# Louisiana Transportation Research Center

## Final Report 562

# Field Instrumentation and Testing to Study Set-up Phenomenon of Piles Driven into Louisiana Clayey Soils

by

Murad Y. Abu-Farsakh, Ph.D., P.E.
Md. Nafiul Haque, Ph.D.
Qiming Chen, Ph.D., P.E.
***LTRC***

4101 Gourrier Avenue | Baton Rouge, Louisiana 70808
(225) 767-9131 | (225) 767-9108 fax | www.ltrc.lsu.edu

| f1. Report No.<br>**FHWA/LA.15/562** | 2. Government Accession No. | 3. Recipient's Catalog No. |
|---|---|---|
| 4. Title and Subtitle<br>**Field Instrumentation and Testing to Study Set-up Phenomenon of Piles Driven into Louisiana Clayey Soils** | 5. Report Date<br>**July 2016**<br>6. Performing Organization Code<br>**LTRC Project Number: 11-2GT**<br>**State Project Number: 736-99-1732** | |
| 7. Author(s)<br>**Murad Y. Abu-Farsakh, Ph.D., P.E., Md. Nafiul Haque, Ph.D. and Qiming Chen, Ph.D., P.E.** | 8. Performing Organization Report No. | |
| 9. Performing Organization Name and Address<br>**Department of Civil and Environmental Engineering**<br>**Louisiana State University**<br>**Baton Rouge, LA 70803** | 10. Work Unit No.<br>11. Contract or Grant No.<br>**LTRC Number: 11-2GT**<br>**State Project No. 736-99-1732** | |
| 12. Sponsoring Agency Name and Address<br>**Louisiana Department of Transportation and Development**<br>**P.O. Box 94245**<br>**Baton Rouge, LA 70804-9245** | 13. Type of Report and Period Covered<br>**Final Report**<br>**June 2011 to Dec 2015**<br>14. Sponsoring Agency Code | |

15. Supplementary Notes
**Conducted in Cooperation with the U.S. Department of Transportation, Federal Highway Administration**


16. Abstract

This research study aims to investigate the pile set-up phenomenon for clayey soils and develop empirical models to predict pile set-up resistance at certain time after end of driving (EOD). To fulfill the objective, a total number of twelve prestressed concrete (PSC) test piles were driven in different soil conditions of Louisiana. Detailed laboratory and in-situ soil testing were performed at each test pile location in order to characterize the subsurface soil condition. Dynamic load tests and static load tests were performed at different times after EOD to verify the axial resistances of piles and to quantify the amount of increase in resistance (i.e., set-up) compared to the EOD. The focus of this research was to calculate the resistance of individual soil layers with time along the length of the pile. In order to implement this goal, all the test piles were instrumented with vibrating wire strain gages. The measurements of vibrating wire strain gages were used to measure the distribution of load transfer along the length of the pile during the static load tests. Vibrating wire piezometers and pressure cells were also installed in the pile face in order to calculate the time for dissipation of excess pore water pressure and corresponding increase in effective stress with time. Case Pile Wave Analysis Program (CAPWAP) was performed in all the dynamic load test data and used to calculate the side resistance of individual soil layers along the length of the pile during dynamic load tests. Logarithmic set-up parameter "A" of individual soil layers were calculated using the unit side resistance. The set-up parameter "A" was correlated with different soil properties such as undrained shear strength, plasticity index, coefficient of consolidation, sensitivity and overconsolidation ratio (OCR). Three different levels of empirical models were developed to estimate the magnitude of pile set-up with time. The developed models were used to predict the total resistance of piles in the database at four different time intervals (i.e., 30 days, 45 days, 60 days and 90 days) after EOD. Reliability analyses were performed to calibrate the set-up resistance factor ($\phi_{set\text{-}up}$) for incorporating it into the LRFD pile design methodology. Accordingly, a set-up resistance factor ($\phi_{set\text{-}up}$) of 0.35 is recommended. A framework for estimating the duration of pile set-up based on consolidation theory of soils at the pile face was introduced.


| 17. Key Words | 18. Distribution Statement<br>**Unrestricted. This document is available through the National Technical Information Service, Springfield, VA 21161.** | | |
|---|---|---|---|
| 19. Security Classif. (of this report) | 20. Security Classif. (of this page) | 21. No. of Pages<br>177 | 22. Price |

# Project Review Committee

Each research project will have an advisory committee appointed by the LTRC Director. The Project Review Committee is responsible for assisting the LTRC Administrator or Manager in the development of acceptable research problem statements, requests for proposals, review of research proposals, oversight of approved research projects, and implementation of findings.

LTRC appreciates the dedication of the following Project Review Committee Members in guiding this research study to fruition.

***LTRC Administrator/ Manager***

Zhongjie "Doc" Zhang, Ph.D., P.E.
Pavement and Geotechnical Research Administrator

***Members***

Jeffrey Lambert, DOTD
Chris Nickel, DOTD
Jesse Rauser, DOTD
Arturo Aguirre, FHWA
Francisco Gudiel, Materials lab, DOTD

***Directorate Implementation Sponsor***

Janice P. Williams, P.E.
DOTD Chief Engineer

# Field Instrumentation and Testing to Study Set-up Phenomenon of Piles Driven into Louisiana Clayey Soils

by

Murad Y. Abu-Farsakh, Ph.D., P.E.
Md. Nafiul Haque, Ph.D.
Qiming Chen, Ph.D., P.E.

Louisiana Transportation Research Center
4101 Gourrier Avenue
Baton Rouge, LA 70808

LTRC Project No. 11-2GT
State Project No. 736-99-1732

conducted for

Louisiana Department of Transportation and Development
Louisiana Transportation Research Center



July 2016

# ABSTRACT

This research study aims to investigate the pile set-up phenomenon for clayey soils and develop empirical models to predict pile set-up resistance at certain time after end of driving (EOD). To fulfill the objective, a total number of 12 prestressed concrete (PSC) test piles were driven in different soil conditions of Louisiana. Detailed laboratory and in-situ soil testing were performed at each test pile location in order to characterize the subsurface soil condition. Dynamic load tests and static load tests were performed at different times after EOD to verify the axial resistances of piles and to quantify the amount of increase in resistance (i.e., set-up) compared to the EOD. The focus of this research was to calculate the resistance of individual soil layers with time along the length of the pile. In order to implement this goal, all the test piles were instrumented with vibrating wire strain gages. The measurements of vibrating wire strain gages were used to measure the distribution of load transfer along the length of the pile during the static load tests. Vibrating wire piezometers and pressure cells were also installed in the pile face in order to calculate the time for dissipation of excess pore water pressure and corresponding increase in effective stress with time. Case Pile Wave Analysis Program (CAPWAP) was performed in all the dynamic load test data and used to calculate the side resistance of individual soil layers along the length of the pile during dynamic load tests. Logarithmic set-up parameter "A" of individual soil layers were calculated using the unit side resistance. The set-up parameter "A" was correlated with different soil properties such as undrained shear strength, plasticity index, coefficient of consolidation, sensitivity and overconsolidation ratio (OCR). Three different levels of empirical models were developed to estimate the magnitude of pile set-up with time. The developed models were used to predict the total resistance of piles in the database at four different time intervals (i.e., 30 days, 45 days, 60 days and 90 days) after EOD. Reliability analyses were performed to calibrate the set-up resistance factor ($\phi_{set\text{-}up}$) for incorporating it into the LRFD pile design methodology. Accordingly, a set-up resistance factor ($\phi_{set\text{-}up}$) of 0.35 is recommended. A framework for estimating the duration of pile set-up based on consolidation theory of soils at the pile face was introduced.

# ACKNOWLEDGEMENT

This research project was funded by the DOTD (SIO No. 736-99-1732) and Louisiana Transportation Research Center (LTRC Project No. 11-2GT). The comments and suggestions of Zhongjie Zhang and Tyson Rupnow of LTRC are gratefully acknowledged.

# IMPLEMENTATION STATEMENT

Piles driven into fine-grained soils usually exhibit increase in resistance (mainly side resistance) over time. This increase in resistance, known as "set-up" or "freeze" phenomenon, has been studied by many researchers in an attempt to develop models that can predict the actual pile resistance at a specific time after pile driving, and to incorporate the set-up effect into pile design. Several empirical models were proposed to estimate pile set-up based on the combined side and tip resistances. These empirical models have some limitations for application due to inter-dependence of back-calculated or assumed variables, complexity of the mechanisms contributing to set-up, and not considering soil layering into the models. The current engineering practice in the design of piles in Louisiana is based on conducting test piles at 14 days after pile driving, ignoring any pile set-up after that, leading to a conservative pile design. In addition, there is a need for a more reliable LRFD design methodology that incorporates the effect of time-dependent gain on pile resistance and takes into consideration soil layering along pile length. This research study focused on developing set-up prediction empirical models that can be used to predict set-up for individual soil layers along the piles, based on different soil properties such as undrained shear strength, plasticity index, coefficient of consolidation, sensitivity, and overconsolidation ratio (OCR), which can be implemented for different soil conditions. The accurate prediction/estimation of the increase in pile resistance with time can be incorporated into a rational design through reducing the number of piles, shortening pile lengths, reducing pile cross-sectional area (using smaller-diameter piles), and/or by reducing the size of driving equipment (using smaller hammers and/or cranes). Incorporating any or a combination of these benefits will result in a significant cost reduction and savings to Louisiana Department of Transportation and Development (DOTD). The resistance factors for the additional set-up resistance using the different empirical models were calibrated, and a set-up resistance factor ($\phi_{set\text{-}up}$) of 0.35 is recommended for all set-up prediction models. This will lead to a successful implementing of pile set-up in LRFD design of piles in Louisiana, which offers a cost-effective and safe pile foundation design in clayey soils.

# TABLE OF CONTENTS

# LIST OF TABLES

# LIST OF FIGURES

# INTRODUCTION

Piles driven into saturated cohesive soils (clays and silts) usually experience a time-dependent increase in pile resistance (mainly frictional), known as "pile set-up" or "freeze." Field observations showed that pile set-up is significant and continues to develop for a long time after installation, especially for fine-grained soils.

The increase of pile resistance over time or set-up is believed to be attributed to three main mechanisms: (1) the increase of effective stress due to dissipation of excess pore water pressure (PWP) generated during pile driving, (2) thixotropy, and (3) stress independent increase or "aging" after the completion of excess PWP dissipation. During pile driving, the soil around the pile (within an influence zone) undergoes large lateral deformations and disturbance, resulting in the development of excess PWP around the pile and change in soil's permeability within the disturbed zone *[1, 2, 3, 4]*. It is believed that a large contribution to pile set-up is related to the dissipation of excess PWP (or consolidation), and the subsequent remolding and reconsolidation of the soil within the influence zone. At early stages, the dissipation of excess PWP can be non-uniform with respect to the log of time depending on soil permeability and extent of soil disturbance. After that, the dissipation becomes uniform. Following that, aging may account for an additional pile set-up *[5]*. Set-up can occur in all pile types driven in different soil types (organic and inorganic, clayey, silty and even sandy soils) *[6]*.

Several empirical relationships*]* have been proposed to estimate the pile set-up resistance with time *[e.g., 7, 8, 9, 10, 11, 12, 13, 14]*. Of these models, the relationship developed by Skov and Denver is the most popular relationship due to its simplicity *[7]*. Most of the available developed models did not consider the soil properties in the model and that the total resistance ($R_t$) was used instead of side resistance ($R_s$) *[8, 10, 11, 12, 13, 14]*. Bullock et al. first proposed the use of side resistance ($R_s$) instead of total resistance ($R_t$) in the set-up model after analyzing the set-up behavior for individual soil layers from instrumented test piles driven in Florida *[15]*. However, very few models incorporated selected soil properties to predict pile set-up *[10, 11, 12]*. The model proposed by Guang-Yu can predict pile set-up only at 14 days after EOD *[12]*. Karlsrud et al. proposed a set-up model that incorporates the plasticity index (PI) and over-consolidation (OCR) ratio *[10]*. Recently, Ng et al. conducted full-scale load tests on instrumented test piles at different locations in Iowa and studied the effect of different soil properties on set-up behavior for steel-H piles *[11]*. The model proposed by Ng et al. incorporates the SPT-N value, horizontal coefficient of consolidation ($c_h$) and equivalent radius of pile ($r_p$) *[11]*. Mostly all of the available models ignored soil properties in their proposed model which are the most important factors to

control set-up behavior. Therefore, there is a need to develop set-up prediction models which can estimate set-up at different soil conditions.

Very few researchers conducted research for the load resistance factor design (LRFD) calibration of set-up resistance factor ($\phi_{set\text{-}up}$) *[16, 17]*. The foundation cost will be reduced by substantial amount if load and resistance factor for set-up ($\phi_{set\text{-}up}$) is incorporated successfully into the LRFD framework. The successful incorporation will aid in design shorter pile length and smaller dimension, less number of piles and finally smaller hammer to drive the pile *[17]*. There are two different set-up factors associated during the calibration of the set-up factor for LRFD framework. They are: $\phi_{EOD}$ and $\phi_{set\text{-}up}$. Because each resistance component has its own individual uncertainties, such as those resulting from the in-situ measurement of soil properties, the components should be adequately reflected in the resistance factors to remain consistent with the LRFD philosophy. Therefore, it is conceptually inappropriate to establish a single resistance factor for both resistance components. Currently the American Association of State Highway and Transportation Officials (AASHTO) do not have any recommendation to incorporate set-up into LRFD framework.

In this research project, field studies were performed on instrumented test piles in order to quantify the amount of set-up after EOD. Laboratory and in-situ testing were performed at each test pile location in order to characterize the subsurface soil condition. Later, set-up of individual soil layers was correlated with soil properties and develop set-up prediction models. LRFD calibration was performed for the calibration of set-up factor for set-up resistance.

# OBJECTIVE

The main objective of this research study is to evaluate the time-dependent increase in pile resistance (or pile set-up phenomenon) for piles driven into Louisiana soils through conducting repeated static and dynamic load testing with time on full-scale instrumented test piles for the purpose of incorporation the pile set-up into DOTD design practice. This will include investigating the mechanism of pile set-up, study the effect of soil type/properties, pile size, and their interaction on pile set-up phenomenon, and develop a model and its reliability to estimate the increase in pile resistance with time.

.

# SCOPE

In order to implement the objectives of this study, full scale load tests were performed on different locations of Louisiana. A series of dynamic load tests and static load tests were conducted on each test pile in order to measure the amount and rate of set-up. The test piles were instrumented with different sensors in order to measure the side resistance of individual soil layers and understand the set-up phenomenon better. Vibrating wire strain gages were installed in pairs in all the test piles in order to measure the side and tip resistances separately and also measure the load distribution along the length of the piles. This load distribution along the length of the pile was used to measure the side resistance of individual soil layers. Skov and Denvers' model was implemented to calculate the logarithmic set-up rate of individual soil layers *[7]*. The logarithmic set-up rate "A" of individual clayey soil layers was correlated with different soil properties (e.g., undrained shear strength, plasticity index, coefficient of consolidation, sensitivity and overconsolidation ratio). Regression analyses were performed with the aid of Statistical Analyses Software (SAS) program in order to develop the set-up prediction model with incorporated soil properties. Finally, load resistance factor calibration was performed in order to calibrate the set-up resistance factor. The LRFD calibration was performed with ΦΦ second moment (FOSM), first order reliability method (FORM) and Monte Carlo simulation methods.

.

# METHODOLOGY

As discussed earlier, the main objective of this research study was to develop models that can predict set-up resistance at certain time after EOD and calibrate the set-up resistance for load resistance factor design (LRFD) calibration. Background information on mechanism of set-up and available set-up prediction model were studied first. Five different sites were selected to perform the set-up study. Laboratory and in-situ soil testing were performed at each test pile location and load tests were performed after EOD. The collected load test data and soil properties were compiled and analyzed. The methodology of collecting, compiling and analyzing the load test data and instrumentation procedure of the test piles are presented in this section.

## Background

### Pile Set-up Mechanism

During pile installation of a driven pile, a volume of soil equal to the volume of pile will be displaced away in the direction of least resistance. A remolded zone will form around the pile followed by a transition zone of slightly changed soil properties. Driving the pile will develop high excess PWP in the remolded zone. The dissipation of excess PWP re-consolidates the remolded zone, leading to increased undrained shear strength and hence increased pile resistance. The increase in pile resistance with time is primarily due to the re-consolidation of the remolded soil around the pile. However, the time-dependent increase in pile resistance continues to increase after complete dissipation of excess PWP *[e.g., 18, 19, 20, 21]*. This additional increase in pile resistance with time is related to soil aging. According to Komurka et al. the pile set-up mechanism can be divided into three phases: Phase 1—logarithmically nonlinear rate of excess PWP dissipation, Phase 2—logarithmically linear rate of excess PWP dissipation, and Phase 3—aging phenomenon *[6]*. However, sometimes it is also possible to have some overlap between successive phases for the same soil layer such that more than one phase may be contributing to set-up at a time. Figure 1 illustrates the three phases of pile set-up.

**Phase 1.** Due to the high disturbance of the soil, the rate of excess PWPs dissipation in this phase is not linear with respect to the log of time. Consequently, the rate of pile set-up during this phase is also not linear with respect to the log of time *[22, 23, 24]*. The lower the soil permeability and the larger the pile size (larger volume of soil displaced and larger extent of the remolded zone), the longer is the duration of the logarithmically nonlinear phase *[25, 26]*. In clean sands, the logarithmic rate of dissipation may become linear almost immediately after driving. In cohesive soils, the logarithmic rate of dissipation may remain nonlinear for several hours to days *[26, 27]*. During pile driving in clays, the surrounding soil undergoes severe disturbance, remolding, and the development of large excess PWP *[11, 20]*. As a result, the

horizontal effective stress along the pile surface can be close to zero. During the non-linear logarithmic phase of consolidation, the dissipation of excess PWP results in increases in effective vertical and horizontal stresses, and thus strength increases in a manner that is not well-understood *[6, 26]*.

**Phase 2.** Following the logarithmic nonlinear phase, after a certain time from pile driving, the rate of excess PWP dissipation becomes linear with respect to the log of time. Consequently, the corresponding pile set-up rate for most soils is also logarithmically linear with respect to the log of time. The time after driving at which the rate of excess PWP dissipation, and hence pile set-up rate, becomes logarithmically linear is referred to as the initial time or reference time, $t_o$, in many empirical models *[7, 9, 11, 28]*. The duration of this logarithmical linear phase is also a function of soil type and properties (permeability and sensitivity) and pile type and size. The duration of this phase is longer for the case of larger-size piles driven in low permeability soils. In clean sands, the duration of logarithmical linear phase ranges from minutes to several hours. While in cohesive soils, this phase may continue for several months or years *[7, 15, 26]*. For example, for a 15 in. (381 mm) diameter pile, 200 to 400 days needed to complete soil consolidation around the pile *[29]*.

**Phase 3.** The third set-up phase is due to aging phenomenon, which is independent of the effective stresses. According to consolidation theory, infinite time is required to complete the dissipation of excess PWP *[5, 21, 27]*. Knowing that the rate of set-up corresponds to the rate of excess PWP dissipation, consequently in some cases infinite time would be required for set-up to be completed. This phenomenon is similar to the case of secondary compression after the primary consolidation is complete. During this phase, the set-up rate is independent of effective stress. This phenomenon is known as aging, which is referred to as the time-dependent change in soil properties at a constant effective stress, which is active for fine-grained as well as coarse-grained soils. Aging is attributed to thixotropy, secondary compression, particle interference, and clay dispersion *[5, 30]*. During the aging phase, the shear strength and stiffness of the soil increases as well as the angle of interface friction between soil and pile *[5, 21]*. It is also associated with reduction in the soil's compressibility *[6, 31, 32]*.

.

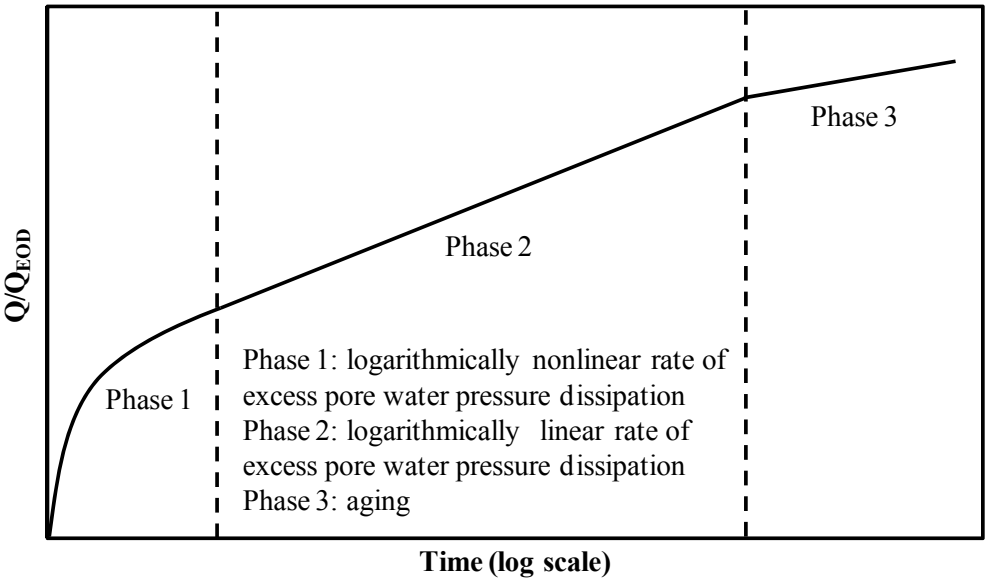


**Figure 1**
**Three phases of pile set-up *[6]***

**Factors Affecting Pile Set-up**

The increase of pile resistance with time depends on many factors including the soil type and properties and the type and size of driven pile.

**Effect of Soil Type.** The increase of pile resistance with time (set-up) after pile installation has been reported in various soil types from cohesive to cohesionless soils. This includes organic and inorganic saturated clays, loose to medium dense silt, sandy silts, silty sands, and fine sand *[30, 33, 34]*. However, the long term pile set-up is not significant in very silty low plasticity cohesive soils and in sands and gravel compared to cohesive soils *[35, 36, 37]*.

During pile driving, the soil around the pile undergoes large radial deformations, which resulted in the development of large excess PWP within the influence zone *[25, 30]*. In cohesive soils, due to the low permeability, the developed excess PWP will dissipate slowly. As a result, small percentage of set-up occurs during the first logarithmically nonlinear dissipation Phase 1, while the majority of set-up occurs during the logarithmically linear dissipation (Phase 2). In cohesive soil, little set-up can be attributed to aging (Phase 3). Soft clays usually exhibit more set-up than stiff clays *[30, 32]*. After pile driving, the consolidation of remolded zone and the increase in effective stress associated with dissipation of excess PWP, usually resulted in increase in the soil's shear strength. Randolph et al. stated that for piles driven in cohesive soils, the soil's shear strength decreases with the logarithmic distance from the pile until it equals the initial soil strength at about 10 pile radii *[25]*. In silts and fine sands, the developed excess PWP around the

pile dissipates at a relatively faster rate than cohesive soils (i.e., almost while driving). As a result, some set-up may occur during the logarithmically linear dissipation (Phase 2), while the majority of set-up occurs during the aging (Phase 3) in these soils *[37, 38]*. Either, or both, of these phases may begin immediately after driving *[39, 40]*. Loose sands and silts have been found to set-up somehow similar to soft clays *[30, 37]*.

The rate of pile set-up in granular soils depends on many factors including soil density, soil grain characteristics (particle size, shape, and gradation), soil shear modulus, moisture content, pile-soil dilatancy, and in-situ stress level *[8, 18, 38, 41]*. Long et al. determined that although the largest set-up occurred in the first 10 days after driving, set-up appeared to continue for up to 500 days, and measured side resistances increased 2 times compared to EOD side resistance *[30]*. An increase in pile resistance of up to 100% has been reported in non-cohesive soil *[18, 30, 38]*. Koutsoftas reported a 125 to 150% increase of pile resistance in dense sand *[42]*. Generally, set-up is greater for dense and well-graded sands, than for loose and uniform sands *[41, 43]*. It is also possible to experience decrease in pile resistance with time, termed relaxation, in dense to very dense silts and fine sands *[8, 30, 37]*.

**Effect of Pile Type.** Set-up has been reported to occur in almost all pile types including pre-stressed concrete (PSC) piles, tapered and fluted steel piles, H-piles, open-end and closed-end pipe piles, and in treated and untreated wood piles. Studies showed that the set-up rate decreases as pile size increases *[44]*. Yang reported greater set-up for wood piles installed in organic silts than for steel H-piles *[45]*.

When concrete and timber piles are driven into clays, excess PWP can dissipate into the pile, causing excess PWP in the soil adjacent to the pile surface to dissipate faster than soil a smaller distance away from the pile *[6]*. As a result, the soil near the pile surface consolidates and increases strength faster than the clay a smaller distance away from the pile. When subjected to a load that causes failure, slippage will occur at some distance away from the pile wall rather than at the pile-soil interface. Because PSC piles have higher soil/pile interface friction, they usually exhibit more set-up than steel piles *[46]*. Chow et al. stated that part of set-up for steel piles installed in sands is attributed to the corrosion-induced bonding of the sand particles with the steel *[47]*.

**Available Methods to Measure Set-up**

**Empirical Models.** Pile set-up can be predicted or quantified using empirical, analytical, or numerical methods. The most popular relationship was proposed by Skov and Denver because of its simplicity to use *[7]*. Both the data from static load tests and dynamic load tests

(CAPWAP) were used to define set-up factor "A" in this model as the rate of increase of resistance ratio per log cycle change of elapsed time ratio. Skov and Denver proposed this logarithmic equation (1) based on three types of soils as clay, chalk and sand *[7]*. They proposed the empirical model as:

$$\frac{R_t}{R_{to}} = 1 + A \log_{10} \frac{t}{t_o} \quad (1)$$

where, $R_t$ = Pile resistance at time, t, $R_{to}$ = Pile resistance at initial time, $t_o$, t = Time elapsed since end of initial pile driving, $t_o$ = a reference time before which the resistance cannot be reliably predicted, and A = Logarithmic set-up rate parameter.

The time $t_o$ is usually taken as the time at which the rate of excess PWP dissipation is linear with respect to log of time. The time $t_o$ is a function of soil type and pile size, which is not easy to calculate. $t_o$ value has to be back-calculated from field data, assumed, or obtained from emperical relationships in the literature *[48]*. For PSC piles and H-piles, Camp and Parmer found that $t_o$ equals to two days, and showed that the use of $t_o$ = 1 day is reasonable *[44]*. Axelsson obtained a value of $t_o$ = 1 day for PSC piles installed in cohesionless soils *[21]*. A value of 1 to 2 days was used for $t_o$ by Svinkin et al. *[8]*. However, some researchers recommernded to standarize $t_o$ = 1 day [*e.g.,7, 28]*.

The logarithmic set-up parameter "A" in equation (1), depends on the soil type, pile material, pile type, pile size and pile resistance *[8, 9, 44]*. Skov and Denver suggested using A = 0.2 for sand and A = 0.6 for clay *[7]*. The "A" parameter either assumed, back-calculated from field data, or obtained from emperical relationships in the literature *[48]*. The results of the literature review by Chow et al. indicated a range of logarithmic set-up parameter "A" from 0.25 to 0.75 *[18]*. Axelsson obtained a range of 0.2 to 0.8 for set-up parameter "A" *[21]*. Bullock reported an average of 0.20 for set-up parameter "A" *[49]*. He also stated that the A and $t_o$ parameters are not independent variables, and the determination of "A" is a function of the value used for $t_o$ *[49]*.

Following by Skov and Denver, some empirical models were proposed *[7]*. Based on some dynamic load test results of Shanghai, China; Huang proposed an empirical model for clayey soils to calculate set-up *[13]*. According to them, the estimate of pile resistance at the time t (day) after driving can be expressed as *[13]:*

$$\frac{R_t}{R_{to}} = 0.263\ [1 + \log(t)]\ R_{max} \quad (2)$$

where, t = the time interval after driving, $R_{max}$ = maximum bearing capacity of pile, and $R_{to}$ = the initial resistance of pile.

Zhu Guang-Yu first introduced the pile set-up related to sensitivity ($S_t$) in cohesive soils *[12]*. The regain of pile resistance increases with $S_t$. About 70 test piles on different 20 sites in the coastal areas of east China were considered in this through analysis. However, during this analysis result of driving and restriking only after 14 days and compared it to the result of static load tests was used to present this empirical expression *[3]*.

$$\frac{R_{14}}{R_{to}} = 0.375S_t + 1 \quad (3)$$

where, sensitivity ($S_t$) equal to the ratio of strength of undisturbed soil to that of remolded soil, $R_{14}$ = pile resistance at 14 days, and $R_{to}$ = the initial pile resistance.

In order to calculate the magnitude and quantify the increase of pile resistance, a series of load tests were performed on five different piles driven on clayey soil in Chicagoland. Lukas and Bushell concluded that the resistance increases mostly in first 10 days due to increase in side resistance as excess PWPs that are generated during pile driving dissipate by this time *[50]*. Beyond this time, the resistance continues to increase but at a slower rate. Compression load tests were performed at four different sites and tension load test were performed on one site during this investigation. An assumption was made that the increase in total pile resistance was attributed entirely due to increase in adhesion along the sides of the pile. The provided approach:

$$\Delta S = S_L \text{ (Long term adhesion)} - S_o \text{ (The time of driving)} \quad (4)$$

where, $S_L = S_u$ (Undrained shear strength) x AF (Adhesion factor)

$S_o = S_u$ (Undrained shear strength) / $S_i$ (Sensitivity of soil)

An empirical relationship was presented by Mesri et al. to predict the set-up in sand *[51]*. This relationship was mainly used to measure to increase in cone resistance with time for clean sands that had been densified by blasting. The two factors that mainly contribute to this increase of strength were: primarily consolidation that occurs for a shorter period of time immediately after blasting and secondary compression at a constant effective stress. This relationship later used to predict the set-up for pile by replacing the increase in cone resistance with time to the increase in pile resistance with time. The following equation is presented to give an empirical relationship for set-up in sand using log-log scale

$$\frac{R_t}{R_{to}} = 1.1\ t^{\alpha} \quad (5)$$

where, $R_t$ = pile resistance at time t day, $R_{to}$ = Pile resistance at the EOD and $\alpha$ = the exponential coefficient. The following values of $\alpha$ are recommended:

Lower bound = 0.05
Upper bound = 0.18
Average = 0.13

Svinkin et al. analyzed two sets of data in sandy soils varying with water table to present a new empirical model for set-up *[8]*. Experimental data showed that the water table has a great influence on the set-up effect in sandy soils. However, the development of soil set-up in saturated sandy soil is generally more complicated. Five different PSC piles with high water table were tested after driving by SLTs and DLTs. Mostly, all of the piles showed soil set-up gradually increases approximately during first 10 days and the tendency followed a similar pattern. However, their set-up coefficient ranged between an upper boundary and lower boundary which are expressed in following two equations:

$$R_t = 1.4\ R_{to} t^{0.1} \quad (6a)$$

$$R_t = 1.025\ R_{to} t^{0.1} \quad (6b)$$

where, t = elapsed time, $R_t$ = pile resistance at t days, and $R_{to}$ = the initial resistance of pile.

The existing model by Skov and Denver yields set-up versus time for assessment of pile resistance after the first restrike and three different values of $t_o$ were recommended depending on types of soil *[7]*. If for various piles this time (i.e., $t_o$) is different, the existing model yields different assessment of set-up at the same site and obtained results of increase in resistance cannot be compared. To provide determination of the soil set-up independently of the time of the first restrike and taking consideration, the actual time in days passed after pile installation Svinkin and Skov proposed a new model *[9]*. For a soil set-up straight line passing through two points corresponding to pile resistance at EOD, $R_{EOD}$ and pile resistance at any time after pile driving, $R_{u(t)}$, a model in logarithmic time scale can be written as

$$\frac{Rt}{R_{to}} - 1 = B\ [\log_{10}(t) + 1] \quad (7)$$

where, t = elapsed time, B = set-up factor, $R_t$ = pile resistance at t days, and $R_{to}$ = the initial resistance of pile.

To predict the set-up more accurately in normally consolidated clay of low plasticity, Karlsrud et al. proposed a new empirical equation (8) based on a database of 49 test piles *[10]*. The proposed model which is known as NGI-99 (Norwegian Geotechnical Institute) considers excess PWP due to installation of pile fully dissipates after 100 days and was taken the resistance at 100 days as reference resistance. The proposed model:

$$\frac{R_{(t)}}{R_{100}} = [1 + \Delta 10.\ \log_{10}(\frac{t}{t_{100}})] \quad (8)$$

where, t = the time between driving and test loading, R(t) = the resistance at any time after 100 days and $R_{100}$ = the reference resistance at 100 days. Δ10 = a dimensionless resistance increase for a ten-fold time increase. Based on results supplemented by Flaate, Δ10 was correlated with PI and OCR value *[52]*.

$$\Delta 10 = 0.1 + 0.4.\ (I - I_p/50).OCR^{-0.8} \quad (9)$$

where, Δ10 ranges from 0.1 to 0.5, $I_p$ = plasticity index and OCR = overconsolidation ratio. $I_p$ and OCR are average values along the pile. The provided methods showed a correlation between calculated and measured value. However, there is a considerable scatter and uncertainties are observed in case of soft clay.

Recently, Ng et al. conducted full-scale load tests on instrumented test piles at different locations of Iowa and studied the effect of different soil properties on set-up behavior for steel-H piles *[11]*. The model proposed by Ng et al. incorporate the SPT-N value, horizontal coefficient of consolidation ($c_h$) and equivalent radius of pile ($r_p$), and the model does not require a reference load test after EOD since the model considered the driving resistance at EOD as a reference resistance *[11]*. However, most of the proposed models in literature require a reference load test data between 1 and 2 days to predict the pile set-up since the duration of the first non-logarithmic phase 1 is uncertain *[e.g.,1, 7]*. They proposed the model to predict the set-up resistance as:

$$\frac{R_{(t)}}{R_{EOD}} = [A \times \log_{10}(\frac{t}{t_{EOD}}) + 1]\frac{L_{(t)}}{L_{EOD}} \quad (10)$$

where, $A = \frac{f_c C_{ha}}{N_a r^2_p} + f_r$, $c_{ha}$= horizontal coefficient of consolidation, $N_a$ = SPT N value, $r_p$ = equivalent pile radius, $f_c$ = consolidation factor, $f_r$ = remolding recovery factor and $L_t/L_{EOD}$= normalized embedded pile length.

**LRFD Calibration Using Reliability Theory**

The basic concept behind LRFD is illustrated in Figure 2 and Figure 3. Here, the distributions of random load (Q) and resistance (R) values are shown in Figure 2 as normal distributions. The performance limit state function for the state of the structural system can be described as follows:

$$g(R, Q) = R - Q$$

where, R is the resistance of a given structure, which is a random variable, and Q is the applied load, which is also a random variable.

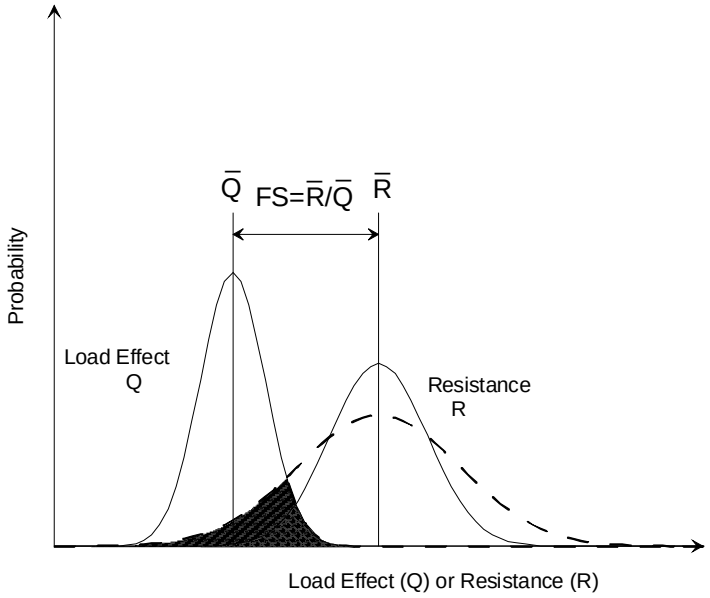


**Figure 2**
**Probability density functions for load effect and resistance**

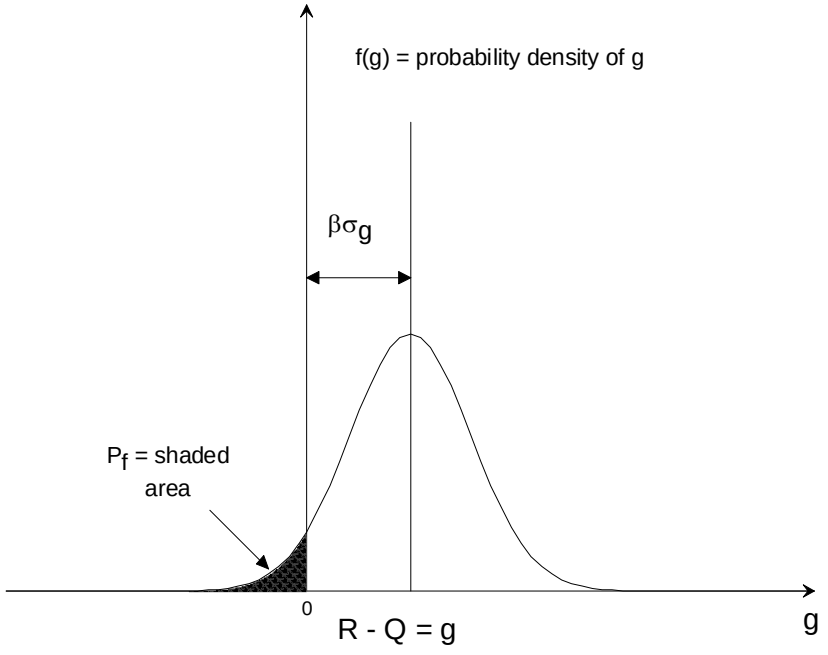


**Figure 3**
**Probability density function of the safety margin *[53]***

The limit state, corresponding to the boundary between desired and undesired performance, would be when g = 0. If g ≥ 0, the structure is safe (desired performance); if g < 0, the structure is unsafe (undesired performance). The probability of failure is then defined as:

$$P_f = p[g(R, Q) < 0] = p\ \{R < Q] \tag{11}$$

In general terms, if X is a random variable such that X = ($x_1$. $x_2$. $x_3$…..$x_n$) with joint probability density function (PDF) $f_x(x)$ and g(x) is a scalar function of input random variable, then g($x_1$. $x_2$. $x_3$…..$x_n$) determines the state of structure such that g(X) > 0 means safe domain and g(X) < 0 indicates failure domain. Also, there exists a limit state surface at the boundary between the two domains defined as an n-dimensional hyper surface {x; g(x) = 0} or the limit state function. The probability of failure is then given by:

$$P_F = \int_{g(x)\leq 0} f_X(x)dx \tag{12}$$

where $f_x(x)$ is the probability density function for a random variable X.

Integration is carried out over the failure domain; in other words, the failure probability is the probability of being in the domain of the n-dimensional space bounded by g(X) ≤ 0. For a normal distribution of g values, the probability of failure can be equated explicitly to the value of reliability index $\beta = \mu_g/\sigma_g$, where $\mu_g$ is the mean value of g and $\sigma_g$ is the standard deviation of g. The relationship between probability of failure and reliability index can be calculated using the following excel function:

$$P_f = 1 - NORMDIST\ (\beta) \tag{13}$$

Also, if the load and resistance values are normally distributed and the limit state function is linear, then β can be determined from the following equation:

$$\beta = \frac{\mu_R - \mu_Q}{\sqrt{{\sigma_R}^2 + {\sigma_Q}^2}} \tag{14}$$

where, $\mu_R$ and $\mu_Q$ are the mean, and $\sigma_R$, and $\sigma_Q$ are the standard deviation of resistance and load, respectively. If both the load and resistance distributions are lognormal and the limit state function is a product of random variables, then β can be calculated using a closed-form solution reported by Withiam et al. and Nowak as follows *[53, 54]:*

$$\beta = \frac{\ln[\mu_R/\mu_Q\sqrt{(1+COV^2_Q)/(1+COV^2_R)}]}{\sqrt{\ln\,[(1+COV^2_Q)(1+COV^2_R)]}} \tag{15}$$

where, $\mu_R$ is the mean value of the resistance R, and $\mu_Q$ is the mean value of the load Q; $COV_R$ and $COV_Q$ are the coefficients of variation for the resistance and load values, respectively. The limit state function for LRFD design for three different methods (i.e., FORM, Monte Carlo simulation method and FOSM) is described later.

**Statistical Characterization of the Collected Data.** To perform an LRFD calibration, the performance limit state equations must be determined. The two limit states that are usually checked in the design of piles and drilled shafts are the ultimate limit state (ULS), or strength limit state, and the serviceability limit state (SLS). Both limit state designs are carried out to satisfy the following criteria *[55]*.

ULS: Factored resistance ≥ Factored load effects
SLS: Deformation ≤ Tolerable deformation to remain serviceable

It is usually considered that the design of deep foundations is controlled by the strength limit state. Therefore, in the following discussion, only the strength I limit state is considered. The following basic equation is recommended to represent limit states design by AASHTO *[56]:*

$$\phi R_n \geq \sum \eta \gamma_i Q_i \tag{16}$$

where, $\phi$ = resistance factor, $R_n$ = nominal resistance, and $\eta$ = load modifier to account for effects of ductility, redundancy, and operational importance. The value of $\eta$ usually is taken as 1.00. The value $Q_i$ = load effect, and $\gamma_i$ = load factor.

The pile resistance is the added value of side resistance ($R_s$) and tip resistance ($R_{tip}$); however, the percentage of side ($R_s$) and tip ($R_{tip}$) resistance to the total resistance ($R_t$) is not constant. Therefore, it is not possible to provide a fixed correlation between in between the three different resistance factors (Total, side and tip). Only the total resistance ($R_t$) is calibrated. Without considering the pile set-up resistance the load combination of dead load and live load for the AASHTO strength I case, the performance limit equation is as follows:

$$\phi R_n = \gamma_{DL} Q_{DL} + \gamma_{LL} Q_{LL} \tag{17}$$

where, $\gamma_{DL}$ and $\gamma_{LL}$ are the load factors for the dead load and live load, respectively, and $Q_{DL}$ and $Q_{LL}$ are dead and live load, respectively. Now, with considering set-up equation (17) can be rewritten as:

$$\phi_{EOD} R_{EOD} + \phi_{set\text{-}up} R_{set\text{-}up} = \gamma_{DL} Q_{DL} + \gamma_{LL} Q_{LL} \tag{18}$$

However, Abu-Farsakh et al. performed the calibration of resistance factors ($\phi$) for the LRFD design of fifty three PSC test piles driven in local Louisiana soil *[57]*. The pile resistances were calculated based on static analysis (Norlund method), three direct CPT methods [Schmertmann method, De-Ruiter and Beringen method, and Bustamante and Gianselli (LCPC) method] and the average of the three CPT methods. The set-up resistance for 14 days after EOD was already included in that resistance factor ($\phi$). Therefore, resistance factor for set-up have to be calibrated for the additional increase in resistance after 14 days and $\phi_{EOD}$ can be replaced in the equation as $\phi_{14}$. Table 1 summarized Abu-Farsakh et al.'s findings for $\phi_{14}$ of fifty three driven test piles and the performance limit equation for set-up can be written as *[57]*:

$$\phi_{14}R_{14} + \phi_{set\text{-}up}R_{set\text{-}up} = \gamma_{DL}Q_{DL} + \gamma_{LL}Q_{LL} \quad (19)$$

**Table 1**

**Proposed resistance factor for initial 14 days at β=2.33 by Abu-Farsakh et al. *[57]***

| Design methods | | Resistance factor ($\phi$) for Local Louisiana soil by Abu-Farsakh et al. *[57]* for initial 14 days | | |
|---|---|---|---|---|
| | | FOSM | FORM | Monte Carlo simulation |
| Static | α-Tomlinson method and Nordlund method | 0.56 | 0.63 | 0.63 |
| Direct CPT method | Schmertmann | 0.44 | 0.48 | 0.49 |
| | LCPC/LCP | 0.54 | 0.60 | 0.59 |
| | De Ruiter and Beringen | 0.66 | 0.74 | 0.73 |
| | CPT average | 0.55 | 0.61 | 0.62 |

The loads applied to the piles are traditionally based on superstructure analysis; whereas, the actual loads transfer to substructure is not fully researched. Most researchers employ the load statistics and the load factors from AASHTO LRFD specifications, which were originally recommended by Nowak, to make the deep foundation design consistent with the bridge superstructure design *[54]*. Both live load and dead loads were assumed to be log normally distributed. In this study, the load statistics and factors from the AASHTO LRFD specifications are adopted as follows *[56]*:

$$\gamma_{LL} = 1.75 \qquad \lambda_{LL} = 1.15 \qquad COV_{LL} = 0.18$$

$$\gamma_{DL} = 1.25 \qquad \lambda_{DL} = 1.08 \qquad COV_{DL} = 0.13$$

where, $\lambda_{DL}$ and $\lambda_{LL}$ are the load bias factors (mean ratio of measured to predicted value) for the dead load and live load, respectively. $COV_{DL}$ and $COV_{LL}$ are the coefficient of variation values for the dead load and live load, respectively. The $Q_{DL}/Q_{LL}$ is the dead load to live load ratio, which varies depending on the span length *[58]*. In this research, $Q_{DL}/Q_{LL}$ of 3 is used for

calibration, since the calibration is insensitive to $Q_{DL}/Q_{LL}$ ratio above 3. The resistance statistics were calculated in terms of the bias factors. The resistance bias factor is defined as the ratio of the measured pile resistance over the predicted pile resistance, i.e.,

$$\lambda_R = \frac{R_m}{R_p} \tag{20}$$

where, $R_m$ = measured resistance and $R_p$ = predicted nominal resistance.

**LRFD Calibration for $\phi_{set\text{-}up}$.** The foundation cost will be reduced by substantial amount if load and resistance factor (LRFD) for set-up ($\phi_{set\text{-}up}$) is incorporated successfully into the LRFD framework. The successful incorporation will aid in design shorter pile length and smaller dimension, less number of piles and finally smaller hammer to drive the pile *[17]*. There are two different set-up factors associated during the calibration of the set-up factor for LRFD framework: $\phi_{EOD}$ and $\phi_{set\text{-}up}$. Because each resistance component has its own individual uncertainties, such as those resulting from the in-situ measurement of soil properties, the components should be adequately reflected in the resistance factors to remain consistent with the LRFD philosophy. Therefore, it is conceptually inappropriate to establish a single resistance factor for both resistance components. Currently the AASHTO do not have any recommendation to incorporate set-up into LRFD framework. As mentioned earlier, $\phi_{EOD}$ is successfully calibrated before by many researchers *[e.g., 59, 60]*. Very few researchers conducted research for the calibration of $\phi_{set\text{-}up}$ *[e.g., 16, 17]*.

Yang and Liang used the first order reliability method (FORM) to compute the separate resistance factors, using Skov and Denver's set-up model *[16, 7]*. A set-up resistance factor of 0.30 specifically at a target reliability index of $\beta = 2.33$ is recommended by Yang and Liang *[16]*. They also concluded that at a low target reliability index ($\beta < 3.00$) incorporation of set-up effect into the prediction of total pile resistance gives an advantageous contribution to predict the total pile resistance. However, incorporation of the set-up resistance into the pile design yields more conservative prediction of the total pile resistance at a higher reliability index ($\beta \geq 3.00$)

Ng et al. used the first order second moment (FOSM) method to calibrate the set-up resistance factor ($\phi_{set\text{-}up}$) *[61]*. A set-up prediction model is first developed (equation 10) in order to estimate the set-up resistance at a specific time. Based on 19 data sets of steel H-piles driven in cohesive soil in IOWA, a set-up resistance factor of 0.36 and 0.31 were recommended for pile set-up for redundant and non-redundant pile groups at a target reliability index of $\beta = 2.33$, respectively bu Ng et al. *[61]*.

**First Order Reliability Method (FORM).** The reliability method proposed by Hasofer and Lind and its subsequent generalization to handle non-Gaussian correlated random variables is commonly called the first order reliability method (FORM) *[62]*. Hasofer and Lind proposed a modified reliability index that did not exhibit the invariance problem *[62]*. The "correction" is to evaluate the limit state function at a point known as the "design point" instead of the mean values. The design point is a point on the failure surface g = 0. Since the design point is generally not known in advance, an iteration technique must be used to solve the reliability index. A detailed procedure regarding FORM can be found in Nowak and Collins *[63]*. Only information on the means and the standard deviations of the resistances and the loads are needed while detailed information on the type of distribution for each random variable is not needed. The Rackwitz and Fiessler algorithm provides a practical and computationally efficient method to compute reliability index (β) with no restriction on the number of random variables *[64]*. β is calculated using the Rackwitz and Fiessler algorithm, as the procedure recommended in Transportation Research Circular E-C079 *[64, 65]*. The "SOLVER" tool in excel is used to perform the calibration for FORM. Steps for FORM using the Rackwitz-Fiessler method *[64]*:

1. The limit state function for LRFD is developed as follows:

(a) The limit state function for $\phi_{14}$ is proposed by Abu-Farsakh et al. *[57]* as:

$\hat{R} - \bar{Q} = 0$ (Limit state)

$\hat{R} - (\lambda_{DL} Q_{DL} + \lambda_{LL} Q_{LL}) = 0$ [Since, $\bar{Q} = \lambda_{DL} Q_{DL} + \lambda_{LL} Q_{LL}$]

$\lambda_R R - (\lambda_{DL} Q_{DL} + \lambda_{LL} Q_{LL}) = 0$

$\lambda_R \frac{\gamma_{DL} Q_{DL} + \gamma_{LL} Q_{LL}}{\phi_{14}} - (\lambda_{DL.} Q_{DL} + \lambda_{LL} Q_{LL}) = 0$ [Since, $\phi_{14} R = \gamma_{DL} Q_{DL} + \gamma_{L.} Q_{LL}$]

$$\lambda_R \frac{\gamma_{DL} + \gamma_{LL} \kappa}{\phi_{14}} - (\lambda_{DL} + \lambda_{LL} \kappa) = 0 \qquad \{\kappa = \frac{Q_{LL.}}{Q_{DL}}\} \tag{21}$$

(b) The limit state function for $\phi_{set\text{-}up}$ can be calculated as:

$$[\gamma_{DL} + \gamma_{LL} \kappa - \phi_{14} \alpha (1 + \kappa)] \lambda_{R_{set-up}} - [\lambda_{DL} + \lambda_{LL} \kappa - \frac{\lambda_{R14}}{\phi_{14}} \left[\left(\gamma_{DL} + \gamma_{LL} \kappa\right)\right] \phi_{set-up} = 0 \tag{22}$$

2. Assuming initial design point ($x_i^*$), mean values are a reasonable choice for most cases. In this case, initial design values for dead load and live load ($x_2$ and $x_3$) assumed and that for resistance ($x_1$) is determined by equating the limit state function equal to zero. Also for lognormal variables equivalent normal parameters are then determined as:

$$\mu^e_x = x^* - \sigma^e_x [\Phi^{-1} F_x (x)]$$

$\sigma^{e}_{x} = \frac{1}{fx(x^*)} \varphi \frac{x^* - \mu^{e}x}{\sigma^{e}x} = \frac{1}{fx(x^*)} \varphi [\Phi^{-1}(F_X(x^*)]$

where, φ and Φ denotes the mass probability density function (PDF) and the cumulative distribution function (CDF) for normal distribution, respectively.

3. Corresponding to the design point x*, the reduced variable is found as:

$z^*_i = \frac{x^* - x\, \mu^{e}x_i}{\sigma^{e}x_i}$

4. Partial derivatives of the limit state function is found at the design point and vector G is defined as:

$G = \begin{Bmatrix} G1 \\ G2 \\ G3 \end{Bmatrix}$, where $G_i = -\frac{\partial g}{\partial zi}\Big|$ at design point $= -\frac{\partial g}{\partial xi}\Big|^*(\sigma^{e}x_i)$ at design point at design point

$\beta = \frac{\{G\}^T\{z*\}}{\sqrt{(G)^T(G)}}$ where, $\{z^*\} = \begin{Bmatrix} z^*_1 \\ z^*_2 \\ z^*_3 \end{Bmatrix}$

$\alpha = \frac{\{G\}}{\sqrt{(G)^T(G)}}$

5. The new design point is determined in the reduced variable as:

$z^*_i = \alpha_i \beta$

$x^*_i = \mu^{e}_{xi} + z_i \sigma^{e}_{xi}$

Also at this step, the new design point for resistance ($x_i$) is determined by inserting new design values for loads ($x_2$ and $x_3$) into the g function. With new design points, steps from 1 to 5 are followed. The procedure is repeated until β and the design point converges.

**Monte Carlo Simulation Method.** For more complicated limit state functions, the application of the general statistical method for the calculation of the reliability index is either extremely difficult or impossible. Under this circumstance, Monte Carlo simulation provides the only feasible way to determine the reliability index or the probability of failure.

The Monte Carlo simulation method employs the generation of random numbers and then it is used to solve deterministic problems. Random values of biases of loads and resistances are generated according to basic statistical parameters [i.e., mean (μ), COV, and an assigned distribution such as lognormal distribution used in this study]. The random values are then combined to form a limit state function (g) according to the equation (22). From the definition of failure (e.g., $g < 0$), the number of failure simulation is counted and the probability of failure is therefore determined. The reliability index can be calculated from known probability of failure. In this study, the random numbers of load and resistance biases with lognormal distributions were generated with a MATLAB code. The steps of Monte Carlo simulation method are as follows:

1. Select a trial resistance factor ($\phi$).
2. Generate random numbers for each set of variables. Here there are four variables (resistance for set-up, resistance for initial 14 days, dead load and live load bias factor), so four sets of random variables have to be generated independently for each case.
3. For each lognormal variable, sample value $x_i$ is estimated as:

$$x^*_i = \exp(\mu_{lnx} + z_i\sigma_{lnx})$$

where, $\sigma^2_{lnx} = \ln(V^2_x + 1)$ and $\mu_{lnx} = \ln(\mu_x) - \frac{1}{2}\sigma^2 lnx$

In the above expressions, $\mu_x$ and $V_x$ are the arithmetic mean and variance of x; $\mu_{lnx}$ and $\sigma_{lnx}$ are equivalent lognormal mean and standard deviation of ln(x).

4. Define the limit state function. The limit state equation developed for FORM method is used for the calibration.

$$[\gamma_{DL} + \gamma_{LL}\text{Ƙ} - \phi_{14}\,\alpha\,(1 + \text{Ƙ})]\,\lambda_{R_{set-up}} - [\lambda_{DL} + \lambda_{LL}\text{Ƙ} - \frac{\lambda_{R14}}{\phi_{14}}\left[\left(\gamma_{DL} + \gamma_{LL}\text{Ƙ}\right)\right]\phi_{set-up} = 0$$

5. Find the number of cases where $g(x_i) \leq 0$. The probability of failure is then defined as:

$$Pf = \frac{\text{count}\,(g \leq 0)}{N}$$

and reliability index $\beta$ is estimated as: $\beta = \phi^{-1}(Pf)$

6. If the calculated reliability index ($\beta$) is different from the selected target reliability index ($\beta_T$), the trial resistance factor ($\phi$) in step 1 should be changed and iteration needs to be done until $|\beta - \beta_T| <$ tolerance (0.01 in this study).

The required number of Monte Carlo trials is based on achieving a particular confidence level for a specified number of random variables and is not affected by the variability of the random variables *[66, 67, 68]*. Using the procedure described by Harr, the number of Monte Carlo trials required for a confidence level of 90% in this study is approximately 4,500 *[66]*. For the probabilistic calculations reported in this study, Monte Carlo simulations with 50,000 trials are performed.

**First Order Second Moment Method (FOSM).** FOSM is easy to use and valid for preliminary analyses, it is preferable to use advance calibration method that is described earlier such as FORM and Monte Carlo simulation method. In the FOSM method, limit state function is linearized by expanding the Taylor series expansion about the mean value of variable. Since only the mean and variance are used in the expansion, it is called first-order, second variance moment. For lognormal distribution of resistance and local statistics, Barker et al. suggested the following relation for calculating reliability index *[69]*:

$$\beta = \frac{\ln\left[\lambda_n FS\left(\frac{\frac{Q_{DL}}{Q_{LL}}+1}{\lambda_{DL}\frac{Q_{DL}}{Q_{LL}}+\lambda_{LL}}\right)\sqrt{\frac{1+COV^2_R+COV^2_{DL}+COV^2_{LL}}{1+COV^2_R}}\right]}{\sqrt{\ln[(1+COV^2_R)(1+COV^2_{DL}+COV^2_{LL})]}} \quad (23)$$

For LRFD, this equation is modified by replacing overall factor of safety by partial factor of safety and then rearranging to express the relation for resistance factor ($\phi$) as follows ($\beta_T$ is the target reliability index):

$$\phi = \frac{\lambda_R\left(\gamma_{DL}\frac{Q_{DL}}{Q_{LL}}+\gamma_{LL}\right)\sqrt{\frac{1+COV^2_{DL}+COV^2_{LL}}{1+COV^2_R}}}{\left(\lambda_{DL}\frac{Q_{DL}}{Q_{LL}}+\lambda_{LL}\right)\exp\left(\beta_T\sqrt{\ln\left[(1+COV^2_R)(1+COV^2_{DL}+COV^2_{LL})\right]}\right)} \quad (24)$$

In order to incorporate $\phi_{set\text{-}up}$ in LRFD strength limit state equation Ng et al. proposed a limit state equation in his developed formulation *[17]*. This formulation was used to calibrate the $\phi_{set\text{-}up}$ for FOSM method *[61]*. The detail procedure of developing this formulation can be found on Ng and Sritharan *[17]*. Here are the summary of the steps:

1. Reliability index ($\beta$) for set-up can be calculated due to set-up as:

$$\beta = \frac{\ln\left(\frac{\lambda_{R_{EOD}}R_{EOD}+\lambda_{R_{set-up}}R_{set-up}}{\lambda_{QDQ}}\right)+\ln\left(\sqrt{\frac{1+COV^2_{Q_{DL}}+COV^2_{Q_{LL}}}{1+COV^2_{R_{EOD}}+COV^2_{R_{set-up}}}}\right)}{\sqrt{\ln[(1+COV^2_{R_{EOD}}+COV^2_{R_{set-up}})(1+COV^2_{Q_{DL}}+COV^2_{Q_{LL}})}} \quad (25)$$

2. Replacing $\phi R$ in the LRFD limit strength equation and the $R_{set\text{-}up}$ can be rearranged as:

$$R_{set\text{-}up} = \frac{\gamma_{DL}Q_{DL}+\gamma_{LL}Q_{LL}-\phi_{EOD}R_{EOD}}{\phi_{set-up}} \quad (26)$$

3. Replacing the equation (26) on equation (25) and rearranging the equation as:

$$\phi_{set\text{-}up} = \frac{\lambda_{set-up}[\gamma_{DL}Q_{DL}+\gamma_{LL}Q_{LL}-\phi_{EOD}R_{EOD}]}{\frac{(\lambda_{DL}Q_{DL}+\lambda_{LL}Q_{LL})e^{\beta\sqrt{\ln[(1+COV^2_{R_{EOD}}+COV^2_{R_{set-up}})(1+COV^2_{Q_{DL}}+COV^2_{Q_{LL}})]}}}{\sqrt{\frac{(1+COV^2_{Q_{DL}}+COV^2_{Q_{LL}})}{(1+COV^2_{R_{EOD}}+COV^2_{R_{set-up}})}}} - \lambda_{EOD}R_{EOD}}$$

By normalizing the above equation by $Q_{DL} + Q_{LL}$ and replacing $\alpha = \frac{R_{EOD}}{Q_{DL}+Q_{LL}}$, the final equation of pile set-up yields to for FOSM method as:

$$\phi_{set\text{-}up} = \frac{\lambda_{set-up}[\frac{\gamma_{DL}\frac{Q_{DL}}{Q_{LL}}+\gamma_{DL}}{1+\frac{Q_{DL}}{Q_{LL}}} - \phi_{EOD}\alpha]}{\frac{\left(\frac{\lambda_{DL}\frac{Q_{DL}}{Q_{LL}}+\lambda_{LL}}{1+\frac{Q_{DL}}{Q_{LL}}}\right)e^{\beta\sqrt{\ln[(1+COV^2_{R_{EOD}}+COV^2_{R_{set-up}})(1+COV^2_{Q_{DL}}+COV^2_{Q_{LL}})]}}}{\sqrt{\frac{(1+COV^2_{Q_{DL}}+COV^2_{Q_{LL}})}{(1+COV^2_{R_{EOD}}+COV^2_{R_{set-up}})}}} - \lambda_{EOD}\alpha}$$

However, in the above equation $\phi_{EOD}$ is replaced with $\phi_{14}$ and the equation becomes:

$$\phi\text{set-up} = \frac{\lambda_{\text{set-up}}\left[\frac{\gamma_{DL}\frac{Q_{DL}}{Q_{LL}}+\gamma_{DL}}{1+\frac{Q_{DL}}{Q_{LL}}} - \phi_{14}\alpha\right]}{\left(\frac{\lambda_{DL}\frac{Q_{DL}}{Q_{LL}}+\lambda_{LL}}{1+\frac{Q_{DL}}{Q_{LL}}}\right)e^{\beta\sqrt{\ln\left[(1+COV^2_{REOD}+COV^2_{Rset-up})(1+COV^2_{QDL}+COV^2_{QLL})\right]}}}{\sqrt{\frac{(1+COV^2_{QDL}+COV^2_{QLL})}{(1+COV^2_{REOD}+COV^2_{Rset-up})}}} - \lambda_{14}\alpha \quad (27)$$

## Laboratory and In-situ Tests

The main objective of this study was to evaluate the pile set-up for individual soil layers and correlate the increase of side resistance (i.e., pile set-up) of individual soil layers with different soil properties (e.g., undrained shear strength, PI, coefficient of consolidation, sensitivity, overconsolidation ratio). To achieve this, laboratory tests were conducted on the collected soil samples in all the investigated sites and in-situ field tests were performed to determine the different soil properties.

### Laboratory Tests

High quality 3-in. Shelby tube samples were retrieved from boreholes at different depths for comprehensive laboratory testing from each test pile location. Water content, unit weight, Atterberg limits and grain size distribution were performed to characterize the subsurface soils. One-dimensional consolidation tests were also conducted to obtain the vertical coefficient of consolidation ($c_v$) and overconsolidation ratio (OCR). Unconsolidated undrained (UU) triaxial tests were performed to estimate the undrained shear strength ($S_u$) of the soils. Small scale laboratory vane shear tests were performed in order to evaluate the sensitivity ($S_t$) of the soil.

### In-situ Tests

The in-situ testing program included both piezocone penetration tests (PCPT) and piezocone dissipation tests. The PCPT is capable of measuring the cone tip resistance ($q_c$), sleeve friction ($f_s$), and pore pressures at different locations, depending on the location of the pressure transducer [at the cone face ($u_1$), behind the base ($u_2$), or behind the sleeve ($u_3$)]. The profile of PCPT tests was used to classify the soil using the Zhang and Tumay probabilistic region estimation method and to evaluate the $S_u$ and over consolidation ratio (OCR) of soil layers *[70]*. The $S_u$ was calculated from PCPT using the equation (28)

$$S_u = (q_t - \sigma_{vo})/N_k \quad (28)$$

with $N_k$ =15 in this study; and the OCR was calculated using the equation (29) proposed by Abu-Farsakh *[71]*:

$$OCR = 0.152\ [(q_t - \sigma_{vo})/\sigma'_{vo}] \quad (29)$$

where, $q_t$ is the corrected tip resistance, $\sigma_{vo}$ is the overburden pressure, and $\sigma'_{vo}$ is the effective overburden pressure.

The soil permeability ($k_h$) was calculated using the equation (30) proposed by Robertson *[72]*:

$$\text{Permeability } (k_h) = c_h \gamma_w / M \quad (30)$$

where, M = 1-D constrained modulus, and $\gamma_w$ = unit weight of water. The constrained modulus (M) was calculated using the equation (31) proposed by Abu-Farsakh *[71]*:

$$M = 3.15\ q_t. \quad (31)$$

The penetration of the piezocone was stopped at pre-specified penetration depths to perform piezocone dissipation test (PDT) with respect to time. The dissipation test plots were used to calculate the horizontal coefficient of consolidation ($c_h$) based on the Teh and Houlsby interpretation method *[73]*. The $c_h$ is then converted to vertical coefficient of consolidation ($c_v$) based on the range of anisoptropic hydraulic conductivity ($k_h/k_v$) of clayey soils.

## Instrumentation

The goal of this research study is to investigate set-up phenomenon by individual soil layers and correlate with different soil properties, hence an instrumentation plan was adopted in all the projects. Sisterbar strain gages were installed in all the test piles of all projects. The test piles of Bayou Zourie and Bayou Lacassine sites were instrumented with pressure cells and piezometers. Multilevel soil piezometers were also installed in the surrounding soils of the pile. A detailed instrumentation plan was adopted in all the projects after characterizing the subsurface soil with laboratory and in-situ soil tests. Instrumentations were placed in all the piles three to four weeks prior to pile driving in the pile casting yard.

### Strain Gages

Sisterbar strain gages were installed in all the test piles of all projects in order to measure the distribution of side resistance along the length of the test pile during the static load test and hence calculate the side ($R_s$) and tip ($R_{tip}$) resistances, separately. Furthermore, load distribution plots were calculated and used to calculate the side resistance of individual soil layers. Vibrating wire "sister bar" strain gages (Geokon Model 4911) were chosen for this study. Strain gages were installed in pairs on opposite sides of the pile as simply attached to the side of a section of rebar at each depth and their average readings were adopted for analysis in order to eliminate the possibility of bending stress. Figure 4a shows the installation procedure of strain gages in the pile at the casting yard.

**Pressure Cells**

Pressure cells were installed at certain locations (i.e., mainly in the clayey soil layer) along the pile (flush with pile surface) to measure the total lateral stress history during the whole testing period. Vibrating wire pressure cells (Geokon Model 4820 "jack-out" style) were chosen in this study. Figure 4b shows the photo of pressure cell that was installed in the pile.

**Piezometers**

Piezometers were installed in the soil-pile interface to measure the buildup and dissipation of excess PWPs with time. The dissipation of excess PWP allowed to establish a correlation between increase in pile resistance and dissipation of excess PWP (or consolidation) or change in effective stress with time along the pile shaft. Vibrating wire piezometer (Geokon model 4500S) were used in this study. Piezometers were installed in pairs with pressure cells at the same location. The piezometers were deaired and saturated in the field, prior to pile driving, using a vacuum pump. To keep the piezometers saturated, the PVC cap, as shown in Figure 4b, stayed on the pile face until they hit the ground and got snapped off during pile driving.

**Multilevel Piezometers**

The soil surrounding the pile was instrumented with piezometers to be arranged at different distances and different depths from the pile surface. Vibrating wire multilevel piezometers (Geokon Model 4500M) was used in this study. The soil piezometers was used to measure the magnitude and extend of buildup pore water presure, characterized the excess pore water disspation curves of the surrounding soil with time and evaluated the extend of influence zone around the pile. Figure 4c shows a photo of the multilevel piezometer that was used in this study.

**Data Acquisition System.** In order to fully capture and record the variation of earth pressure, PWPs and the measured side resistance of individual soil layers along the pile length with time, the instrumentations were setup for collecting the data continuously starting immediately before pile driving until the last restrike. Continuous recordings were performed to fully record the variation of PWP and collect the strain gage readings during the static load test. During these periods, a data acquisition system of CR-1000 with a solar panel was used for recording the data as shown in Figure 4d.

**Accelerometers and Strain Transducers.** Dynamic measurements were obtained by attaching pairs of strain transducers and accelerometers near the top of the pile prior to pile driving and every restrike event (Figure 4e). The responses of accelerometers and strain transducers were monitored thorough pile driving analyzer (PDA).


(a) Sister bar Strain gages

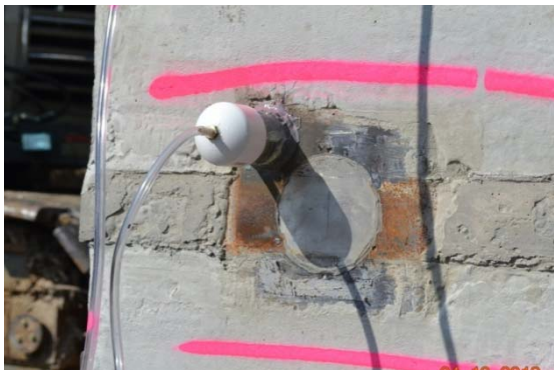

(b) Piezometer and Pressure cell


(c) Multilevel Piezometer

(d) Data acquisition system

(e) Installation of accelerometer and strain transducer

**Figure 4**
**Photos of the instruments**

## Load Test

For measuring the pile set-up, it is essential that the pile resistance should be determined at two different time intervals. However, the timings and methods of resistance measurement are very significant, as the value of the information obtained and the conclusions can differ with time and method. There are several methods available to measure the pile resistance: dynamic load test, static load test, and osterberg cell load test.

### Dynamic Load Test (DLT)

The DLT with a Pile Driving Analyzer (PDA) was conducted in all the test piles of all projects during driving and at different times following EOD in order to measure the pile resistance. The test was conducted according to ASTM D-4945 [*74*]. The pile was instrumented with one pair of accelerometer and one pair of strain transducer and connected to a portable digital microcomputer before performing the test. A simple pile model (CASE model) was applied on the collected data in the field to predict the combined tip and side resistances. The data was further analyzed using the CAPWAP (Case Pile Wave Analysis Program) to calculate the distribution of side resistance along the pile length.

### Static Load Test (SLT)

The SLT is a full scale test that was mainly performed in this study to measure the ultimate pile resistance. The test was performed following the procedure described by ASTM D1143 *[75]*. SLT is expensive and required more time to perform compared to the DLTs. A reaction frame needs to be designed and constructed in order to perform the SLT. The reaction frame normally consists of sixteen pipe piles, hydraulic jack and a diagonal beam. Figure 5 shows a typical load frame arrangement that was used in Bayou Lacassine project. The usual practice of DOTD to perform the SLT is at 14 days after EOD.

### Osterberg Cell Load Test (OCLT)

The Osterberg cell (O-cell) instrumented at the tip in order to perform the load test on the pile. The O-cell is a cylindrical hydraulic jack that is used to load the soil below the pile tip taking the pile's side resistance as a reaction. As a result, the pile side is loaded upward using the tip resistance of the soil as a reaction. Since both the side and tip resistances were used as reactions to test each other, the Osterberg cell load test worked as a full-scale proof test to either the tip resistance or the side resistance, depending on which one fails first.

**Figure 5**
**Load frame arrangement for TP-2 at Bayou Lacassine site**

## Investigated Sites

Five different sites were selected in Louisiana to perform the pile set-up study: Bayou Zourie, Bayou Lacassine, Bayou Teche, Bayou Bouef, and LA-1. The other sites with sufficient pile set-up and soil information (Appendix-A) are selected for verification of the developed model. Brief descriptions of these five sites with the test pile information, instrumentation plan and laboratory test results are discussed below:

### Bayou Zourie Site

The project consisted of constructing a two-lane highway bridge on the northbound lane of U.S.171 over Bayou Zourie in Vernon Parish of Louisiana. The existing bridge required

replacement due to substandard load carrying capacity and embankment protection is severely undermined. Square prestressed concrete (PSC) pile foundations having a width of 24 in. were selected to support the bridge structure and abutment retaining wall. The photo of the bridge site is depicted in Figure 6a.

**Test Pile.** The test pile was a square, nominally 24 in. wide, 55 ft. long, PSC pile (Figure 6b). The embedment depth of the pile is 50 ft. The design scour depth was estimated to be 20 ft. and the diameter of the pre-bored hole was 44 in. As such, the test pile location was pre-augered to a depth of 20 ft. The pile was driven to the design depth of 50 ft. below the ground surface, using an ICE I-46 open-end diesel hammer. This hammer had a ram weight of 10,145 lbs. and a rated energy of 107,700 ft-lb.

(a) Construction site (b) Test Pile

**Figure 6**
**Bayou Zourie bridge site**

**Geotechnical Conditions.** The test site was characterized using Standard Penetration Tests (SPT), Piezocone Penetration Tests (PCPT). Laboratory triaxial and one dimensional consolidation tests were also performed on undisturbed samples. A soil boring log, along with PCPT data are presented in Figure 7. The liquid limit (*LL*), *PI*, particle size distribution, $S_u$, SPT *N*-values, and $c_v$ are also shown in Figure 7. The detail description of the subsurface soil condition can be found in Chen et al. and Haque *[23, 76]* The subsurface conditions consist of layers of loose to medium sand and silty sand with occasional clayey pockets to a depth of 17 ft. A medium to dense sand exists between 17 ft. and 33 ft. The pile is terminated in a stiff clay that underlies the sand. The SPT number of the sand layers varies from 2 to 25 and the $S_u$ of the clay layers ranges from 2.9 to 7.1 ksf (from UU test) and 3.2 to 10.2 ksf (estimated from CPT). The groundwater level is about 4 ft. below the ground surface. The results of PCPT dissipation tests

at different depths are shown in Figure 8. Based on the dissipation tests, the values $c_h$ were estimated using the Teh and Houlsby method with $t_{50}$ *[73]*.The values of $c_v$ were ranging from 0.0012 to 0.012 $in^2$/min. The values of $c_v$ estimated from one dimensional consolidation tests on shelby tube soil samples at different depths are also presented in Figure 7, with values range from 0.002 to 0.006 $in^2$/min, which are in agreement with the values estimated from dissipation tests.

**Instrumentation Plan.** To characterize the change in pile resistance with time, an instrumentation plan, which included earth pressure cells, piezometers, and "sister bar" strain gages was developed and implemented. Figure 9 shows the instrumentation plan that was implemented for the test pile and in the surrounding soil. Vibrating wire pressure cells and piezometers were installed at four locations along the test pile 25, 35, 40, and 45 ft. below the ground surface. The pressure cells and piezometers were installed in pairs to measure the horizontal effective stress acting on the pile face. Vibrating wire "sister bar" strain gages were installed in pairs at each level (i.e. two per level) along the pile at depths of 1, 15, 20, 25, 33, 40, 45, and 48 ft. below ground surface. They provided strain measurements near the pile tip and at/near soil layer boundaries established from the boring log. As such, it is possible to evaluate the pile side shear set-up for each soil layer along the pile length. Nine vibrating wire multilevel piezometers were installed one week before pile installation at three distances (1B, 2B, and 4B from the pile face, where B is the width of the pile) and three depths (35, 40, and 45 ft. below the ground surface) to measure the PWP distribution in the ground to help determine the disturbed zone of soil due to pile driving. Each multilevel piezometer was deaired and saturated prior to installation.

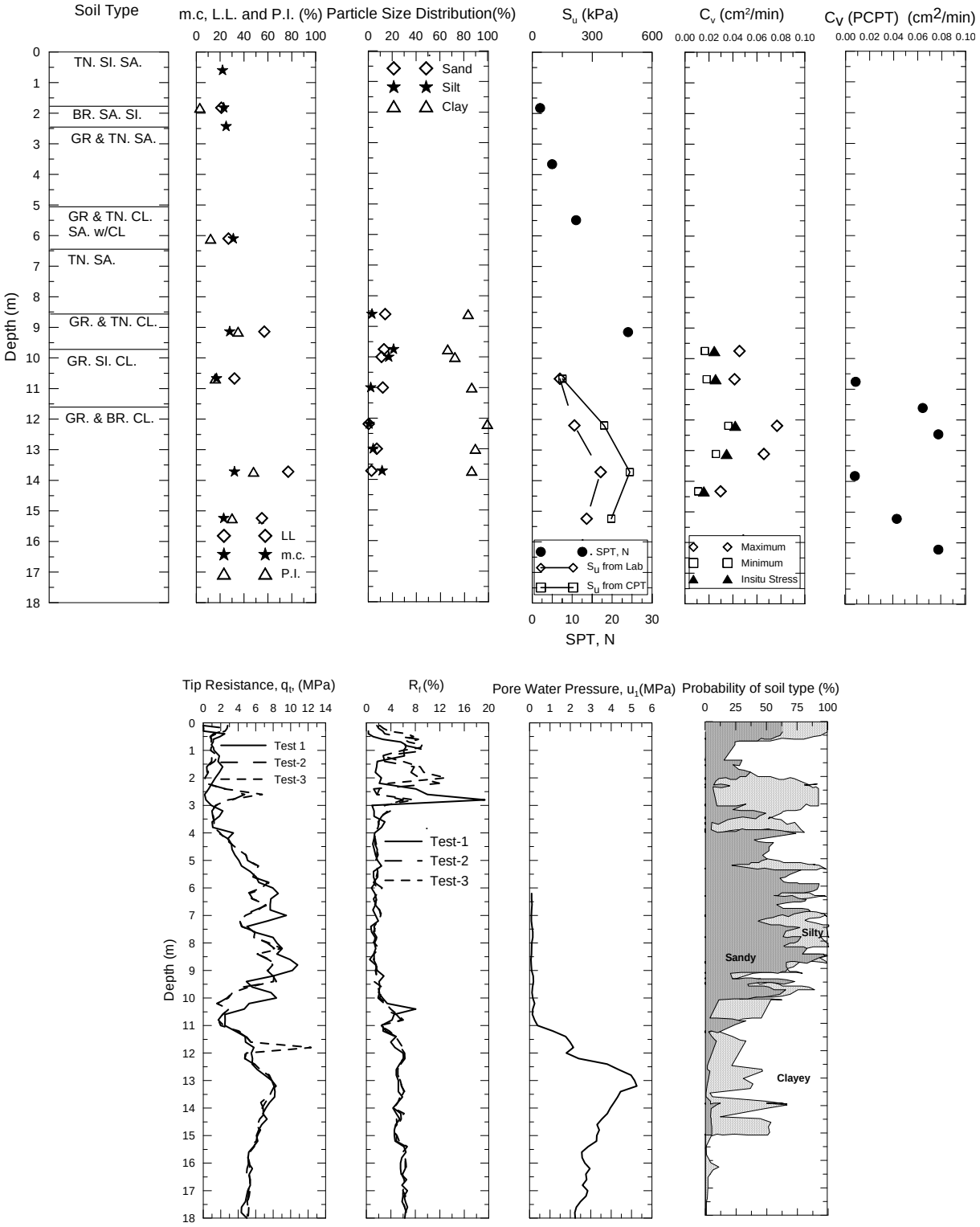


**Figure 7**

**Soil boring and PCPT soil classification at test pile location of Bayou Zourie site**

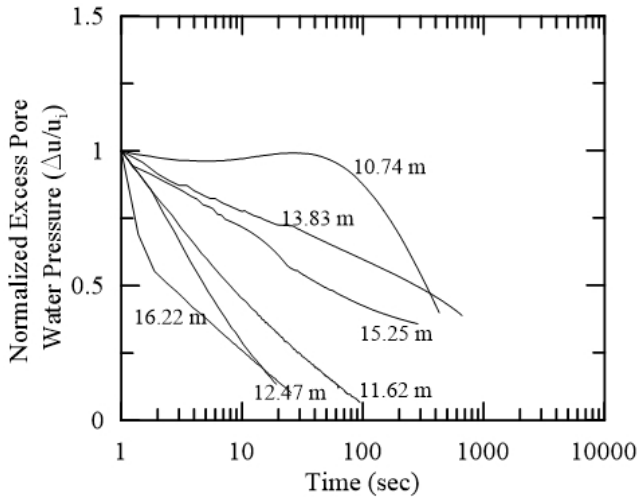


**Figure 8**
**Dissipation test results of test pile location of Bayou Zourie site**

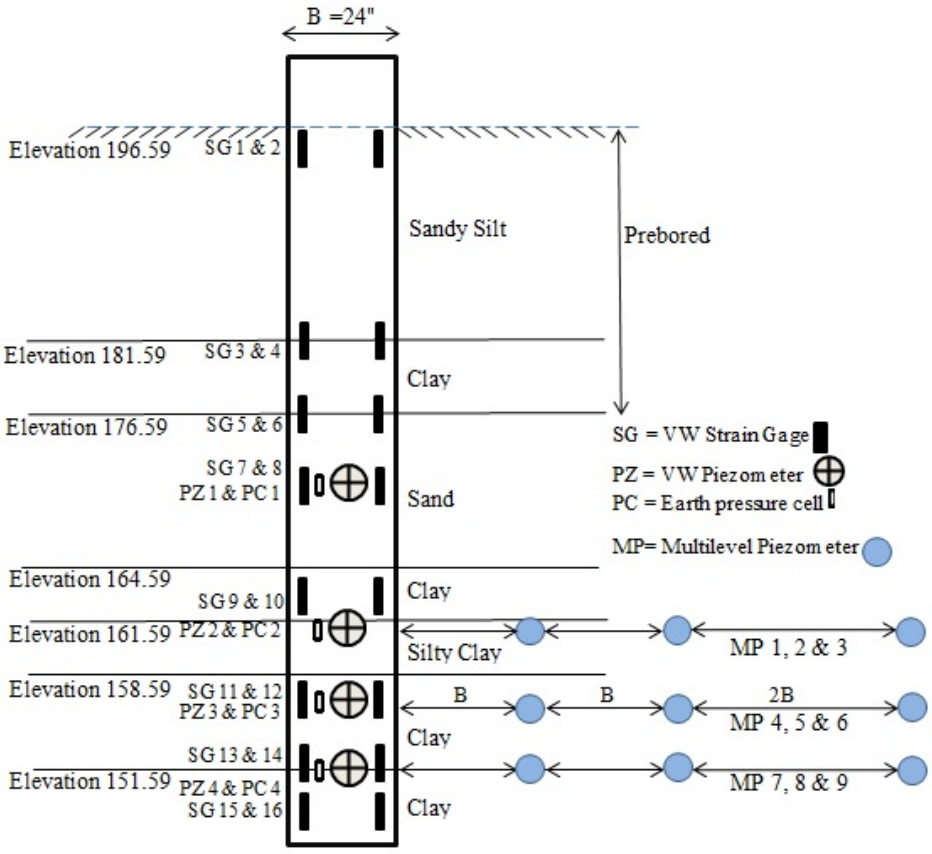


**Figure 9**
**Instrumentation plan for the test pile of Bayou Zourie site**

**Bayou Lacassine Site**

Louisiana DOTD replaced the old Bayou Lacassine Bridge on Highway 14 in Jefferson Davis Parish, Louisiana. The new bridge was built with PSC piles supported by concrete bents. The bridge was approximately 1920 ft. in length and it consisted of two end bents and sixteen intermediate piers, which were supported by a total 152 square PSC piles. The photos of Bayou Lacassine bridge site are shown in Figure 10a. The detail description of the bridge site can be found in Haque et al. *[77]*.

**Test Pile.** Three test piles were installed in order to verify the design and for research purposes. Two test piles: Test Pile-1 (TP-1) and Test Pile-3 (TP-3) were instrumented and driven on each side of the new bridge. Test Pile-2 (TP-2) was driven in the middle of waterway between TP-1 and TP-3 and was not instrumented due to inaccessibility of data collection. All of the test piles were close ended square PSC piles with 30 in. width. A circular void of 16.5 in. diameter ran from 8 ft. below the top of the pile to 5 ft. above the base of the pile (Figure 10b). The total length of TP-1, TP-2, and TP-3 were 75 ft., 82 ft., and 75 ft., respectively. The test piles TP-1, TP-2, and TP-3 were driven to an embedment depth of about 67 ft., 75 ft., and 67 ft., respectively. An oversized casing of 36 in diameter with length equal to scour depth was installed at each test pile location. The casings' installation depths were 21 ft., 18 ft., and 21 ft. for TP-1, TP-2, and TP-3, respectively. The test piles were driven using an I62V2 diesel impact hammer. The hammer had the ram weight of 14,600 lbs and rated stroke energy 165,000 ft.-lbs.

(a) Construction site

(b) Casing

**Figure 10**
**Bayou Lacassine bridge site**

**Geotechnical Conditions.** Laboratory and in-situ testing programs were performed to characterize the subsurface soil conditions at the locations of the test piles. Boreholes were drilled at the three test pile locations and high-quality 3-in. Shelby tube samples were extracted at different depths for comprehensive laboratory testing. The laboratory soil classification tests for TP-1, TP-2, and TP-3 are depicted in Figure 11, Figure 12, and Figure 13, respectively. The in-situ testing program included performing both PCPT and PDTs near the test pile locations. Figure 14a and Figure 14b depict the piezocone dissipation tests obtained at TP-1 and TP-3 locations, respectively. The $c_h$ was calculated from piezocone dissipation tests using Teh and Housby method *[73]*. The PCPT provided measurements of cone tip resistance ($q_c$) and sleeve friction ($f_s$). The profile of PCPT tests was used to classify the soil using the Zhang and Tumay probabilistic region estimation method and to evaluate the $S_u$ and over consolidation ratio (OCR) of soil layers *[70]*. The laboratory and in-situ PCPT test in the project site revealed the subsurface soil conditions for TP-1, TP-2 and TP-3 location as follows:

TP-1: The subsurface soil profile at the test pile location consisted of soft to medium soft clay down to 26 ft. Underneath it, there was a layer of silty clay with sand pockets from 26 ft. to 43 ft. followed by a medium to stiff clay with lenses of silt down to 69 ft. The soil boring, laboratory test results, CPT profiles and CPT soil classification of TP-1 location are presented in Figure 11.

TP-2: It was revealed that the subsurface soil condition at the TP-2 location consisted of mainly medium to stiff silty clay to clayey soil with small silt and sand pockets down to about 52 ft. with some lenses of silt 23 ft. to 29 ft. A sandy layers lies from 54 ft. to 59 ft. with traces of silt. Below that, soft to medium clay with interlayers of silt was found between 59 ft. to 69 ft. The soil boring, laboratory test results, CPT profiles, and CPT soil classification of TP-2 location are presented in Figure 12.

TP-3: The soil boring and CPT profile show that the profile consisted of soft to medium brown lean clay down to 36 ft., which was underlain by gray fat silty clay layer 36 ft. to 48 ft. This is followed by medium to stiff sandy clay layer interbedded with lenses of silt down to about 69 ft. The soil profile, laboratory test results, CPT profiles, and CPT soil classification of TP-3 location are presented in Figure 13.

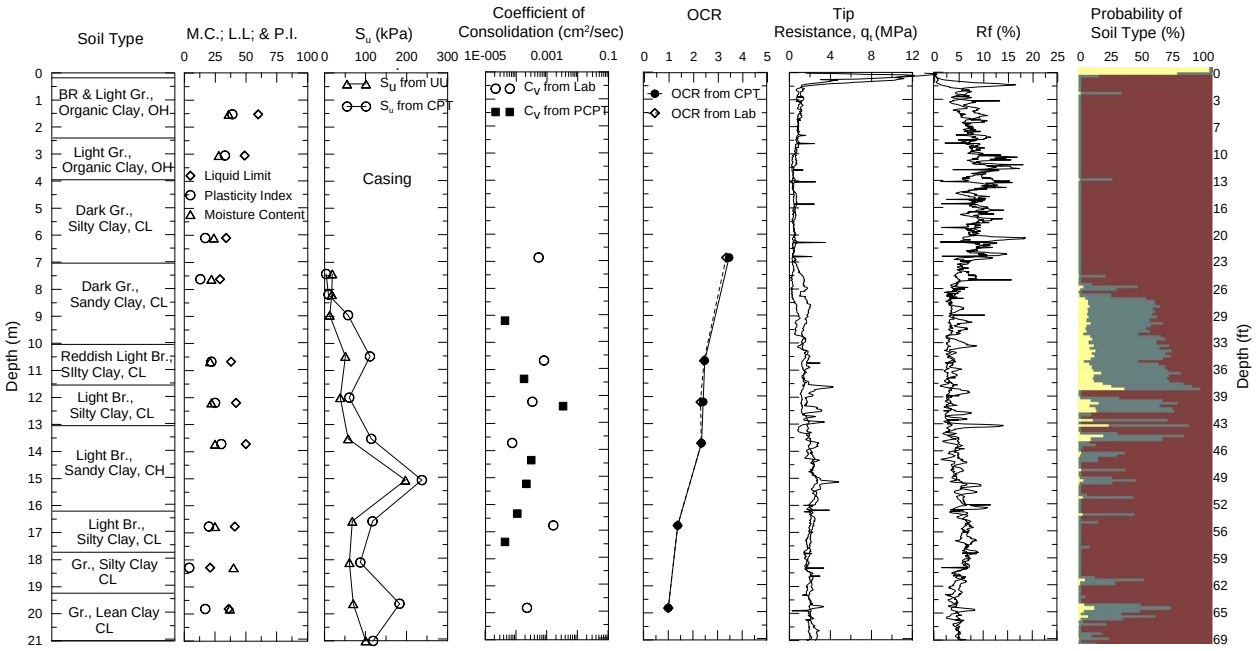


**Figure 11**

**Soil boring and PCPT soil classification at TP-1 location of Bayou Lacassine site**

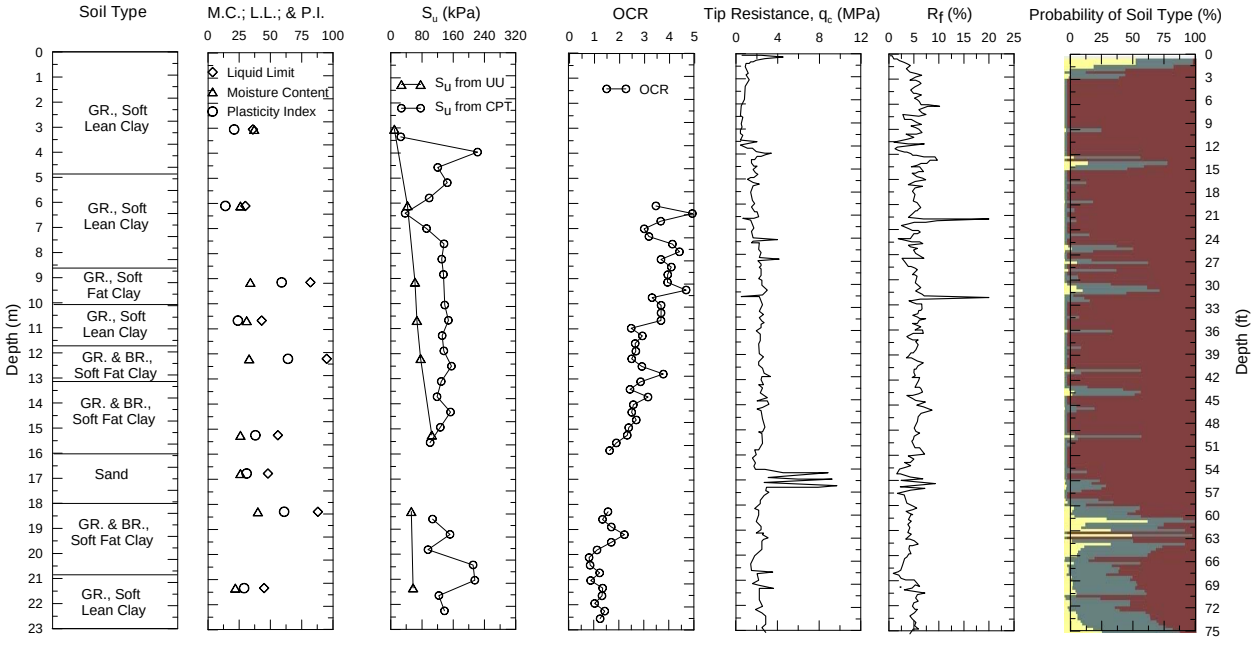


**Figure 12**

**Soil boring and PCPT soil classification at TP-2 location of Bayou Lacassine site**

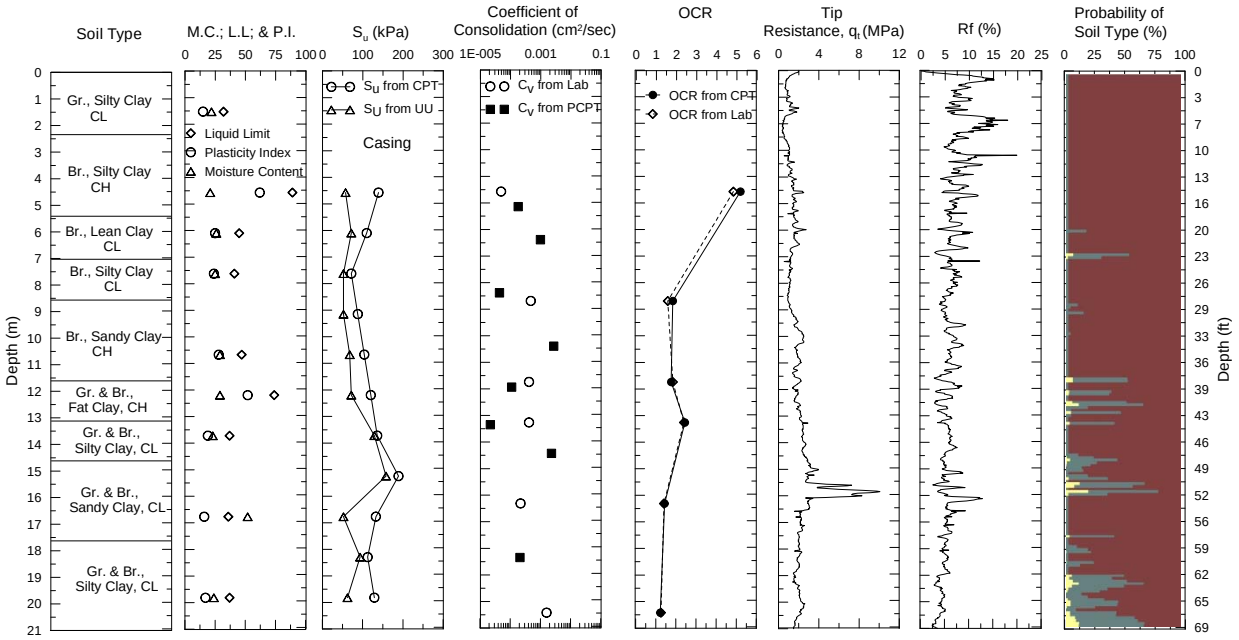


**Figure 13**
**Soil boring and PCPT soil classification at TP-3 location of Bayou Lacassine site**

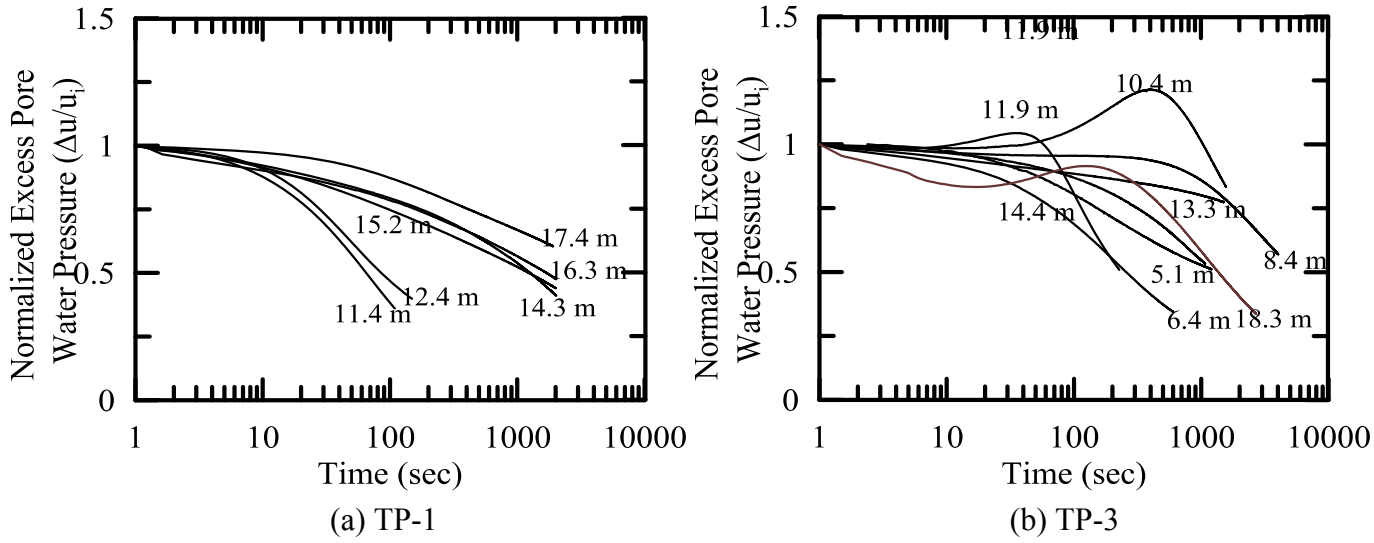


**Figure 14**
**Dissipation test results at test pile locations of Bayou Lacassine site**

**Instrumentation Plan.** The instrumentation plan of the TP-1 and TP-3 of Bayou Lacassine bridge site are depicted in Figure 15a and Figure 15b, respectively. In order to measure the side

resistance for each soil layer along the piles' length during the SLTs, TP-1 and TP-3 were instrumented in pairs with sixteen vibrating wire strain gages located at eight different depths below the ground surface as shown in Figure 15. Four sets of vibrating wire pressure cells and piezometers were installed in TP-1 and TP-3 faces to measure the total earth pressure, excess PWP, and hence the effective stress with time. In addition, nine multilevel piezometers of vibrating wire type were installed in the surrounding soil to measure the spatial distribution of excess PWP induced by pile driving. They were placed at three different depths and three different distances from the face of test piles, designated as MP-1 to MP-9 in Figure 15. The selected distances were 1B, 2B, and 3B from the face of the test pile, with B being the pile width. In order to fully capture and record the variation of earth pressure, PWPs and the measured side resistance of individual soil layers along the length of pile with time, the instrumentations were setup for collecting the data continuously starting immediately before pile driving until the last restrike. During these periods, a data acquisition system with a solar panel was used for recording the data.

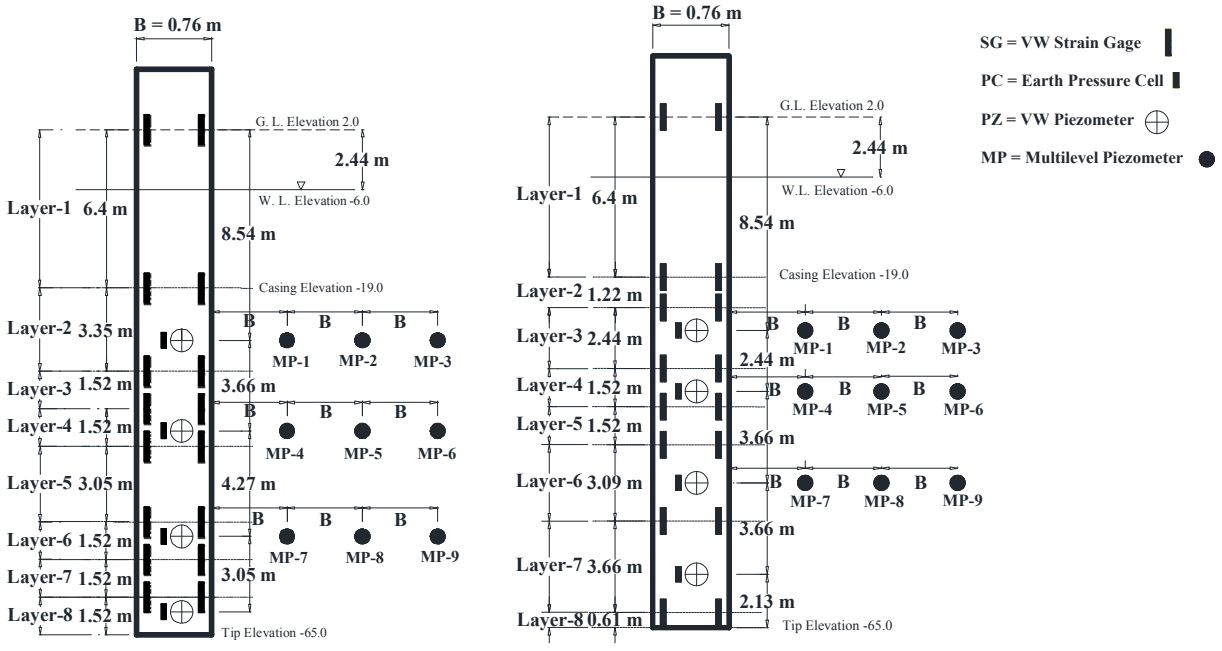


(a) Test Pile-1 (TP-1)

(b) Test Pile-3 (TP-3)

**Figure 15**
**Instrumentation plan for the test piles of Bayou Lacassine site**

**Bayou Teche Site**

This project located in New Iberia on LA 3156 and replaced the existing Jefferson street bridge over Bayou Teche. The new structure composed of a wider more decorative bridge and sidewalk which is providing the service for traveling public to and from the downtown area. The total length of the bridge is 212 ft**.** Figure 16 shows a photo of the Bayou Teche bridge site.

**Figure 16**
**Bayou Teche bridge site**

**Test Pile.** The test pile was 24-in. square PSC pile with 64 ft. in length. The penetration depth of the pile was 60 ft. The pile was driven with the aid of the hammer ICE-I-36. The test pile was not instrumented due to the conflict of construction schedule with the delivery of the instrumentation.

**Geotechnical Conditions.** Laboratory testing programs were performed to characterize the subsurface soil conditions at the location of the test pile. It was revealed that the subsurface soil condition at the test pile location consisted of mainly brown lean clayey soil down to about 34 ft. followed by brown sandy silt soil up to 40 ft. A brown color sand layers lied from 40 ft. to 52 ft. with traces of silt. Below that, gray sand was found between 52 ft. to 60 ft. The soil boring, laboratory test results at test pile location are presented in Figure 17.

.

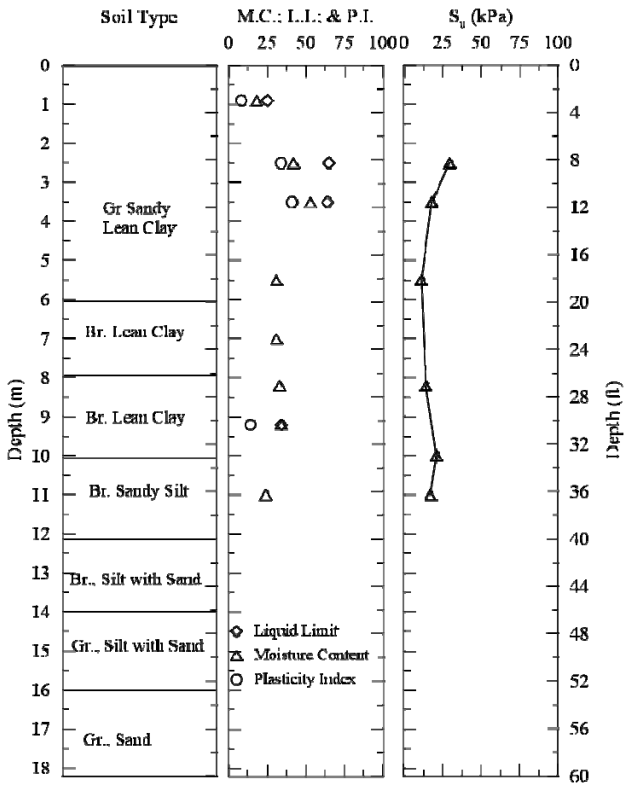


**Figure 17**
**Soil boring at test pile location of Bayou Teche site**

**Bayou Bouef Site**

The long-term pile set-up study was conducted during the construction of the Bayou Bouef bridge extension on relocated U.S. 90, east of Morgan City, Louisiana. The maximum design pile load was typically 163 tons. Plan pile lengths ranged from 125 to 150 ft. long. The long term pile set-up study was conducted next to TP-3 of this project between pile bents 210 and 211.

**Test Pile.** An instrumented 30-in. square PSC pile was driven in the Bayou Bouef bridge site to perform this set-up study. The total length of the pile was 142 ft. The pile was driven to the design depth of 130 ft. below the ground surface, using a HPSI 2005 hammer.

**Geotechnical Conditions.** The subsurface conditions were characterized during the pre-design phase of the project by taking soil borings. Extensive laboratory and in-situ testing programs were performed to characterize the subsurface soil conditions at the test pile location. The subsurface soils consisted of normally consolidated soft to medium clays to approximately elevation -124 ft. followed by medium to dense sand. A 12 ft. layer of loose to medium sand was found at elevation -60 ft. The soil profile at test pile location is shown in Figure 18.

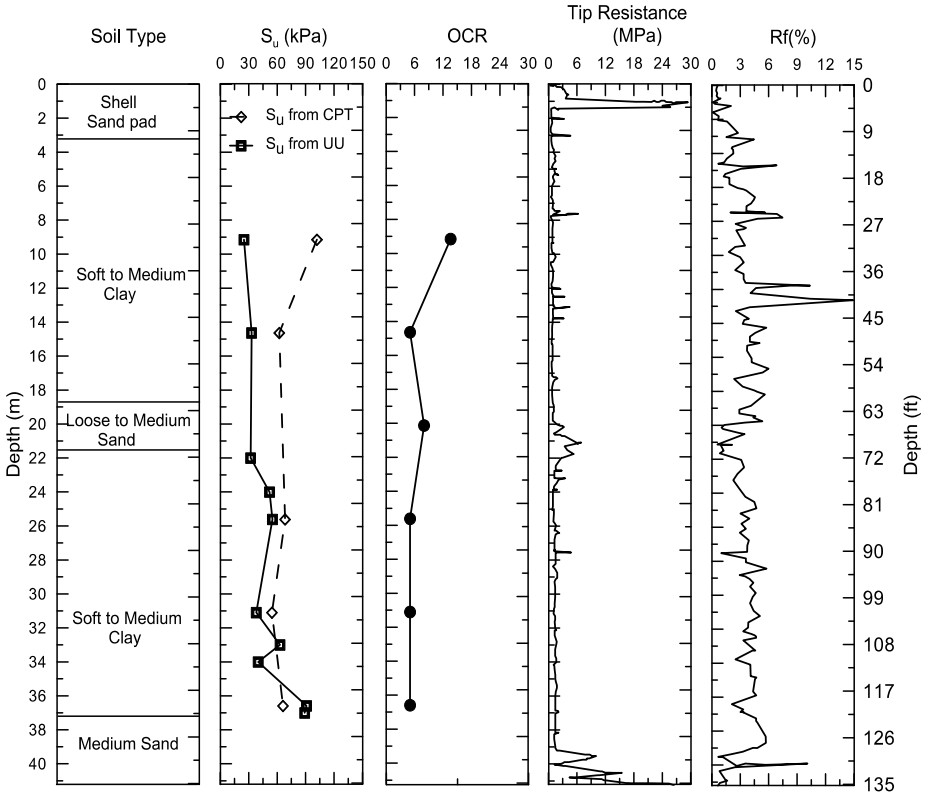


**Figure 18**

**Soil boring and CPT soil classification at test pile location of Bayou Bouef site**

**Instrumentation Plan.** The instrumented test pile was fabricated at Gulf Coast Pre-Stress, Inc. DOTD and Loadtest, Inc. personnel supervised the fabrication and assisted in the installation of instrumentation of the Osterberg Cell in the test pile. An Osterberg Cell (O-Cell) was cast at the tip of the pile. Tell-tale pairs were attached to the bottom plate of the O-Cell and above the top of the O-Cell to measure the relative movement of the top and bottom of the O-Cell as the O-Cell is expanded during load testing. The pile was also instrumented with 16 vibrating wire strain gages placed in diametrically opposed pairs at 8 different levels as shown in Figure 19.

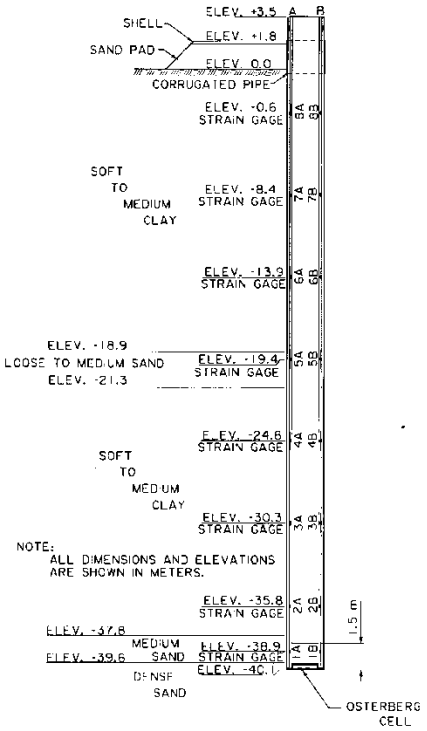


**Figure 19**
**Instrumentation plan for test pile of Bayou Bouef site**

**LA-1 Site**

An elevated highway between Golden Meadow and Port Fourchon was constructed to replace the previously existing LA-1 highway. This project involved the construction of approximately 17 miles of access-controlled, elevated roadway consisting of low-level and medium-level bridges, two elevated interchanges, and one fixed high-level bridge over Bayou Lafourche. A pre-design pile load testing program was performed on various sizes and types of piles at four different locations along the project alignment. The four locations represented the northern mid-level bridge, the high-level Bayou Lafourche crossing, the south connector, and the low-level bridge segment. Figure 20 shows the photo of TP-2 and TP-3 locations of LA-1 site.

(a) Test site 2

(b) Test site 3

**Figure 20**
**LA-1 bridge site**

**Test Pile.** Nine test piles were driven at four different locations along the LA-1 project. These test piles consisted of six different sizes of PSC piles, two 54-in. spun cast cylinder piles and one 30-in. open-ended steel pipe pile. At the location of TP-2, one PSC 16-in. square and 130-ft. long solid PSC pile was tested in addition to a 54-in. diameter concrete spun-cast cylinder pile. The PSC pile at the location of TP-3 has a lateral dimension of 30-in. and 190 ft. length with a 16.5-in. diameter void. One 30-in. diameter steel pipe pile and 195 ft. in length was installed here. Another 54-in. diameter cylindrical pile with 160 ft. in length was installed in this location. Two piles were installed close to each other at two test piles locations (TP-4 and TP-5). The test piles of same size and type (24-in. PSC piles) were installed at 10 ft. apart within a very short period of time. At the location of TP-4, TP-4a and TP-4b were 160 ft. and 210 ft. long, respectively. At the location of TP-5, the test consisted of two 24 in. PSC piles with 145 ft. and 170 ft. in lengths. All of the piles at TP-4 and TP-5 locations had a 10.5-in diameter void in center. Table 2 presents the details of the test piles for LA-1 project.

**Geotechnical Conditions.** Extensive laboratory and in-situ testing programs were performed to characterize the subsurface soil conditions at each of the test pile locations. Boreholes were drilled at each test pile location and in-situ testing program such as piezocone penetration tests (PCPT) were performed. The Zhang and Tumay probabilistic region estimation method was used to classify the subsurface soils *[70]*. The soil stratification from soil borings and their associated results of laboratory tests, in addition to tip resistance ($q_c$) and friction ratio ($R_f$) from PCPT tests of four test piles locations are presented in Figure 21 to Figure 24. Generally the soil conditions consisted of clays within the depths of explorations with some silty and sandy soils between the depths of about 30 ft. and 40 ft. and again between 120 ft. and 125

ft. depths. The locations of sand/silt strata varied from location to location. The detail description of soil condition can be found on Haque et al. *[78]*.

**Table 2**
**Information of test piles for LA-1 project**

| Pile ID | Width | Length | | | Hammer Type |
|---|---|---|---|---|---|
| | | Total | Embedment | Left above GL | |
| | in. | ft. | ft. | ft. | |
| TP-2 | 16 | 130 | 120 | 10 | Vulcan 010 |
| TP-3 | 30 | 190 | 180 | 10 | Vulcan 010 / Vulcan 020 |
| TP-4a | 24 | 160 | 150 | 10 | Vulcan 020 |
| TP-4b | 24 | 210 | 200 | 10 | Vulcan 020 |
| TP-5a | 24 | 145 | 139 | 6 | Vulcan 020 |
| TP-5b | 24 | 170 | 163 | 7 | Vulcan 020 |

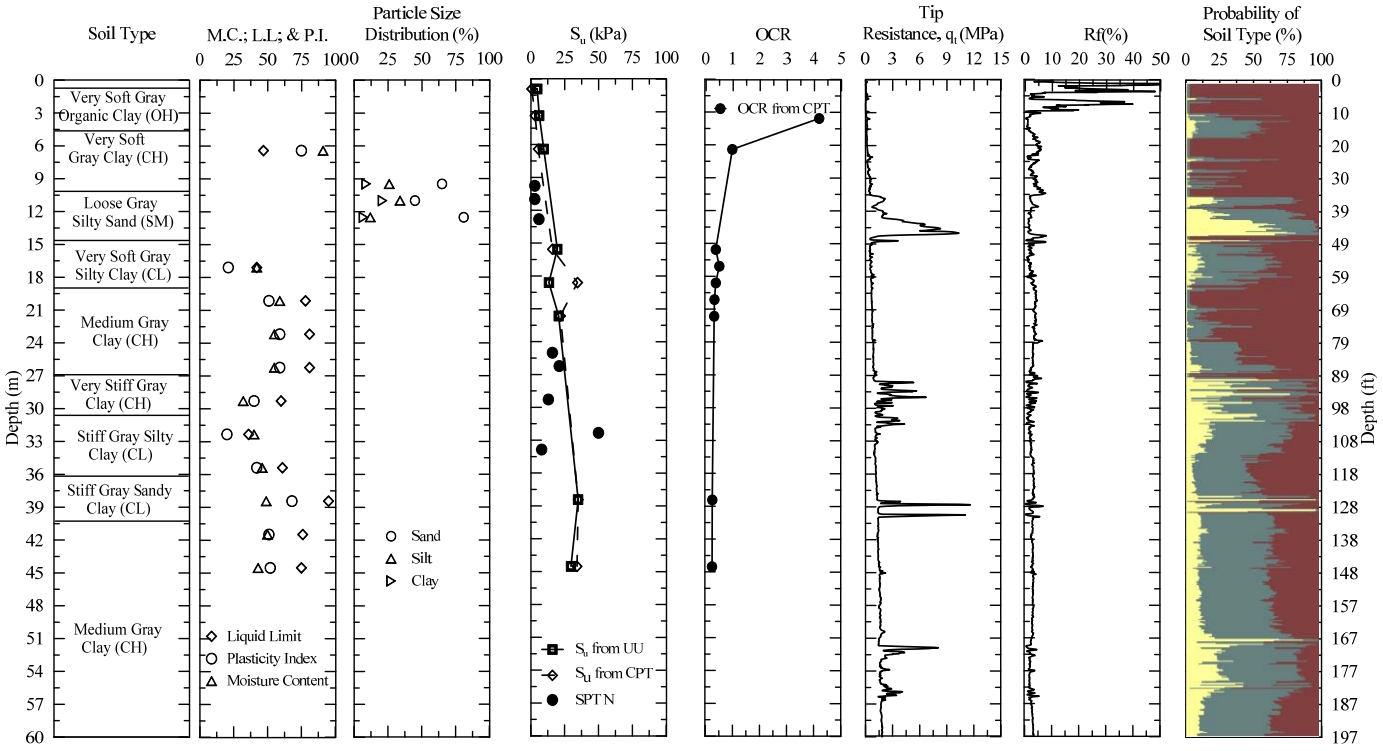


**Figure 21**
**Soil boring and PCPT soil classification at TP-2 location of LA-1 site**

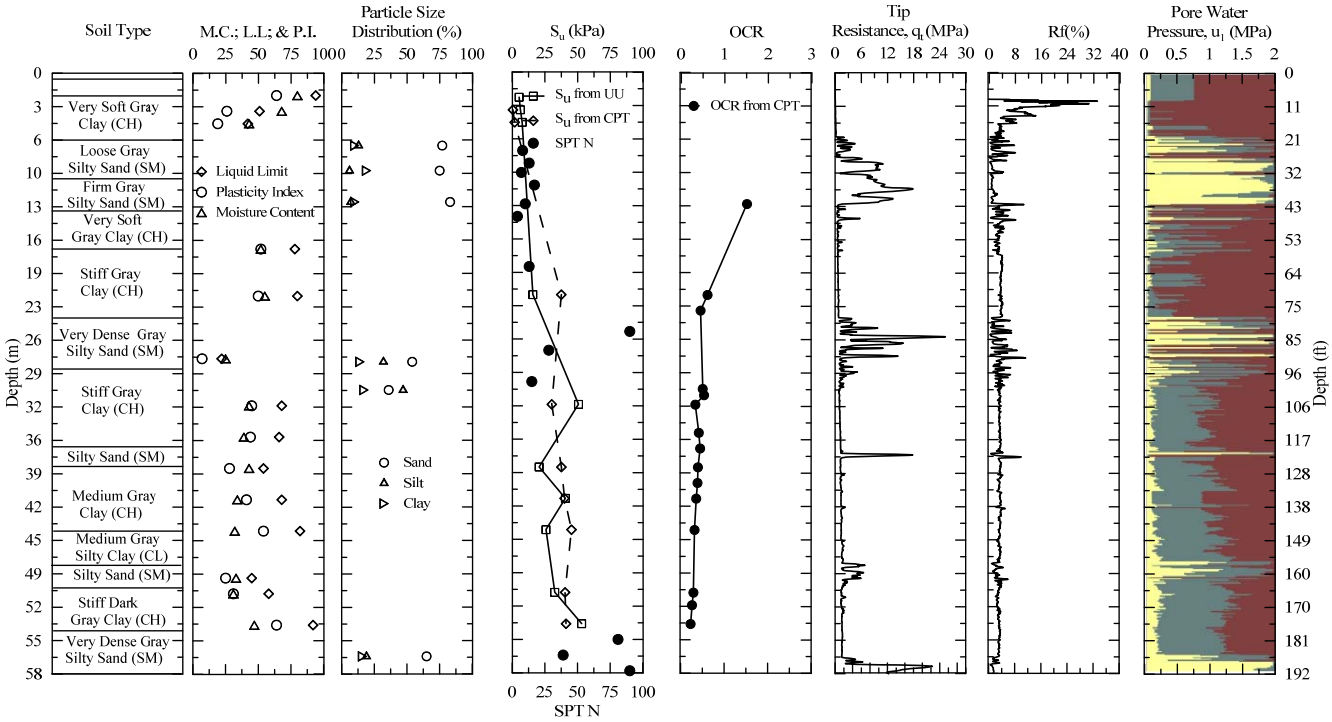


**Figure 22**

**Soil boring and PCPT soil classification at TP-3 location of LA-1 site**

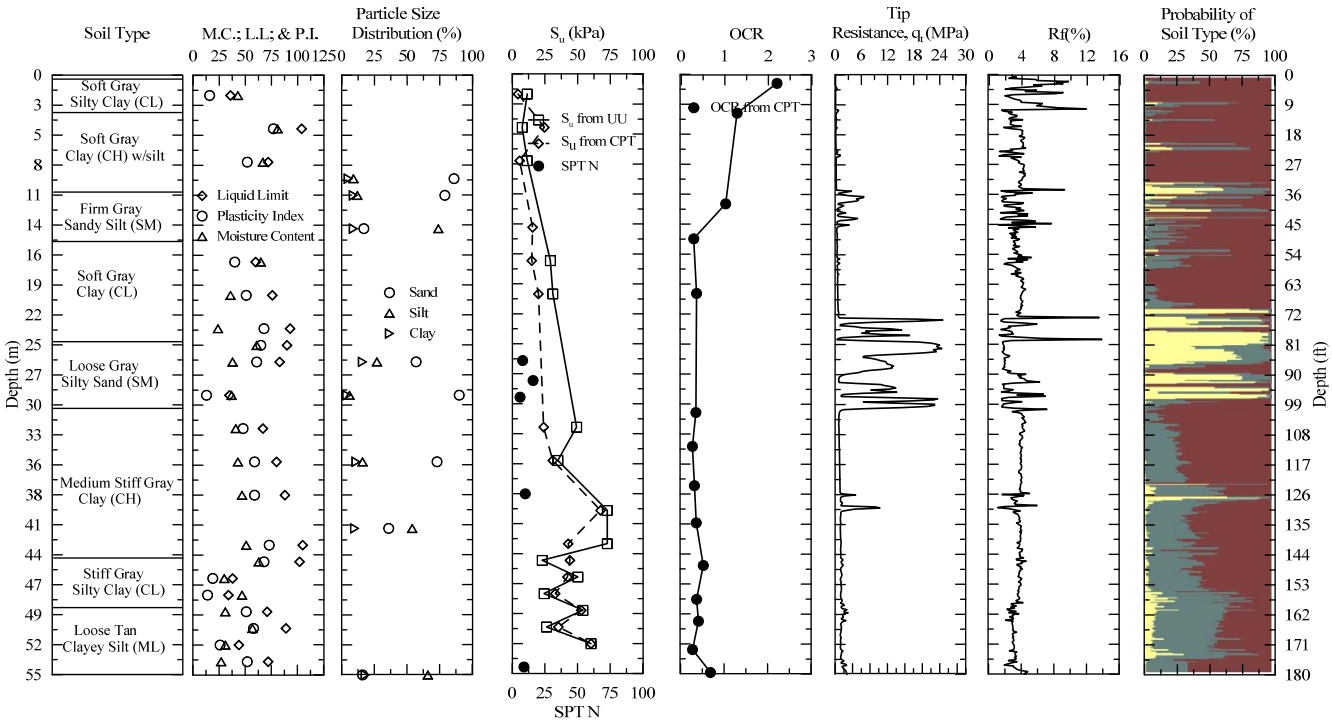


**Figure 23**

**Soil boring and PCPT soil classification at TP-4 location of LA-1 site**

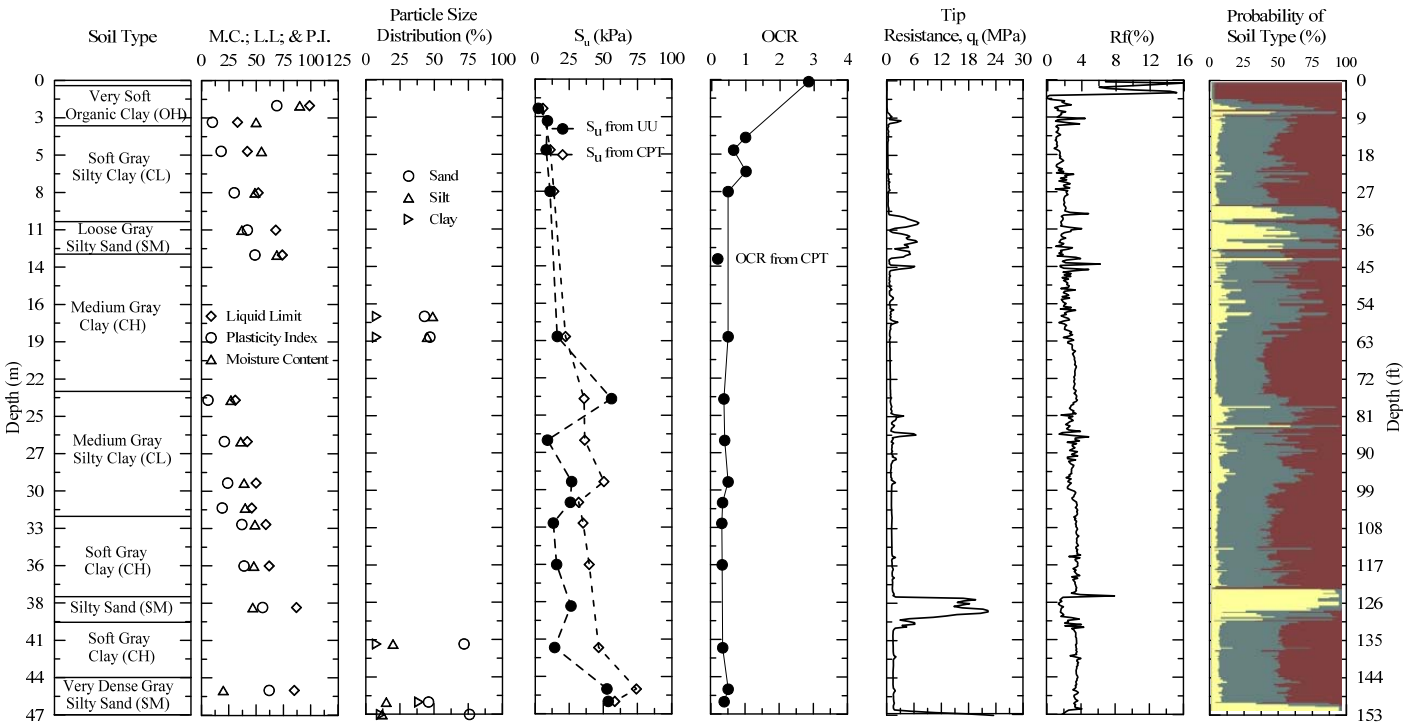


**Figure 24**
**Soil boring and PCPT soil classification at TP-5 location of LA-1 site**

**Instrumentation Plan.** The PSC piles were each instrumented with seven to eight levels of strain gages in order to evaluate load distribution along the length of the piles and measure the side and tip resistances separately. Two gages were placed on opposite faces of the pile at each level. The Sure-Lock mechanical splices were modified to provide a through hole for these lead wires. After the sections had been spliced in the field, the wires from the bottom section were pulled through the PVC pipes embedded in the upper section, and exposed wires and notches were grouted to protect the lead wires from the subsequent pile driving damages. An example of the instrumentation plans of TP-4a and TP-5a for LA-1 project are depicted in Figure 25a and Figure 25b**,** respectively.

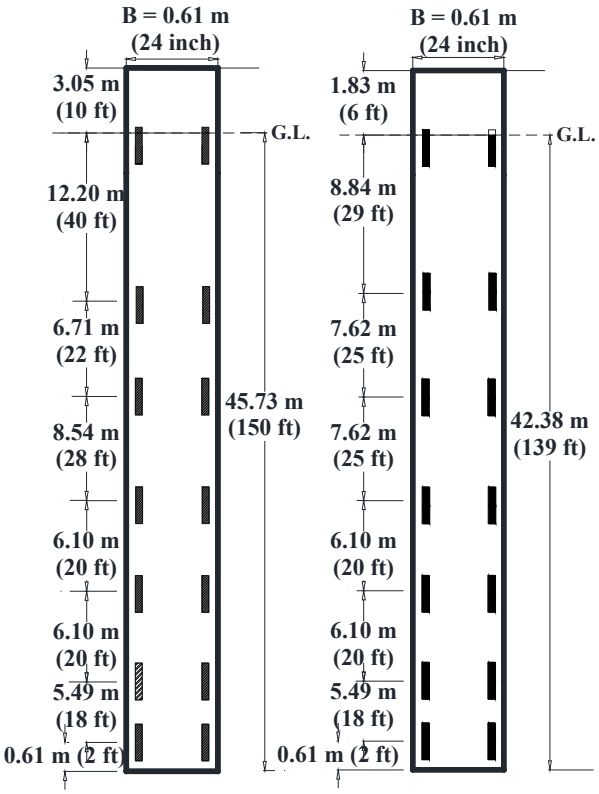


(a) TP-4a (b) TP-5a

**Figure 25**
**Instrumentation plan for the test piles of LA-1 site**

# DISCUSSSION OF RESULTS

## Bayou Zourie Site

For estimating pile set-up, the pile resistances were measured at different time intervals after EOD for this Bayou Zourie project. The load test program included three DLTs and two SLTs after EOD. Restrikes were conducted on the test pile at predetermined intervals to assess the development of "pile set-up" following EOD. In addition, two SLTs were conducted on the test pile at 14 and 30 days after EOD. The load test result of the test pile is tabulated in Table 3. The set-up plot for total resistance ($R_t$) of the test pile is depicted in Figure 26.

**Table 3**
**Set-up information for test pile of Bayou Zourie site**

| Events | Time | Side Resistance $R_s$ | | Tip Resistance $R_{tip}$ | | Total Resistance $R_t$ | | Blows | EMX kN-m (kip-ft) | Set Per Blow mm (in.) |
|---|---|---|---|---|---|---|---|---|---|---|
| | Days | kN (kips) | Ratio ($R_s/R_{so}$) | kN (kips) | Ratio | kN (kips) | Ratio ($R_t/R_{to}$) | | | |
| EOD | - | 1624 (365) | 1.0 | 1054 (237) | 1.0 | 2678 (602) | 1.0 | - | 40.8 (30.1) | - |
| 1st DLT | 0.07 | 2033 (457) | 1.3 | 983 (221) | 0.9 | 3016 (678) | 1.1 | 14 | 41.2 (30.4) | 75 (3) |
| 2nd DLT | 1 | 2095 (471) | 1.3 | 1090 (245) | 1.0 | 3185 (716) | 1.2 | 16 | 51.8 (38.2) | 75 (3) |
| 3rd DLT | 77 | 2918 (656) | 1.8 | 988 (222) | 0.9 | 3906 (878) | 1.5 | 28 | 46.6 (34.4) | 63.5 (2.5) |
| 1st SLT | 14 | - | - | - | - | - | - | - | - | - |
| 2nd SLT | 30 | - | - | - | - | - | - | - | - | - |

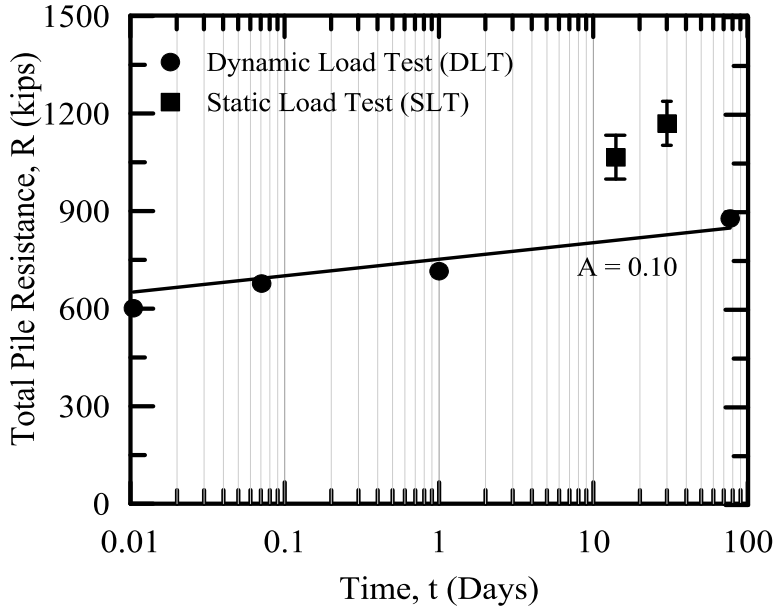


**Figure 26**
**Total pile resistance versus time for the test pile of Bayou Zourie site**

**Set-up of Total Pile Resistance**

**Dynamic Load Test (DLT).** Three high strain restrikes were carried out on the test pile at different time intervals from 60 minutes after EOD, up to a maximum of 77 days after EOD for the test pile. To determine the resistance distribution along the side and measure the side and tip resistances separately for restrikes, Case Pile Wave Analysis Program (CAPWAP) analyses were performed on selected blows at the EOD and the first high energy blow of each restrike event. The set-up results for DLT of Bayou Zourie are presented in Table 3. The set-up ratio of side ($R_s/R_{so}$) and total ($R_t/R_{to}$) pile resistance at different times after EOD measured by restrikes are also presented in Table 3. The change in total ($R_t$), side ($R_s$), and tip ($R_{tip}$) resistances are listed separately in Table 3 to illustrate the different effects of set-up. Both total ($R_t$) and side ($R_s$) resistance increased with time after EOD. Referring to the last restrike (77 days after EOD), the increase in CAPWAP calculated side resistance ($R_s$) was 80% while the increase in total pile resistance ($R_t$) was 46%. The tip resistance ($R_{tip}$) component remained virtually the same even after 77 days. This indicates that the pile set-up was mainly due to the increase in side resistance ($R_s$). As shown in Figure 26, the CAPWAP based total resistance as a function of time (t) was best fitted to a logarithmic time scale with a relatively high coefficient of correlation ($R^2$) of 0.93, suggesting a logarithmic time relationship similar to the model proposed by Skov and Denver *[7]*. However, neither of the two SLTs were loaded to failure, as will be discussed in the following section. Therefore, a direct comparison of SLTs and CAPWAP results was not possible specifically for this site. As such, the observed pile set-up in DLT and SLTs are discussed separately specifically for this case.

**Static Load Test (SLT).** The compression SLTs were conducted by means of a 1000 kips hydraulic jack reacting against beams connected to the reaction piles. Based on preliminary calculations, which later proved to have been underestimated, it was assumed that the pile could be tested to failure with a 1000 kips test system. Two SLTs were performed on the test pile at 14 and 30 days after EOD. Each SLT consisted of three stages: loading, unloading, and reloading: the pile was first loaded to 504 kips with 28 kips increments, then unloaded to zero load with 168 kips decrements. After the load was removed, the pile was reloaded the pile to 504 kips in increments of 168 kips, then the load was increased in increments of 28 kips until either the pile or hydraulic jack reached their maximum capacity. The load was maintained constant during each load increment.

In the SLTs, the pile was loaded to the maximum capacity of the hydraulic jack (1000 kips), which corresponds to about 3 times the pile design load. However, the test pile still did not reach failure. The higher anticipated capacity may be partially due to the contribution of the upper 20 ft. which was pre-augured and therefore ignored in the preliminary capacity estimate. Load-

settlement curves of the two SLTs are presented in Figure 27. Extrapolation of the measured load-settlement curves was performed based on engineering judgment. The possible range of the extrapolated load-settlement curves is indicated in the figure by the "hatched region" at the end of the measured data for each curve. The ultimate pile resistances were estimated using the extrapolated curves and the Davisson method for piles with diameter of 24 in. or less *[79]*. The extrapolated pile resistances were 1,010 kips to 1,165 kips and 1,135 kips to 1,287 kips for 14 and 30 days, respectively. The static load capacities are also included in Figure 26 for comparison with the dynamic load resistances from CAPWAP analyses.

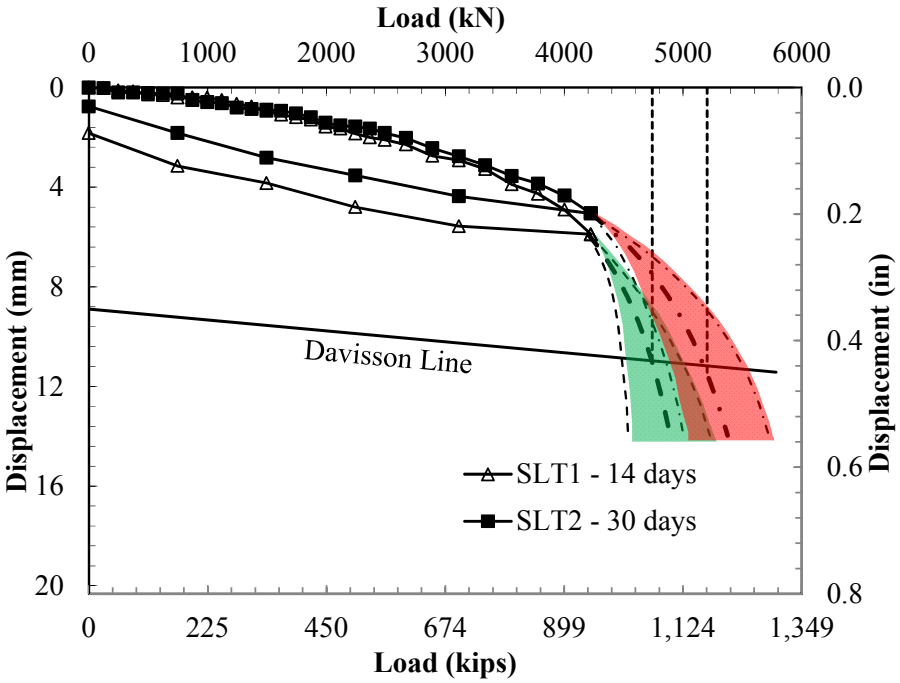


**Figure 27**

**Load settlement plot for the test pile of Bayou Zourie site**

The strain gage readings obtained during the load tests were used to estimate the distribution of load transfer along the pile, as presented in Figure 28. As can be seen from Figure 28, the load transferred to the tip of the pile decreased with time (for example, at the applied load of 1073 kips, the load estimated by the bottom strain gage measurements decreased from 144 kips to 133 kips with time). Based on these load transfer curves, the distribution of unit side resistance ($f_s$) and total side resistance along the pile at a specific displacement was calculated, as shown in Figure 29. This was necessary to understand the pile set-up since the pile was not loaded to failure. These curves appear to support the conclusion of time-dependent increase of side resistance in clayey soil. In the sandy soil layer, the side resistance changed slightly after first SLT, which is consistent with the observation in the DLTs.

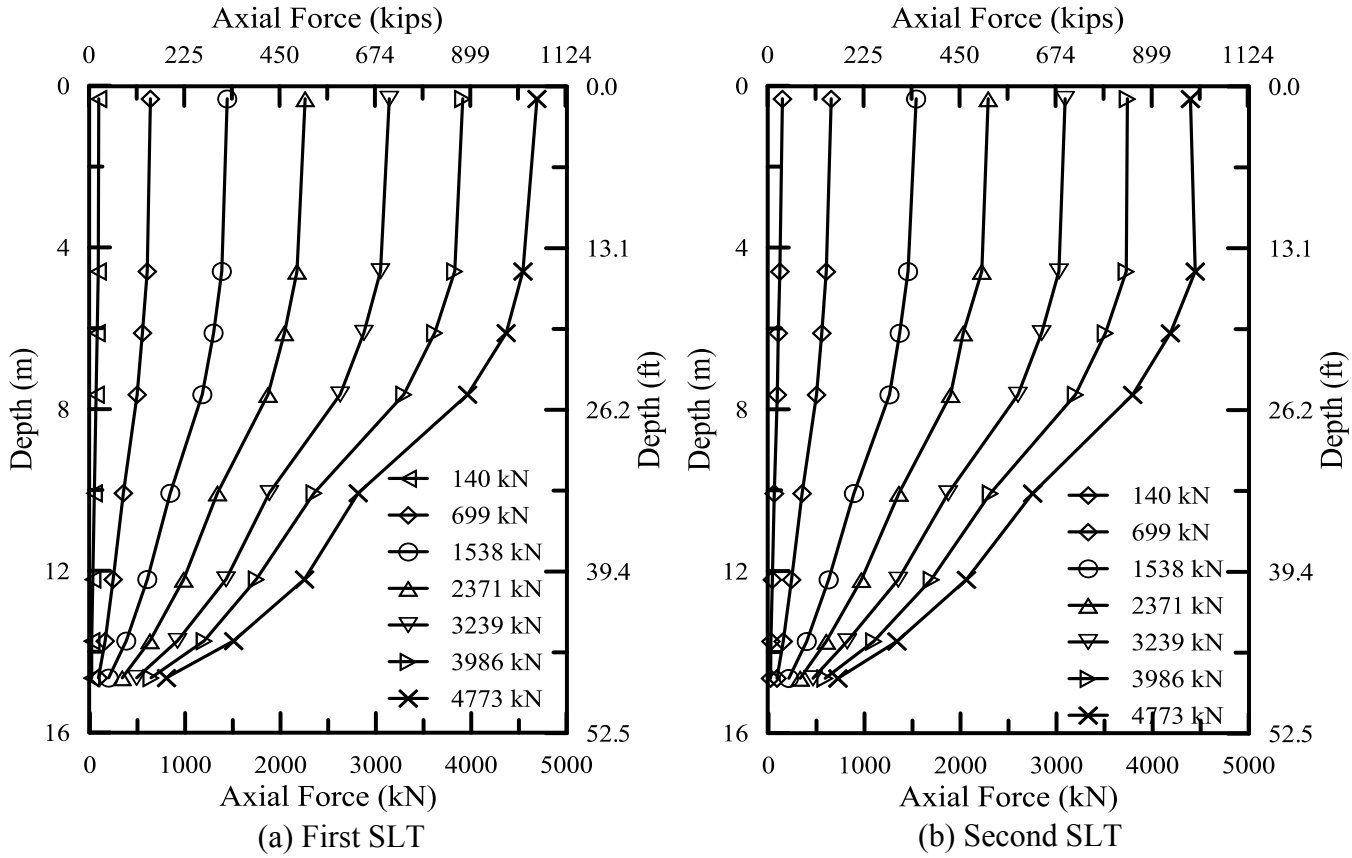


**Figure 28**

**Load distribution plot for the test pile of Bayou Zourie site (a) first SLT (b) second SLT**

**Set-up of Individual Soil Layers**

Set-up of soils needs to be analyzed for individual soil layers along the pile length rather than the total pile resistance for better prediction of set-up phenomenon. The resistances estimated from the DLTs were analyzed using the data obtained from the CAPWAP program in order to estimate the side resistance for individual soil layers along the piles. The load transfer distribution plots (Figure 28) were not used specifically for this site since the piles did not reach the failure load during the SLT. The calculated side resistances of all the individual soil layers, ratio of side resistance set-up and the depths of individual soil layers for test piles are tabulated in Table 4. The subsurface soil properties for the corresponding layers are provided in Figure 7. Logarithmic "A" parameter for individual soil layers were also calculated using the unit side resistance and tabulated in Table 4.

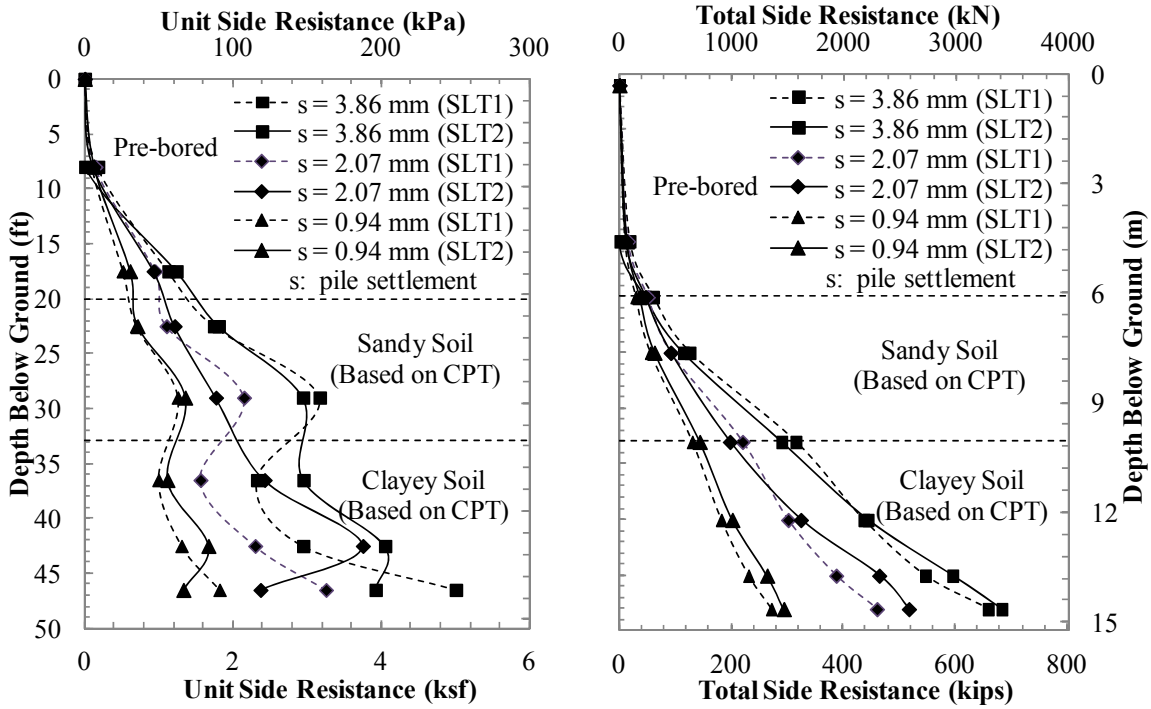


(a) Comparison of unit side resistance (b) Comparison of total side resistance

**Figure 29**

**Comparison of unit and total side resistance during first SLT and second SLT**

**Table 4**

**Set-up information of individual soil layers for the test pile of Bayou Zourie site.**

| Layer No | Layer Depth m (ft.)* | EOD | | 1st DLT | | 2nd DLT | | 3rd DLT | | A Parameter |
|---|---|---|---|---|---|---|---|---|---|---|
| | | Time | | | | | | | | |
| | | - | | 1.7 Hour | | 1 Day | | 77 Days | | |
| | | Res. kN (kips) | Set-up Ratio | Res. kN (kips) | Set-up Ratio | Res. kN (kips) | Set-up Ratio | Res. kN (kips) | Set-up Ratio | |
| 1 | 0-6.0 (0-19.7) | 284 (64) | 1.0 | 393 (88) | 1.4 | 314 (71) | 1.1 | 468 (105) | 1.6 | 0.10 |
| 2 | 6.0-8.6 (19.7-28.2) | 501 (113) | 1.0 | 574 (129) | 1.1 | 457 (103) | 0.9 | 438 (99) | 0.9 | 0.00 |
| 3 | 8.6-10.4 (28.2-34.1) | 183 (41) | 1.0 | 230 (52) | 1.2 | 260 (58) | 1.4 | 353 (79) | 1.9 | 0.15 |
| 4 | 10.4-12.1 (34.1-39.7) | 146 (33) | 1.0 | 245 (55) | 1.7 | 384 (86) | 2.6 | 716 (161) | 4.9 | 0.34 |
| 5 | 12.1-13.8 (39.7-45.3) | 182 (41) | 1.0 | 247 (56) | 1.4 | 361 (81) | 2.0 | 637 (143) | 3.5 | 0.29 |
| 6 | 13.8-15.6 (45.3-51.0) | 328 (73) | 1.0 | 344 (77) | 1.0 | 319 (72) | 1.0 | 306 (69) | 0.9 | 0.00 |
| Total Side Res. kN (kips) | | 1624 (365) | 1.0 | 2033 (457) | 1.3 | 2095 (471) | 1.3 | 2918 (656) | 1.8 | |

*Soil layers were chosen based on PCPT soil profile

The soil layers along the length of the test pile were divided into six individual soil layers to facilitate the analyses of individual soil layers. The top 20 ft. was pre-bored before driving and no casing was installed. Therefore, a small amount of resistance 64 kips was observed during driving due to soil-pile interaction. A small amount of set-up was observed for this layer (0 ft. – 19.7 ft.) and the final DLT showed that the set-up ratio for this layer was 1.6. Layers 2 and 6 represented the sandy soil layers for this test pile location and layers 3, 4, and 5 represented the clayey soil layers. The sandy soil layers exhibited relaxation whereas the clayey soil layers exhibited increase in resistance or set-up behavior. The tabulated data of Table 4 shows that during the first DLT (i.e., 1.7 hour after EOD), the side resistance of those two sandy soil layers (i.e., layer 2 and 6) was higher than the EOD side resistance followed by decrease in side resistance or exhibited relaxation behavior. The quick dissipation of excess PWP immediately after pile driving may contribute to this behavior. The consolidation behavior related to set-up for both sandy and clayey soil layers are depicted in Figure 30a to Figure 30d. The side resistances of individual soil layers are also presented in the figures as function of time.

Figure 30a shows that most of the excess PWP dissipated before second DLT (24 hours after EOD). As stated earlier, the side resistance of the sandy soil layer increased logarithmically with time followed by a decrease in the resistance (i.e., relaxation). On the contrary, all the three clayey soil layers exhibited significant amount of set-up and the maximum amount (i.e., 4.9 times higher compared to EOD side resistance) of set-up was exhibited by layer 4. The side resistances were 1.9 and 3.5 times higher compared to EOD side resistances for the clayey soil layers 3 and 5, respectively. Logarithmic "A" parameter that was calculated using the unit side resistance ($f_s$) was also higher for layer 4 compared to layers 3 and 5. Logarithmic "A" parameter for layer 4 was 0.34, whereas the "A" parameter for layers 3 and 5 were 0.15 and 0.29, respectively. The lower $S_u$ (i.e., 1 tsf) of layer 4 and slower dissipation of excess PWP compared to other clayey soil layers (i.e., layers 3 and 5) may contribute to this higher amount of set-up and rate of set-up. Figure 30b to Figure 30d show that all the clayey soil layers exhibited slower dissipation of excess PWP compared to the sandy soil layers (i.e., layer 2) due to low permeability. As can be observed from Figure 30d, about 98% of the excess PWP that was developed during pile driving in clayey soil layer dissipated in about 60 days after EOD. During this period (i.e., EOD to 60 days), 80% of the total set-up was completed and this is due to consolidation and thixotropic behavior. The remaining 20% of total set-up can be attributed to aging effect. The results agree well with the published studies in literature, which showed that set-up for clayey soil layer is dominated by consolidation behavior *[e.g. 1, 6, 21]*. The piezometers installed in layer 4 showed that 98% of excess pore water dissipated in 60 days whereas the piezometer installed in sandy soil layer (i.e., layer 2) exhibited that 98% of excess PWP dissipated before 1 day after EOD (Figure 30a).

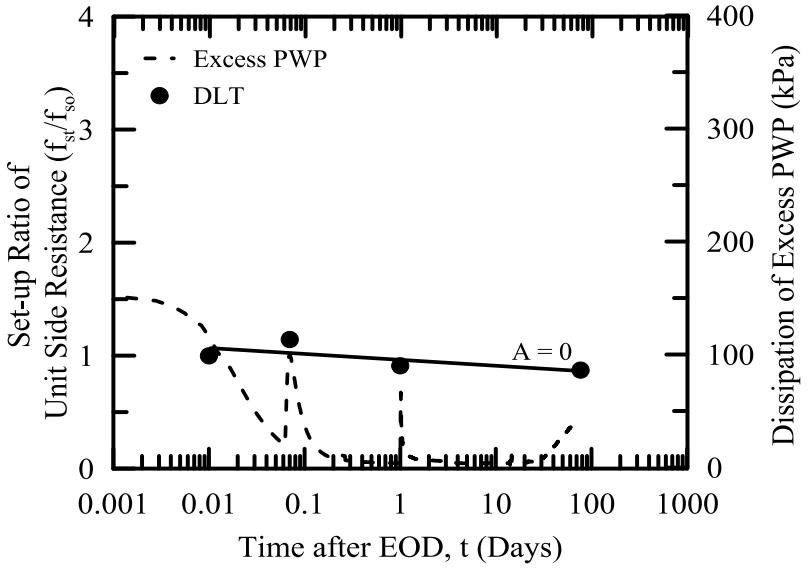


(a) Layer-2: Piezometer installed at 25 ft. (7.6 m)

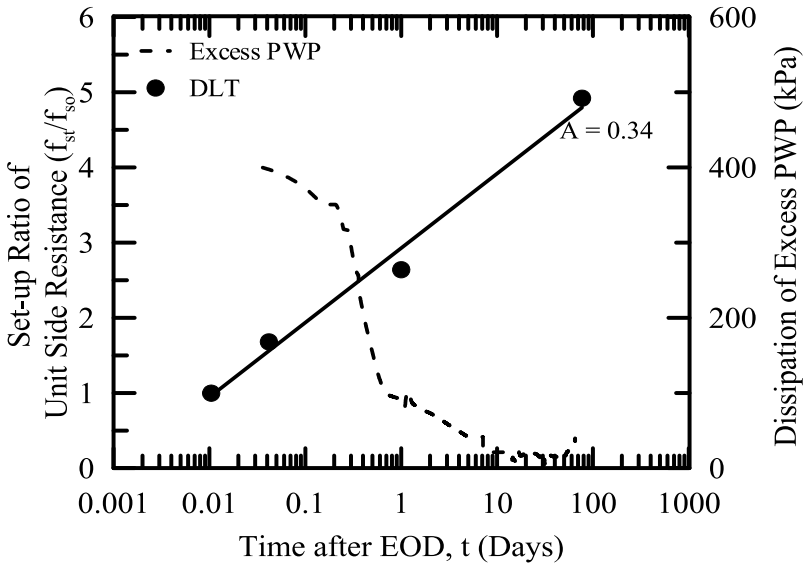


(b) Layer-4: Piezometer installed at 35 ft. (10.7 m)

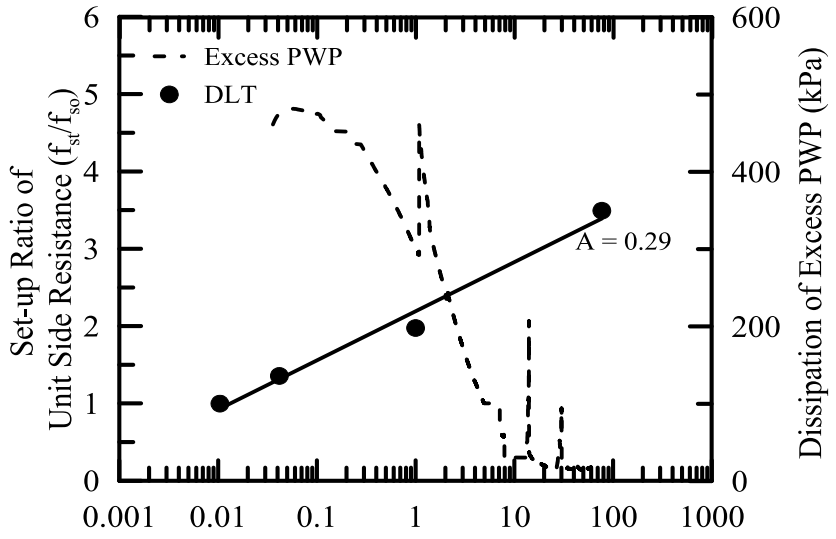


(c) Layer-5: Piezometer installed at 40 ft. (12.2 m)

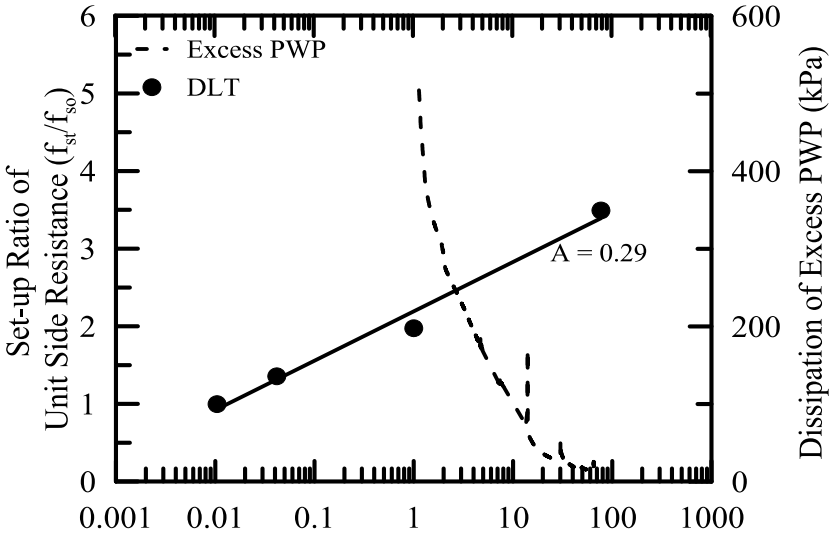


(d) Layer-5: Piezometer installed at 45 ft. (13.7 m)

**Figure 30**
**Set-up of individual soil layers and correlation with dissipation of excess PWP of Bayou Zourie site**

**Distribution of Excess PWP in the Remolded Zone.** Figure 31 presents the distribution of excess PWP measured at different depths, 8 minutes after EOD. As shown in the figure, the excess PWP sharply decreased from the pile face to a distance of 2B from pile face, after which

it decreased at a much lower rate. This suggests that the surrounding soil along the pile (within 2B) is significantly disturbed or compressed due to pile driving; the influence of pile driving extends beyond 4B.

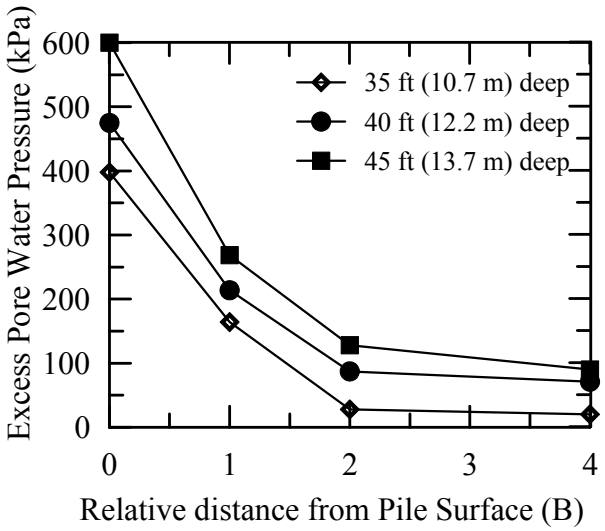


**Figure 31**
**Excess PWP distributions with the distance after EOD in Bayou Zourie site**

### Bayou Lacassine Site

An extensive load test program was carried out after pile installation using both SLTs and DLTs. To start estimating the set-up immediately after pile driving, two initial DLTs were performed within 24 hours after EOD for the three test piles. Five SLTs were then conducted on the two instrumented test piles (TP-1 and TP-3) over a period of six months and one SLT was performed on the other non-instrumented test pile (TP-2) at twenty two days after EOD. A final restrike was also performed on each test pile after the last SLT. The measured side, tip and total resistances with time for all tests are tabulated in Table 5. The plots of total pile resistance with time after EOD are presented in Figure 32a, Figure 32b and Figure 32c for TP-1, TP-2 and TP-3, respectively.

**Set-up of Total Pile Resistance**

**Dynamic Load Test (DLT).** Three high strain DLTs were carried out on each test pile at different time intervals from 30 minutes after EOD, up to a maximum of 217 days after EOD for TP-1, 23 days after EOD for TP-2, and 181 days after EOD for TP-3. The time intervals of conducting the DLTs and corresponding total, side and tip resistances are tabulated in Table 5 for all test piles. The test results showed a significant increase in resistance for all test piles started immediately after driving. The first restrike, which was conducted within 1 hour after EOD on

all test piles, showed that the total resistance was increased by 9%, 7% and 17% for TP-1, TP-2, and TP-3, respectively. Initial excess PWP dissipation and thixotropic effect may contribute to this significant amount of set-up over a very short time period. The final restrike showed that the total resistances were 2.1, 1.7, and 1.6 times higher compared to the EOD total resistance for TP-1, TP-2, and TP-3, respectively.

The final restrike demonstrated that the side resistance was increased by 129%, 99%, and 91% for TP-1, TP-2, and TP-3, respectively, as compared to the EOD values. The tip resistance was almost constant over time for TP-2 and TP-3, which implies that the set-up was primarily occurred along the side for the test piles. However, the tip resistance of TP-1 was almost constant until the fourth SLT, and then was increased by 33% in the last restrike (217 days after EOD). This behavior will be discussed later.

**Table 5**
**Set-up information of test piles for Bayou Lacassine site**

| Events | Time | Side Resistance $R_s$ | | Tip Resistance $R_{tip}$ | | Total Resistance $R_t$ | | EMX kN-m (kip-ft) | Set Per Blow mm (in) |
|---|---|---|---|---|---|---|---|---|---|
| | Days | kN (kips) | Ratio ($R_s/R_{so}$) | kN (kips) | Ratio | kN (kips) | Ratio ($R_t/R_{to}$) | | |
| Test Pile-1 (TP-1) | | | | | | | | | |
| EOD | - | 1038 (233) | 1.0 | 339 (76) | 1.0 | 1377 (309) | 1.0 | 42.0 (31.0) | 8.4 (0.3) |
| 1st DLT | 0.02 | 1139 (256) | 1.1 | 355 (80) | 1.1 | 1494 (336) | 1.1 | 39.4 (29.1) | 7.9 (0.3) |
| 2nd DLT | 1 | 1545 (348) | 1.5 | 354 (79) | 1.0 | 1899 (427) | 1.4 | 60.7 (44.8) | 8.4 (0.3) |
| 1st SLT | 13 | 1695 (381) | 1.6 | 316 (71) | 0.9 | 2011 (452) | 1.5 | - | - |
| 2nd SLT | 53 | 1901 (427) | 1.8 | 323 (73) | 0.9 | 2224 (500) | 1.6 | - | - |
| 3rd SLT | 127 | 2130 (479) | 2.1 | 361 (81) | 1.1 | 2491 (560) | 1.8 | - | - |
| 4th SLT | 148 | 2191 (493) | 2.1 | 407 (91) | 1.2 | 2598 (584) | 1.9 | - | - |
| 5th SLT | 208 | 2094 (471) | 2.0 | 415 (93) | 1.2 | 2509 (564) | 1.8 | - | - |
| 3rd DLT | 217 | 2376 (534) | 2.3 | 451 (102) | 1.3 | 2827 (636) | 2.1 | 57.2 (42.2) | 3.3 (0.1) |
| Test Pile-2 (TP-2) | | | | | | | | | |
| EOD | - | 1372 (308) | 1.0 | 592 (133) | 1.0 | 1964 (441) | 1.0 | 56.6 (41.8) | 12.2 (0.5) |
| 1st DLT | | 1534 (345) | 1.1 | 574 (129) | 1.0 | 2108 (474) | 1.1 | 59.5 (43.9) | 6.4 (0.25) |
| 2nd DLT | 1 | 2302 (518) | 1.7 | 632 (142) | 1.1 | 2934 (660) | 1.5 | 78.2 (57.7) | 8.4 (0.3) |
| 1st SLT | 22 | | | | | 3345 (752) | 1.7 | - | - |
| 3rd DLT | 23 | 2733 (614) | 2.0 | 597 (134) | 1.0 | 3330 (748) | 1.7 | 65.2 (48.1) | 1.8 (0.07) |
| Test Pile-3 (TP-3) | | | | | | | | | |
| EOD | - | 1495 (336) | 1.0 | 765 (172) | 1.0 | 2260 (508) | 1.0 | 42.3 (31.2) | 8.4 (0.3) |
| 1st DLT | 0.04 | 1851 (416) | 1.2 | 791 (178) | 1.0 | 2642 (594) | 1.2 | 47.2 (34.8) | 5.1 (0.2) |
| 2nd DLT | 1 | 2171 (488) | 1.4 | 720 (162) | 0.9 | 2891 (650) | 1.3 | 68.6 (50.6) | 5.1 (0.2) |
| 1st SLT | 15 | 3100 (697) | 2.1 | 681 (153) | 0.9 | 3781 (850) | 1.7 | - | - |
| 2nd SLT | 29 | 2909 (654) | 1.9 | 667 (150) | 0.9 | 3576 (804) | 1.6 | - | - |
| 3rd SLT | 93 | 2821 (634) | 1.9 | 693 (156) | 0.9 | 3514 (790) | 1.5 | - | - |
| 4th SLT | 129 | 2786 (626) | 1.9 | 657 (148) | 0.9 | 3443 (774) | 1.5 | - | - |
| 5th SLT | 175 | 2896 (651) | 1.9 | 645 (145) | 0.8 | 3541 (796) | 1.6 | - | - |
| 3rd DLT | 181 | 2856 (642) | 1.9 | 765 (172) | 1.0 | 3621 (814) | 1.6 | 45.3 (33.4) | 2.0 (0.08) |

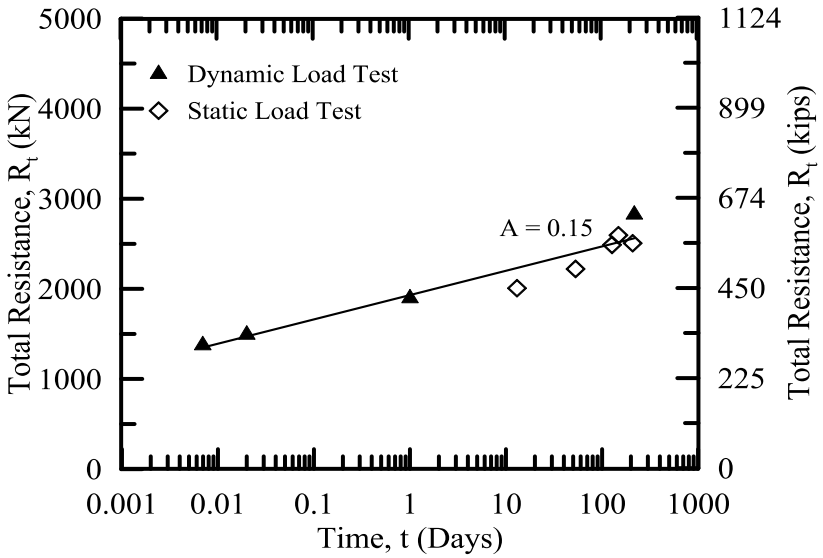


(a) Test Pile-1 (TP-1)

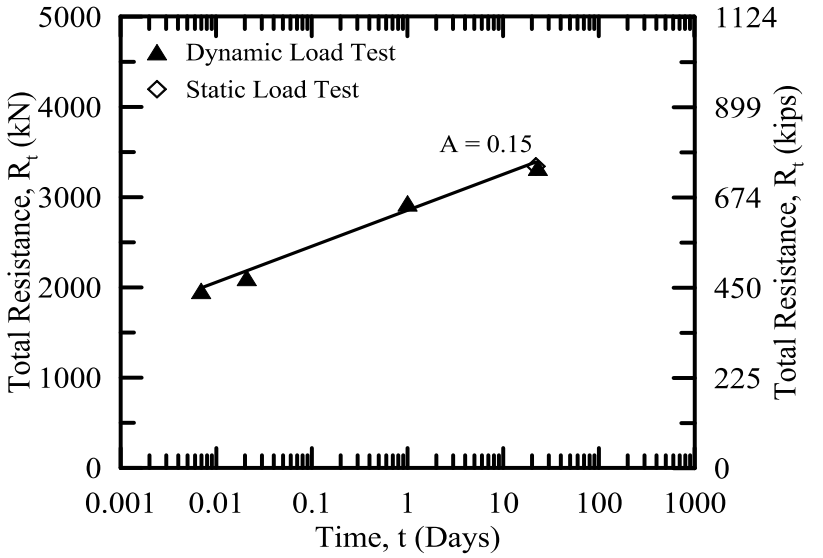


(b) Test Pile-2 (TP-2)

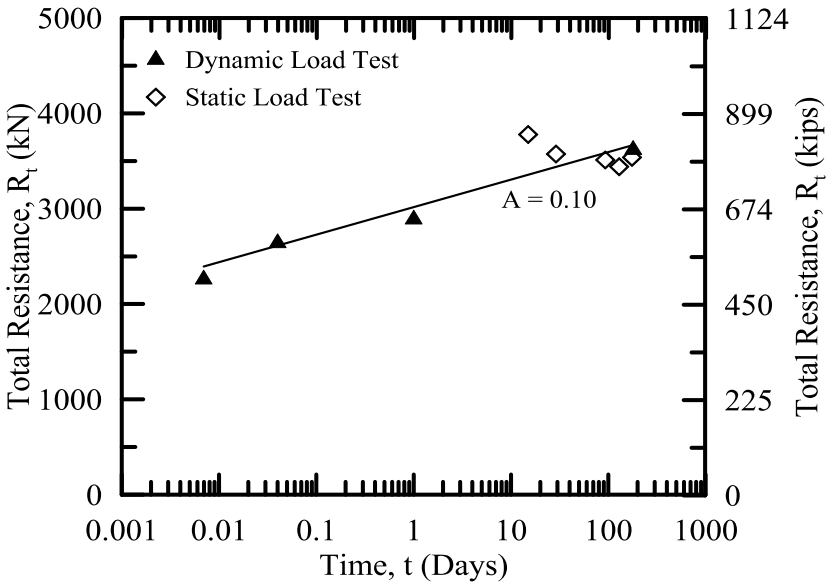

(c) Test Pile-3 (TP-3)

**Figure 32**
**Total pile resistance versus time elapsed for (a) TP-1 (b) TP-2 and (c) TP-3 of bayou Lacassine site**

**Static Load Test (SLT).** Five SLTs were conducted on both instrumented test piles (TP-1 and TP-3) over a period of six months after EOD in accordance with ASTM Standard D1143 and one SLT was conducted on Test Pile-2 *[75]*. The time schedule of each SLT is tabulated in Table 5. Sixteen reaction pipe piles of 24 in. diameter were installed at each test pile location after 8-10 days from pile driving. Compressive axial loads were applied to the pile using a 1,500 kip capacity hydraulic jack reacting against the load frame. The load was applied in increments of 10% of the proposed design load 274 kips with a constant time interval of 5 minutes between increments (quick test). Load was added until continuous jacking was required to maintain the test load. The load was applied in three different stages: loading (up to 250 kips) followed by unloading to 10 kips and then reloading to failure point. At the end, the load was removed in decrements of 25% of the maximum failure load.

According to DOTD design criteria, the minimum settlement of the tested pile at the plunging load during the SLT should be at least 10% of the pile diameter. However, in order to minimize the soil disturbance and remolding effect, the research team decided to limit the plunge of both instrumented test piles at the failure load to 1 in. after the second SLT. Figure 33a, Figure 33b and Figure 33c present the measured static load-settlement curves for TP-1, TP-2 and TP-3,

respectively. The ultimate resistance of each pile was calculated using the modified Davisson interpretation method, and the values are presented in Table 5 *[79]*. Test results of TP-1 showed that the total pile resistance ($R_t$) increased by approximately 46% by the first SLT (13 days after EOD) and increased up to 89% by the fourth SLT (148 days after EOD).

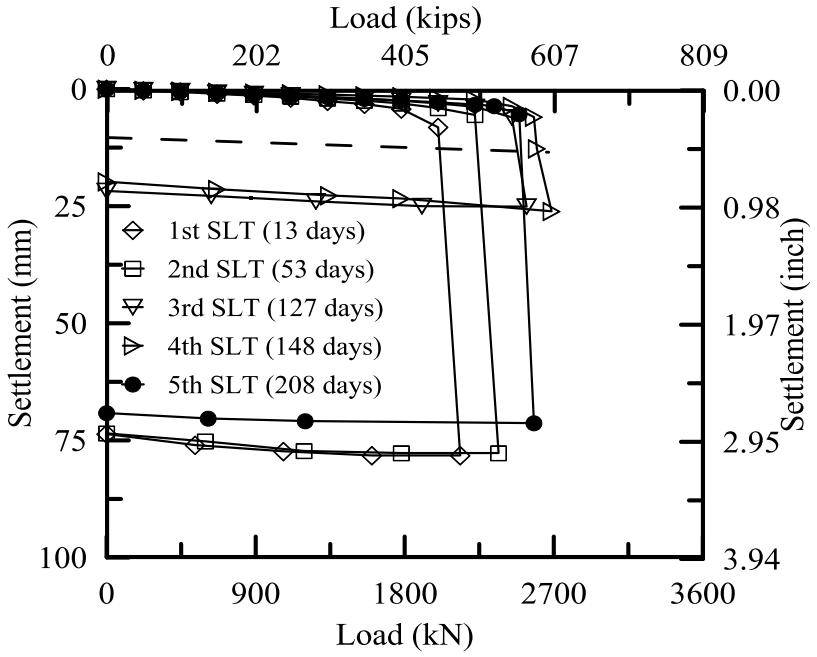


(a) Test Pile-1 (TP-1)

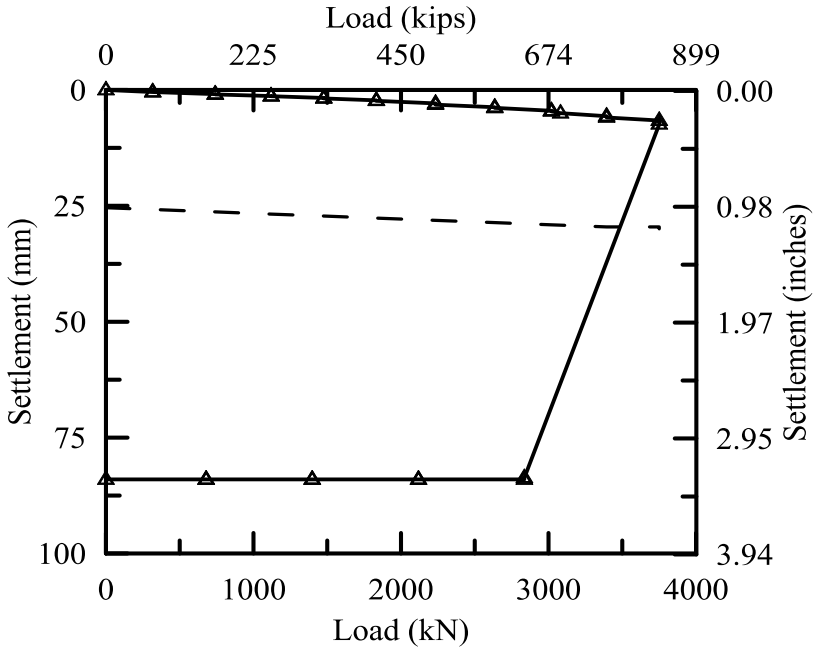


(b) Test Pile-2 (TP-2)

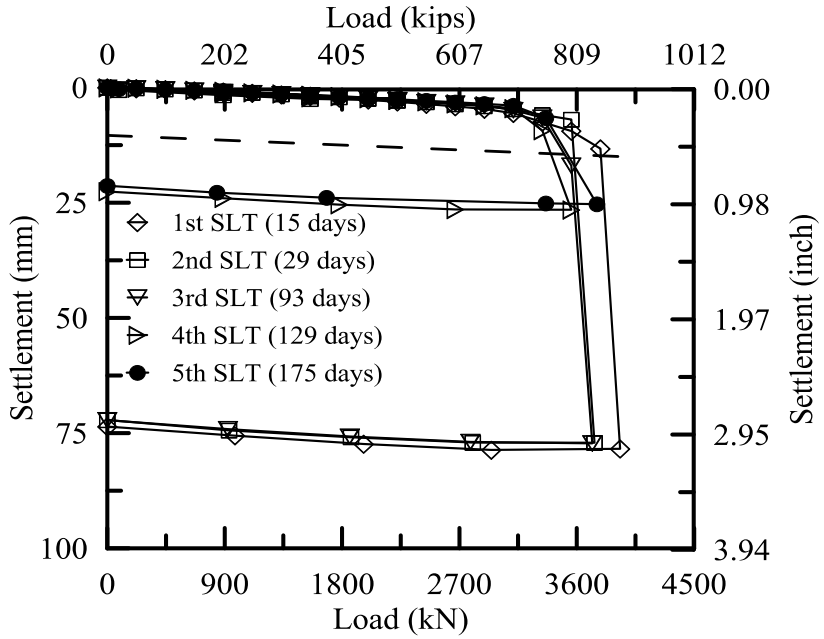


(c) Test Pile-3 (TP-3)

**Figure 33**
**Load settlement plots for (a) TP-1 (b) TP-2 and (c) TP-3 of Bayou Lacassine site**

However, the pile resistance decreased slightly (~5%) during the fifth SLT (208 days after EOD) as compared to the fourth SLT, which was still 1.8 times higher compared to EOD. The last restrike (217 days after EOD) immediately after the fifth SLT supports the set-up trend, and the total resistance was finally 2.1 times higher compared to the EOD total resistance. It was observed that during the 4$^{th}$ SLT and 5$^{th}$ SLT the tip resistance was increased by a small amount (20%), which was also observed in the last restrike of TP-1. As discussed earlier, the increase in tip resistance for TP-1 may be due to the additional compaction of the soil below the tip caused by SLTs and/or long-term increase in strength due to aging and delay in consolidation process. Only one SLT was conducted on TP-2. The total resistance was 1.7 times higher during the SLT (22 days after EOD) compared to the EOD total resistance for TP-2. The behavior of TP-3 during the SLTs was slightly different from TP-1. The total resistance of TP-3 increased significantly by 67% at the first SLT (15 days after EOD) as compared to EOD total resistance. However, the total resistance stayed almost constant during the following SLTs. The total resistance for TP-3 at the fifth SLT (175 days after EOD) was 1.6 times higher than the EOD value. Figure 34 and Figure 35 present the load distribution plots of the SLTs for TP-1 and TP-3, respectively. In order to capture the strain gage measurements for every incremental load during SLTs, the data acquisition system was set to collect the data at two minute intervals during each SLT. The strain data at each incremental load were obtained with referenced to the strain measured reading taken just before the SLT. The axial load transfer can be determined from the

strain measurements, the cross-sectional area and the Young's modulus of the pile. The loads were calculated from the vibrating wire strain gage measurements, in which the measured strains at the start of the load test were set as reference points (i.e., assuming no load prior to starting the SLT) at the eight levels. No residual load was considered in this study. The side resistance was then derived from the load distribution plots.

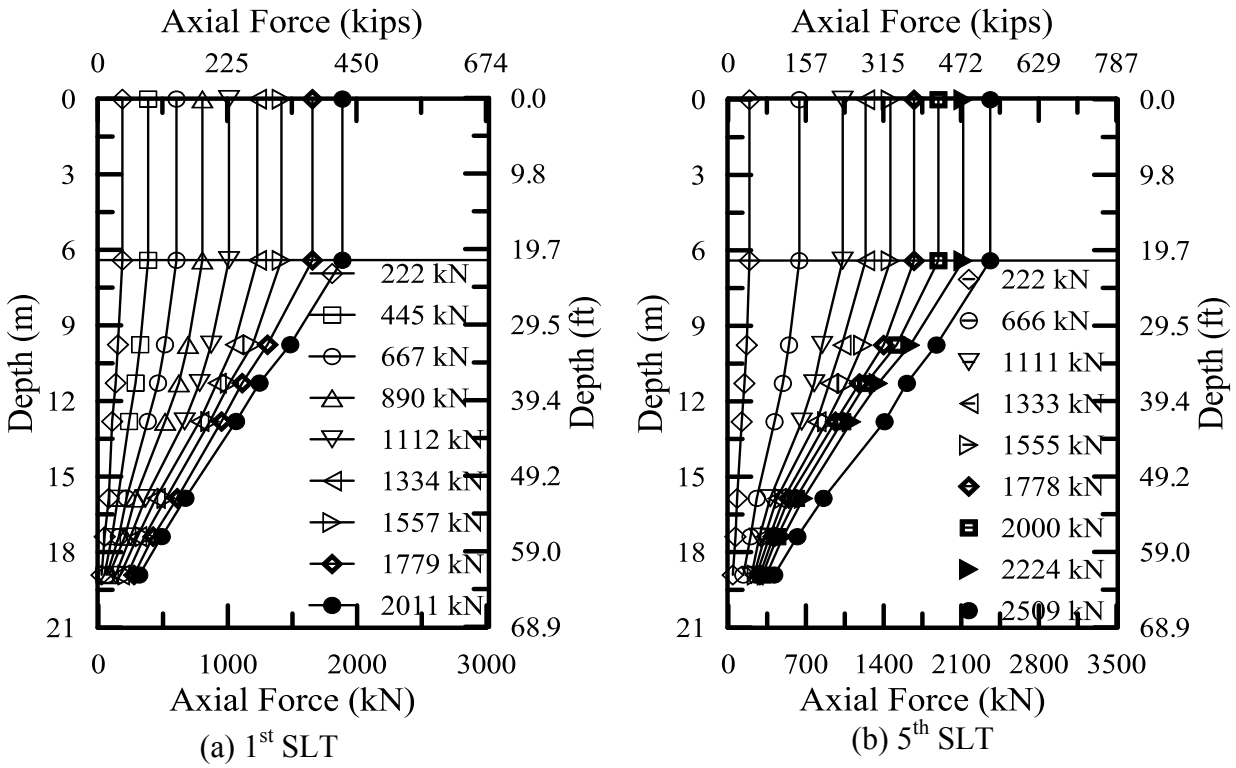


**Figure 34**
**Load distribution plots for TP-1 of Bayou Lacassine site**

**Set-up of Individual Soil Layers**

Set-up of soils needs to be analyzed for individual soil layers along the piles' length rather than the total pile resistance for better prediction of set-up phenomenon. The resistances estimated from the DLTs were analyzed using the data obtained from the CAPWAP program in order to estimate the side resistance for individual soil layers along the piles. The load transfer distribution plots (Figure 34 and Figure 35) were generated and used to estimate the side resistances for all the soil layers along TP-1 and TP-3 from the SLTs. For TP-2, only the side resistance evaluated from CAPWAP analyses was used to estimate the side resistance of individual soil layers.

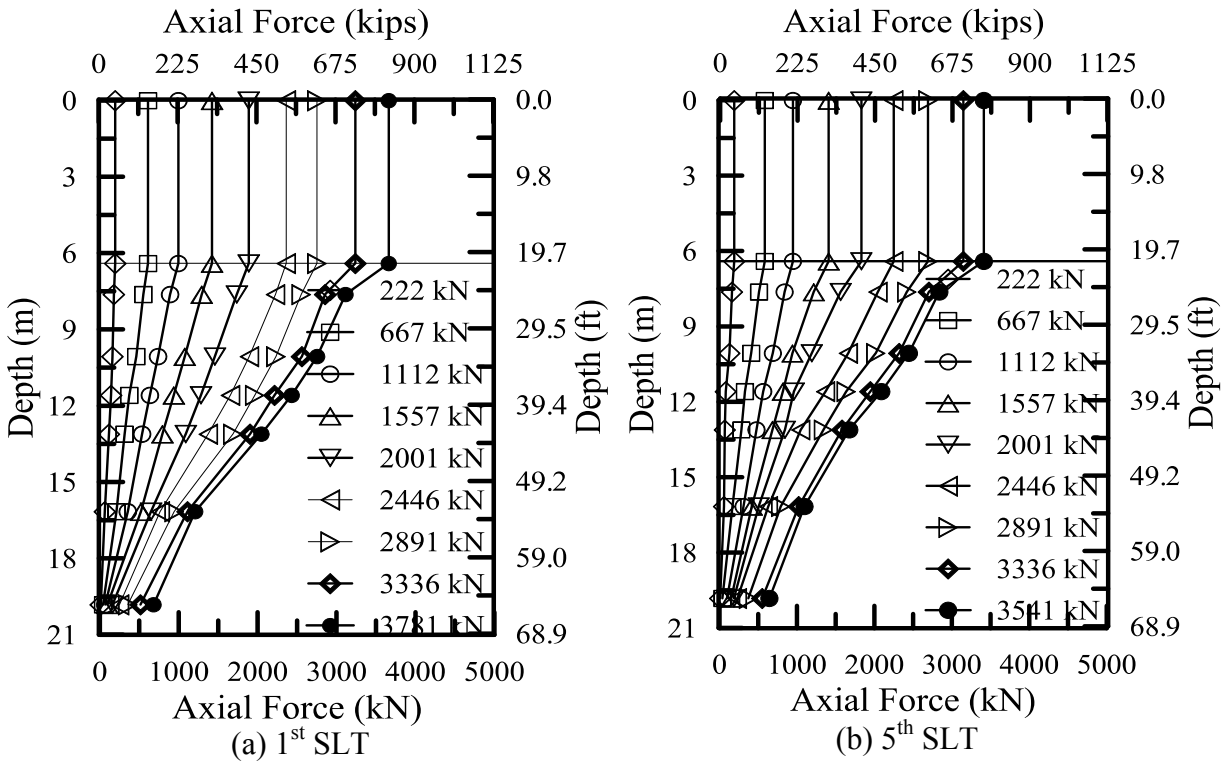


**Figure 35**
**Load distribution plots for TP-3 of Bayou Lacassine site**

**Soil Layers along Test Pile-1 (TP-1).** Each soil layer along the length of TP-1 experienced certain degree of set-up. The side resistance of individual soil layers and set-up ratio of side resistance of individual soil layers are tabulated in Table 6. Figure 36a, Figure 36b, Figure 36c, and Figure 36d present the set-up ratio of unit side resistance ($f_s/f_{so}$) for individual soil layers and the corresponding dissipation plots of excess PWP (consolidation process) for layers 2, 4, 6, and 8 of TP-1, respectively. The logarithmic rate of set-up parameter (A) is also presented for all the layers in the figures in order to correlate with soil properties such as PI, $S_u$, $S_t$, permeability ($k_h$) and $c_h$.

**Table 6**

**Set-up information for individual soil layers for TP-1 of Bayou Lacassine site**

| Events | Time (Days) | 1st Layer | 2nd Layer | | 3rd Layer | | 4th Layer | | 5th Layer | | 6th Layer | | 7th Layer | | 8th layer | |
|---|---|---|---|---|---|---|---|---|---|---|---|---|---|---|---|---|
| | | | Res. kN (kips) | Set-up Ratio | Res. kN (kips) | Set-up Ratio | Res. kN (kips) | Set-up Ratio | Res. kN (kips) | Set-up Ratio | Res. kN (kips) | Set-up Ratio | Res. kN (kips) | Set-up Ratio | Res. kN (kips) | Set-up Ratio |
| EOD | - | Casing | 152 (34) | 1.0 | 89 (20) | 1.0 | 151 (34) | 1.0 | 329 (74) | 1.0 | 125 (28) | 1.0 | 107 (24) | 1.0 | 85 (19) | 1.0 |
| 1st DLT | | | 173 (39) | 1.1 | 95 (21) | 1.1 | 172 (39) | 1.1 | 349 (78) | 1.1 | 136 (31) | 1.1 | 123 (28) | 1.1 | 91 (20) | 1.1 |
| 2nd DLT | 1 | | 306 (69) | 2.0 | 166 (37) | 1.9 | 185 (42) | 1.2 | 444 (100) | 1.3 | 179 (40) | 1.4 | 150 (34) | 1.4 | 115 (26) | 1.3 |
| 1st SLT | 13 | | 371 (83) | 2.4 | 196 (44) | 2.2 | 193 (43) | 1.3 | 471 (106) | 1.4 | 187 (42) | 1.5 | 161 (36) | 1.5 | 116 (26) | 1.4 |
| 2nd SLT | 53 | | 462 (104) | 3.0 | 218 (49) | 2.4 | 197 (44) | 1.3 | 489 (110) | 1.5 | 228 (51) | 1.8 | 168 (38) | 1.6 | 139 (31) | 1.6 |
| 3rd SLT | 127 | | 480 (108) | 3.2 | 254 (57) | 2.8 | 231 (52) | 1.5 | 598 (134) | 1.8 | 232 (52) | 1.9 | 193 (43) | 1.8 | 142 (32) | 1.7 |
| 4th SLT | 148 | | 491 (110) | 3.2 | 261 (59) | 2.9 | 242 (54) | 1.6 | 613 (138) | 1.9 | 236 (53) | 1.9 | 205 (46) | 1.9 | 143 (32) | 1.7 |
| 5th SLT | 208 | | 485 (109) | 3.2 | 240 (54) | 2.7 | 218 (49) | 1.4 | 560 (126) | 1.7 | 236 (53) | 1.9 | 208 (47) | 1.9 | 147 (33) | 1.7 |
| 3rd DLT | 217 | | 498 (112) | 3.3 | 280 (63) | 3.1 | 257 (58) | 1.7 | 704 (158) | 2.1 | 250 (56) | 2.0 | 219 (49) | 2.0 | 168 (38) | 2.0 |
| Set-up parameter "A" | | | 0.26 | | 0.12 | | 0.10 | | 0.15 | | 0.15 | | 0.14 | | 0.13 | |

Layers 2 and 3 exhibited the highest increase of side resistances among all the soil layers of TP-1 with time. The calculated side resistances during the last restrike (217 days after EOD) were 3.3 times higher for layer 2, compared to the EOD side resistance. The $S_u$ measured by UU test for layer 2 was 0.2 tsf; which was lower than the other soil layers of TP-1, and the OCR of this layer from consolidation test was 3.5, which was also higher than the other soil layers. The lower value of $S_u$ for layer 2 contributes to the higher magnitude of set-up in this layer as compared to the other soil layers. The piezometer installed at 28 ft. depth of layer 2 recorded 0.5 tsf (48 kPa) of peak excess PWP generated during pile driving, and that 99% of this excess PWP was dissipated at 52 days after EOD (Figure 36a). The low permeability ($k_h = 0.9 \times 10^{-8}$ cm/sec) contributes to this longer period of dissipation time that affects the rate of set-up (A = 0.26). Figure 36b showed that the piezometer installed at 40 ft. depth of layer 4 recorded a peak value of 3.1 tsf (295 kPa) of excess PWP that was generated during pile driving and achieved 99% dissipation in a shorter period of time (35 days after EOD). Layer 4 has relatively higher permeability ($k_h = 7.8 \times 10^{-8}$ cm/sec) and higher $c_h$ value ($c_h = 4.1 \times 10^{-2}$ cm$^2$/sec) compared to other soil layers. In addition, the CPT profile revealed presence of sand and silt lenses in this layer (36.0 to 43.0 ft. depth). The relatively high $k_h$ and $c_h$ attribute to the lower rate of set-up (A = 0.10) for layer 4 compared to other soil layers along the length of TP-1 pile. The set-up of both

layers 2 and 4 continued to increase at a slower rate after the excess PWP was completely dissipated, which can be attributed to aging effect. Layers 5, 6, and 7 exhibited closer amount of set-up. The side resistances during the last DLT (217 days after EOD) were 2.1, 2.0, and 2.0 times higher than the EOD side resistances for layers 5, 6, and 7, respectively of TP-1. The $S_u$ values for these layers ranges from 0.40 tsf (38.6 kPa) to 0.71 tsf (68 kPa) and the OCR ranges from 2.3 to 1.3. The soil profile and CPT soil classification [see Figure 11] reveal that the soil deposits consists of silty clay that almost homogeneous throughout these three layers (layer 5 to 7), which contributes to similar amount of set-up. Figure 36c showed that a peak value of 6.1 tsf (585 kPa) of excess PWP was developed during pile driving for layer 6 and that 99% of this excess PWP was dissipated in 53 days after EOD mainly due to relatively lower permeability ($k_h$ = 0.2 x $10^{-8}$ cm/sec) and lower $c_h$ ($c_h$ = 1.3 x $10^{-3}$ $cm^2$/sec) compared to layer 1-4; thus higher rate of set-up (A = 0.15) was observed for this layer compared to layer 4 (A = 0.15). Similar behavior was also observed for layer 8 of TP-1 as depicted in Figure 36d.

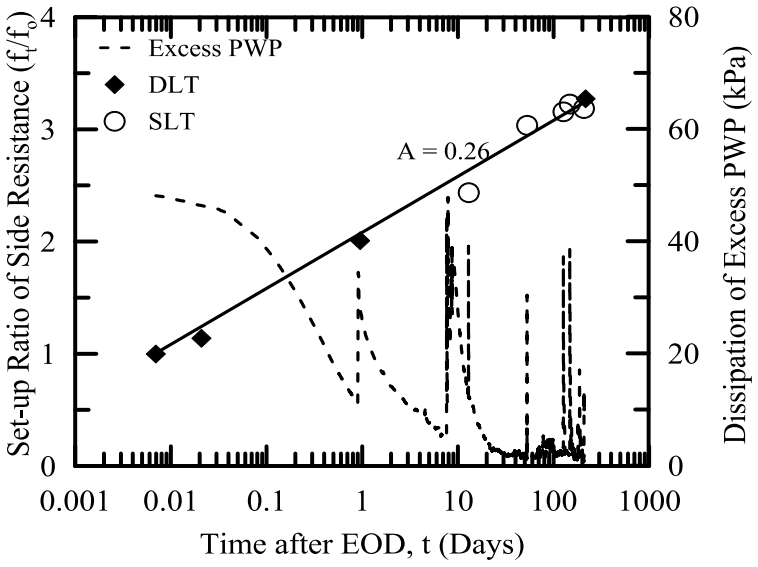

(a) Layer 2

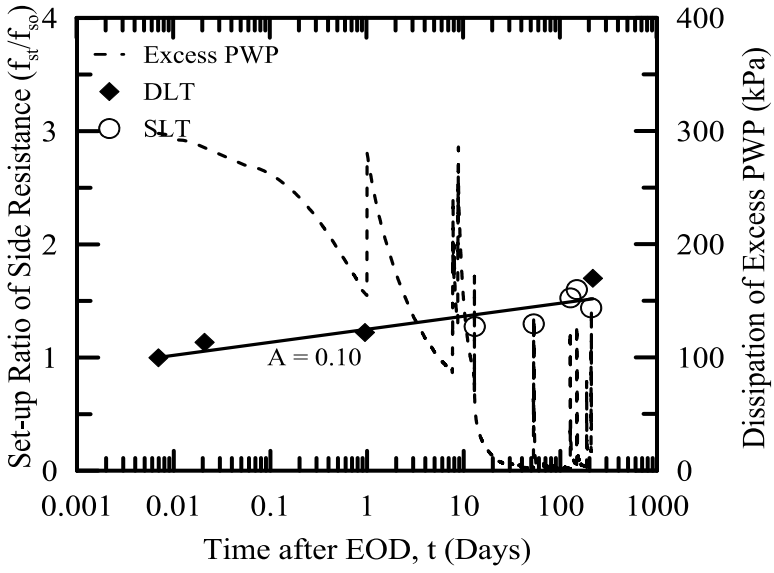


(b) Layer 4

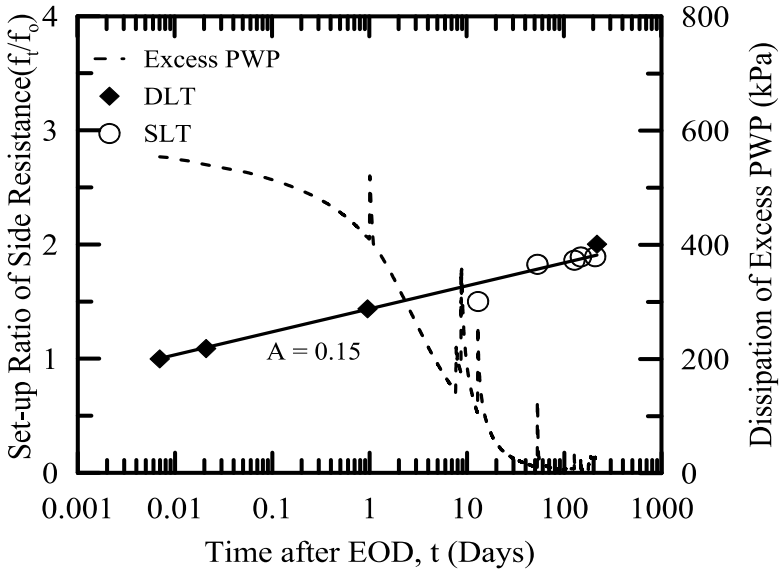


(c) Layer 6

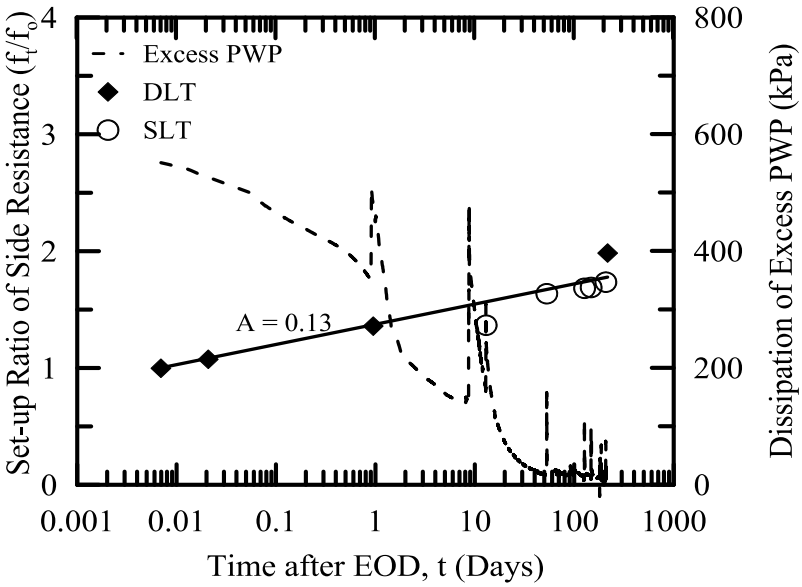


(d) Layer 8

**Figure 36**
**Set-up of individual soil layers and correlation with dissipation of excess PWP for TP-1 of Bayou Lacassine site**

**Soil Layers along Test Pile-2 (TP-2).** The side resistance of individual soil layers of TP-2 is tabulated in Table 7. The $S_u$ measured from UU test for layer 2 was the lowest among all the soil layers of TP-2. $S_u$ for this layer was 0.45 tsf (43.1 kPa), which helped to exhibit the highest amount of set-up. The final restrike at 23 days after EOD showed that the side resistance was 2.8 times higher than the EOD side resistance for this layer. Layers 4, 5, 7, and 8 exhibited closer amount of set-up. The side resistances during the last restrike (23 days after EOD) were 1.8, 1.9, 1.9 and 2.0 times higher than the EOD side resistances for layers 4, 5, 7, and 8, respectively. The $S_u$ for these layers varied from 0.55 tsf (52.7 kPa) to 1.10 tsf (105.3 kPa). The UU test revealed that the $S_u$ was higher [1.60 tsf (153.2 kPa)] for layer 6 compared to the all other soil layers along the length of TP-2; and thus set-up was lower for this layer. The side resistance was only 1.3 times higher than the EOD resistance for layer 6 during the last DLT (23 days after EOD). It should be noted here that, the side resistances calculated for TP-2 was only from the CAPWAP analyses, since the TP-2 was not instrumented.

**Table 7**

**Set-up information for individual soil layers for TP-2 of Bayou Lacassine site**

| Events | Time (Days) | 1st Layer | 2nd Layer | | 3rd Layer | | 4th Layer | | 5th Layer | | 6th Layer | | 7th Layer | | 8th layer | |
|---|---|---|---|---|---|---|---|---|---|---|---|---|---|---|---|---|
| | | | Res. kN (kips) | Set-up Ratio | Res. kN (kips) | Set-up Ratio | Res. kN (kips) | Set-up Ratio | Res. kN (kips) | Set-up Ratio | Res. kN (kips) | Set-up Ratio | Res. kN (kips) | Set-up Ratio | Res. kN (kips) | Set-up Ratio |
| EOD | - | Casing | 157 (35) | 1.0 | 239 (54) | 1.0 | 312 (70) | 1.0 | 127 (29) | 1.0 | 279 (63) | 1.0 | 168 (38) | 1.0 | 90 (20) | 1.0 |
| 1st DLT | 0.02 | | 174 (39) | 1.1 | 269 (60) | 1.1 | 373 (84) | 1.2 | 148 (33) | 1.2 | 290 (65) | 1.0 | 176 (40) | 1.0 | 104 (23) | 1.2 |
| 2nd DLT | 1 | | 336 (76) | 2.1 | 465 (105) | 1.9 | 524 (118) | 1.7 | 209 (47) | 1.6 | 354 (80) | 1.3 | 282 (63) | 1.7 | 132 (30) | 1.5 |
| 1st SLT | 22 | | Not Instrumented | | | | | | | | | | | | | |
| 3rd DLT | 23 | | 438 (98) | 2.8 | 614 (138) | 2.6 | 571 (128) | 1.8 | 243 (55) | 1.9 | 365 (82) | 1.3 | 324 (73) | 1.9 | 178 (40) | 2.0 |
| Set-up parameter "A" | | | 0.27 | | 0.23 | | 0.16 | | 0.17 | | 0.08 | | 0.19 | | 0.18 | |

**Soil Layers along Test Pile-3 (TP-3):** The side resistance of individual soil layers of TP-3 for Bayou Lacassine is tabulated in Table 8. The soil layers along the length of TP-3 exhibited very slow rate of set-up after the first SLT (15 days after EOD). The dissipation of excess PWP for layers 3, 4, 6, and 7 of TP-3 and the corresponding increase in side resistance are presented in Figure 37a, Figure 37b, Figure 37c, and Figure 37d, respectively. Piezometers for TP-3 recorded faster dissipation of excess PWPs compared to piezometers for TP-1 due to higher permeability and higher $c_v$ value. It can be seen from Figure 37a that 4.30 tsf (412 kPa) of peak excess PWP was generated during driving in layer 3 of TP-3 and that 99% dissipation of excess PWP was completed in 57 days after EOD. This slower dissipation rate of excess PWP for layer 3 was mainly due to lower permeability ($k_h = 0.2 \times 10^{-8}$ cm/sec) and lower $c_h$ ($c_h = 5.3 \times 10^{-4}$ cm$^2$/sec) compared to the other soil layers of TP-3, which contributed to the significant increase in side resistance and higher set-up rate (A = 0.27) for layer 3. Figure 37b showed that 2.74 tsf (262 kPa) of peak excess PWP was generated in layer 4 and that 99% of this excess PWP was dissipated in only 19 days after EOD, mainly due to relatively higher permeability ($k_h = 47.3 \times 10^{-8}$ cm/sec) and higher $c_h$ ($c_h = 3.3 \times 10^{-2}$ cm$^2$/sec). The high permeability ($k_h = 79.7 \times 10^{-8}$ cm$^2$/sec) and the presence of silt and sand, contributed to the fast dissipation of excess PWP, and hence relaxation or constant resistance of layer 6 after the first SLT (Figure 37c). The side resistance for layer 6 during the first SLT (15 days after EOD) was 1.3 times higher than the EOD side resistance; however, it reduced to 1.04 times higher compared to EOD side resistance during the final DLT (181 days after EOD). The piezometer installed in layer 7 (Figure 37d)

exhibited faster dissipation of excess PWP thus relatively slow set-up rate (A = 0.14) was observed for this layer. However, layer 6 experienced a significant reduction in side resistance (or relaxation) after the first SLT, which resulted on no more set-up and almost constant total resistance for TP-3 after the 1st SLT.

**Table 8**

**Set-up information for individual soil layers for TP-3 of bayou Lacassine site**

| Events | Time (Days) | 1st Layer | 2nd Layer | | 3rd Layer | | 4th Layer | | 5th Layer | | 6th Layer | | 7th Layer | | 8th layer | |
|---|---|---|---|---|---|---|---|---|---|---|---|---|---|---|---|---|
| | | | Res. kN (kips) | Set-up Ratio | Res. kN (kips) | Set-up Ratio | Res. kN (kips) | Set-up Ratio | Res. kN (kips) | Set-up Ratio | Res. kN (kips) | Set-up Ratio | Res. kN (kips) | Set-up Ratio | Res. kN (kips) | Set-up Ratio |
| EOD | - | Casing | 133 (30) | 1.0 | 128 (29) | 1.0 | 179 (40) | 1.0 | 144 (32) | 1.0 | 637 (143) | 1.0 | 229 (52) | 1.0 | 45 (10) | 1.0 |
| 1st DLT | | | 271 (61) | 2.0 | 162 (36) | 1.3 | 180 (40) | 1.0 | 205 (46) | 1.4 | 673 (151) | 1.1 | 302 (68) | 1.3 | 58 (13) | 1.3 |
| 2nd DLT | 1 | | 339 (76) | 2.6 | 226 (51) | 1.8 | 221 (50) | 1.2 | 241 (54) | 1.7 | 716 (161) | 1.1 | 363 (82) | 1.6 | 65 (15) | 1.4 |
| 1st SLT | 15 | | 547 (123) | 4.1 | 360 (81) | 2.8 | 322 (72) | 1.8 | 384 (86) | 2.7 | 840 (189) | 1.3 | 527 (118) | 2.3 | 120 (27) | 2.7 |
| 2nd SLT | 29 | | 556 (125) | 4.2 | 378 (85) | 2.9 | 338 (76) | 1.9 | 382 (86) | 2.6 | 690 (155) | 1.1 | 444 (100) | 1.9 | 121 (27) | 2.7 |
| 3rd SLT | 93 | | 559 (126) | 4.2 | 380 (85) | 2.9 | 345 (78) | 1.9 | 389 (87) | 2.7 | 576 (129) | 0.9 | 447 (101) | 1.9 | 125 (28) | 2.8 |
| 4th SLT | 129 | | 564 (127) | 4.2 | 384 (86) | 3.0 | 347 (78) | 1.9 | 391 (88) | 2.7 | 525 (118) | 0.8 | 449 (101) | 1.9 | 126 (28) | 2.8 |
| 5th SLT | 175 | | 577 (130) | 4.3 | 393 (88) | 3.1 | 346 (78) | 1.9 | 418 (94) | 2.9 | 578 (130) | 0.9 | 454 (102) | 1.9 | 130 (29) | 2.9 |
| 3rd DLT | 181 | | 479 (108) | 3.6 | 425 (95) | 3.3 | 310 (70) | 1.7 | 380 (85) | 2.6 | 661 (149) | 1.0 | 464 (104) | 2.0 | 137 (31) | 3.0 |
| Set-up parameter "A" | | | 0.26 | | 0.27 | | 0.17 | | 0.22 | | 0.00 | | 0.14 | | 0.26 | |

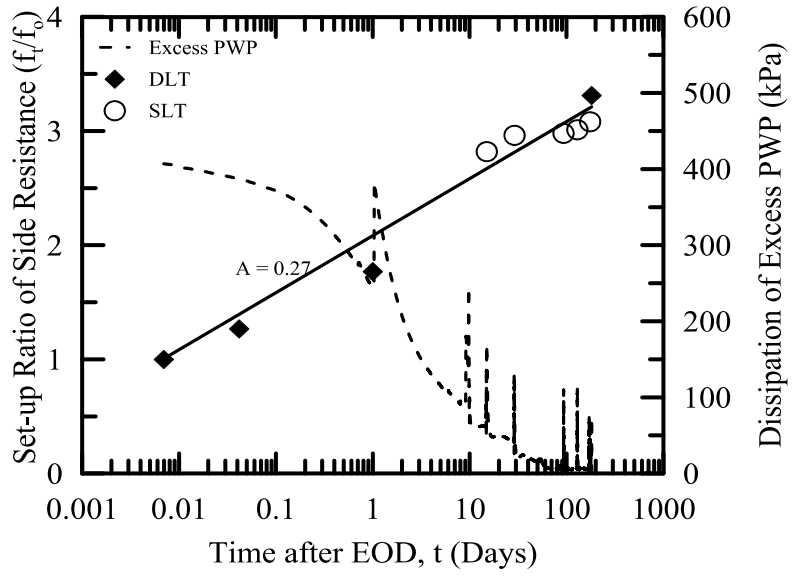


(a) Layer 3

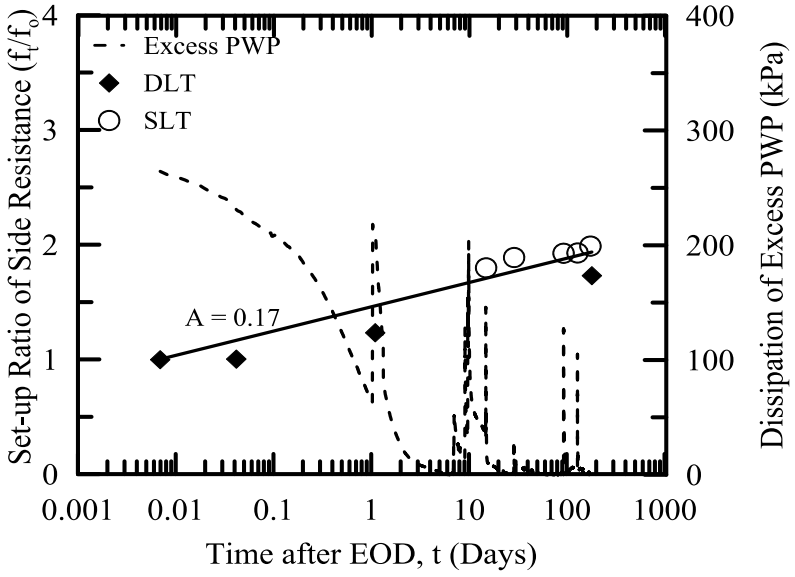


(b) Layer 4

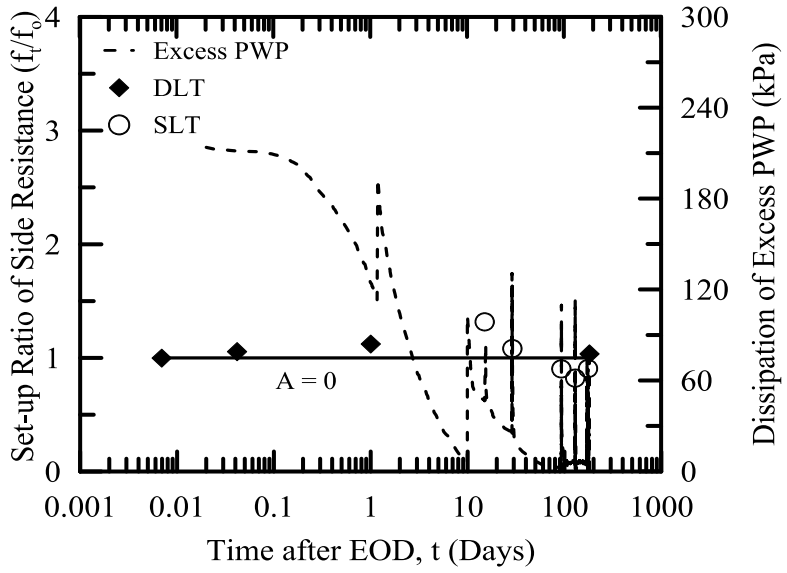


(c) Layer 6

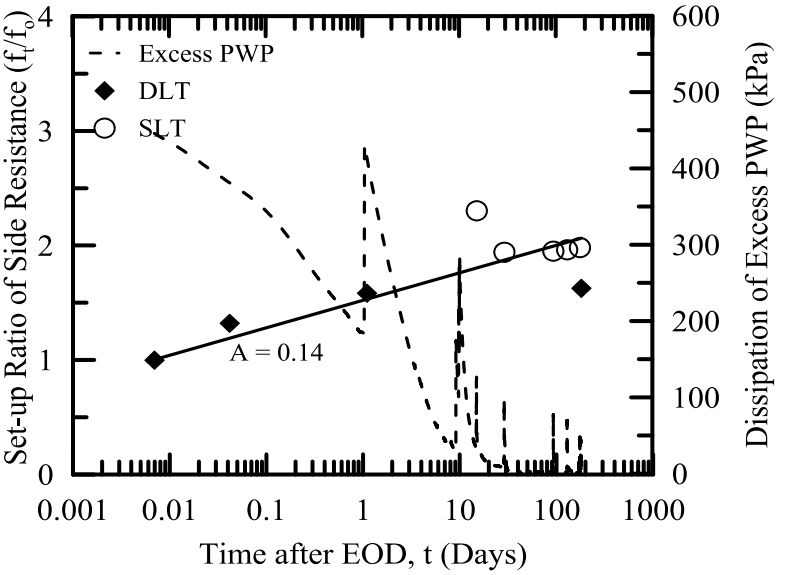


(d) Layer 7

**Figure 37**
**Set-up of individual soil layers and correlation with dissipation of excess PWP for TP-3 of Bayou Lacassine site**

**Horizontal Effective Stress Analyses and Corresponding Set-up.** Figure 38 shows that the horizontal effective stress increased with time in each soil layer along the instrumented test piles (i.e., TP-1 and TP-3). The rate of increase was faster until the dissipation of excess PWP was completed. The pressure cells installed in layers 4 and 6 of TP-1 exhibited increase in

horizontal effective stresses by 201% and 164%, respectively, after six months from EOD. However, the 99% dissipation of excess PWP for layers 4 and 6 was completed in 35 and 53 days after EOD, respectively. The corresponding horizontal effective stress of those layers during the same period was increased by 181% and 155%, respectively. It may be postulated that the remaining increase of 20% and 9% can be attributed to aging effect. Similar behavior was also observed in the effective stress analyses for TP-3. The horizontal effective stresses were increased significantly for layers 3 and 7 of TP-3 until the consolidation process was completed. An increase in horizontal effective stress of 3% and 6% was observed after 99% dissipation of excess PWP for layers 3 and 7 of TP-3, respectively. In contrast, layer 6 of TP-3 exhibited the lowest increase (24%) in horizontal effective stress, and slight relaxation was observed in side resistance of this layer at later stages. Close proximity of silty-sandy interlayer and high permeability contributed to this behavior. Measurements of all pressure cells installed in clayey soil layers for both test piles demonstrated significant increase in horizontal effective stresses during the consolidation period. However, the pressure cells installed in sandy-silty layers did not exhibit noticeable increase in horizontal effective stress.

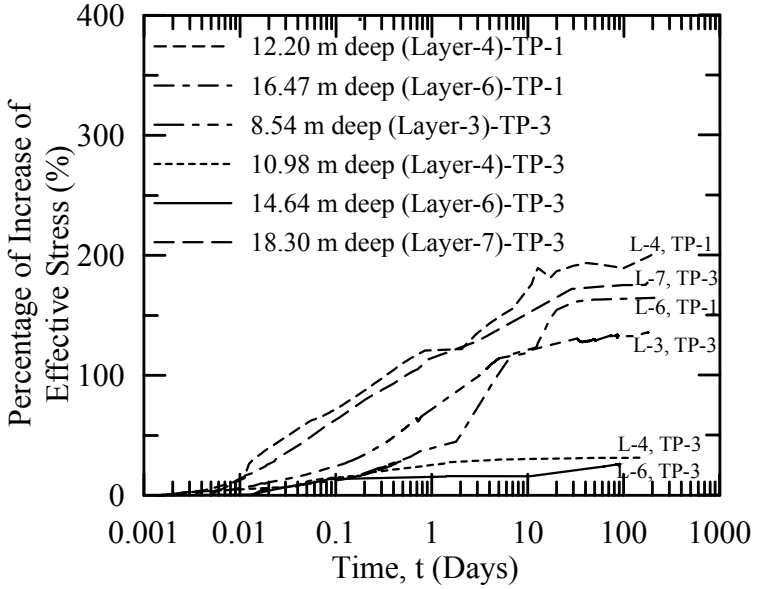


**Figure 38**

**Horizontal effective stress analyses for instrumented test piles for Bayou Lacassine site**

**Distribution of Excess PWP in the Remolded Zone.** In order to identify the remolded zone caused by pile driving in addition to the consolidation process, the piezometers installed in the surrounding soil and on faces of the instrumented piles were monitored continuously for the Bayou Lacassine site. During pile driving, the piezometers installed on the pile face exhibited the maximum excess PWP followed by an exponential decay with radial distance from pile face

(Figure 39). The values of excess PWP presented in this figure were recorded 30 minutes after EOD. The figure shows that the measured excess PWP due to pile driving decreased rapidly with the increase in radial distance from pile face. The figure also demonstrates that the influence zone due to pile driving extended beyond the 3B radial distance from pile face (B was the width of the pile).

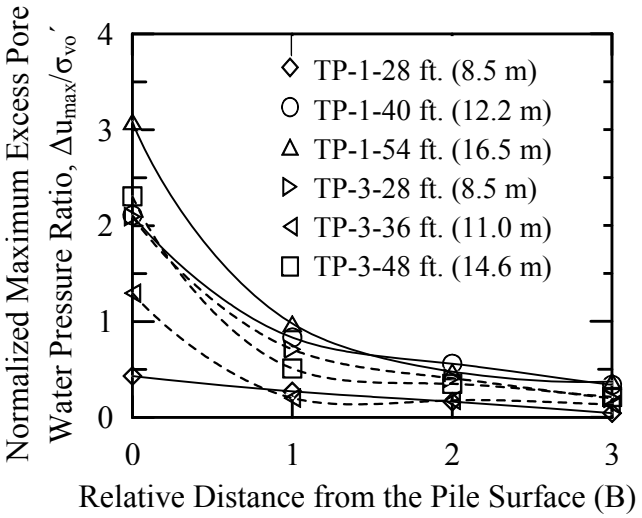


**Figure 39**
**Excess PWP distributions with the distance after EOD in Bayou Lacassine site**

**Bayou Teche Site**

A load test program was conducted at the Bayou Teche site to evaluate the set-up. The load test program consisted of four DLTs after EOD and one SLT. The set-up results of the test pile at Bayou Teche site are presented in Table 9. Both the total ($R_t$) and side ($R_s$) resistance increased with time after EOD. The set-up ratio of side resistance ($R_s/R_{so}$) and total resistance ($R_t/R_{to}$) are also tabulated in Table 9 for each load test. The set-up plot for total resistances ($R_t$) and side resistances ($R_s$) are depicted in Figure 40a and Figure 40b, respectively.

**Table 9**
**Pile set-up information of Bayou Teche bridge site**

| Events | Time | Side Resistance $R_s$ | | Tip Resistance | | Total Resistance $R_t$ | | EMX kN-m (kip-ft.) | Set Per Blow mm (in) |
|---|---|---|---|---|---|---|---|---|---|
| | Days | kN (kips) | Ratio ($R_s/R_{so}$) | kN (kips) | Ratio | kN (kips) | Ratio ($R_t/R_{to}$) | | |
| EOD | - | 422 (95) | 1.0 | 1106 (249) | 1.0 | 1528 (344) | 1.0 | 20.4 | 5.1 (0.20) |
| 1st DLT | 0.04 | 507 (114) | 1.2 | 1088 (245) | 1.0 | 1595 (359) | 1.0 | 21.9 | 5.1 (0.20) |
| 2nd DLT | 1 | 605 (136) | 1.4 | 1128 (254) | 1.0 | 1733 (390) | 1.1 | 27.7 | 4.1 (0.16) |
| 3rd DLT | 7 | 702 (158) | 1.6 | 996 (224) | 0.9 | 1698 (382) | 1.1 | 28.7 | 5.1 (0.20) |
| 4th DLT | 32 | 805 (181) | 1.9 | 872 (196) | 0.8 | 1677 (377) | 1.1 | 27.5 | 8.4 (0.33) |
| SLT | 26 | - | - | - | - | 1806 (407) | 1.2 | - | - |

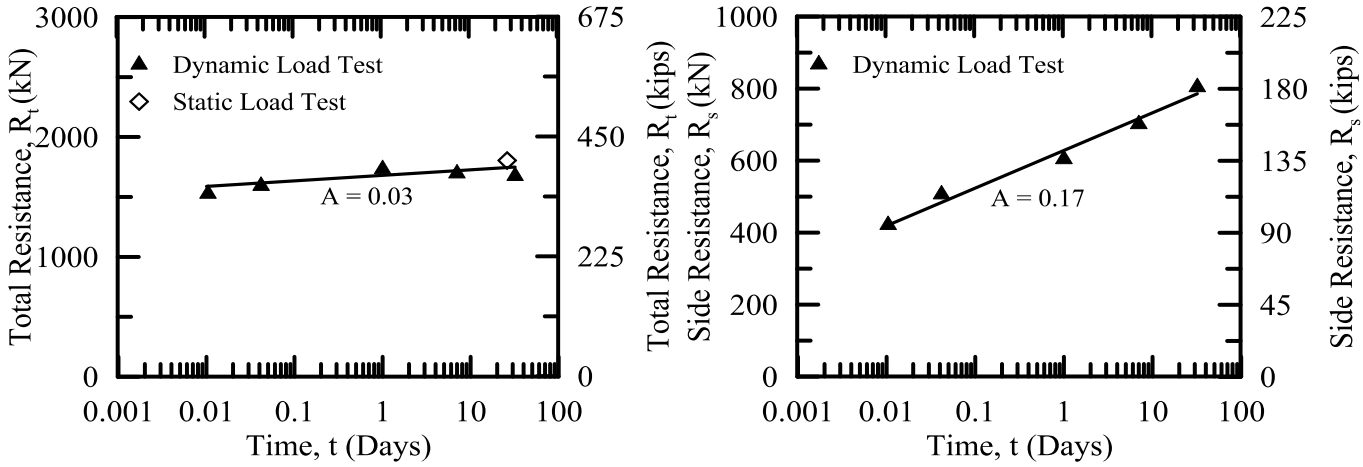


(a) Total resistance ($R_t$) versus elapsed time (b) Side resistance ($R_s$) versus elapsed time

**Figure 40**
**Set-up results for Bayou Teche site**

**Set-up of Total Pile Resistance**

**Dynamic Load Test (DLT).** Four high strain DLTs were carried out on the test pile at different time intervals from 1 hour after EOD, up to a maximum of 32 days. The time intervals of conducting the DLTs and corresponding total, side, and tip resistances are tabulated in Table 9 for the test pile. The test results showed that a significant increase in side resistance for the test pile started immediately after driving. The first restrike, which was conducted within 1 hour after EOD on the test pile, showed that the side resistance was increased by 20% compared to EOD side resistance. Initial excess pore water dissipation and thixotropic effect may contribute to this significant amount of set-up over a very short time period. The final restrike (32 days after EOD) showed that the total resistance was 1.1 times higher compared to the EOD total resistance. The final restrike demonstrated that the side resistance was increased by 90% as compared to EOD values.

**Static Load Test (SLT).** One SLT was conducted on the test pile 26 days after EOD in accordance with ASTM Standard D1143 *[75]*. Figure 41 presents the measured load settlement plot for the test pile. The ultimate resistance of the test pile was calculated using the modified Davisson interpretation method; the value of total resistance ($R_t$) is presented in Table 9 *[79]*. The result showed that the total pile resistance ($R_t$) increased by approximately 18% during the SLT (26 days after EOD).

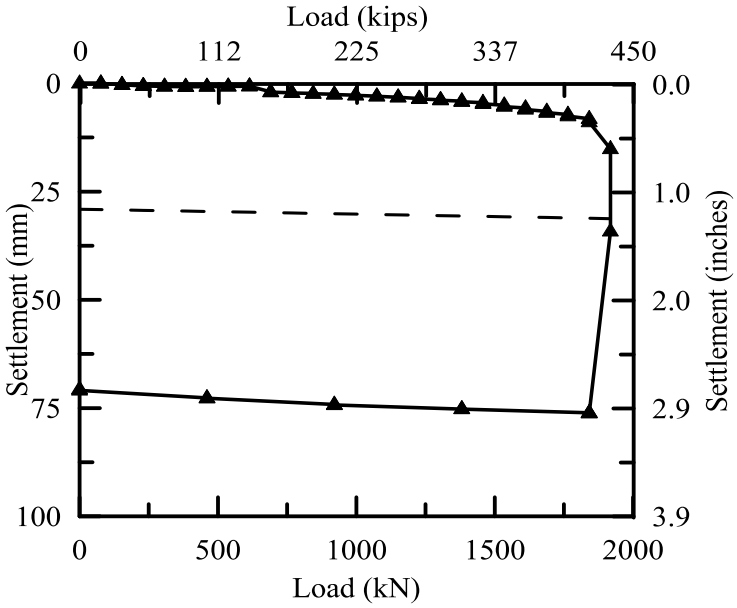


**Figure 41**

**Load settlement plot for the test pile of Bayou Teche site**

**Set-up of Individual Soil Layers**

In an attempt to study the influence of soil type to the set-up behavior, the soil profiles along the piles were broken down into individual soil layers. The resistance distributions of DLTs were analyzed using the CAPWAP analyses. The calculated side resistances for individual soil layers and corresponding set-up ratios with time are tabulated in Table 10. The set-up behavior for clayey and sandy soil layers are depicted in Figure 42a and Figure 42b, respectively.

Layers 2, 3, and 4 represented the clayey soil layers of the test pile for Bayou Teche site. The set-up behavior of clayey soil layers is depicted in Figure 42a. The maximum amount of set-up and logarithmic rate of set-up "A" was observed for layer 4 and the minimum amount of set-up was exhibited by layer 3 among the clayey soil layers. The DLT performed 32 days after EOD showed that the side resistances were 6.2 and 7.6 times higher compared to the EOD side resistances for layers 2 and 4, respectively. The set-up parameters for layers 2, 3, and 4 were 0.37, 0.29, and 0.40, respectively. The low $S_u$ [0.17 tsf (17 kPa)] and high PI (52%) as compared to other clayey soil layers may contributed to the higher amount and rate of set-up behavior for layer 4.

The sandy soil layers exhibited smaller amount of set-up than the clayey soil layers. Layers 5, 6, and 7 represented the sandy soil layers in this study. The set-up behavior of sandy soil layers are depicted in Figure 42b. It is observed from Figure 42b and Table 10 that all sandy soil layers exhibited smaller amounts and rates of set-up compared to the clayey soil layers.

**Table 10**

**Set-up information for individual soil layers for Bayou Teche test pile**

| Events | Time (Days) | 1st Layer | 2nd Layer | | 3rd Layer | | 4th Layer | | 5th Layer | | 6th Layer | | 7th Layer | |
|---|---|---|---|---|---|---|---|---|---|---|---|---|---|---|
| | | | Res. kN (kips) | Set-up Ratio | Res. kN (kips) | Set-up Ratio | Res. kN (kips) | Set-up Ratio | Res. kN (kips) | Set-up Ratio | Res. kN (kips) | Set-up Ratio | Res. kN (kips) | Set-up Ratio |
| EOD | - | Casing | 17 (4) | 1.0 | 49 (11) | 1.0 | 22 (5) | 1.0 | 111 (25) | 1.0 | 89 (20) | 1.0 | 134 (30) | 1.0 |
| 1st DLT | 0.04 | | 44 (10) | 2.6 | 76 (17) | 1.5 | 49 (11) | 2.3 | 111 (25) | 1.0 | 93 (21) | 1.0 | 134 (30) | 1.0 |
| 2nd DLT | 1 | | 52 (12) | 3.0 | 111 (25) | 2.3 | 107 (24) | 4.8 | 112 (25) | 1.0 | 94 (21) | 1.0 | 129 (29) | 1.0 |
| 3rd DLT | 7 | | 82 (18) | 4.7 | 130 (30) | 2.7 | 142 (32) | 6.5 | 120 (27) | 1.1 | 94 (21) | 1.0 | 134 (30) | 1.0 |
| 4th DLT | 32 | | 107 (24) | 6.2 | 169 (38) | 3.5 | 169 (38) | 7.6 | 133 (30) | 1.2 | 94 (21) | 1.0 | 133 (30) | 1.0 |
| Set-up parameter "A" | | | 0.37 | | 0.29 | | 0.40 | | 0.10 | | 0.03 | | 0.02 | |

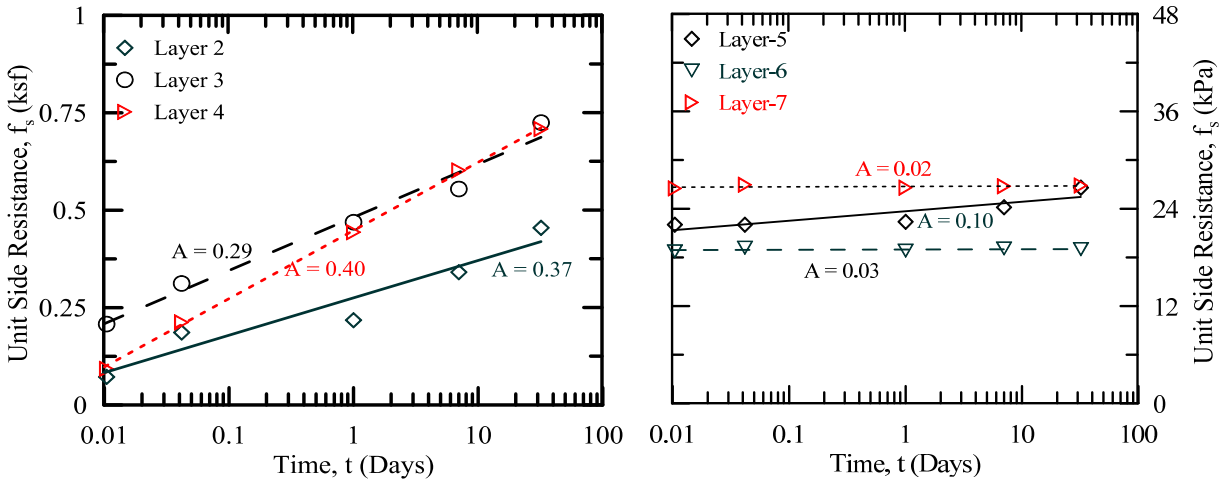


(a) Clayey soil layers (b) Sandy soil layers

**Figure 42**

**Set-up behavior of individual soil layers for the test pile of Bayou Teche site**

### Bayou Bouef Site

The pile resistances were measured at different time intervals after EOD for the Bayou Bouef bridge site in order to measure the pile set-up. The load test program included one DLT at 1 day after EOD and five Osterberg Cell load tests (OCLT) that were performed over a two year period after the DLT was performed. Both total ($R_t$) and side ($R_s$) resistances increased with time after EOD. The set-up ratio of side ($R_s/R_{so}$) and total ($R_t/R_{to}$) resistances are also tabulated in Table 11

for each load test. The total side resistances shown in Table 11 are plotted with respect to time in Figure 43a and Figure 43b, respectively.

**Table 11**
**Set-up information of Bayou Bouef test site**

| Events | Time | Side Resistance $R_s$ | | Tip Resistance $R_{tip}$ | | Total Resistance $R_t$ | | Set Per Blow mm (in.) |
|---|---|---|---|---|---|---|---|---|
| | Days | kN (kips) | Ratio ($R_s/R_{so}$) | kN (kips) | Ratio | kN (kips) | Ratio ($R_t/R_{to}$) | |
| EOD | - | 1254 (282) | 1.0 | 1750 (394) | 1.0 | 3004 (676) | 1.0 | - |
| 1st DLT | 1 | 1939 (436) | 1.5 | 1789 (402) | 1.0 | 3728 (838) | 1.2 | 4.1 (0.16) |
| 1st OCLT | 7 | 3281 (738) | 2.6 | 1803 (406) | 1.0 | 5084 (1144) | 1.7 | |
| 2nd OCLT | 14 | 3707 (833) | 3.0 | 1810 (407) | 1.0 | 5517 (1240) | 1.8 | |
| 3rd OCLT | 28 | 4126 (928) | 3.3 | 1800 (406) | 1.0 | 5926 (1334) | 2.0 | |
| 4th OCLT | 247 | 4758 (1070) | 3.8 | | | | | |
| 5th OCLT | 716 | 4758 (1070) | 3.8 | | | | | |

**Set-up of Total Pile Resistance ($R_t$)**

**Dynamic Load Test (DLT).** Two DLTs were conducted and CAPWAP analyses were performed on dynamic data recorded with the Pile Driving Analyzer (PDA) for the EOD and the 1 day restrike. The DLT was performed in general accordance with ASTM standard D 4945 [*74*]. The DLT performed at 1 day exhibited a 50% increase in side resistance ($R_s$) compared to the EOD side resistance. The tip resistance was almost constant during this period.

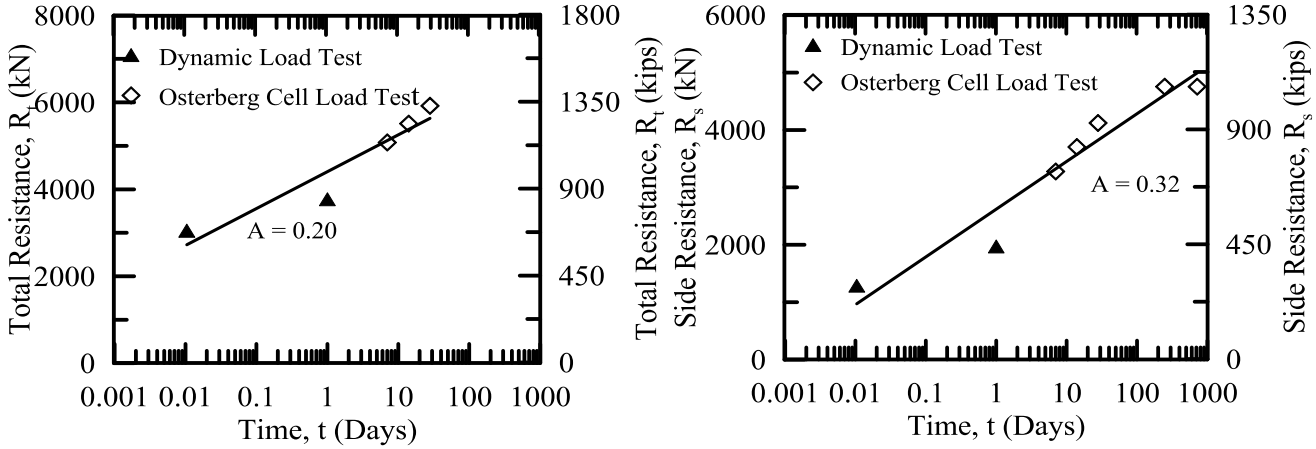


(a) Total resistance ($R_t$) versus elapsed time

(b) Side resistance ($R_s$) versus elapsed time

**Figure 43**
**Set-up results of Bayou Bouef site**

**Osterberg Cell Load Test (OCLT).** Five Osterberg cell load tests (OCLT) were conducted on the test pile starting from 7 days after EOD to 2 years. The O-cell was driven in a fully closed condition. The peak side resistances from OCLT had been used to evaluate the increase in pile side resistance. All load tests conducted with the Osterberg cell failed in side resistance. Full tip resistance was not mobilized during any of the OCLTs. The osterberg cell load settlement plots for tests 1 and 3 are presented in Figure 44a and Figure 44b, respectively. The side resistances measured by OCLT are plotted with logarithmic of time in Figure 43b and exhibited a relatively high (i.e., 0.89) coefficient of correlation ($R^2$) suggesting a logarithmic time relationship exist for side resistance similar to the model proposed by Skov and Denver *[7]*. The side resistance ($R_s$) increased by 196% from the EOD to the typical load testing time at 14 days after EOD and the total resistance was 1.8 times higher compared to the EOD total resistance. The dissipation of excess PWP and thixotropic effect may contribute to this higher rate and amount of set-up at early stage. However, a further 28% increase in side resistance was observed between the $2^{nd}$ OCLT and $4^{th}$ OCLT. This slower rate and amount of set-up after the $2^{nd}$ OCLT may be due to aging effect. However, no set-up was observed for side resistance in between the fourth and fifth OCLT which implies that after a certain time aging had also no effect on set-up. The tip resistances remained constant during the testing period. The load distribution plots for first and third OCLT are depicted in Figure 45a and Figure 45b, respectively. In order to capture the strain gage measurements for every incremental load during OCLTs, the data acquisition system was set to collect the data at two minute intervals during each OCLT. The load distribution plots indicate increasing axial resistance as the depth increases, as expected from the soil boring data. The load distribution plots were used to calculate the side resistance of individual soil layers.

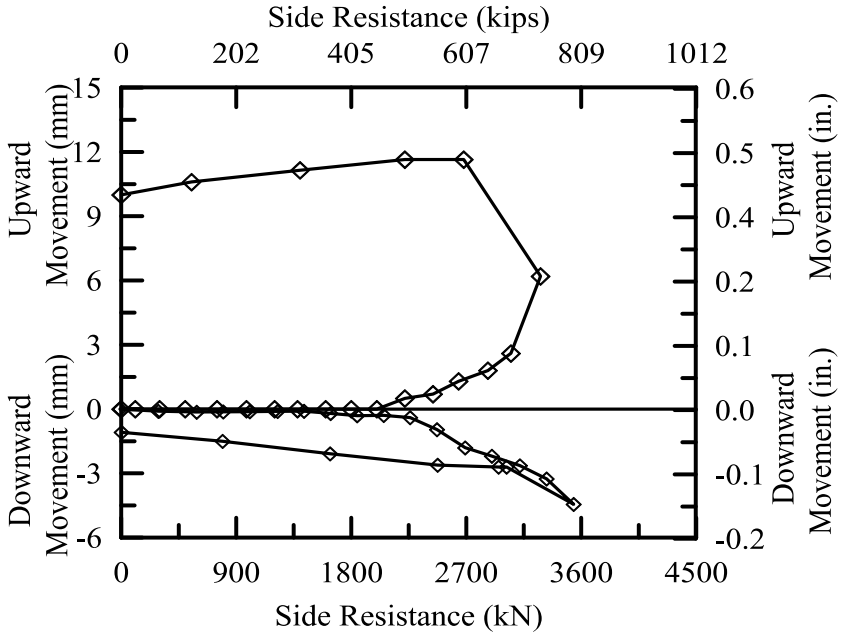


(a) 1st OCLT

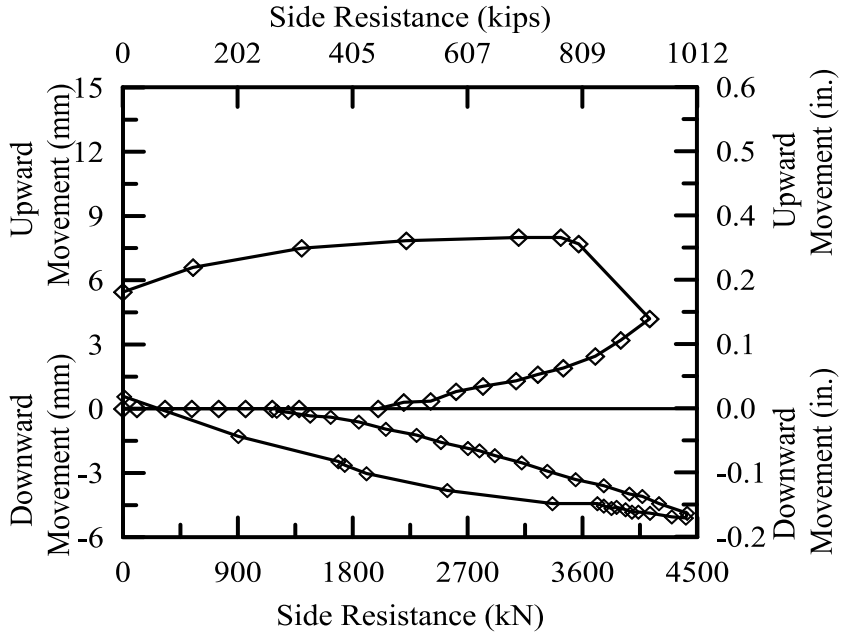


(b) 3rd OCLT

**Figure 44**
**Load settlement plots for the test pile of Bayou Bouef site**

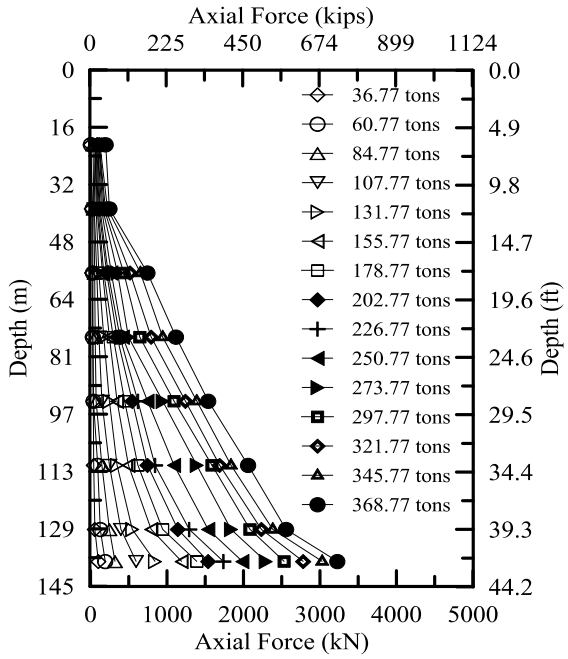


(a) 1st OCLT

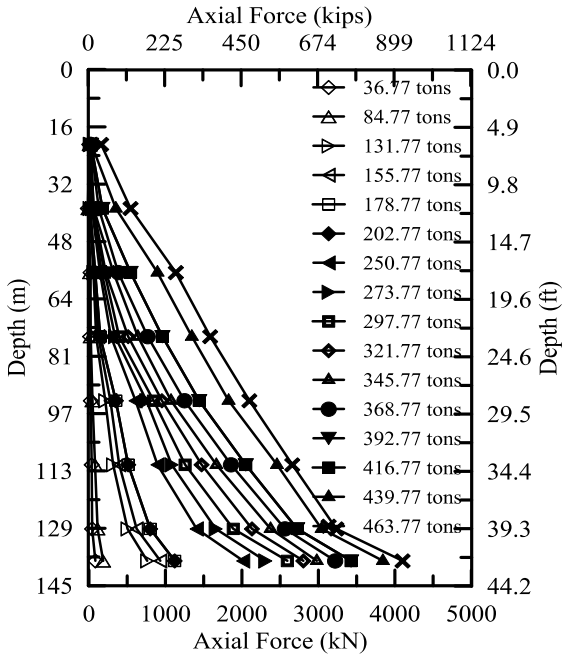


(b) 3rd OCLT

**Figure 45**

**Load distribution plots for the Osterberg cell load test of test pile for Bayou Bouef**

**Set-up of Individual Soil Layers**

The CAPWAP analyses distribution from DLTs and load transfer distribution from OCLTs were used to estimate the side resistance for individual soil layers along the length of the pile. The set-up behavior of clayey and sandy soil layers are depicted in Figure 46a and Figure 46b, respectively. Layers 3 and 6 represented the sandy soil layers along the length of the test pile. Clayey soil layers exhibited higher amount of set-up compared to the sandy soil layers with the exception of layer 6. The set-up ratios of clayey soil layers (i.e., Layers 1, 2, 4, and 5) during the third OCLT were 4.4, 3.6, 3.0, and 4.2 times higher compared to the EOD side resistance. The back-calculated logarithmic "A" parameter for layers 1, 2, 4 and 5 were 0.29, 0.29, 0.31, and 0.48, respectively. The higher $S_u$ [i.e., 0.67 tsf (63 kPa)] and lower PI (i.e., 39%) for layer 2 compared to the other clayey soil layers contributed to the lower amount and rate of set-up. The higher amount and rate of set-up for layer 5 may be attributed to the lower $S_u$ [i.e. 0.60 tsf (57 kPa)] and higher PI (i.e., 75%) compared to the other clayey soil layers. However, the amount and rate of set-up for the sandy soil layers along the length of the pile for Bayou Bouef site was higher compared to the other sandy soil layers of other project site. The logarithmic "A" parameter for layers 3 and 6 were 0.25 and 0.36, respectively. The presence of smaller amount of fine content may contributed to this behavior.

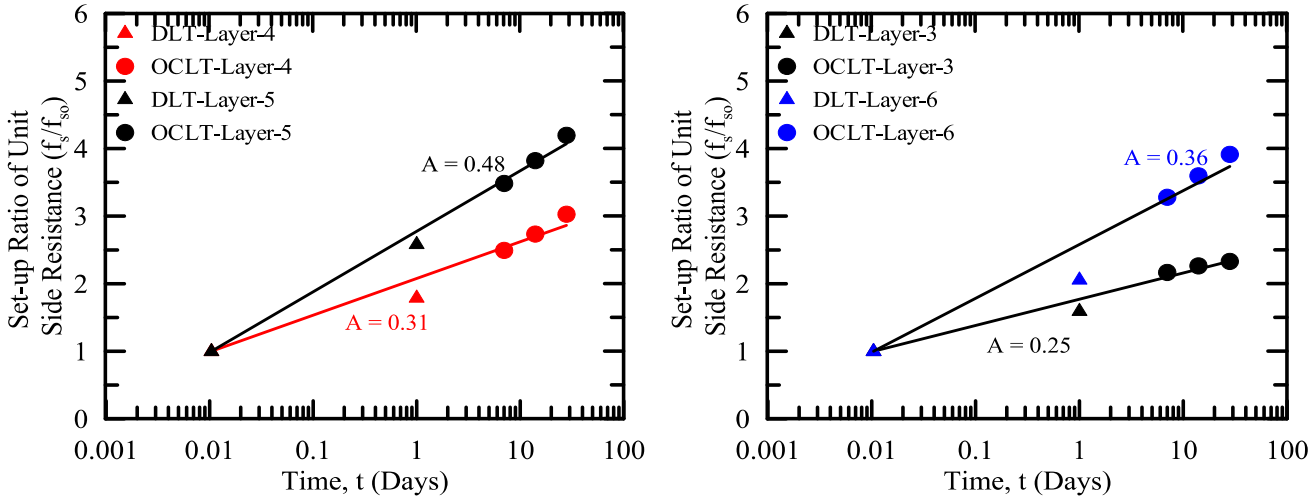


(a) Clayey soil layers

(b) Sandy soil layers

**Figure 46**

**Set-up behavior of individual soil layers for the test pile of Bayou Bouef site**

## LA-1 Site

For estimating the pile set-up, the pile resistances were measured at different time intervals after EOD for LA-1 project. The load test program included several DLTs and one SLT on each test pile. The load test results of TP-2, TP-3, TP-4a, TP-4b, TP-5a, and TP-5b are presented in Table 12, Table 13, Table 14, Table 15, Table 16, and Table 17, respectively. The set-up plots for total resistance ($R_t$) of TP-2, TP-3, TP-4, and TP-5 are depicted in Figure 47a, Figure 47b, Figure 47c, and Figure 47d, respectively. The figure demonstrates that the total resistance as a function of time (t) was best fitted to a logarithmic time scale with a relatively high coefficient of correlation ($R^2$) for all test piles, suggesting a logarithmic time relationship similar to the model proposed by Skov and Denver *[7]*. The logarithmic set-up parameters "A" for the total pile resistance of TP-2, TP-3, TP-4a, TP-4b, TP-5a, and TP-5b were 0.33, 0.25, 0.23, 0.32, 0.18, and 0.31, respectively.

**Table 12**
**Load test results for TP-2**

| Events | Time | Side Resistance, $R_s$ | | Tip Resistance. $R_{tip}$ | | Total Resistance. $R_t$ | |
|---|---|---|---|---|---|---|---|
| | Hours | kN (kips) | Set-up Ratio ($R_s/R_{so}$) | kN (kips) | Set-up Ratio ($R_{tip}/R_{tipo}$) | kN (kips) | Set-up Ratio ($R_t/R_{to}$) |
| EOD | - | 237 (53) | 1.0 | 153 (34) | 1.0 | 390 (87) | 1.0 |
| 1st DLT | 2.2 | 613 (138) | 2.6 | 219 (49) | 1.4 | 832 (187) | 2.1 |
| 2nd DLT | 3.9 | 914 (205) | 3.9 | 144 (32) | 0.9 | 1058 (237) | 2.7 |
| 3rd DLT | 6.0 | 1077 (242) | 4.5 | 161 (36) | 1.1 | 1238 (278) | 3.2 |
| 4th DLT | 21.6 | 1253 (282) | 5.3 | 186 (42) | 1.2 | 1439 (324) | 3.7 |
| 5th DLT | 56.0 | 1317 (296) | 5.6 | 186 (42) | 1.2 | 1503 (338) | 3.9 |
| 6th DLT | 76.9 | 1543 (347) | 6.5 | 167 (37) | 1.1 | 1710 (384) | 4.4 |
| 7th DLT | 96.9 | 1615 (363) | 6.8 | 181 (41) | 1.2 | 1796 (404) | 4.6 |
| Static Test | 168.0 | 1779 (400) | 7.5 | 120 (27) | 0.8 | 1899 (427) | 4.9 |

**Table 13**
**Load test results for TP-3**

| Events | Time | Side Resistance, $R_s$ | | Tip Resistance. $R_{tip}$ | | Total Resistance. $R_t$ | |
|---|---|---|---|---|---|---|---|
| | Hours | kN (kips) | Set-up Ratio ($R_s/R_{so}$) | kN (kips) | Set-up Ratio ($R_{tip}/R_{tipo}$) | kN (kips) | Set-up Ratio ($R_t/R_{to}$) |
| EOD | - | 1678 (377) | 1.0 | 1440 (324) | 1.0 | 3118 (701) | 1.0 |
| 1st DLT | 2.0 | 2340 (526) | 1.4 | 1536 (345) | 1.1 | 3876 (871) | 1.2 |
| 2nd DLT | 23.6 | 2767 (622) | 1.6 | 1731 (389) | 1.2 | 4498 (1011) | 1.4 |
| 3rd DLT | 69.2 | 3318 (746) | 2.0 | 1513 (340) | 1.0 | 4831 (1086) | 1.5 |
| 4th DLT | 162.4 | 4051 (911) | 2.4 | 1090 (245) | 0.8 | 5141 (1156) | 1.6 |
| Static Test | 312.0 | 5067 (1139) | 3.0 | 2318 (521) | 1.6 | 7385 (1660) | 2.4 |

**Table 14**
**Load test results for TP-4a**

| Events | Time | Side Resistance, $R_s$ | | Tip Resistance. $R_{tip}$ | | Total Resistance. $R_t$ | |
|---|---|---|---|---|---|---|---|
| | Hours | kN (kips) | Set-up Ratio ($R_s/R_{so}$) | kN (kips) | Set-up Ratio ($R_{tip}/R_{tipo}$) | kN (kips) | Set-up Ratio ($R_t/R_{to}$) |
| EOD | - | 349 (78) | 1.0 | 422 (95) | 1.0 | 771 (173) | 1.0 |
| 1st DLT | 2.0 | 1540 (346) | 4.4 | 431 (97) | 1.0 | 1971 (443) | 2.6 |
| 2nd DLT | 3.6 | 1983 (446) | 5.7 | 445 (100) | 1.1 | 2428 (546) | 3.1 |
| 3rd DLT | 5.8 | 2084 (469) | 6.0 | 408 (92) | 1.0 | 2492 (561) | 3.2 |
| 4th DLT | 20.6 | 2679 (602) | 7.7 | 408 (92) | 1.0 | 3087 (694) | 4.0 |
| 5th DLT | 44.9 | 2923 (657) | 8.4 | 439 (99) | 1.0 | 3362 (756) | 4.4 |
| 6th DLT | 68.5 | 3064 (689) | 8.8 | 451 (101) | 1.1 | 3515 (790) | 4.6 |
| 7th DLT | 89.2 | 3224 (725) | 9.3 | 459 (103) | 1.1 | 3683 (828) | 4.8 |
| Static Test | 144.0 | 3452 (776) | 9.9 | 378 (85) | 0.9 | 3830 (861) | 5.0 |

**Table 15**
**Load test results for TP-4b**

| Events | Time | Side Resistance, $R_s$ | | Tip Resistance. $R_{tip}$ | | Total Resistance. $R_t$ | |
|---|---|---|---|---|---|---|---|
| | Hours | kN (kips) | Set-up Ratio ($R_s/R_{so}$) | kN (kips) | Set-up Ratio ($R_{tip}/R_{tipo}$) | kN (kips) | Set-up Ratio ($R_t/R_{to}$) |
| EOD | - | 2087 (469) | 1.0 | 1103 (248) | 1.0 | 3190 (717) | 1.0 |
| 1st DLT | 3.1 | 3151 (708) | 1.5 | 1099 (247) | 1.0 | 4250 (955) | 1.3 |
| 2nd DLT | 4.4 | 3217 (723) | 1.5 | 1180 (265) | 1.1 | 4397 (988) | 1.4 |
| 3rd DLT | 6.6 | 3572 (803) | 1.7 | 1100 (247) | 1.0 | 4672 (1050) | 1.5 |
| 4th DLT | 8.4 | 3796 (853) | 1.8 | 1238 (278) | 1.1 | 5034 (1131) | 1.6 |
| 5th DLT | 23.7 | 4282 (963) | 2.1 | 1165 (262) | 1.1 | 5447 (1225) | 1.7 |
| 6th DLT | 48.2 | 4700 (1057) | 2.3 | 1254 (282) | 1.1 | 5954 (1339) | 1.9 |
| 7th DLT | 72.3 | 4989 (1122) | 2.4 | 1229 (276) | 1.1 | 6218 (1398) | 1.9 |
| 8th DLT | 92.9 | 5833 (1311) | 2.8 | 1119 (252) | 1.0 | 6952 (1563) | 2.2 |
| Static Test | 144 | 5829 (1310) | 2.8 | 1538 (346) | 1.4 | 7367 (1656) | 2.3 |

**Table 16**
**Load test results for TP-5a**

| Events | Time | Side Resistance, $R_s$ | | Tip Resistance. $R_{tip}$ | | Total Resistance. $R_t$ | |
|---|---|---|---|---|---|---|---|
| | Hours | kN (kips) | Set-up Ratio ($R_s/R_{so}$) | kN (kips) | Set-up Ratio ($R_{tip}/R_{tipo}$) | kN (kips) | Set-up Ratio ($R_t/R_{to}$) |
| EOD | - | 593 (133) | 1.0 | 196 (44) | 1.0 | 789 (177) | 1.0 |
| 1st DLT | 2.6 | 1259 (283) | 2.1 | 255 (57) | 1.3 | 1514 (340) | 1.9 |
| 2nd DLT | 4.2 | 1457 (328) | 2.5 | 285 (64) | 1.4 | 1742 (392) | 2.2 |
| 3rd DLT | 21.7 | 2170 (488) | 3.7 | 300 (67) | 1.5 | 2470 (555) | 3.1 |
| 4th DLT | 46.6 | 2391 (538) | 4.0 | 251 (56) | 1.3 | 2642 (594) | 3.3 |
| 5th DLT | 70.0 | 2592 (583) | 4.4 | 237 (53) | 1.2 | 2829 (636) | 3.6 |
| % DLT | 90.6 | 2692 (605) | 4.5 | 238 (53) | 1.2 | 2930 (658) | 3.7 |
| Static Test | 144.0 | 3095 (696) | 5.2 | 192 (43) | 1.0 | 3287 (739) | 4.2 |

**Table 17**
**Load test results for TP-5b**

| Events | Time | Side Resistance, $R_s$ | | Tip Resistance, $R_{tip}$ | | Total Resistance, $R_t$ | |
|---|---|---|---|---|---|---|---|
| | Hours | kN (kips) | Set-up Ratio ($R_s/R_{so}$) | kN (kips) | Set-up Ratio ($R_{tip}/R_{tipo}$) | kN (kips) | Set-up Ratio ($R_t/R_{to}$) |
| EOD | - | 1260 (283) | 1.0 | 462 (104) | 1.0 | 1722 (387) | 1.0 |
| 1st DLT | 3.2 | 1999 (449) | 1.6 | 463 (104) | 1.0 | 2462 (553) | 1.4 |
| 2nd DLT | 5.3 | 2059 (463) | 1.6 | 447 (100) | 1.0 | 2506 (563) | 1.4 |
| 3rd DLT | 7.5 | 2183 (491) | 1.7 | 432 (97) | 0.9 | 2615 (588) | 1.5 |
| 4th DLT | 23.6 | 2227 (501) | 1.8 | 501 (113) | 1.1 | 2728 (614) | 1.6 |
| 5th DLT | 48.1 | 2435 (547) | 1.9 | 493 (111) | 1.1 | 2928 (658) | 1.7 |
| 6th DLT | 72.0 | 2582 (580) | 2.0 | 494 (111) | 1.1 | 3076 (691) | 1.8 |
| 7th DLT | 92.2 | 2771 (623) | 2.2 | 451 (101) | 1.0 | 3222 (724) | 1.9 |
| Static Test | 144.0 | 3065 (689) | 2.4 | 374 (84) | 0.8 | 3439 (773) | 2.0 |

**Set-up in Terms of Total Pile Resistance**

**Dynamic Load Test (SLT).** All six test piles were monitored during driving and during the subsequent restrikes using PDA. The monitoring was performed in general accordance with ASTM standard D 4945 [*74*]. To determine the resistance distribution along the length of the pile during the DLTs, Case Pile Wave Analysis Program (CAPWAP) analyses were performed on selected blows at the EOD and the first high energy blow of each restrike event. The CAPWAP side resistances were further broken down into layers that were consistent with the strain gage locations along the pile shaft. The results of CAPWAP analyses indicated an increase in resistance for each restrike event. The change in total ($R_t$), side ($R_s$), and tip ($R_{tip}$) resistances are listed separately to illustrate the different effects of set-up on resistances in Table 12 to Table 17. As is observed from Table 12 to Table 17, the tip resistances were almost constant over the time for all test piles, albeit with some variations from CAPWAP and strain readings. Therefore, it is reasonable to use the side resistance only to analyze the set-up behavior of clayey soils. Due to high initial excess PWP and thixotropic effect, the first DLT that was normally conducted 2 hours after EOD exhibited high amount of set-up on all test piles. The first DLT showed that the side resistances were 2.6, 1.4, 4.4, 1.5, 2.1, and 1.6 times higher than the EOD side resistances for TP-2, TP-3, TP-4a, TP-4b, TP-5a, and TP-5b, respectively. The side resistances at 24 hours were 5.3, 1.6, 7.7, 2.1, 3.7, and 1.8 times higher for TP-2, TP-3, TP-4a, TP-4b, TP-5a, and TP-5b, respectively, as compared to the EOD side resistances. The side resistances were increased by 34%, 46%, 45%, 54%, 41%, and 65% of the total set-up at 2 hours after EOD for TP-2, TP-3, TP-4a, TP-4b, TP-5a, and TP-5b, respectively, as measured by the DLT. The rate became much slower in between the 24 hour's DLT and the SLT that was conducted at 6 days to 13 days after EOD for the different test piles.

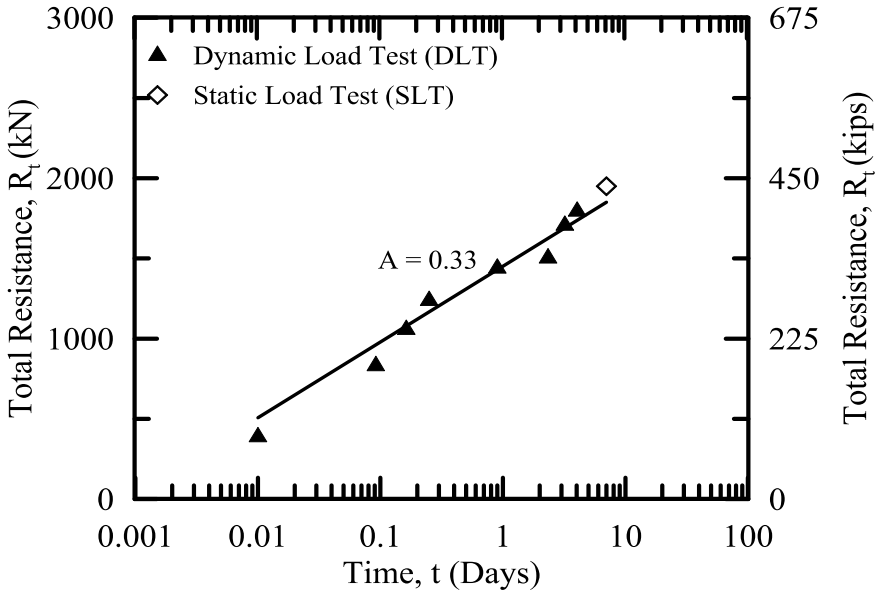


(a) Test Pile-2 (TP-2)

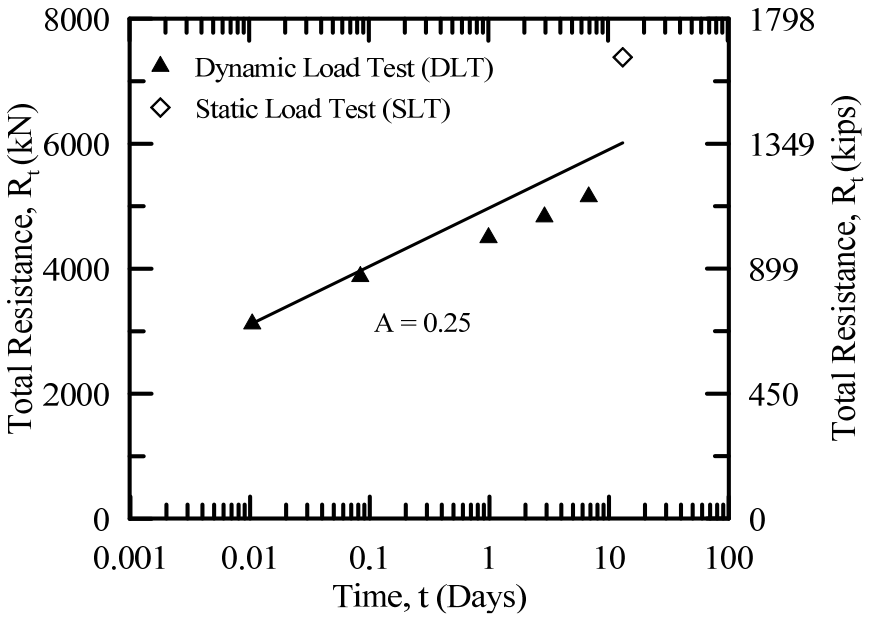


(b) Test Pile-3 (TP-3)

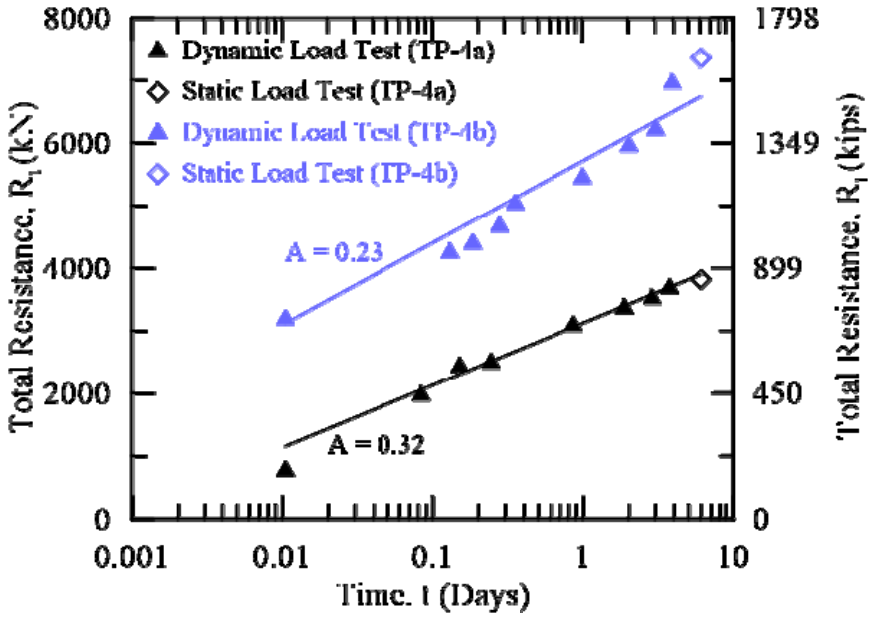


(c) Test Pile-4 (TP-4)

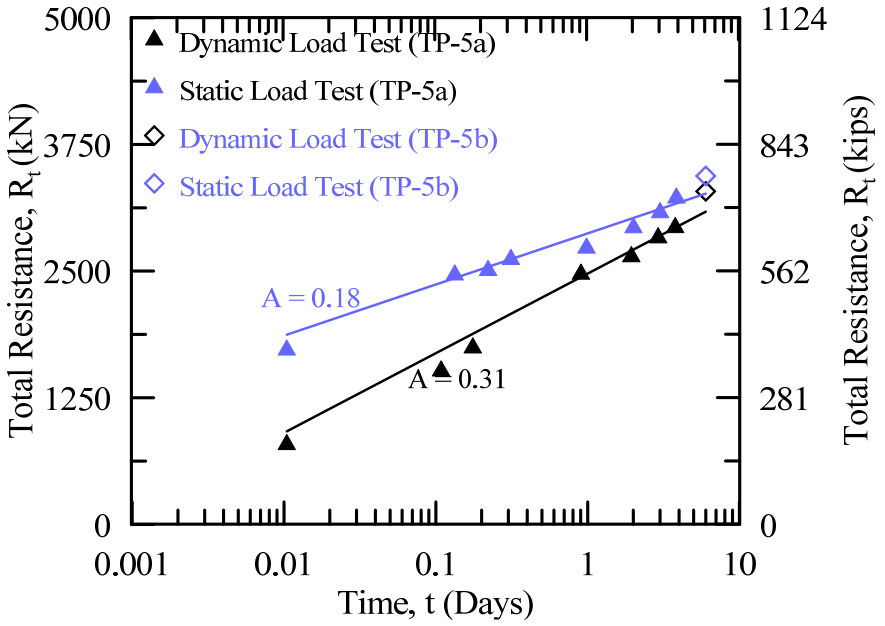


(d) Test Pile-5 (TP-5)

**Figure 47**
**Total pile resistance versus original time elapsed for all test piles of LA-1 site**

**Static Load Test (SLT).** Axial compression SLT was conducted on each test pile. The test loads were applied to the test piles using a 1200 ton capacity hydraulic jack manufactured by Elgood-Mayo Corp. It should be mentioned here that the SLTs for TP-2 and TP-3 were performed using a single loading frame arrangement. However, since at TP-4 and TP-5 locations, two piles were installed in 10 ft. apart, a single load frame was designed to perform the SLT on two piles together.

The test piles were loaded following the quick load test method for individual piles. The load was applied in increments of 10 to 15 % of the proposed design load with a constant time increment of 2.5 minutes between the increments. Load was applied until continuous jacking was required to maintain the test load. After a 5 minute holding period, the applied load was removed in four equal decrements with a 5 minute holding period between decrements so the shape of the rebound curve could be determined.

The SLT results of LA-1 projects are depicted in Figure 48. Based on the Davisson's criteria, the total resistances of the test piles were computed as 427 kips, 1660 kips, 861 kips, 1656 kips, 739 kips, and 773 kips for TP-2, TP-3, TP-4a, TP-4b, TP-5a, and TP-5b, respectively *[79]*. In order to capture the strain gage measurements for every load increment during SLTs, the data acquisition system was set to collect the data at 2.5 minutes intervals. The load distribution plots measured by strain gage during the SLTs for all the test piles are presented in Figure 49. The measurements of strain gages located at 2 ft. above the tip were used to calculate the tip resistance for all test piles.

The total resistances of TP-2, TP-3, TP-4a, TP-4b, T-5a, and TP-5b measured after the final SLTs were 4.9, 2.4, 5.0, 2.3, 4.2, and 2.0 times higher than the EOD total resistances, respectively. The side resistances for the SLTs were 7.5, 3.0, 9.9, 2.8, 5.2, and 2.4 times the EOD side resistances for TP-2, TP-3, TP-4a, TP-4b, TP-5a, and TP-5b, respectively. As mentioned earlier, the tip resistances remained nearly constant. A noteworthy observation is that the test pile at TP-3 had a much higher tip resistance compared to other test piles. The tip resistance measured at failure during the SLT for this pile was 388 kips. The pile was driven to bear in dense sand layer, which can be observed from the soil profile (Figure 22). Similar behavior was also observed for TP-4b.

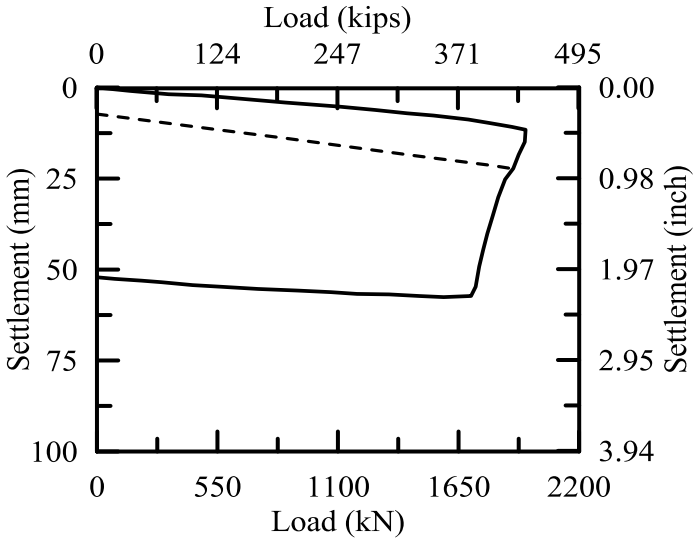


(a) Test Pile-2 (TP-2)

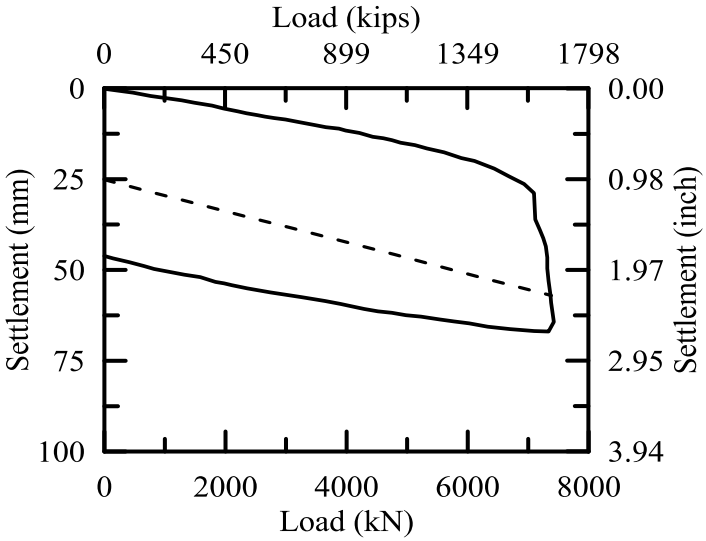


(b) Test Pile-3 (TP-3)

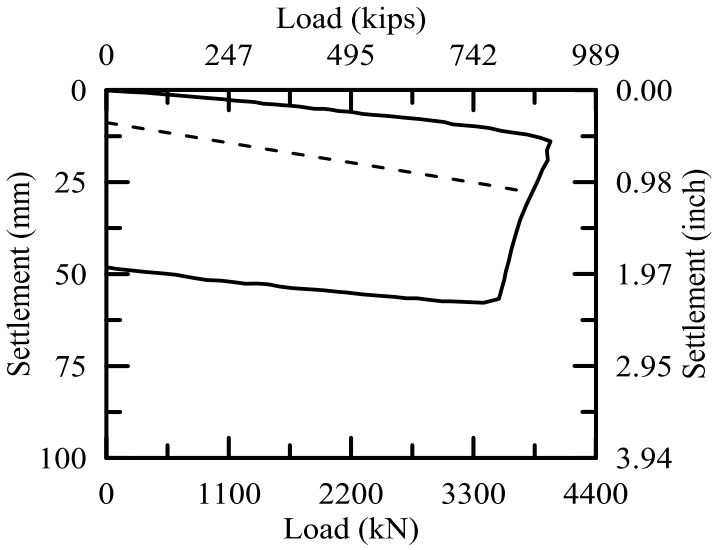


(c) Test Pile-4a (TP-4a)

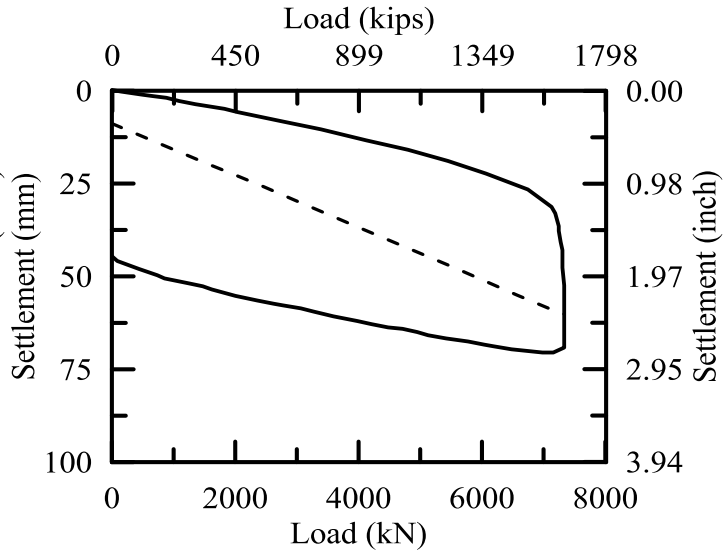


(d) Test Pile-4b (TP-4b)

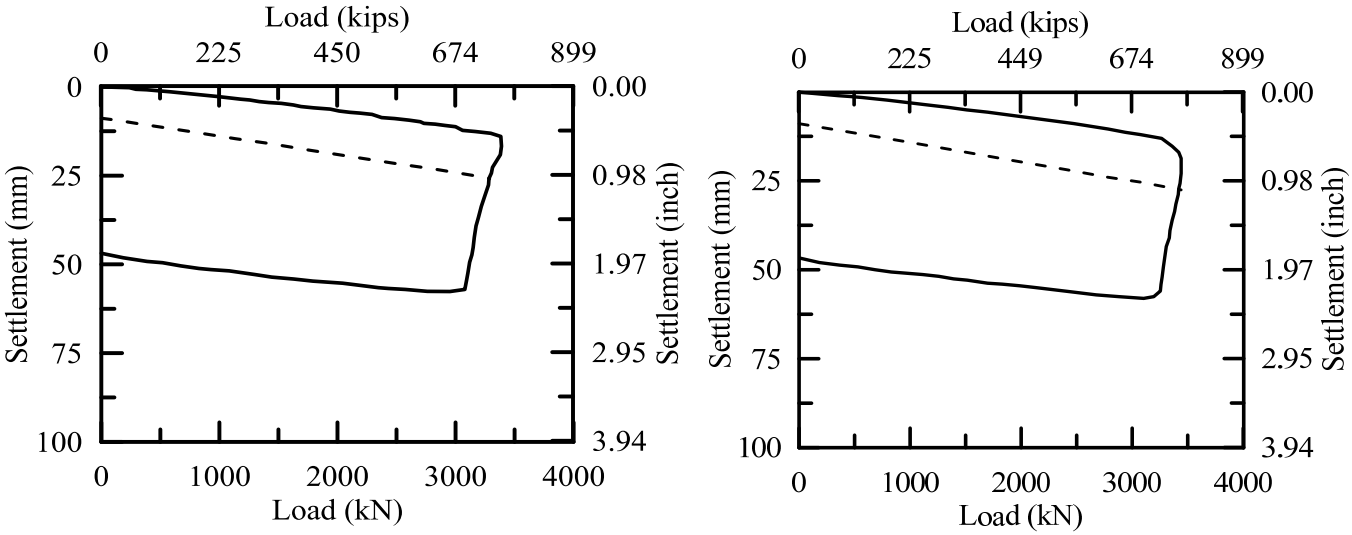


(e) Test Pile-5a (TP-5a)

(f) Test Pile-5b (TP-5b)

**Figure 48**
**Load settlement plots for LA-1 site**

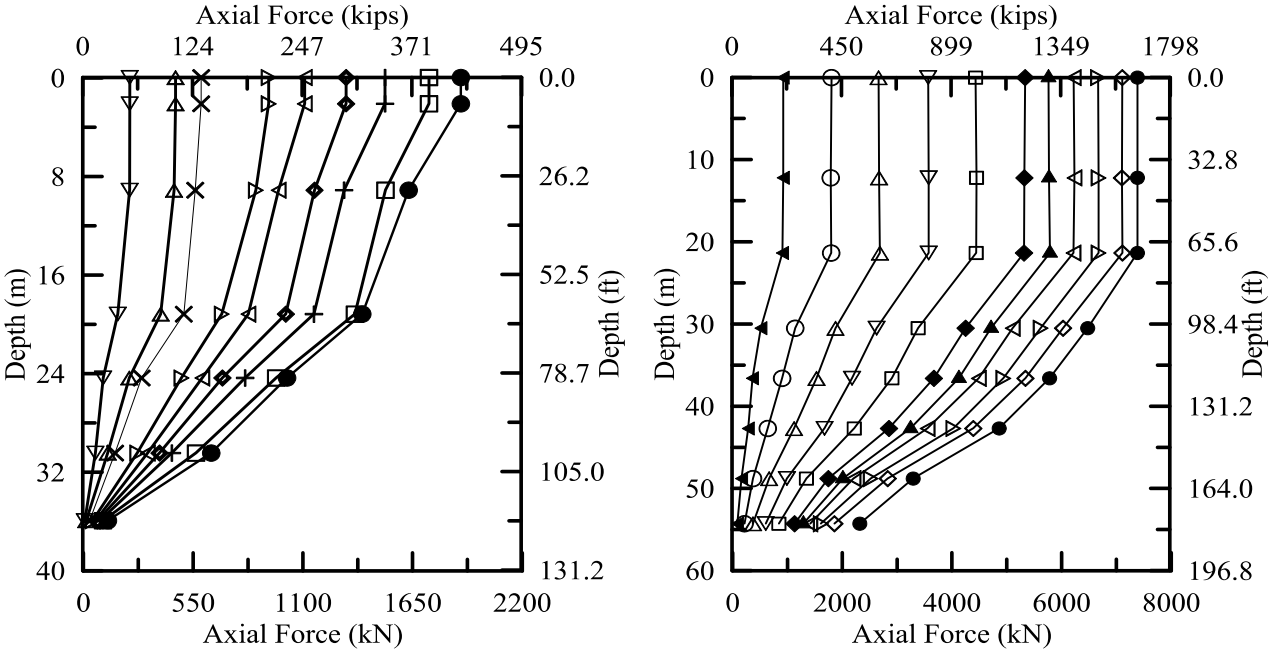


(a) Test Pile-2 (TP-2)

(b) Test Pile-3 (TP-3)

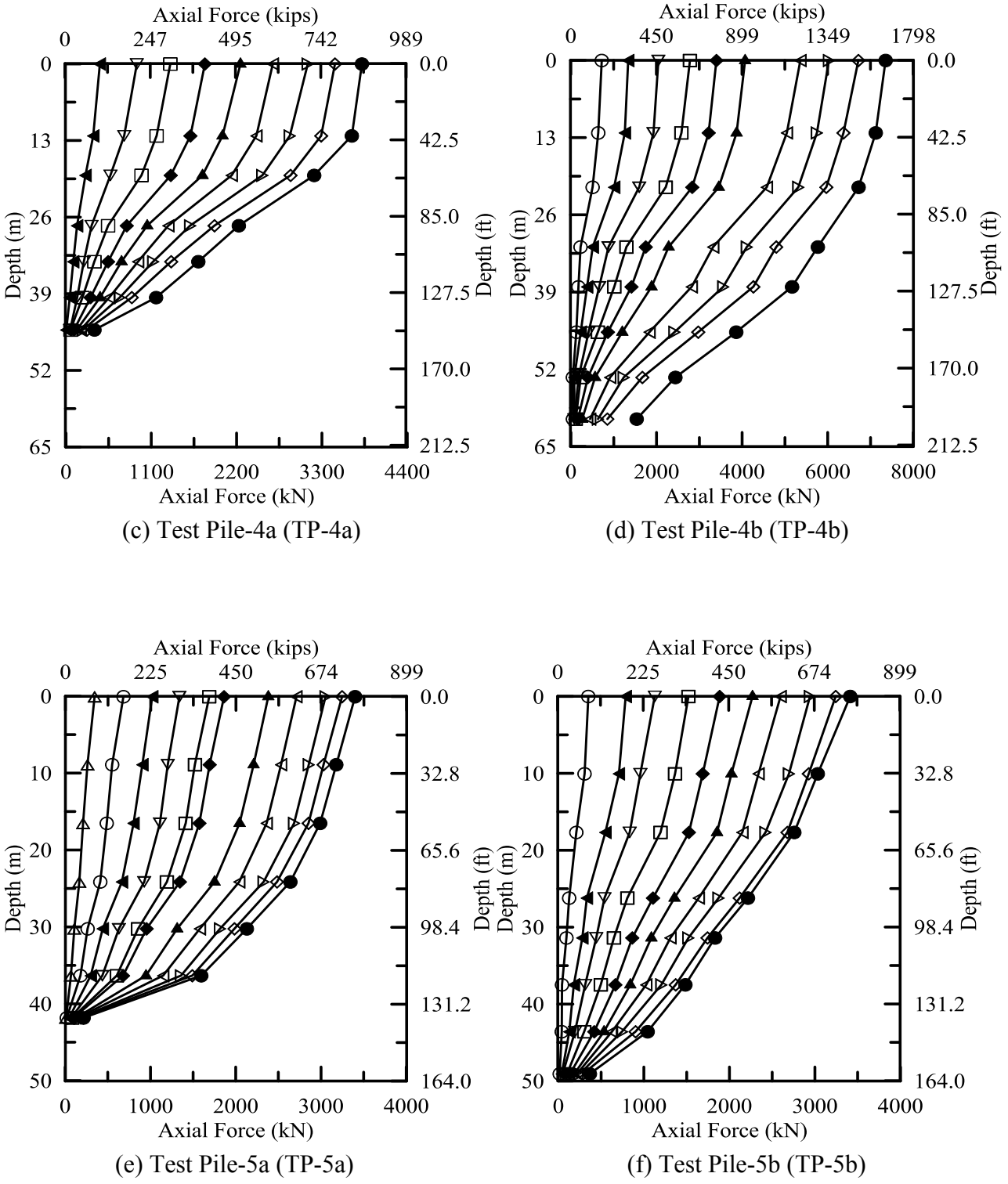


**Figure 49**
**Load distribution plots for the test piles of LA-1**

The behavior of the test piles installed at TP-4 and TP-5 locations was interesting. In order to evaluate the effect of pile installation sequence on set-up behavior, two piles were installed close to each other at two selected test pile locations (TP-4 and TP-5), two test piles were installed at the TP-4 and TP-5 locations with 10 ft. distance apart and driven within a very short period of time (i.e., 3 hours at TP-4 location and 2 hours at TP-5 location). At both locations, the piles that were installed later (i.e., TP-4a and TP-5a) experienced relatively smaller driving resistances compared to the piles that were installed first (i.e., TP-4b and TP-5b). The side resistance during driving of TP-4b was approximately 6 times higher than the side resistance of TP-4a. However, during the SLT (6 days after EOD), the side resistance of TP-4b was only 1.7 times higher than the side resistance of TP-4a. Similar behavior was also observed at TP-5 location. Though the side resistance (133 kips) of TP-5a during driving was approximately half of TP-5b (283 kips), however, TP-5a exhibited higher side resistance during the SLT (6 days after EOD) compared to TP-5b. The high set-up rate of TP-4a and TP-5a compared to TP-4b and TP-5b may be attributable to the effect of pile installation sequence. The TP-4b and TP-5b pile were installed first, which showed higher initial pile resistance compared to the TP-4a and TP-5a piles. It may be postulated that the driving of the TP-4b and TP-5b piles resulted in the development of excess PWP in the surrounding soils and it was postulated that excess PWP do exist at the TP-4a and TP-5a pile locations due to driving the TP-4b and TP-5b piles. As a result, the initial resistances of the TP-4a and TP-5a piles were artificially low. As the excess PWP dissipated with time, the final resistances of the two piles converge to a smaller gap. It may be postulated that 10 ft. center-to-center distance between the two test piles at both location (i.e., TP-4a, TP-4b and TP-5a, TP-5b) was insufficient to minimize pile-soil-pile interaction. In addition, the small time lag (i.e., 2 hours) between the installations of the two piles also contributed to this difference.

**Set-up of Individual Soil Layers**

The resistance distributions of DLTs were analyzed using the CAPWAP analyses. These distributions are used along with the measured load distribution from the SLTs. The resistance distribution calculated from an instrumented pile can be used to determine the load transfer at the locations of the strain gages. The example of calculated side resistances of individual soil layers of TP-2, TP-3, TP-4a, TP-4b, TP-5a, and TP-5b of LA-1 projects are presented Table 18, Table 19, Table 20, Table 21, Table 22, and Table 23, respectively.

**Table 18**

**Side resistance for individual soil layers for TP-2**

| Events | Side Res. Info. | Layer No | | | | | | | | Total Side Res. kN (kips) |
|---|---|---|---|---|---|---|---|---|---|---|
| | | 2-1 | 2-2 | 2-3* | 2-4 | 2-5 | 2-6 | 2-7 | 2-8 | |
| EOD | Res. kN (kips) | 17 (4) | 17 (4) | 35 (8) | 14 (3) | 30 (7) | 35 (8) | 61 (13) | 28 (6) | 237 (53) |
| 2.2 Hour | Res. kN (kips) | 31 (7) | 28 (6) | 58 (13) | 40 (9) | 98 (22) | 112 (25) | 115 (26) | 131 (30) | 613 (138) |
| | $R_{si}/R_{soi}$ | 1.8 | 1.7 | 1.6 | 3.0 | 3.2 | 3.2 | 1.9 | 4.7 | 2.6 |
| 3.9 Hour | Res. kN (kips) | 50 (11) | 59 (13) | 70 (16) | 54 (12) | 134 (30) | 174 (39) | 164 (37) | 209 (47) | 914 (205) |
| | $R_{si}/R_{soi}$ | 2.9 | 3.5 | 2.0 | 4.0 | 4.4 | 5.0 | 2.7 | 7.4 | 3.9 |
| 6.0 Hour | Res. kN (kips) | 81 (18) | 62 (14) | 70 (16) | 58 (13) | 154 (35) | 192 (43) | 198 (44) | 262 (59) | 1077 (242) |
| | $R_{si}/R_{soi}$ | 4.7 | 3.8 | 2.0 | 4.3 | 5.1 | 5.5 | 3.3 | 9.3 | 4.5 |
| 21.6 Hour | Res. kN (kips) | 94 (21) | 97 (22) | 83 (19) | 67 (15) | 211 (48) | 227 (51) | 211 (47) | 263 (59) | 1253 (282) |
| | $R_{si}/R_{soi}$ | 5.5 | 6.0 | 2.4 | 5.0 | 7.0 | 6.5 | 3.5 | 9.3 | 5.3 |
| 56.0 Hour | Res. kN (kips) | 106 (24) | 118 (26) | 79 (18) | 79 (18) | 233 (52) | 226 (51) | 196 (44) | 280 (63) | 1317 (296) |
| | $R_{si}/R_{soi}$ | 6.2 | 7.3 | 2.2 | 5.9 | 7.7 | 6.4 | 3.2 | 9.9 | 5.6 |
| 76.9 Hour | Res. kN (kips) | 151 (34) | 126 (28) | 92 (21) | 85 (19) | 246 (55) | 252 (57) | 261 (59) | 330 (74) | 1543 (347) |
| | $R_{si}/R_{soi}$ | 8.9 | 7.8 | 2.6 | 6.3 | 8.1 | 7.2 | 4.3 | 11.7 | 6.5 |
| 96.9 Hour | Res. kN (kips) | 155 (35) | 135 (30) | 94 (21) | 84 (19) | 263 (59) | 274 (62) | 261 (59) | 349 (78) | 1615 (363) |
| | $R_{si}/R_{soi}$ | 9.1 | 8.3 | 2.6 | 6.2 | 8.7 | 7.8 | 4.3 | 12.4 | 6.8 |
| Static (168 Hour) | Res. kN (kips) | 165 (37) | 134 (30) | 99 (22) | 92 (20) | 280 (63) | 301 (68) | 305 (69) | 403 (91) | 1779 (400) |
| | $R_{si}/R_{soi}$ | 9.7 | 8.3 | 2.8 | 7.4 | 9.6 | 8.8 | 5.0 | 14.3 | 7.5 |
| Calculated "A" parameter | | 0.53 | 0.51 | 0.15 | 0.40 | 0.45 | 0.41 | 0.35 | 0.44 | |

## Table 19
## Side resistance for individual soil layers for TP-3

| Events | Side Res. Info. | Layer No | | | | | | | | | Total Side Res. kN (kips) |
|---|---|---|---|---|---|---|---|---|---|---|---|
| | | 3-1 | 3-2* | 3-3 | 3-4 | 3-5* | 3-6 | 3-7 | 3-8* | 3-9 | |
| EOD | Res. kN (kips) | 64 (14) | 311 (70) | 114 (26) | 103 (23) | 69 (16) | 215 (48) | 318 (71) | 296 (67) | 188 (42) | 1678 (377) |
| 2 Hour | Res. kN (kips) | 119 (27) | 394 (89) | 219 (49) | 165 (37) | 78 (17) | 445 (100) | 364 (82) | 312 (70) | 244 (55) | 2340 (526) |
| | $R_{si}/R_{soi}$ | 1.9 | 1.3 | 1.9 | 1.6 | 1.1 | 2.1 | 1.1 | 1.1 | 1.3 | 1.4 |
| 24 Hour | Res. kN (kips) | 152 (34) | 437 (98) | 240 (54) | 218 (49) | 81 (18) | 546 (123) | 463 (104) | 327 (74) | 303 (68) | 2767 (622) |
| | $R_{si}/R_{soi}$ | 2.4 | 1.4 | 2.1 | 2.1 | 1.2 | 2.5 | 1.5 | 1.1 | 1.6 | 1.6 |
| 69 Hour | Res. kN (kips) | 218 (49) | 467 (105) | 301 (68) | 297 (67) | 85 (19) | 627 (141) | 587 (132) | 334 (75) | 402 (90) | 3318 (746) |
| | $R_{si}/R_{soi}$ | 3.4 | 1.5 | 2.6 | 2.9 | 1.2 | 2.9 | 1.9 | 1.1 | 2.1 | 2.0 |
| Static (312 Hour) | Res. kN (kips) | 363 (82) | 515 (115) | 447 (101) | 416 (93) | 94 (21) | 839 (189) | 1195 (269) | 396 (89) | 802 (180) | 5067 (1139) |
| | $R_{si}/R_{soi}$ | 5.7 | 1.6 | 3.9 | 4.0 | 1.3 | 3.9 | 3.8 | 1.3 | 4.3 | 3.0 |
| Calculated "A" parameter | | 0.43 | 0.13 | 0.32 | 0.37 | 0.08 | 0.31 | 0.37 | 0.07 | 0.37 | |

## Table 20
## Side resistance for individual soil layers for TP-4a

| Events | Side Res. Info. | Layer No | | | | | | | | | | | Total Side Res. kN (kips) |
|---|---|---|---|---|---|---|---|---|---|---|---|---|---|
| | | 4a-1 | 4a-2 | 4a-3* | 4a-4 | 4a-5 | 4a-6* | 4a-7 | 4a-8 | 4a-9* | 4a-10 | 4a-11 | |
| EOD | Res. kN (kips) | 8 (2) | 8 (2) | 26 (6) | 26 (6) | 27 (6) | 59 (13) | 35 (8) | 36 (8) | 35 (8) | 38 (9) | 51 (11) | 349 (78) |
| 2 Hour | Res. kN (kips) | 11 (2) | 15 (3) | 70 (16) | 127 (29) | 135 (30) | 497 (112) | 113 (25) | 168 (38) | 45 (10) | 143 (32) | 216 (49) | 1540 (346) |
| | $R_{si}/R_{soi}$ | 1.4 | 1.8 | 2.7 | 4.9 | 5.0 | 8.4 | 3.2 | 4.7 | 1.3 | 3.7 | 4.3 | 4.4 |
| 4 Hour | Res. kN (kips) | 19 (4) | 22 (5) | 56 (13) | 142 (32) | 160 (36) | 584 (131) | 195 (44) | 234 (53) | 47 (11 | 240 (54) | 284 (64) | 1983 (446) |
| | $R_{si}/R_{soi}$ | 2.5 | 2.7 | 2.1 | 5.4 | 5.9 | 9.9 | 5.5 | 6.6 | 1.3 | 6.3 | 5.6 | 5.7 |
| 6 Hour | Res. kN (kips) | 23 (5) | 27 (6) | 61 (14 | 180 (41) | 199 (45) | 588 (132) | 245. (55) | 217 (49) | 48 (11) | 214 (48) | 282 (63) | 2084 (469) |
| | $R_{si}/R_{soi}$ | 3.0 | 3.4 | 2.3 | 6.9 | 7.4 | 9.9 | 7.0 | 6.1 | 1.4 | 5.6 | 5.6 | 6.0 |
| 45 Hour | Res. kN (kips) | 47 (11) | 41 (9) | 64 (14) | 300 (67) | 317 (71) | 700 (157) | 320 (72) | 310 (70) | 51 (12) | 348 (78) | 425 (96) | 2923 (657) |
| | $R_{si}/R_{soi}$ | 6.2 | 5.0 | 2.4 | 11.5 | 11.8 | 11.8 | 9.1 | 8.8 | 1.5 | 9.4 | 8.4 | 8.4 |
| 69 Hour | Res. kN (kips) | 50 (11) | 43 (10) | 66 (15) | 336 (76) | 348 (78) | 741 (166) | 343 (77) | 346 (78) | 52 (12) | 349 (78) | 390 (88) | 3064 (689) |
| | $R_{si}/R_{soi}$ | 6.5 | 5.3 | 2.5 | 12.8 | 12.9 | 12.5 | 9.7 | 9.8 | 1.5 | 9.1 | 7.7 | 8.8 |
| 89 Hour | Res. kN (kips) | 51 (12) | 48 (11) | 71 (16) | 371 (83) | 370 (83) | 756 (170) | 359 (81) | 358 (80) | 54 (12) | 372 (84) | 414 (93) | 3224 (725) |
| | $R_{si}/R_{soi}$ | 6.7 | 5.9 | 2.7 | 14.1 | 13.7 | 12.8 | 10.2 | 10.1 | 1.5 | 9.7 | 8.2 | 9.3 |
| Static (144 Hour) | Res. kN (kips) | 53 (12) | 49 (11) | 72 (16) | 353 (79) | 401 (90) | 868 (195) | 395 (89) | 381 (86) | 55 (12) | 382 (86) | 443 (100) | 3452 (776) |
| | $R_{si}/R_{soi}$ | 6.9 | 6.0 | 2.8 | 13.5 | 14.9 | 14.7 | 11.2 | 10.8 | 1.5 | 10.0 | 8.8 | 9.9 |
| Calculated "A" parameter | | 0.51 | 0.44 | 0.13 | 0.48 | 0.48 | 0.24 | 0.45 | 0.41 | 0.13 | 0.42 | 0.38 | |

**Table 21**
**Side resistance for individual soil layers for TP-4b**

| Events | Side Res. Info. | Layer No | | | | | | | | | | | Total Side Res. kN (kips) |
|---|---|---|---|---|---|---|---|---|---|---|---|---|---|
| | | 4b-1 | 4b-2 | 4b-4 | 4b-5 | 4b-7 | 4b-8 | 4b-10 | 4b-11 | 4b-12 | 4b-13 | 4b-14 | |
| EOD | Res. kN (kips) | 18 (4) | 14 (3) | 52 (12) | 42 (9) | 111 (25) | 124 (28) | 145 (33) | 172 (39) | 171 (38) | 243 (55) | 486 (109) | 2087 (469) |
| 3 Hour | Res. kN (kips) | 34 (8) | 36.6 (8) | 112.5 (25) | 110.2 (25) | 233.8 (53) | 240 (54) | 253 (57) | 220 (50) | 189 (43) | 309.8 (70) | 705 (159) | 3151 (708) |
| | $R_{si}/R_{soi}$ | 1.9 | 2.6 | 2.2 | 2.6 | 2.1 | 1.9 | 1.8 | 1.3 | 1.1 | 1.3 | 1.5 | 1.5 |
| 4 Hour | Res. kN (kips) | 39 (9) | 45 (10) | 118 (27) | 112 (25) | 237 (53) | 258 (58) | 256 (58) | 230 (52) | 195 (44) | 313 (70) | 714 (161) | 3217 (723) |
| | $R_{si}/R_{soi}$ | 2.1 | 3.2 | 2.3 | 2.7 | 2.1 | 2.1 | 1.8 | 1.3 | 1.1 | 1.3 | 1.5 | 1.5 |
| 6 Hour | Res. kN (kips) | 40 (9) | 49 (11) | 122 (27) | 121 (27) | 250 (56) | 271 (61) | 268 (60) | 318 (71) | 229 (52) | 394 (88) | 779 (175) | 3572 (803) |
| | $R_{si}/R_{soi}$ | 2.2 | 3.5 | 2.3 | 2.9 | 2.3 | 2.2 | 1.9 | 1.9 | 1.4 | 1.6 | 1.6 | 1.7 |
| 8 Hour | Res. kN (kips) | 55 (12) | 57 (13) | 142 (32) | 124 (28) | 269 (61) | 277 (62) | 279 (63) | 328 (74) | 273 (61) | 406 (91) | 825 (185) | 3796 (853) |
| | $R_{si}/R_{soi}$ | 3.0 | 4.1 | 2.7 | 3.0 | 2.4 | 2.2 | 1.9 | 1.9 | 1.6 | 1.7 | 1.7 | 1.8 |
| 24 Hour | Res. kN (kips) | 70 (16) | 65 (15) | 157 (35) | 139 (31) | 316 (71) | 303 (68) | 281 (63) | 346 (78) | 363 (82) | 541 (122) | 863 (194) | 4282 (963) |
| | $R_{si}/R_{soi}$ | 3.8 | 4.7 | 3.0 | 3.3 | 2.9 | 2.4 | 1.9 | 2.0 | 2.1 | 2.2 | 1.8 | 2.1 |
| 48 Hour | Res. kN (kips) | 72 (16) | 73 (16) | 171 (39) | 153 (34) | 355 (80) | 335 (75) | 346 (78) | 433 (97) | 403 (91) | 608 (137) | 894 (201) | 4700. (1057) |
| | $R_{si}/R_{soi}$ | 3.9 | 5.2 | 3.3 | 3.6 | 3.2 | 2.7 | 2.4 | 2.5 | 2.4 | 2.5 | 1.8 | 2.3 |
| 72 Hour | Res. kN (kips) | 75 (17) | 74.0 (17) | 181 (41) | 164 (37) | 363 (82) | 360 (81) | 366 (82) | 451 (101) | 409 (92) | 722 (162) | 943 (212) | 4989 (1122) |
| | $R_{si}/R_{soi}$ | 4.1 | 5.3 | 3.5 | 3.9 | 3.3 | 2.9 | 2.5 | 2.6 | 2.4 | 3.0 | 1.9 | 2.4 |
| 93 Hour | Res. kN (kips) | 90 (20) | 90.5 (20) | 208 (47) | 206 (46) | 436 (98) | 379 (85) | 498 (112) | 534 (120) | 524 (118) | 849 (191) | 1046 (235) | 5833 (1311) |
| | $R_{si}/R_{soi}$ | 5.0 | 6.5 | 4.0 | 4.9 | 3.9 | 3.1 | 3.4 | 3.1 | 3.1 | 3.5 | 2.2 | 2.8 |
| Static (144 Hour) | Res. kN (kips) | 117 (26) | 90 (20) | 213 (48) | 188 (42) | 414 (93) | 410 (92) | 489 (110) | 544 (122) | 546 (123) | 821 (184) | 1051 (236) | 5829 (1310) |
| | $R_{si}/R_{soi}$ | 6.5 | 6.4 | 4.1 | 4.5 | 3.8 | 3.3 | 3.4 | 3.2 | 3.2 | 3.4 | 2.2 | 2.8 |
| Calculated "A" parameter | | 0.47 | 0.42 | 0.35 | 0.35 | 0.35 | 0.30 | 0.34 | 0.37 | 0.40 | 0.42 | 0.22 | |

**Table 22**

**Side resistance for individual soil layers for TP-5a**

| Events | Side Res. Info. | Layer No | | | | | | Total Side Res. kN (kips) |
|---|---|---|---|---|---|---|---|---|
| | | 5a-1 | 5a-2* | 5a-3 | 5a-4 | 5a-5 | 5a-6* | |
| EOD | Res. kN (kips) | 51 (11) | 65 (15) | 118 (26) | 83 (19) | 114 (26) | 162 (36) | 593 (133) |
| 2 Hour | Res. kN (kips) | 108 (24) | 70 (16) | 270 (61) | 192 (43) | 316 (71) | 303 (68) | 1259 (283) |
| | $R_{si}/R_{soi}$ | 2.1 | 1.1 | 2.3 | 2.3 | 2.8 | 1.9 | 2.1 |
| 4 Hour | Res. kN (kips) | 115 (26) | 71 (16) | 309 (70) | 259 (58) | 365 (82) | 338 (76) | 1457 (328) |
| | $R_{si}/R_{soi}$ | 2.3 | 1.1 | 2.6 | 3.1 | 3.2 | 2.1 | 2.5 |
| 22 Hour | Res. kN (kips) | 162 (37) | 117 (26) | 497 (112) | 357 (80) | 569 (128) | 468 (105) | 2170 (488) |
| | $R_{si}/R_{soi}$ | 3.2 | 1.8 | 4.2 | 4.3 | 5.0 | 2.9 | 3.7 |
| 47 Hour | Res. kN (kips) | 191 (43) | 135 (30) | 560 (126) | 390 (88) | 608 (137) | 507 (114) | 2391 (538) |
| | $R_{si}/R_{soi}$ | 3.8 | 2.1 | 4.7 | 4.7 | 5.3 | 3.1 | 4.0 |
| 70 Hour | Res. kN (kips) | 204 (46) | 137 (31) | 627 (141) | 422 (95) | 653 (147) | 549 (123) | 2592 (583) |
| | $R_{si}/R_{soi}$ | 4.1 | 2.1 | 5.3 | 5.1 | 5.7 | 3.4 | 4.4 |
| Static (144 Hour) | Res. kN (kips) | 258 (58) | 113 (25) | 591 (133) | 440 (99) | 764 (172) | 929 (209) | 3095 (696) |
| | $R_{si}/R_{soi}$ | 5.1 | 1.7 | 5.0 | 5.3 | 6.7 | 5.7 | 5.2 |
| Calculated "A" parameter | | 0.33 | 0.23 | 0.36 | 0.35 | 0.36 | 0.24 | |

**Table 23**

**Side resistance for individual soil layers for TP-5b**

| Events | Side Res. Info. | Layer No | | | | | | | | Total Side Res. kN (kips) |
|---|---|---|---|---|---|---|---|---|---|---|
| | | 5b-1 | 5b-2* | 5b-3 | 5b-4 | 5b-5 | 5b-6* | 5b-7 | 5b-8 | |
| EOD | Res. kN (kips) | 107 (24) | 103 (23) | 251 (56) | 167 (38) | 130 (29) | 163 (37) | 49 (11) | 290 (65) | 1260 (283) |
| 3 Hour | Res. kN (kips) | 243 (54) | 133 (30) | 402 (90) | 281 (63) | 352 (79) | 234 (53) | 101 (23) | 253 (57) | 1999 (449) |
| | $R_{si}/R_{soi}$ | 2.3 | 1.3 | 1.6 | 1.7 | 2.7 | 1.4 | 2.0 | 0.9 | 1.6 |
| 5 Hour | Res. kN (kips) | 227 (51) | 137 (31) | 427 (96) | 248 (56) | 380 (85) | 252 (57) | 108 (24) | 280 (63) | 2059 (463) |
| | $R_{si}/R_{soi}$ | 2.1 | 1.3 | 1.7 | 1.5 | 2.9 | 1.6 | 2.2 | 1.0 | 1.6 |
| 8 Hour | Res. kN (kips) | 249 (56) | 146 (33) | 458 (103) | 264 (59) | 402 (90) | 252 (57) | 108 (24) | 304 (69) | 2183 (491) |
| | $R_{si}/R_{soi}$ | 2.3 | 1.4 | 1.8 | 1.6 | 3.1 | 1.6 | 2.2 | 1.1 | 1.7 |
| 24 Hour | Res. kN (kips) | 269 (60) | 151 (34) | 471 (106) | 271 (61) | 449 (101) | 267 (60) | 114 (26) | 235 (53) | 2227 (501) |
| | $R_{si}/R_{soi}$ | 2.5 | 1.5 | 1.9 | 1.6 | 3.5 | 1.6 | 2.3 | 0.8 | 1.8 |
| 48 Hour | Res. kN (kips) | 302 (68) | 170 (38) | 570 (128) | 323 (72) | 495 (111) | 245 (55) | 105 (24) | 225 (51) | 2435 (547) |
| | $R_{si}/R_{soi}$ | 2.8 | 1.7 | 2.3 | 1.9 | 3.8 | 1.5 | 2.1 | 0.8 | 1.9 |
| 72 Hour | Res. kN (kips) | 319 (72) | 173 (39) | 606 (136) | 350 (79) | 540 (121) | 269 (60) | 115 (26) | 210 (47) | 2582 (580) |
| | $R_{si}/R_{soi}$ | 3.0 | 1.7 | 2.4 | 2.1 | 4.2 | 1.7 | 2.3 | 0.7 | 2.0 |
| Static (144 Hour) | Res. kN (kips) | 400 (90) | 164 (37) | 652 (147) | 384 (86) | 348 (78) | 309 (69) | 132 (30) | 676 (152) | 3065 (689) |
| | $R_{si}/R_{soi}$ | 3.7 | 1.6 | 2.6 | 2.3 | 2.7 | 1.9 | 2.7 | 2.3 | 2.4 |
| Calculated "A" parameter | | 0.28 | 0.15 | 0.25 | 0.23 | 0.23 | 0.15 | 0.20 | 0.21 | |

Layer 8 of TP-2 with $S_u$ of 0.28 tsf (26.5 kPa) and PI of 68% and layer 1 of TP-2 with $S_u$ of 0.07 tsf (7 kPa) and PI of 84% exhibited the highest amount of set-up after 7 days from EOD among all the clayey soil layers along the length of TP-2. The set-up behavior of clayey soil layers of TP-2 is depicted in Figure 50a. Layers 3-1, 3-3, 3-4, 3-6, 3-7, and 3-9 represented the clayey soil layers of TP-3. The maximum amount of set-up was observed for layer 1 and the minimum amount of set-up was exhibited by layer 7 of TP-3. The SLT (performed 13 days after EOD) showed that the side resistance set-up were 5.7 and 3.8 times higher compared to the EOD side resistances for layers 1 and 7 of TP-3, respectively. The set-up trend for the clayey soil layers of TP-3 are presented in Figure 50b.

Figure 50c and Figure 50d show the set-up trend for the clayey soil layers for TP-4a and TP-4b, respectively. Layers 2 and 5 exhibited the minimum ($R_{si}/R_{soi}$ = 6.0) and maximum ($R_{si}/R_{soi}$ = 14.9) set-up ratio among the clayey soil layers of TP-4a, respectively. The maximum ($R_{si}/R_{soi}$ = 6.5) and minimum ($R_{si}/R_{soi}$ = 2.2) of set-up ratio among the clayey soil layers of TP-4b were exhibited by layers 1 and 14, respectively. It appears that the higher $S_u$ [0.81 tsf (78.0 kPa)] and the lower PI (26%) for the soil layer 14 of TP-4b as compared to the other clay layers at TP-4 location may be the main factors for the lowest set-up ratio. Similarly the lower $S_u$ and higher PI for layers 1 and 2 at TP-4b location resulted in higher amount of set-up ratio compared to the other clayey layers for TP-4b. Similar behavior was also observed for the clayey soil layers of TP-5. Figure 50e and Figure 50f depict the set-up trend for the clayey soil layers for TP-5a and TP-5b, respectively. As can been observed from the set-up behavior of the soil layers of TP-5a and TP-5b, the same conclusions can be made regarding the effect of soil property's impact on the set-up behavior for individual soil layers.

The sandy soil layers exhibited smaller amount of set-up than the clayey soil layers for all test piles of LA-1 project. Layers 2-3, 3-2, 3-5, 3-8, 4a-3, 4a-6, 4a-9, 4b-3, 4b-6, 4b-9, 5a-2, 5a-6, 5b-2 and 5b-6 represented the sandy soil layers in this study. The set-up behavior of sandy soil layers of all test piles of LA-1 are depicted in Figure 51. It is observed from Figure 51 that all sandy soil layers exhibited smaller amounts and rates of set-up compared to the clayey soil layers. The maximum ($R_{si}/R_{soi}$ = 2.79) and the minimum ($R_{si}/R_{soi}$ = 1.34) amount of set-up ratios for the sandy soil layers of all LA-1 test piles were exhibited by layer 6 of TP-4b and layer 8 of TP-3, respectively at the time of performing the SLT.

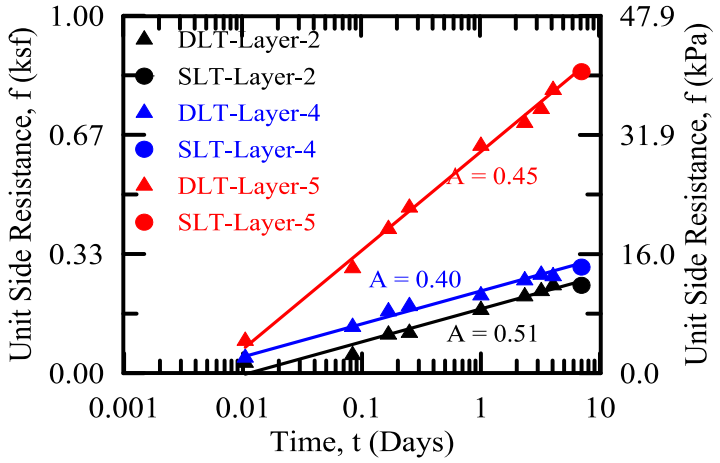


(a) Test Pile-2 (TP-2)

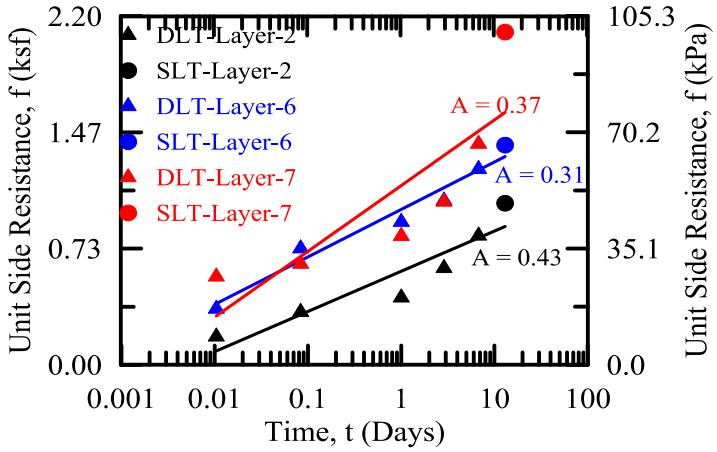


(b) Test Pile-3 (TP-3)

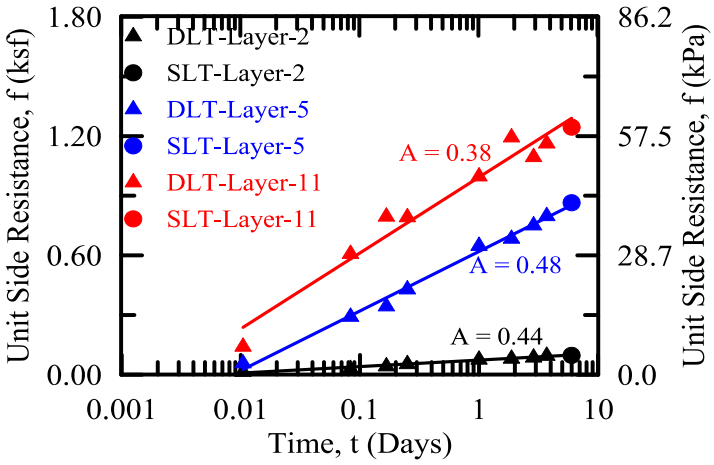


(c) Test Pile-4a (TP-4a)

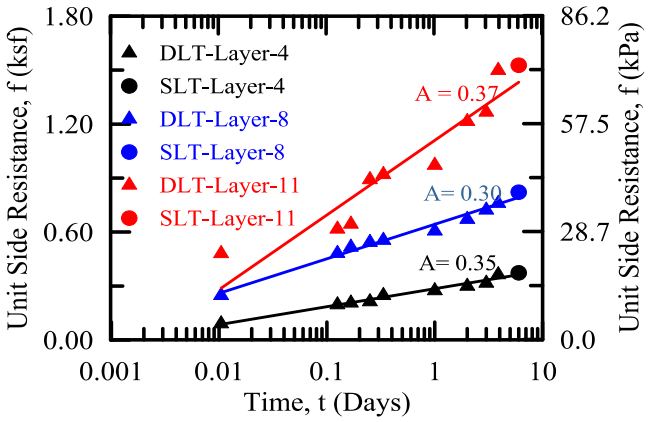


(d) Test Pile-4b (TP-4b)

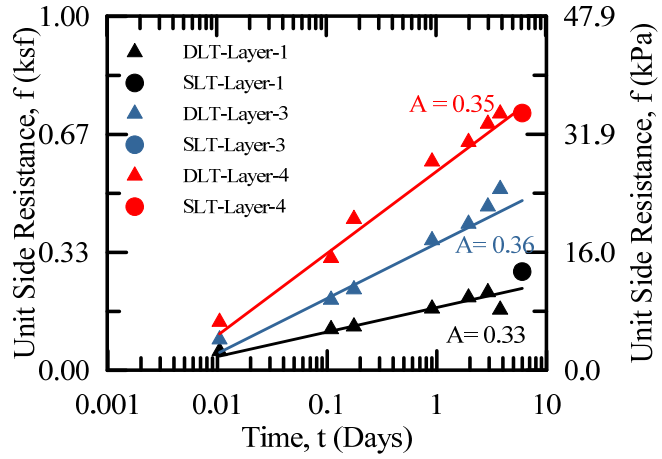


(e) Test Pile-5a (TP-5a)

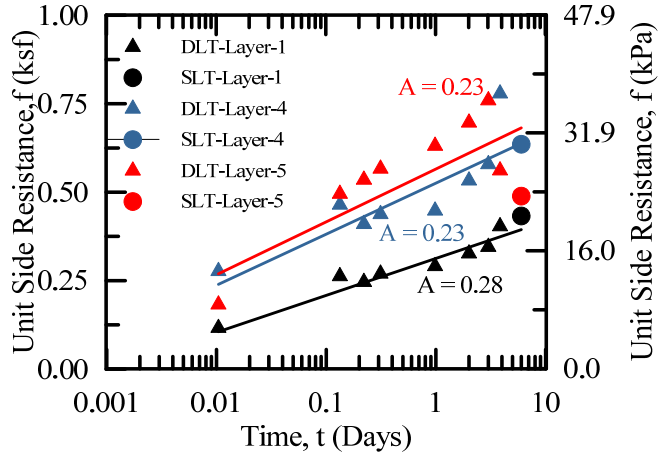


(f) Test Pile-5b (TP-5b)

**Figure 50**

**Set-up of individual soil layers for clayey soil of LA-1 site**

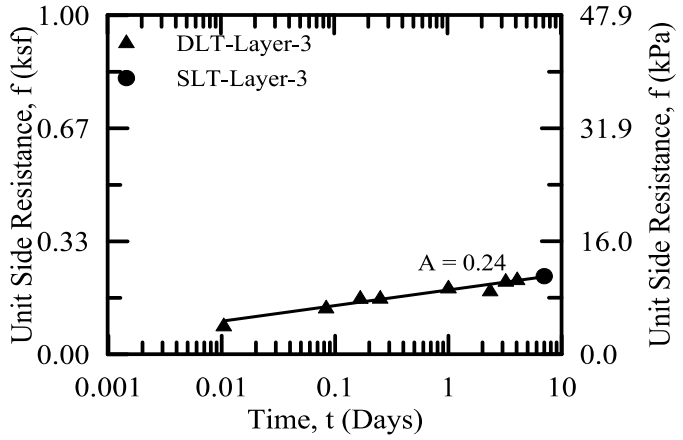


(a) Test Pile-2 (TP-2)

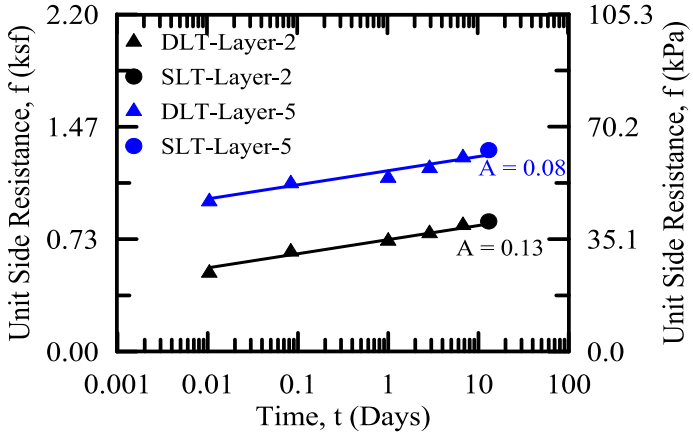


(b) Test Pile-3 (TP-3)

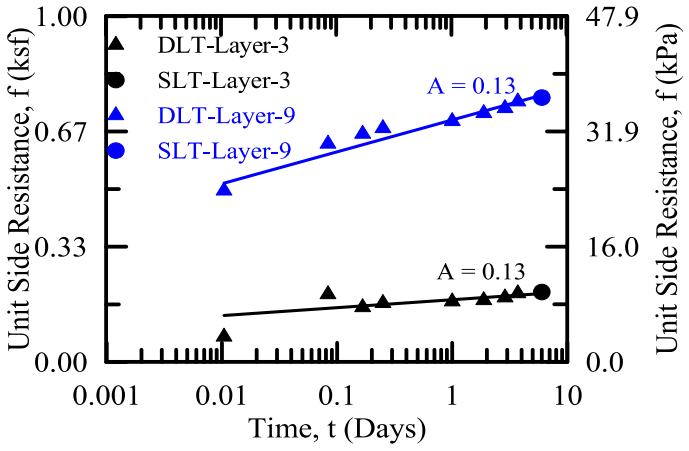


(c) Test Pile-4a (TP-4a)

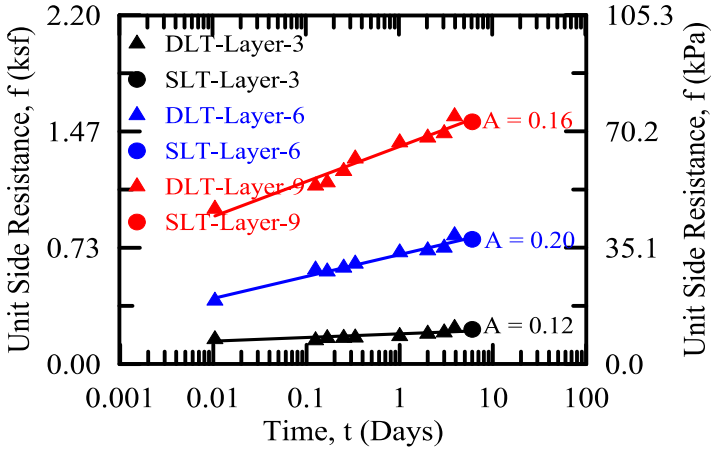


(d) Test Pile-4b (TP-4b)

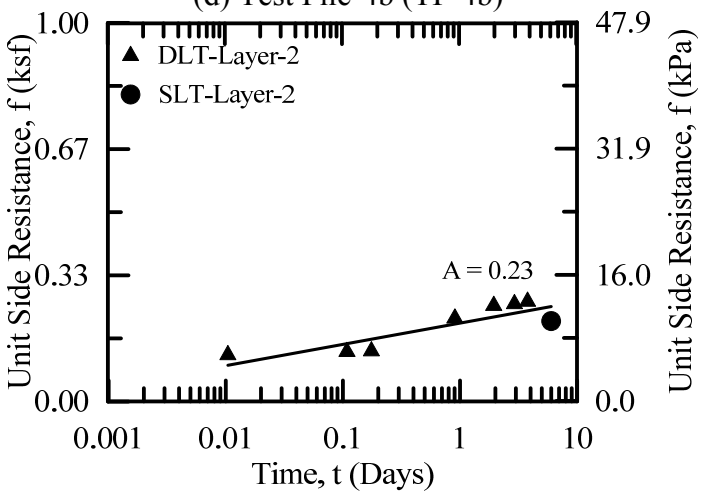


(e) Test Pile-5a (TP-5a)

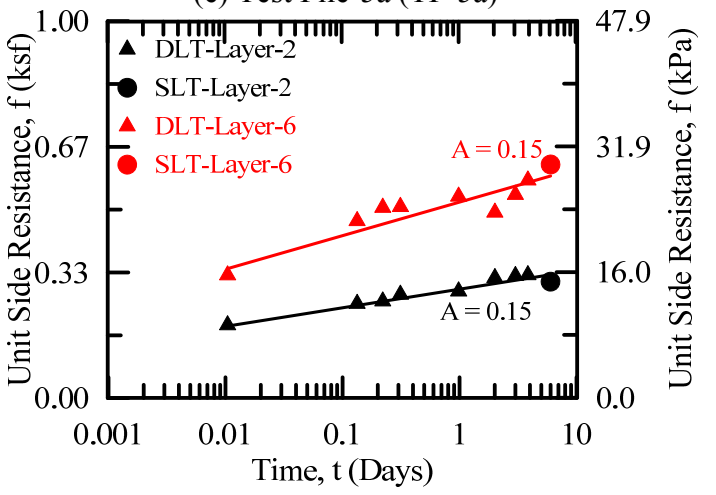


(f) Test Pile-5b (TP-5b)

**Figure 51**
**Set-up of individual soil layers for sandy soil of LA-1 site**

## Correlation in Between Soil Properties and Pile Set-up

The set-up of soils needs to be analyzed for individual soil layers along the pile length rather than the total pile resistance ($R_t$) for better prediction of set-up. The soil properties such as PI, $S_u$, permeability ($k_h$), OCR, $S_t$ and $c_v$ have significant effect on the set-up process that cannot be incorporated in pile set-up unless analyses were performed for individual soil layers.

The logarithmic set-up parameters "A" were used to back-calculate using the model proposed by Skov and Denver for the total resistances ($R_t$) of test piles *[7]*. However, in this study, set-up parameter "A" was back-calculated using the unit side resistance ($f_s$) [i.e., side resistance of the layer / (length of the layer x perimeter)] instead of total resistance to analyze the set-up behavior for individual soil layers.

$$\frac{f_s}{f_{so}} = 1 + A \log \frac{t}{t_o} \quad (32)$$

Usually, the elapsed time for the EOD is assumed to be at about 10 minutes in the logarithmic scale of set-up plot in the literature. However, it is found from the load test program at this site that an elapsed time of 15 minutes after EOD produces the most reasonable fit of set-up with the time as shown in set-up plots. A total of 94 soil layers from 12 PSC test piles of five different project sites were used in the analyses for this study. Clayey soil behavior was dominant in 70 clayey soil layers and the rest of the soil layers (i.e., 24) exhibited sandy soil behavior. The maximum and minimum "A" values for the clayey soil layers were 0.53 and 0.12, respectively; while for sandy soil, the maximum and minimum values of "A" parameter were 0.26 and 0.02, respectively. The average value of "A" parameter for clayey and sandy soil layers were 0.31 and 0.15, respectively. The effects of soil properties on these back-calculated logarithmic "A" parameters were investigated and tried to correlate with the soil properties.

### Effect of Undrained Shear Strength ($S_u$)

The $S_u$ was correlated in this study with the set-up parameter "A" for the individual clayey soil layers. It was observed that the layer-1 of TP-2 of LA-1 site exhibited the maximum rate of set-up (i.e., 0.53), on the contrary the soil layer (i.e., Layer 5 of Bayou Zourie site) with highest $S_u$ exhibited lower magnitude of set-up as well lower rate of set-up (i.e., 0.29). In general, the clayey soil layers of LA-1 project with lower $S_u$ exhibited higher rate and magnitude of set-up compared to the clayey soil layers of other sites. The correlation between $S_u$ and set-up parameter "A" is depicted in Figure 52. The figure shows that there exists an inverse-power relationship in between the "A" parameter and $S_u$. The coefficient of correlation ($R^2$) of this relationship is higher ($R^2 = 0.68$) as observed from the figure. Stiff clayey soil layers with high $S_u$ values exhibited less amount of set-up with low rate of set-up parameter "A." On the other hand, soft clayey soil layers with low $S_u$ value exhibited high amount and rate of set-up

parameter “A” since the thixotropic effect is more significant and the excess PWP that was generated during pile driving takes prolonged period to dissipate in soft clayey soil layers.

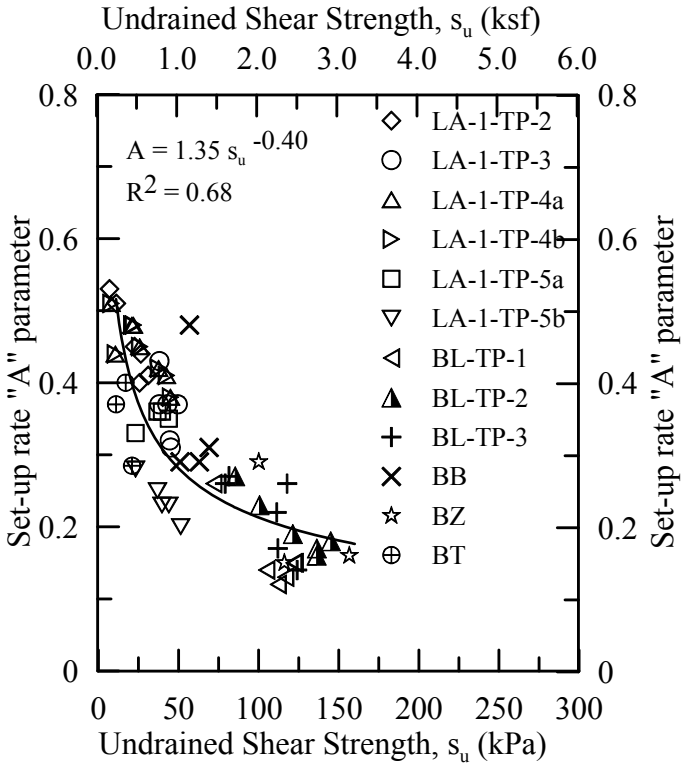


**Figure 52**

**Correlation between $S_u$ and set-up parameter “A”**

**Effect of Plasticity Index (PI)**

The correlation between the PI of clayey soil layers and the set-up parameter “A” is shown in Figure 53. Layer-2 of TP-2 at LA-1 site with maximum PI (i.e., PI = 84%) exhibited higher magnitude and rate of set-up (i.e., A = 0.53) compared to the other clayey soil layers, whereas, layer-7 of TP-1 at Bayou Lacassine site exhibited lower amount and rate of set-up (i.e., A = 0.14) with the minimum PI (i.e., PI = 4%) among all the clayey soil layers. This observation is consistent with Figure 53, where a linear proportional relationship between the PI and the “A” parameter is observed and the coefficient of correlation ($R^2$) is high ($R^2$ = 0.73) for this correlation. The clayey soil layers with low PI values usually exhibited lower amount of set-up as well as low values of logarithmic set-up parameter “A”; while clayey soil layers with high PI values exhibited higher amount of set-up with higher values of set-up parameter “A.”

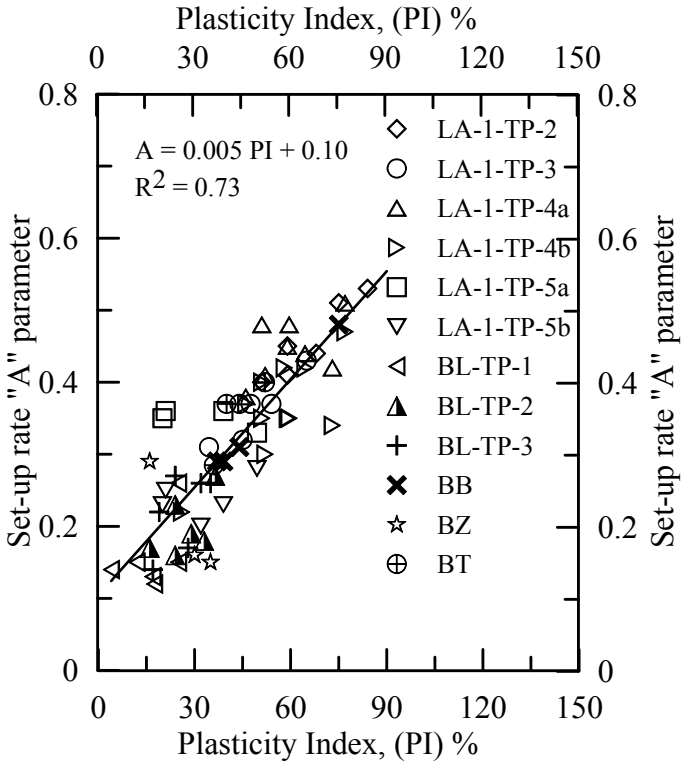


**Figure 53**

**Correlation between PI and set-up parameter "A"**

**Effect of Overconsolidation Ratio (OCR)**

PCPT evaluated OCR was tried to correlate with the set-up parameter "A." For the procedure of calculating OCR from PCPT data, see Abu-Farsakh *[71]*. Layer-2 of TP-2 in Bayou Lacassine site with maximum OCR (i.e., OCR = 3.05) exhibiting lower amount of set-up rate (i.e., A= 0.27), whereas, Layer-13 of TP-4b in LA-1 site exhibited higher amount of set-up rate (i.e., A = 0.42) with minimum OCR value (i.e., OCR = 0.25). The correlation between OCR and set-up parameter "A" is presented in Figure 54. The figure shows that there is an inverse power relationship exist in between OCR and set-up parameter "A" same as $S_u$ – "A" parameter relationship. The coefficient of correlation ($R^2$) of this relationship is 0.48. This may conclude that overconsolidated clayey soils exhibited lower amount and rate of set-up compared to the normally consolidated clayey soil.

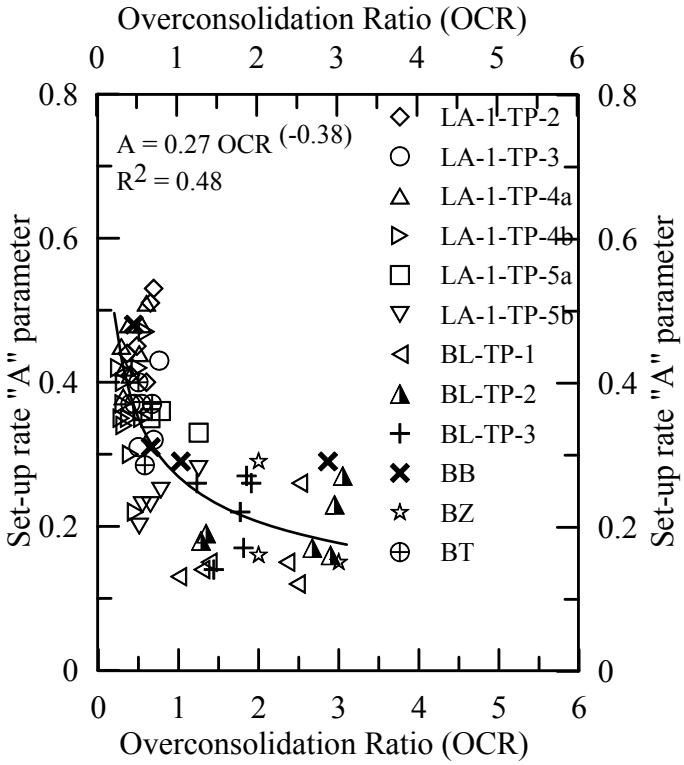


**Figure 54**

**Correlation between OCR and set-up parameter "A"**

**Effect of Sensitivity ($S_t$)**

Due to the thixotropic property of the soil, the subsequent remolding and reconsolidation of the disturbed soil at the soil-pile interface zone will also be associated with long-term gain in soil strength, depending on $S_t$ of the soil. Small scale lab vane shear test was used to perform the test and determine the $S_t$ of the collected soil samples from three test pile locations of Bayou Lacassine site and the test pile location of Bayou Zourie site. Layer-2 of TP-1 in Bayou Lacassine site with maximum $S_t$ exhibited higher amount of set-up rate (A = 0.26) and Layer-3 of Bayou Zourie site exhibited lower amount of set-up rate (A = 0.15) compared to the other clayey soil layers due to low $S_t$. The correlation in between $S_t$ and set-up parameter "A" is depicted in Figure 55. The figure shows that there exist a linear proportional relationship in between $S_t$ and set-up parameter "A" and the coefficient of correlation ($R^2$) of this correlation is 0.44.

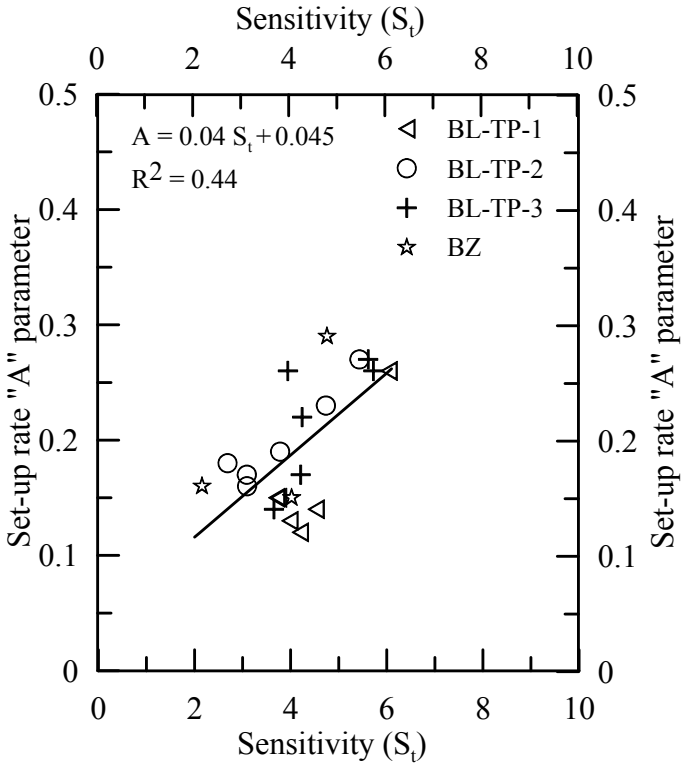


**Figure 55**

**Correlation between $S_t$ and set-up parameter "A"**

**Effect of Coefficient of Consolidation ($c_v$)**

The coefficient of consolidation ($c_v$ *or* $c_h$) is believed to be one of the most important factor to influence the set-up behavior of clayey soils. In-situ piezocone dissipation tests were performed and the $c_h$ was calculated using Teh and Houlsby method *[73].* The $c_h$ is then converted to the $c_v$ based on the range of anisoptropic hydraulic conductivity ($k_h/k_v$) of clayey soils. Laboratory consolidation tests were also performed on soil samples collected at LA-1 and Bayou Teche pile test sites. The correlation between the $c_v$ and set-up parameter "A" for this study is depicted in Figure 56**.** In order to better represent the relationship, the normalized logarithmic value of $c_v$ is considered in this analyses. The figure shows that there exist an inverse linear proportional relationship between the set-up rate parameter "A" and the log $c_v$ values. This is expected, since the excess PWP that was generated during pile driving dissipated fast in soils with high $k_h$ and high $c_h$ values and that the set-up rate is mainly attributable to the dissipation of excess PWP (consolidation); therefore, it can be concluded that the soil layers with high $k_h$ and high $c_v$ or $c_h$ values exhibited lower set-up rate "A" compared to the soil layers with low $k_h$ and low $c_v$ values.

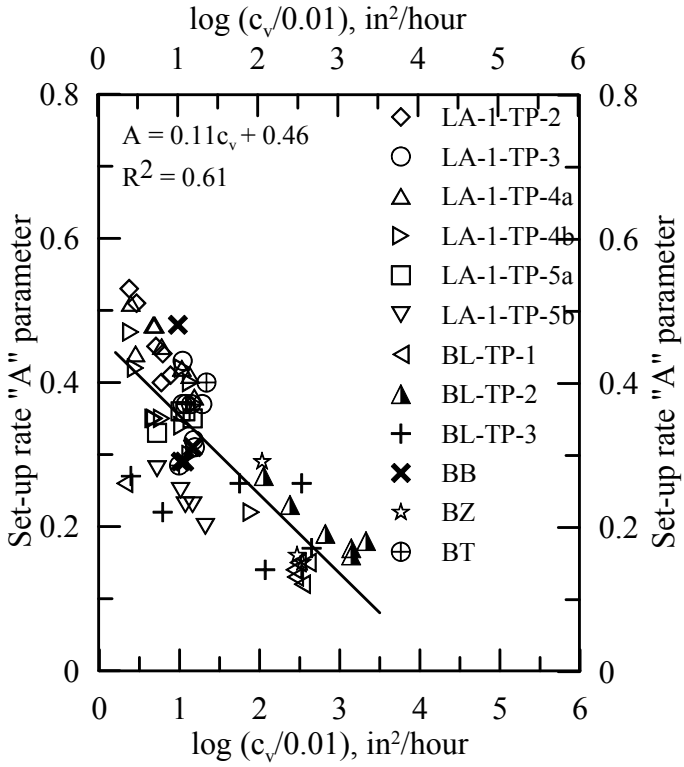


**Figure 56**
**Correlation between $c_v$ and set-up parameter "A"**

### Development of Pile Set-up Prediction Model

Non-linear multivariable regression analyses were performed to develop the set-up prediction models. Three different levels of model were developed. The procedure for developing the models for every level was similar; however, the difference is only in incorporation of different soil properties in different levels of model. The correlations that were described for individual soil properties earlier were analyzed together to develop the models. Two soil parameters (i.e., $S_u$ and PI) were focused and correlated with set-up parameter "A" in Level-1. Level-2 contains three soil parameters: $S_u$, PI and $c_v$. $S_t$ was incorporated in Level-3 in addition of $S_u$, PI and $c_v$. In addition to the soil properties of Level-3, OCR was tried to incorporate in the models. However, it was found from the statistical analyses that OCR did not have a significant influence on the set-up prediction models. Regression analyses were performed with the aid of SAS program on 70 clayey soil layers from these 12 instrumented test piles that were used to develop the models.

**Empirical Model for Level-1, [A=f ($S_u$, PI)]**

Comprehensive statistical analyses were carried out on the collected field measurements to develop nonlinear regression model between the logarithmic set-up parameter "A" and the soil

properties (i.e., $S_u$ and PI) that was selected to incorporate in Level-1. PI was normalized with 100 and $S_u$ was normalized with 1 tsf (95.76 kPa) in order to make the set-up parameter unit less. Once some preliminary models were selected, detail statistical analyses such as the significance of the model as a whole (F test) and the significance of the partial multiple regression coefficient (t test) were carried out on each model to find out the influence of each parameters on the model. Four initial models were selected for Level-1 after initial screening. These four models were evaluated furthermore to predict the best model. Based on the statistical analyses the following empirical model was proposed to calculate the set-up parameter "A" for clayey soil layers of Level-1:

$$A=\frac{0.79\left(\frac{PI}{100}\right)+0.49}{\left(\frac{S_u}{1\ tsf}\right)^{2.03}+2.27} \tag{33}$$

The coefficient of correlation ($R^2$) of this model was 0.98, whereas the mean and standard deviation of the measured and predicted values were 0.99 and 0.16, respectively. This set-up parameter "A" was incorporated in Skov and Denvers' model to predict the unit side resistance ($f_s$) at certain time (t) after EOD for individual clayey soil layers *[7]*.

$$\frac{f_s}{f_{so}}=1+\left[\frac{0.79\left(\frac{PI}{100}\right)+0.49}{\left(\frac{S_u}{1\ tsf}\right)^{2.03}+2.27}\right]\log\frac{t}{t_o} \tag{34}$$

where, $t_o$ = 1 day and $f_{so}$ = measured unit side resistance at 1 day restrike.

As mentioned earlier, to determine the effectiveness of the entire model, a significant test for overall model was performed (i.e., F-test). The null hypothesis for F-test was rejected because α value was less than 0.0001 for Pr>F. This suggested that at least one of the independent variables ($S_u$, PI) was non-linearly related to the dependent variable ("A" parameter). The t-test was then performed in order to evaluate the effectiveness of the incorporated parameters (i.e., $S_u$, PI) on the model. The null hypothesis was rejected since α was less than 0.05 for Pr>|t| which means that all independent variables were effectively related to the dependent variable. Figure 57a presents the comparison of measured versus predicted total resistance ($R_t$) due to set-up for the test piles that was used to develop the model for Level-1. The bias (μ) and the standard deviation (σ) of the model for the total resistance ($R_t$) due to set-up was 0.96 and 0.16, respectively. Other available pile set-up data from DOTD were analyzed here to verify the developed model. 18 non-instrumented test piles (Appendix-A) were used for the model verification and Figure 57b depicts the comparison of measured and estimated total pile resistance predicted by the Level-1. The comparison shows that the pile set-up model for Level-1 can predict the set-up with good accuracy by having the mean of resistance ratio (i.e., ratio of measured to estimated pile resistance) close to unity (i.e., 0.95) and with a small coefficient of variation (0.20) of total pile resistance ($R_t$).

**Empirical Model for Level-2, [A=f ($S_u$, PI, $c_v$)]**

$c_v$ was considered along with $S_u$ and PI in Level-2 pile set-up prediction model. Comprehensive statistical analyses were carried out on the collected field measurements to develop the nonlinear multivariable regression model between the logarithmic set-up parameter "A" and the soil properties (i.e., $S_u$, PI and $c_v$) for Level-2. Logarithmic value of $c_v$ which was normalized with 0.01 $in^2$/hour was used in the correlation. PI was normalized with 100 and $S_u$ was normalized with 1 tsf (95.76 kPa) in order to make the set-up parameter "A" unit less. As mentioned earlier, F-test and t-test were performed for detail statistical analyses.

Four initial models were selected for Level-2 after initial screening. These four models were evaluated furthermore to predict the best model. Statistical test were performed to find the best model. Finally, sum of square error (SSE) was calculated for each model with the data that were not used to prepare the model. Based on the statistical analyses the following regression model was proposed to calculate the set-up parameter "A" for clayey soil layers of Level-2:

$$A = \frac{1.12*\left(\frac{PI}{100}\right)+0.69}{\left[\left(\frac{S_u}{1\ tsf}\right)^{1.44}\right]*\left[\log\left(\frac{c_v}{0.01\frac{in^2}{hour}}\right)\right]^{0.54}+3.19} \quad (35)$$

The coefficient of correlation ($R^2$) of this model was 0.98, whereas the mean and standard deviation of the measured and predicted values were 0.99 and 0.14, respectively. The developed correlation in between set-up parameter "A" and soil properties will need to be incorporated in Skov and Denvers' model to predict the unit side resistance ($f_s$) at certain time (t) after EOD for individual clayey soil layers *[7]*.

$$\frac{f_s}{f_{so}} = 1 + \left[\frac{1.12*\left(\frac{PI}{100}\right)+0.69}{\left[\left(\frac{S_u}{1\ tsf}\right)^{1.44}\right]*\left[\log\left(\frac{c_v}{0.01\frac{in^2}{hour}}\right)\right]^{0.54}+3.19}\right] \log\frac{t}{t_o} \quad (36)$$

where, $t_o$ = 1 day and $f_{so}$ = measured unit side resistance at 1 day restrike.

In order to determine the effectiveness of the entire model, an F-test for overall model was performed. The null hypothesis was rejected because α value was less than 0.0001 for Pr>F. t-test was then performed in order to evaluate the effectiveness of the incorporated parameters (i.e., $S_u$, PI and $c_v$) on the model. The null hypothesis was rejected as well since α was less than for 0.05 for Pr>|t| which means that all independent variables were effectively related to the dependent variable.

Figure 58a compares the measured versus predicted total resistance ($R_t$) due to set-up of 12 test piles that was used to developed the model. The bias (μ) and standard deviation (σ) of these

values were 0.97 and 0.13, respectively. Figure 58b demonstrates that the proposed pile set-up model for Level-2 can predict the set-up with good accuracy by comparing the measured versus predicted total resistance for 18 non-instrumented test piles that was used only for verification purpose.

**Empirical Model for Level-3, [A=f ($S_u$, PI, $c_v$, $S_t$)]**

$S_t$ was incorporated along with $S_u$, PI and $c_v$ in Level-3 pile set-up prediction model. Comprehensive statistical analyses were carried out on the collected field measurements to develop the nonlinear multivariable regression model between the logarithmic set-up parameter "A" and the soil properties (i.e., $S_u$, PI, $c_v$ and $S_t$) for Level-3. Laboratory evaluated $S_t$ was incorporated in the set-up prediction model in order to incorporate the remolding effect due to pile driving.

Three initial models were selected for Level-3 after initial screening. These three models were evaluated furthermore to predict the best model. As mentioned earlier, statistical tests were performed. Finally, sum of square error (SSE) was calculated for each model with the data that were not used to prepare the model. Based on the statistical analyses the following regression model was proposed to calculate the set-up parameter "A" for clayey soil layers of Level-3:

$$A = \frac{0.44*\left(\frac{PI}{100}\right)(S_t)+2.20}{\left[\left(\frac{S_u}{1tsf}\right)^{1.94}\right]*\left[\log\left(\frac{c_v}{0.01\frac{in^2}{hour}}\right)\right]^{1.06}+10.65} \quad (37)$$

The coefficient of correlation ($R^2$) of this model was 0.98, whereas the mean and standard deviation of the measured and predicted values were 0.99 and 0.12, respectively. This set-up parameter "A" will need to be incorporated in Skov and Denvers' model to predict the unit side resistance ($f_s$) at certain time (t) after EOD for individual clayey soil layers *[7]*.

$$\frac{f_s}{f_{so}} = 1 + \left[\frac{0.44*\left(\frac{PI}{100}\right)(S_t)+2.20}{\left[\left(\frac{S_u}{1tsf}\right)^{1.94}\right]*\left[\log\left(\frac{c_v}{0.01\frac{in^2}{hour}}\right)\right]^{1.06}+10.65}\right] \log\frac{t}{t_o} \quad (38)$$

where, $t_o$ = 1 day and $f_{so}$ = measured unit side resistance at 1 day restrike.

In order to determine the effectiveness of the entire model, an F-test for overall model was performed. The null hypothesis was rejected because α value was less than 0.0001 for Pr>F. t-test was then performed in order to evaluate the effectiveness of the incorporated parameters (i.e., $S_u$, PI, $c_v$ and $S_t$) on the model. The null hypothesis was rejected since α was less than for 0.05 for Pr>|t| which means that all independent variables were effectively related to the dependent variable.

Figure 59a presents the comparison of measured versus predicted total resistance ($R_t$) due to set-up for the test piles that was used to develop the model for Level-3. The bias ($\mu$) and the standard deviation ($\sigma$) of the model for the total resistance ($R_t$) due to set-up was 0.99 and 0.11, respectively. Figure 59b demonstrates that the proposed pile set-up model for Level-3 can predict the set-up with good accuracy by having the mean (i.e., ratio of measured to estimated pile resistance) close to unity (i.e., 0.97) and with a small COV (0.12) of total pile resistance ($R_t$).

Equations (33), (35), and (37) were developed with respect to initial normalized time, $t_o$ = 1 day. Recalibrations were performed on the same equations with respect to the initial normalized time, $t_o$ = 1 hour. The developed models for set-up parameter "A" with soil properties (for $t_o$ = 1 hour) were:

$$A=\frac{1.02*\left(\frac{PI}{100}\right)+0.26}{\left(\frac{S_u}{1\ tsf}\right)^{0.68}+0.50} \tag{39}$$

$$A=\frac{1.18*\left(\frac{PI}{100}\right)+0.32}{\left[\left(\frac{S_u}{1\ tsf}\right)^{0.40}\right]*\left[\log\left(\frac{C_v}{0.01\frac{in^2}{hour}}\right)\right]^{0.37}+0.53} \tag{40}$$

$$A=\frac{0.11*\left(\frac{PI}{100}\right)(S_t)+0.23}{\left[\left(\frac{S_u}{1tsf}\right)^{0.07}\right]*\left[\log\left(\frac{C_v}{0.01\frac{in^2}{hour}}\right)\right]^{0.17}-0.06} \tag{41}$$

This set-up parameter "A" was incorporated into Skov and Denvers' model to predict the unit side resistance ($f_s$) at certain time (t) after EOD for individual clayey soil layers for $t_o$ = 1 hour *[7]*. The corresponding unit side resistance ($f_s$) can be calculated as:

$$\frac{f_s}{f_{so(1\text{-}hr)}}=1+\left[\frac{1.02*\left(\frac{PI}{100}\right)+0.26}{\left(\frac{S_u}{1\ tsf}\right)^{0.68}+0.50}\right]\log\frac{t}{t_{o(1\text{-}hr)}} \tag{42}$$

$$\frac{f_s}{f_{so(1\text{-}hr)}}=1+\left[\frac{1.18*\left(\frac{PI}{100}\right)+0.32}{\left[\left(\frac{S_u}{1\ tsf}\right)^{0.40}\right]*\left[\log\left(\frac{C_v}{0.01\frac{in^2}{hour}}\right)\right]^{0.37}+0.53}\right]\log\frac{t}{t_{o(1\text{-}hr)}} \tag{43}$$

$$\frac{f_s}{f_{so(1\text{-}hr)}}=1+\left[\frac{0.11*\left(\frac{PI}{100}\right)(S_t)+0.23}{\left[\left(\frac{S_u}{1tsf}\right)^{0.07}\right]*\left[\log\left(\frac{C_v}{0.01\frac{in^2}{hour}}\right)\right]^{0.17}-0.06}\right]\log\frac{t}{t_{o(1\text{-}hr)}} \tag{44}$$

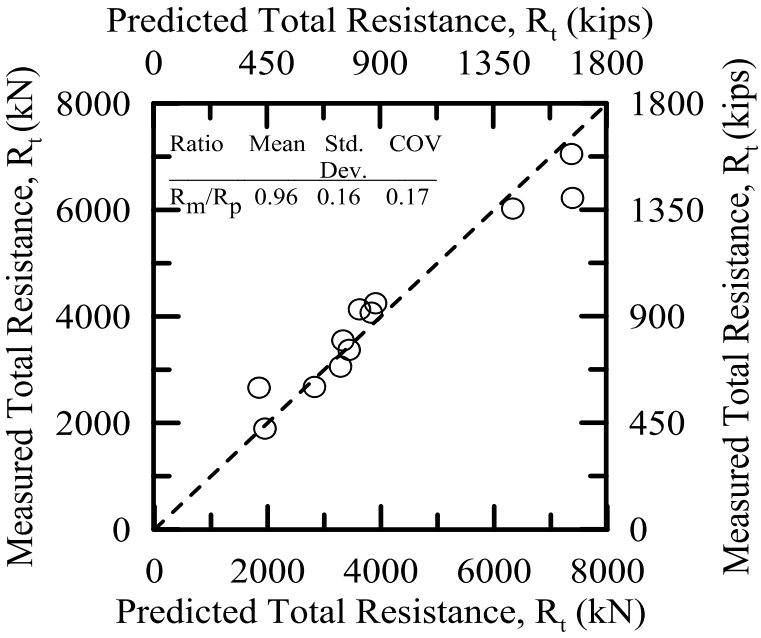


(a) Predicted versus measured "$R_t$" for the preparation of model of Level-1

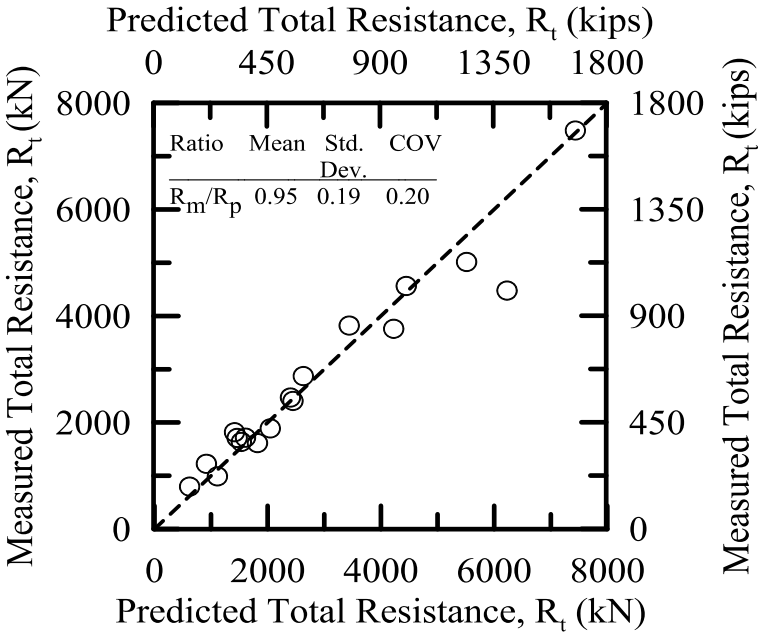


(b) Predicted versus measured "$R_t$" for the validation of model for Level-1

**Figure 57**
**Statistical analyses for developed model for Level-1**

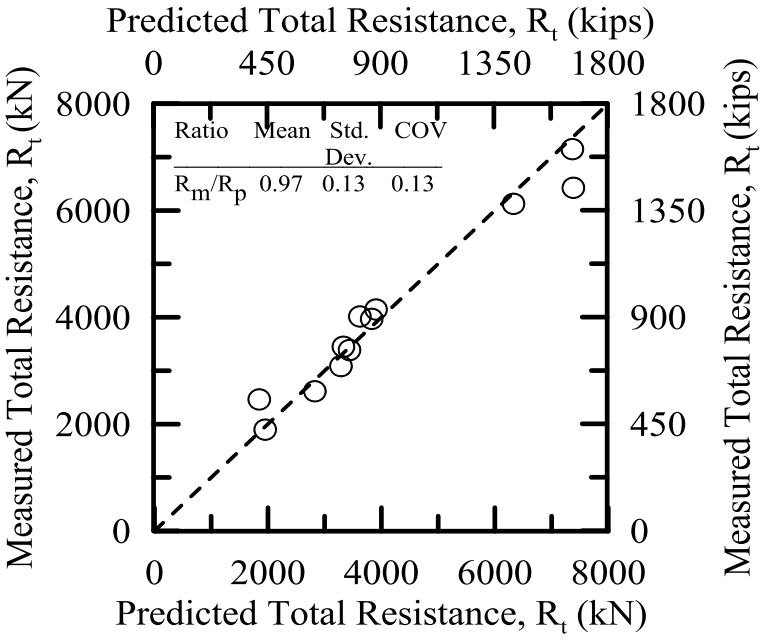


(a) Predicted versus measured "$R_t$" for the preparation of model of Level-2

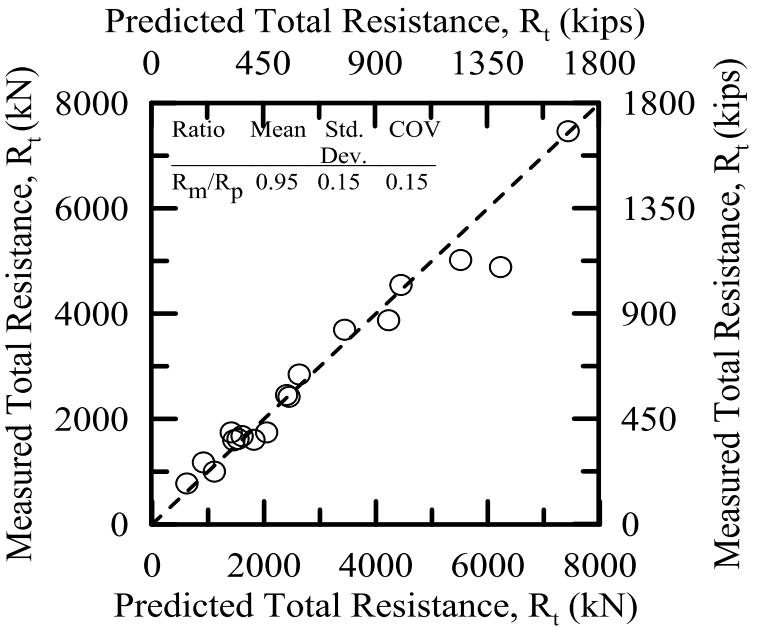


(b) Predicted versus measured "$R_t$" for the validation of model for Level-2

**Figure 58**
**Statistical analyses for developed model for Level-2**

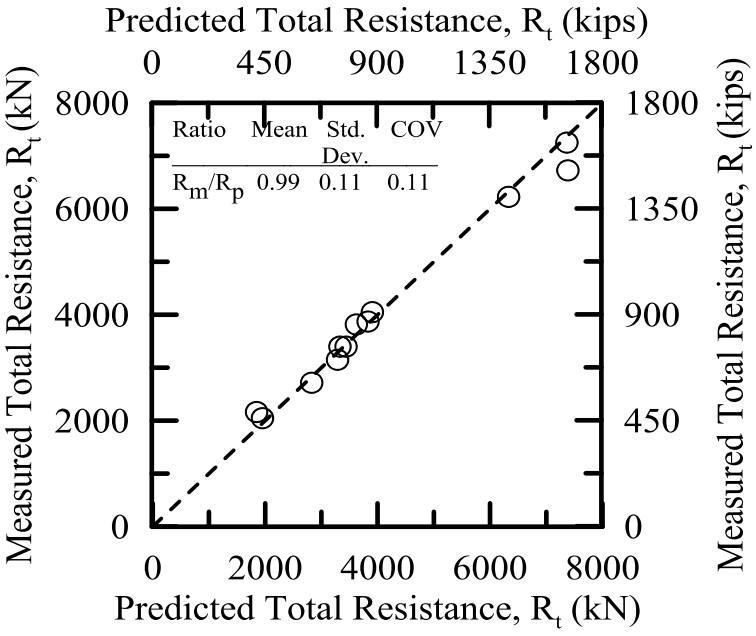


(a) Predicted versus measured "$R_t$" for the preparation of model of Level-3

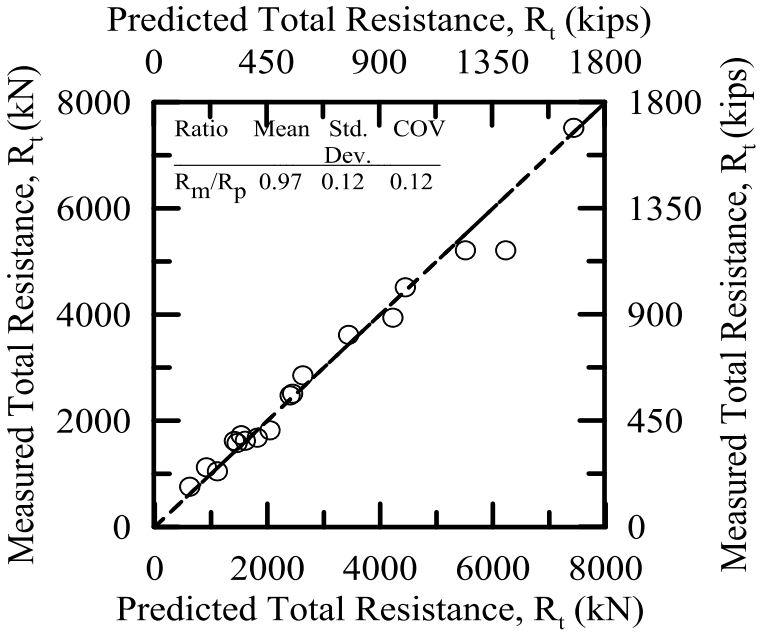


(b) Predicted versus measured "$R_t$" for the validation of model for Level-3

**Figure 59**
**Statistical analyses for developed model for Level-3**

**Predicted versus Measured Total Resistances**

Statistical analyses were performed on the data set of total resistance ($R_t$) for 30 test piles including 12 instrumented test piles and 18 non-instrumented test piles. Total resistances ($R_t$) of piles were estimated using the developed model at Level-1 and compared with the measured resistance at specific time intervals (i.e., 30 days, 45 days, 60 days and 90 days after EOD). Increases of resistances were considered only after 14 days. Table 24 presents the data set of increase in resistance after 14 days for both measured and predicted resistances using Level-1 model. From the results of Table 24 a statistical analysis was first conducted on the collected database of 30 test piles to evaluate the statistical characteristics of the increase in total resistance ($R_t$) at four different time intervals (i.e., 30 days, 45 days, 60 days and 90 days after EOD) after 14 days from EOD. The corresponding resistance bias factor ($\lambda_R=R_m/R_p$), which is the mean ratio between the measured resistance and the predicted resistance ($R_m/R_p$), was determined. The standard deviation ($\sigma$) and the coefficient of variation (COV) of the bias ($\lambda_R$) were also calculated and summarized in Table 25.

Figure 60 presents the comparison between the measured and predicted total set-up resistances after 14 days using the Level-1 model. A simple regression analysis was also conducted to obtain a line of best fit of the predicted/measured additional set-up resistances (i.e., increase o resistance after 14 days). The mean ratio of $R_p/R_m$ equals to 1.03 for the additional set-up at 30 days from 14 days, while the slope of the best fit line was 0.90 and indicates a 10% underestimation of additional set-up resistance using the Level-1 model for 30 driven piles (Figure 60a). On the other hand, the mean ratio of $R_p/R_m$ equals 1.18 for the additional set-up at 45 days from 14 days, while the slope of the best fit line was 0.99 and indicates a 1 % underestimation of additional set-up resistance using the Level-1 model (Figure 60b). The mean ratio of $R_p/R_m$ equals 1.22 for the additional set-up at 60 days from 14 days, while the slope of the best fit line was 1.04 and indicates a 4% overestimation of additional set-up resistance using the Level-1 model for 30 driven piles (Figure 60c). Finally, the mean ratio of $R_p/R_m$ equals 1.23 for the additional set-up at 90 days from 14 days, while the slope of the best fit line was 1.05 and indicates a 5% overestimation of additional set-up resistance using the Level-1 model for 30 driven piles (Figure 60d). The COV of $R_m/R_p$ for the additional set-up resistances at 30 days, 45 days, 60 days and 90 days after 14 days were 0.41, 0.33, 0.29 and 0.27, respectively.

**Table 24**

**Set-up information with respect to 14 days using Level-1 model**

| Nos | Project Name | Resistance increased with respect to 14 days using Level-1 model | | | | | | | |
|---|---|---|---|---|---|---|---|---|---|
| | | ($R_{30}$ - $R_{14}$), kN | | ($R_{45}$ - $R_{14}$), kN | | ($R_{60}$ - $R_{14}$), kN | | ($R_{90}$ - $R_{14}$), kN | |
| | | Mea | Pre | Mea | Pre | Mea | Pre | Mea | Pre |
| 1 | Bayou Liberty | 146.80 | 145.53 | 224.80 | 222.95 | 280.20 | 277.88 | 358.30 | 355.30 |
| 2 | US 90 LA 668 | 153.81 | 96.55 | 194.14 | 147.91 | 222.75 | 184.36 | 263.08 | 235.72 |
| 3 | New Starc | 77.99 | 84.85 | 119.48 | 129.99 | 148.92 | 162.02 | 190.41 | 207.16 |
| 4 | JCT LA-1 US 190 | 123.48 | 86.48 | 165.12 | 132.50 | 194.66 | 165.14 | 236.30 | 211.15 |
| 5 | Calcasieu River TP-1 | 239.36 | 242.77 | 366.70 | 371.93 | 457.05 | 463.57 | 584.39 | 592.72 |
| 6 | Calcasieu River TP-2 | 290.52 | 363.33 | 445.08 | 556.62 | 554.74 | 693.77 | 709.30 | 887.06 |
| 7 | St. Louis Canal Bridge | 92.99 | 62.83 | 118.79 | 96.25 | 137.11 | 119.97 | 162.91 | 153.39 |
| 8 | Joyce Lasalle IND1 | 149.94 | 113.10 | 212.90 | 173.27 | 257.57 | 215.96 | 320.53 | 276.13 |
| 9 | Joyce Lasalle IND2 | 84.31 | 90.97 | 123.35 | 139.36 | 151.06 | 173.70 | 190.10 | 222.09 |
| 10 | Morman Slough TP-1 | 124.98 | 150.33 | 181.10 | 230.30 | 225.72 | 287.04 | 288.60 | 367.02 |
| 11 | Bayou Bouef (west) | 181.68 | 101.39 | 230.12 | 155.33 | 264.49 | 193.60 | 312.94 | 247.54 |
| 12 | Fort Buhlow | 71.35 | 67.22 | 109.30 | 102.99 | 136.23 | 128.36 | 174.19 | 164.12 |
| 13 | Caminada Bay TP-3 | 485.64 | 356.16 | 744.01 | 545.65 | 927.32 | 680.09 | 1185.69 | 869.57 |
| 14 | Caminada Bay TP-5 | 571.89 | 300.83 | 496.15 | 460.87 | 618.40 | 574.42 | 790.69 | 734.46 |
| 15 | Caminada Bay TP-6 | 337.96 | 344.60 | 517.76 | 527.94 | 645.33 | 658.01 | 825.13 | 841.34 |
| 16 | Caminada Bay TP-7 | 173.12 | 193.46 | 265.22 | 296.39 | 330.57 | 369.42 | 422.67 | 472.34 |
| 17 | Bayou Lacassine TP-1 | 309.90 | 113.14 | 359.32 | 173.33 | 394.40 | 216.04 | 443.85 | 276.23 |
| 18 | Bayou Lacassine TP-2 | 138.34 | 155.38 | 211.94 | 238.05 | 264.16 | 296.70 | 337.76 | 379.36 |
| 19 | Bayou Lacassine TP-3* | - | - | - | - | - | - | - | - |
| 20 | Bayou Zourie | 101.14 | 189.76 | 154.94 | 290.71 | 193.12 | 362.34 | 246.92 | 463.29 |
| 21 | Bayou Bouef* | - | - | - | - | - | - | - | - |
| 22 | Bayou Teche | 58.72 | 149.17 | 40.87 | 228.53 | 50.94 | 284.84 | 65.14 | 364.20 |
| 23 | LA-1 TP-2 | 175.73 | 171.57 | 269.21 | 262.85 | 335.55 | 327.62 | 429.03 | 418.90 |
| 24 | LA-1 TP-3* | - | - | - | - | - | - | - | - |
| 25 | LA-1 TP-4a | 362.36 | 357.58 | 555.14 | 547.81 | 691.92 | 682.78 | 884.69 | 873.01 |
| 26 | LA-1 TP-4b | 492.87 | 613.02 | 755.08 | 939.14 | 941.12 | 1170.54 | 1203.33 | 1496.67 |
| 27 | LA-1 TP-5a | 292.73 | 294.33 | 448.47 | 450.92 | 558.96 | 562.02 | 714.70 | 718.60 |
| 28 | LA-1 TP-5b | 186.72 | 252.84 | 286.05 | 387.35 | 356.53 | 482.78 | 455.87 | 617.29 |
| 29 | LA-1 TP-6 | 352.28 | 349.01 | 539.69 | 534.69 | 672.66 | 666.43 | 860.08 | 852.11 |
| 30 | LA-1 TP-10 | 115.53 | 112.45 | 176.99 | 172.27 | 220.59 | 214.71 | 282.05 | 274.54 |

* Data after 30 days were not relevant and unused.

**Table 25**

**Statistical analysis of the set-up resistance for Level-1 model**

| Time Interval | Summary Statistics | | | |
|---|---|---|---|---|
| | $R_m/R_p$ | | | $R_p/R_m$ |
| | Mean ($\lambda_R$) | σ | COV | Mean |
| 14-30 | 1.13 | 0.47 | 0.41 | 1.03 |
| 14-45 | 1.02 | 0.33 | 0.33 | 1.18 |
| 14-60 | 1.00 | 0.29 | 0.29 | 1.22 |
| 14-90 | 0.97 | 0.26 | 0.27 | 1.23 |

Figure 61 presents the histogram and the normal and lognormal distributions of bias of the additional set-up resistance at four different time intervals using the Level-1 model. Figure 62 illustrates the CDFs of the resistance bias for the additional set-up resistance at four different

time intervals after 14 days. As shown in these figures, for all the four specific time intervals, lognormal distribution matches the histogram and the CDF of additional set-up resistance better than the normal distribution. In addition, the resistance bias factor ($\lambda_R = R_m/R_p$) can range theoretically from 0 to infinity, with an optimal value of one; therefore the distribution of the resistance bias can be assumed to follow a log-normal distribution *[80]*. In this study, the lognormal distribution was used for the reliability calibration analysis at four specific time intervals (i.e., 30 days, 45 days, 60 days and 90 days after 14 days from EOD).

**LRFD Calibration**

This study follows the calibration procedure based on the first order reliability method (FORM), Monte Carlo simulation method and first order second moment (FOSM) to determine the additional set-up resistance factors ($\phi_{set\text{-}up}$) at four specific time intervals from 14 days after EOD. Reliability analyses were conducted and the resistance factors for all different time intervals were calibrated at a dead load to live load ratio ($Q_{DL}/Q_{LL}$) of 3.0 since $\beta$ converges for $Q_{DL}/Q_{LL}$ exceeding 3.0. Figure 63 presents the additional set-up resistance factors ($\phi_{set\text{-}up}$) determined for various reliability indices ($\beta$) at four specific time intervals. As shown in the figures, the additional set-up resistance factors ($\phi_{set\text{-}up}$) determined by the advanced method (FORM and Monte Carlo Simulation method) are relatively close and generally higher than the additional set-up resistance factors ($\phi_{set\text{-}up}$) obtained from FOSM. The additional set-up resistance factor using the FORM and Monte Carlo Simulation method were generally 20% higher than those calculated using the FOSM method, indicating that $\phi_{set\text{-}up}$ values calculated using the simpler and closed-form FOSM method were relatively more conservative than those advanced methods. This difference in $\phi_{set\text{-}up}$ may attribute to (a) the different reliability theory implemented in calculating the $\phi_{set\text{-}up}$ values, (b) the assumed distribution for the probabilistic characteristics of the random variable $R_{set\text{-}up}$ *[17]*.

A review of the literature indicates that required reliability indices are between 2.33 and 3.00 for geotechnical applications *[16, 17, 57]*. The additional set-up resistance factors ($\phi_{set\text{-}up}$) for different time intervals to a reliability index ($\beta$) of 2.33 are tabulated in Table 26. The resistance factor ($\phi_{set\text{-}up}$) for additional set-up resistance at 30 days, 45 days, 60 days and 90 days from 14 days were in a range of 0.26 ~ 0.29, 0.29 ~ 0.34. 0.30 ~ 0.37 and 0.32 ~ 0.37, respectively for three different models at a target reliability index ($\beta$) of 2.33.The value is close to the reported value in literature. Yang and Liang before calibrated the set-up resistance factor using the FORM method and recommended to use $\phi_{set\text{-}up}$ as 0.30 *[16]*. Recently Ng and Sritharan also calibrated the set-up resistance factor for steel H-piles and recommended $\phi_{set\text{-}up}$ as 0.36 *[17]*. Finally, it was recommended to use additional set-up resistance factor ($\phi_{set\text{-}up}$) as 0.28, 0.30, 0.35 and 0.35 at 30 days, 45 days, 60 days and 90 days after 14 days, respectively for driven piles in Louisiana.

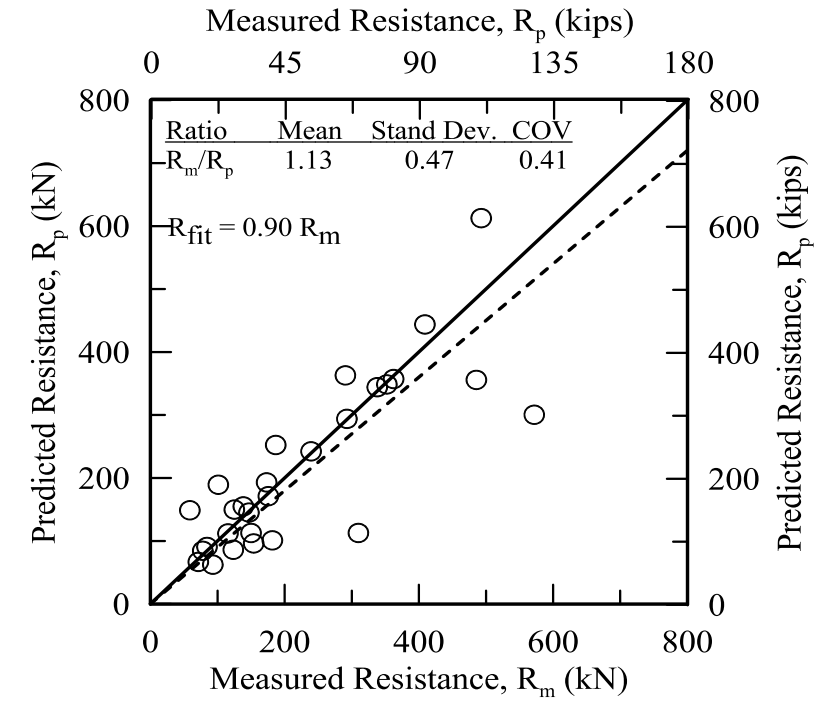


(a) Comparison of ($R_{30}$ - $R_{14}$) for Level-1

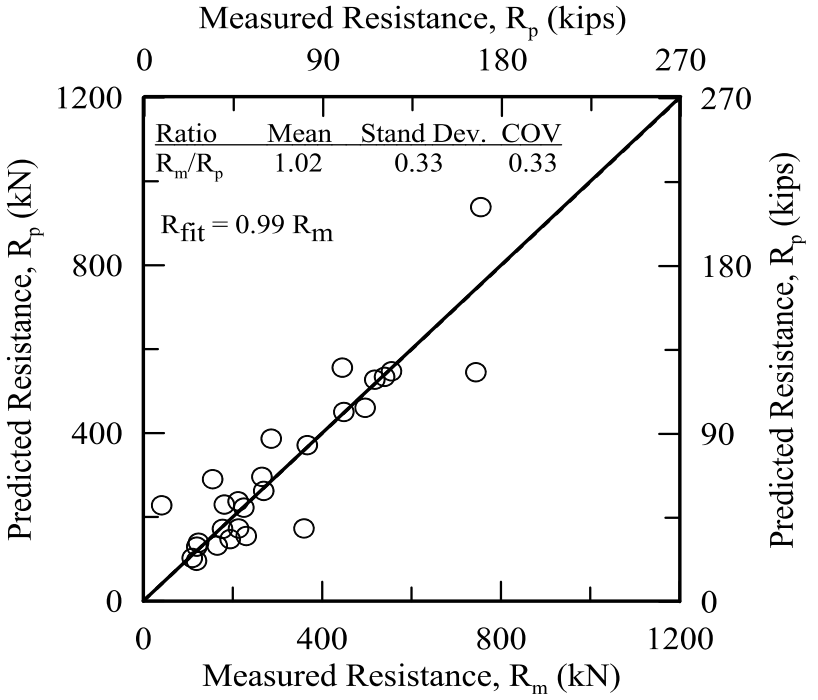


(b) Comparison of ($R_{45}$ - $R_{14}$) for Level-1 model

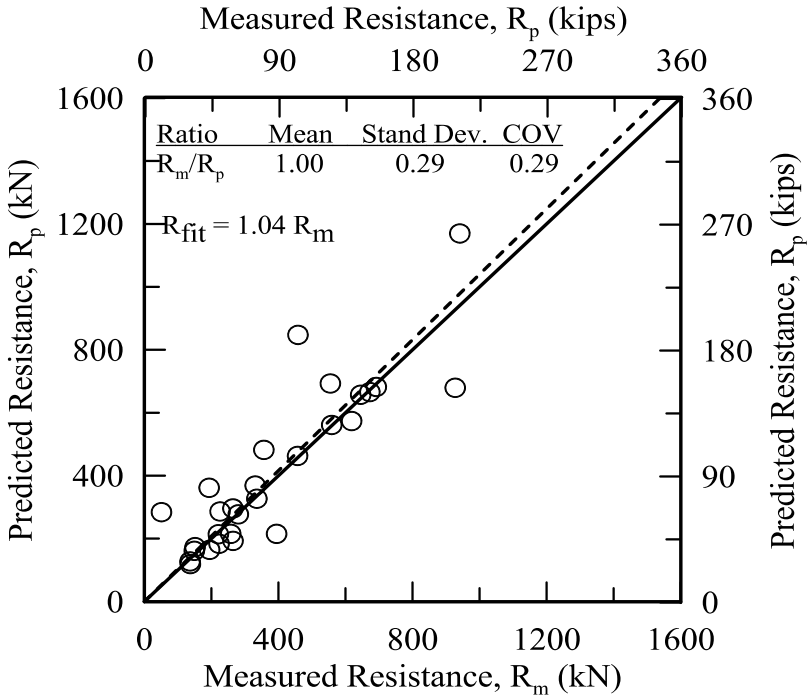


(c) Comparison of ($R_{60}$ - $R_{14}$) for Level-1

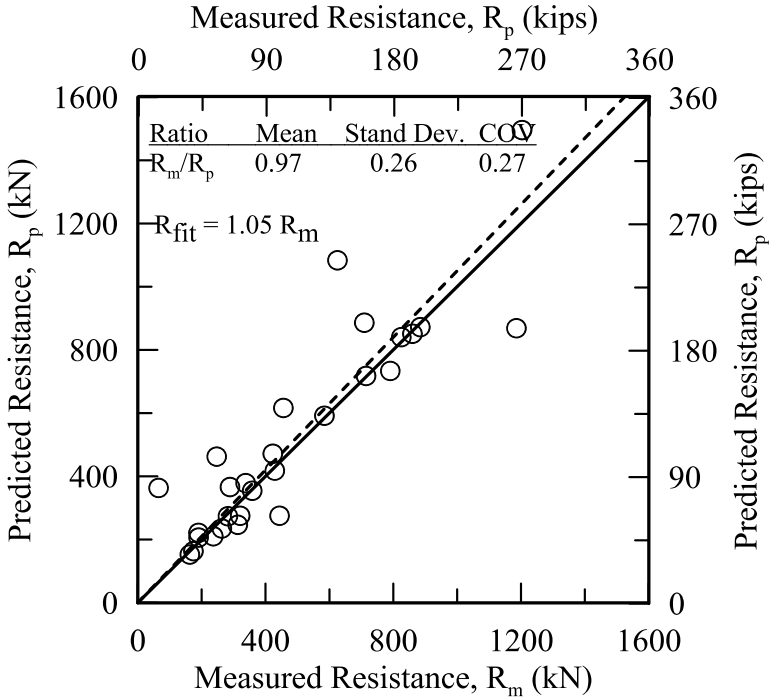


(d) Comparison of ($R_{90}$ - $R_{14}$) for Level-1 model

**Figure 60**
**Measured versus predicted resistance for set-up from 14 days for Level-1**

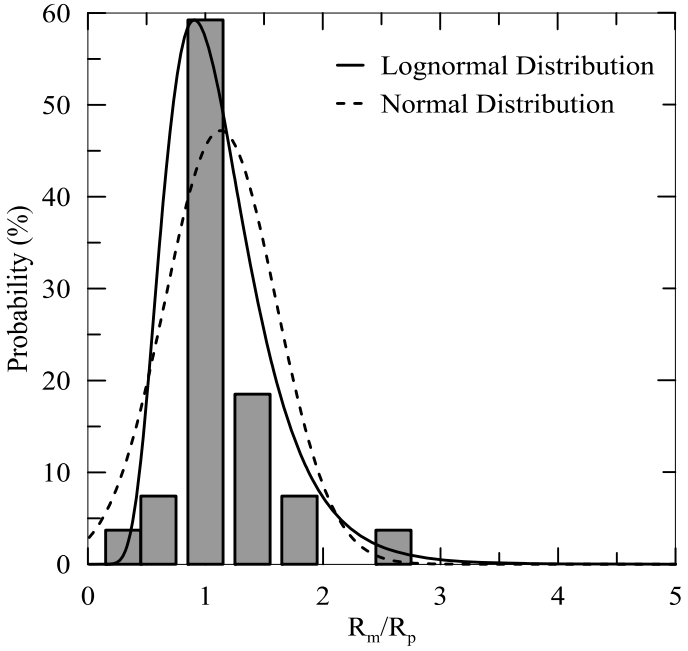


(a) Histogram of bias factors for $R_{30}$ - $R_{14}$

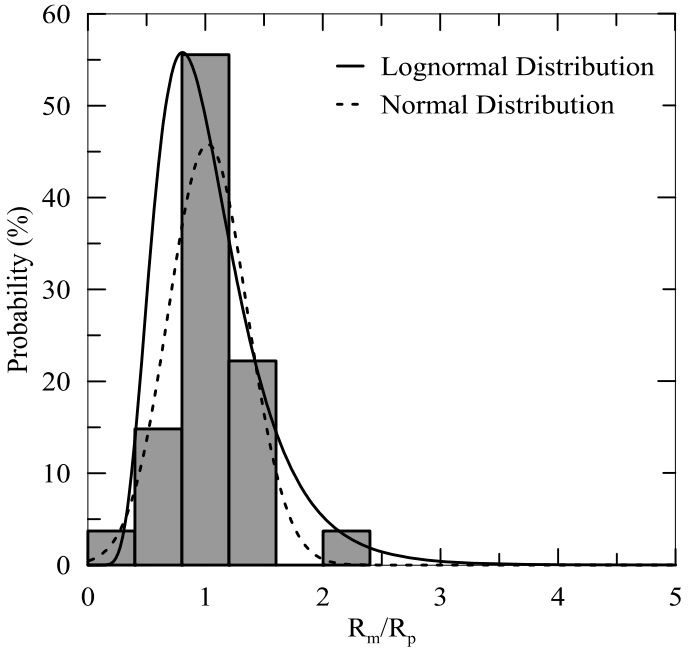


(b) Histogram of bias factors for $R_{45}$ - $R_{14}$

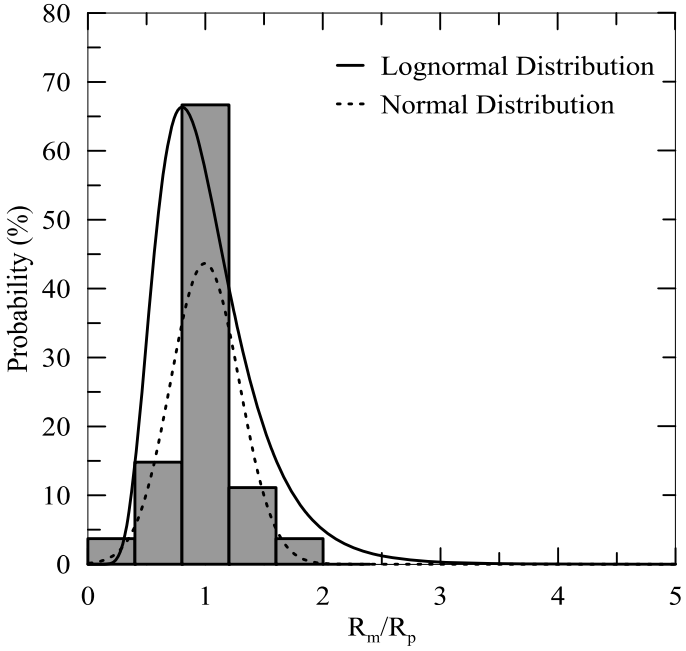


(c) Histogram of bias factors for $R_{60}$ - $R_{14}$

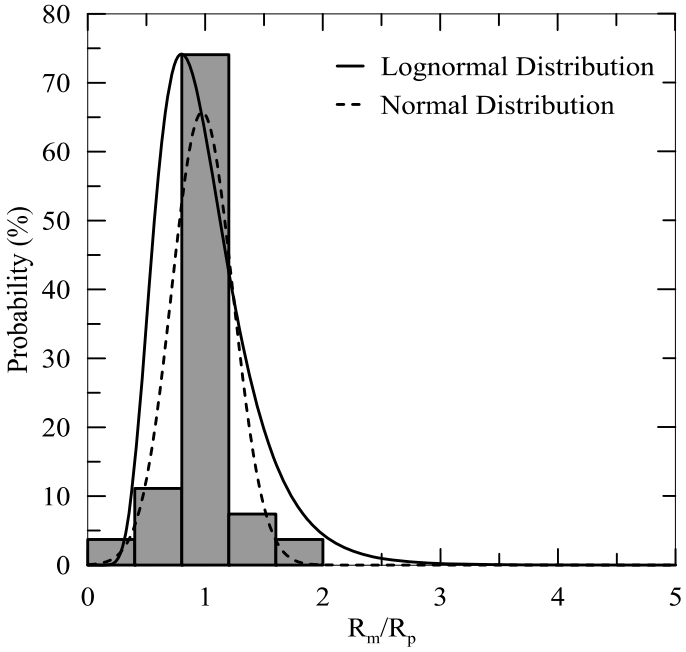


(d) Histogram of bias factors for $R_{90}$ - $R_{14}$

**Figure 61**
**Histograms of bias factors for interpretation criteria for Level-1 model**

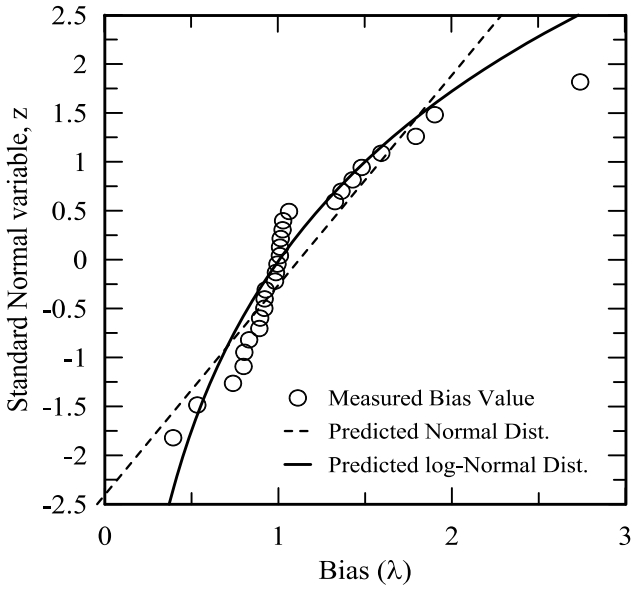


(a) Cumulative distribution function (CDF) of bias values for additional set-up resistance ($R_{30}$-$R_{14}$)

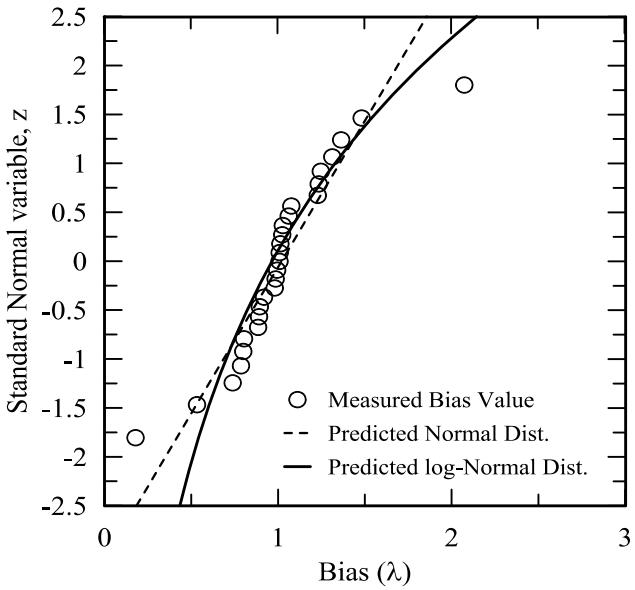


(b) Cumulative distribution function (CDF) of bias values for additional set-up resistance ($R_{45}$-$R_{14}$)

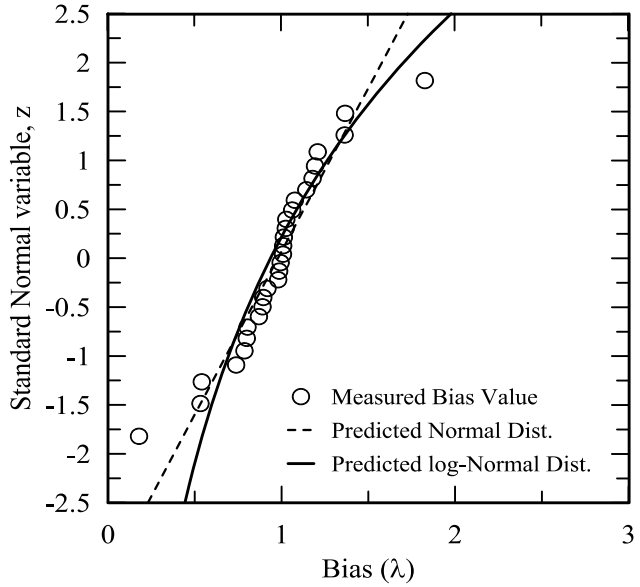


(c) Cumulative distribution function (CDF) of bias values for additional set-up resistance ($R_{60}$-$R_{14}$)

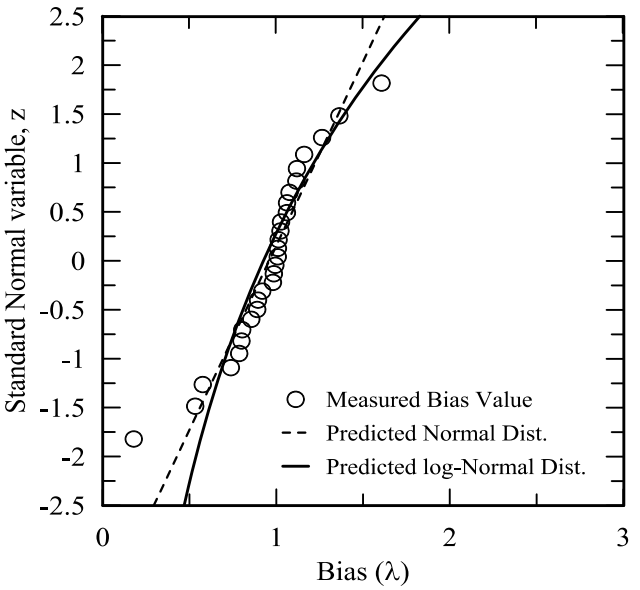


(d) Cumulative distribution function (CDF) of bias values for additional set-up resistance ($R_{90}$-$R_{14}$)

**Figure 62**
**Cumulative distribution function (CDF) of bias values for additional resistances after 14 days at four different time intervals**

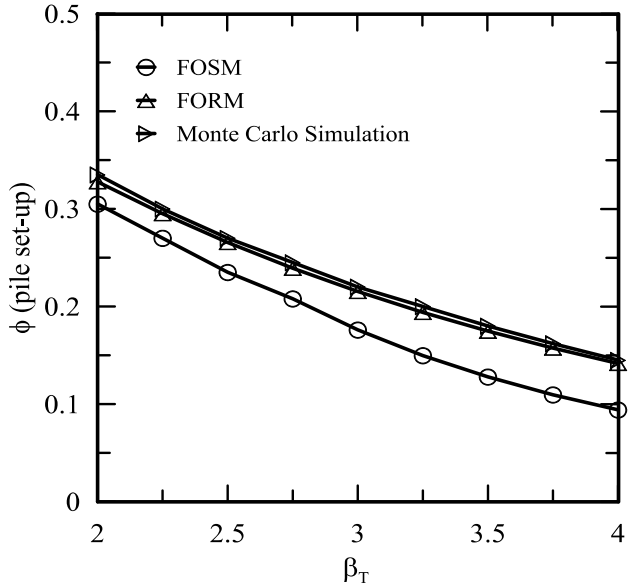


(a) Resistance factor calibrated for $R_{30}$-$R_{14}$ set-up resistance

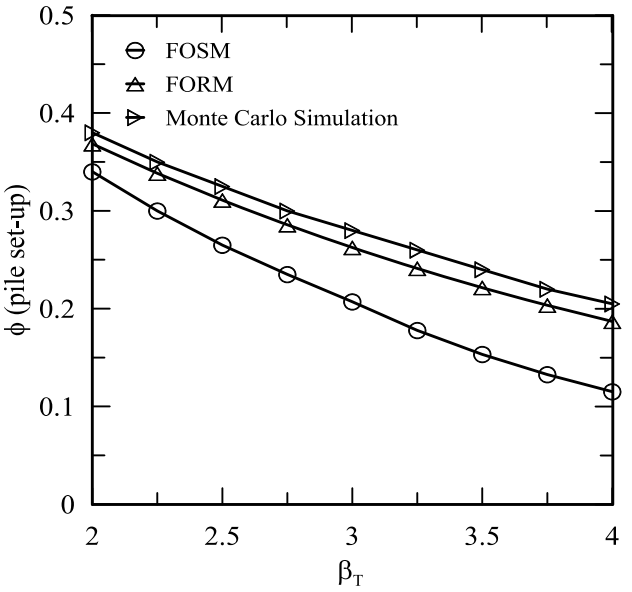


(b) Resistance factor calibrated for $R_{45}$-$R_{14}$ set-up resistance

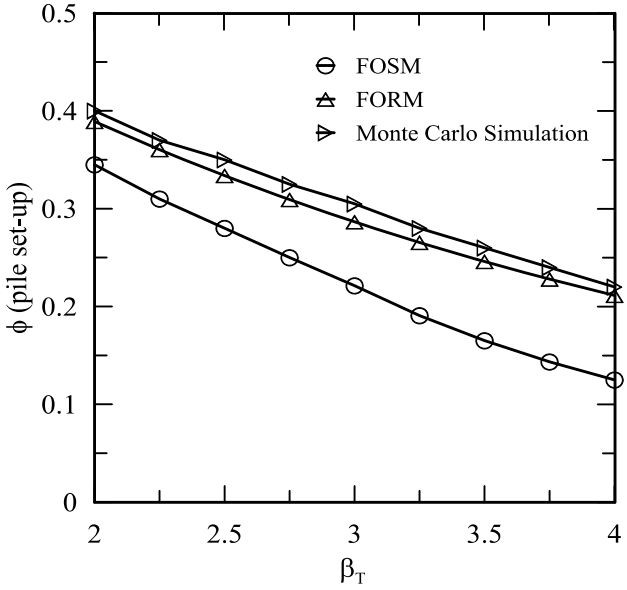


(c) Resistance factor calibrated for $R_{60}$-$R_{14}$ set-up resistance

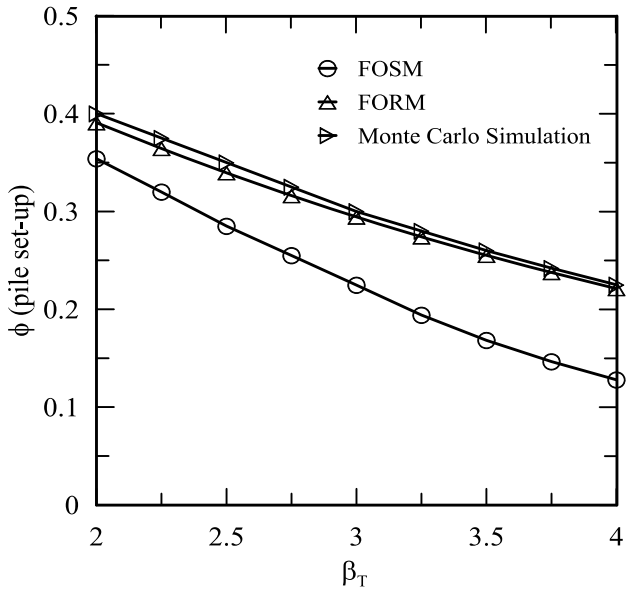


(d) Resistance factor calibrated for $R_{90}$-$R_{14}$ set-up resistance

**Figure 63**
**Set-up resistance factors for different reliability indexes of Level-1 model**

**Table 26**

**Set-up resistance factors ($\phi_{set\text{-}up}$) for driven piles**

| | FOSM | | | FORM | | | MCS | | | Recommended |
|---|---|---|---|---|---|---|---|---|---|---|
| | Level-1 | Level-2 | Level-3 | Level-1 | Level-2 | Level-3 | Level-1 | Level-2 | Level-3 | |
| $\phi_{set\text{-}up}$ for additional set-up at 30 days | 0.26 | 0.27 | 0.27 | 0.28 | 0.30 | 0.30 | 0.29 | 0.30 | 0.31 | 0.28 |
| $\phi_{set\text{-}up}$ for additional set-up at 45 days | 0.29 | 0.30 | 0.31 | 0.33 | 0.34 | 0.35 | 0.34 | 0.36 | 0.37 | 0.30 |
| $\phi_{set\text{-}up}$ for additional set-up at 60 days | 0.30 | 0.32 | 0.33 | 0.35 | 0.35 | 0.36 | 0.37 | 0.37 | 0.38 | 0.35 |
| $\phi_{set\text{-}up}$ for additional set-up at 90 days | 0.32 | 0.34 | 0.34 | 0.35 | 0.36 | 0.36 | 0.37 | 0.38 | 0.38 | 0.35 |
| Ng and Sritharan [17] | 0.36 | | | | | | | | | |
| Yang and Liang [16] | 0.30 | | | | | | | | | |
| **Overall Recommended** | **0.35** | | | | | | | | | |

**Implementation Procedure**

Two scenarios (or phases) will be considered here to implement the pile set-up resistance in the design and analysis of driven piles. They are:

- Design Phase (No load tests are available)
- Construction Phase (Restrikes and/or static load tests are performed)

**Design Phase**

The increase in pile resistance due to set-up from EOD to 14 days was already included in a previous research study for static and direct CPT pile design methods, which was incorporated in the local design guidelines *[57]*. In the previous study, LRFD calibration was performed for pile resistances corresponding to 14 days after EOD ($R_{14}$), and the resistance factors ($\phi_{14}$) that include set-up from EOD to 14 days were recommended for the different pile design methods, which range from 0.48 to 0.74 (Table 1). Incorporating pile set-up for any time beyond the 14 days after EOD can be achieved through either estimating the increase in side resistance of the pile ($R_s$) or estimating the increase in side resistance of individual soil layers ($R_{si}$) along the pile length. In either approach, two steps are needed in order to incorporate pile set-up in the design phase beyond the 14 days after EOD. First step: calculate the initial side resistance of the pile ($R_{so}$) (or the initial side resistance for individual soil layers ($R_{soi}$)). Second step: estimate the total side resistance of the pile ($R_{st}$) using the weighted average value of A (or sum of $R_{sti}$ for individual soil layers) at any specific time (t) beyond the 14 days. The additional pile set-up resistance from 14 days to any specific time t after EOD will be equal to the increase in total side resistance of

the pile from 14 days, $R_{set\text{-}up} = R_{st} - Rs_{14}$. No change in tip resistance with time. The corresponding strength limit state equation (equation 19) for design of piles including set-up at any time will be as follows:

$$\phi_{14}R_{14} + \phi_{set\text{-}up}R_{set\text{-}up} \geq \gamma_{DL}Q_{DL} + \gamma_{LL}Q_{LL} \quad (19)$$

**Steps to calculate the initial pile resistance ($R_o$) (or $R_{soi}$ for individual soil layers)**

i. Perform subsurface soil investigation (soil boring and/or in-situ tests) to identify the soil stratification and layers' thicknesses ($H_1$, $H_2$, … $H_n$), and to evaluate the soil properties.

ii. Calculate the total and side resistance of the pile at 14 days ($R_{14}$ and $R_{s14}$) using the static design methods or CPT design methods.

iii. Calculate the set-up parameter "A" for individual clayey soil layers using the proposed correlations (i.e., the correlations with respect to the initial reference time, $t_o$ =1 day) in this study. Any of the following three correlations can be used based on available soil properties [equation (33) is recommended].

$$A = \frac{0.79\left(\frac{PI}{100}\right) + 0.49}{\left(\frac{S_u}{1\ tsf}\right)^{2.03} + 2.27} \qquad \text{(recommended)} \quad (33)$$

$$A = \frac{1.12*\left(\frac{PI}{100}\right)+0.69}{\left[\left(\frac{S_u}{1\ tsf}\right)^{1.44}\right]*\left[\log\left(\frac{C_v}{0.01\frac{in^2}{hour}}\right)\right]^{0.54}+3.19} \quad (35)$$

$$A = \frac{0.44*\left(\frac{PI}{100}\right)(S_t)+2.20}{\left[\left(\frac{S_u}{1tsf}\right)^{1.94}\right]*\left[\log\left(\frac{C_v}{0.01\frac{in^2}{hour}}\right)\right]^{1.06}+10.65} \quad (37)$$

For sandy soil layers, a constant value of 0.15 will be used as set-up parameter "A". The set-up parameter "$A_{av}$" for the total length of the pile will be calculated using the weighted average method.

$$A_{av} = \frac{H_1*A_1+H_2*A_2....H_n*A_n}{H_{total}} \quad (45)$$

iv. Back-calculate the initial pile side resistance ($R_{so}$ using $A_{av}$) (or $R_{soi}$ for individual soil layers using $A_i$) corresponding to 1 day after EOD using the Skov and Denver's model *[7]* as follows:

$$\frac{R_{s14}}{Rso} = 1 + A_{av}\log\frac{t\ (t=14\ day)}{t_o(t_o=1\ day)} \quad (46)$$

$$R_{so} = R_{s14} / \left[1 + A_{av}\log\frac{t\ (t=14\ day)}{t_o(t_o=1\ day)}\right] \quad (47)$$

**Steps to calculate the pile set-up resistance beyond 14 days ($R_{st}$, t >14 days)**

i. The initial side resistance of the pile ($R_{so}$) (or $R_{soi}$ for individual soil layers) that was calculated from previous steps will be used to predict the total side resistance set-up ($R_{st}$) (or $R_{sti}$ for individual soil layers) at any time t after EOD (i.e., 45 days, 60 days, 90 days, 120 days or other times).

ii. The weighted average set-up parameter "$A_{av}$" that was that was used to back-calculate the initial pile side resistance ($R_{so}$) will be used to estimate the pile side resistance ($R_{st}$) (or $R_{sti}$ for individual soil layers using $A_i$) at any time by implementing the Skov and Denver's model *[7]*. The model is

$$\frac{R_{st}}{Rso} = 1 + A_{av} \log \frac{t}{t_o(t_o=1\ day)}$$

iii. The resistance factor ($\phi_{14}$) of the specific pile design method (Table 1) will be applied in LRFD design to the total pile resistance at 14 days ($R_{14}$) [i.e., $\phi_{14}R_{14}$ in equation (19)]. A resistance factor ($\phi_{set\text{-}up} = 0.35$) will be applied to the additional side resistance set-up ($R_{set\text{-}up} = R_{st} - R_{s14}$) from14 days to any specific time t after EOD ($\phi_{set\text{-}up}R_{set\text{-}up}$).

**Construction Phase**

Restrikes and/or load tests are usually performed during the construction phase. Therefore, a different approach will be followed to incorporate set-up in the construction phase. The first restrikes usually performed from 1 hour to 1 day after EOD. Three different models were developed to predict the unit side resistance ($f_s$) set-up after EOD with respect to the normalized time $t_o$ =1 hour and another three different models were developed to predict the unit side resistance ($f_s$) set-up after EOD with respect to the normalized time $t_o$ for 1 day. The following steps summarize the implementation of set-up during the construction phase:

i. Perform the 1st restrike (preferably at 1 hour to 1 day after EOD).

ii. Perform CAPWAP analyses on the restrike data to calculate the initial unit side resistance ($f_{so}$) of individual soil layers along the pile length.

iii. Use equations (34), (36), or (38) [equation (34) is recommended] to calculate the unit side resistance set-up if the restrike is performed at t = 1 day, or equations (42), (43) or (44) [equation (42) is recommended] if a restrike is conducted at t = 1 hour after EOD. The necessary steps to predict the unit side resistance set-up if a restrike is performed in between 1 hour to 1 day are also described in the following section.

iv. The set-up for total resistance can be calculated using two approaches. First approach: estimate the side resistance set-up for individual soil layers. Second approach: use the weighted average value of A (or weighted average soil properties) to estimate the side resistance set-up of the pile ($R_s$). The detail steps for both approaches are described in the following section.

v. It is recommended to use a set-up resistance factor ($\phi_{set\text{-}up}$) of 0.5 in the construction phase, which is 50% higher than the resistance factors in the design phase ($\phi_{set\text{-}up}$ is design phase is 0.35), since the set-up rate A can be verified during the construction phase.

The developed models to estimate set-up for unit side resistance ($f_s$) (for first approach) with respect to the normalized time $t_o$ = 1 day are:

$$\frac{f_s}{f_{so(1\text{-}day)}} = 1 + \left[\frac{0.79*\left(\frac{PI}{100}\right)+0.49}{\left(\frac{S_u}{1\ tsf}\right)^{2.03}+2.27}\right] \log\frac{t}{t_{o(1\text{-}day)}} \quad \text{(Recommended)} \tag{34}$$

$$\frac{f_s}{f_{so(1\text{-}day)}} = 1 + \left[\frac{1.12*\left(\frac{PI}{100}\right)+0.69}{\left[\left(\frac{S_u}{1\ tsf}\right)^{1.44}\right]*\left[\log\left(\frac{C_v}{0.01\frac{in^2}{hour}}\right)\right]^{0.54}+3.19}\right] \log\frac{t}{t_{o(1\text{-}day)}} \tag{36}$$

$$\frac{f_s}{f_{so(1\text{-}day)}} = 1 + \left[\frac{0.44*\left(\frac{PI}{100}\right)(S_t)+2.20}{\left[\left(\frac{S_u}{1tsf}\right)^{1.94}\right]*\left[\log\left(\frac{C_v}{0.01\frac{in^2}{hour}}\right)\right]^{1.06}+10.65}\right] \log\frac{t}{t_{o(1\text{-}day)}} \tag{38}$$

The developed models with respect to the normalized time $t_o$ = 1 hour are:

$$\frac{f_s}{f_{so(1\text{-}hr)}} = 1 + \left[\frac{1.02*\left(\frac{PI}{100}\right)+0.26}{\left(\frac{S_u}{1\ tsf}\right)^{0.68}+0.50}\right] \log\frac{t}{t_{o(1\text{-}hr)}} \text{ (Recommended)} \tag{42}$$

$$\frac{f_s}{f_{so(1\text{-}hr)}} = 1 + \left[\frac{1.18*\left(\frac{PI}{100}\right)+0.32}{\left[\left(\frac{S_u}{1\ tsf}\right)^{0.40}\right]*\left[\log\left(\frac{C_v}{0.01\frac{in^2}{hour}}\right)\right]^{0.37}+0.53}\right] \log\frac{t}{t_{o(1\text{-}hr)}} \tag{43}$$

$$\frac{f_s}{f_{so(1\text{-}hr)}} = 1 + \left[\frac{0.11*\left(\frac{PI}{100}\right)(S_t)+0.23}{\left[\left(\frac{S_u}{1tsf}\right)^{0.07}\right]*\left[\log\left(\frac{C_v}{0.01\frac{in^2}{hour}}\right)\right]^{0.17}-0.06}\right] \log\frac{t}{t_{o(1\text{-}hr)}} \tag{44}$$

**For Initial Restrike Between 1 Hour and 1 Day**

Usually, the initial restrike is performed between 1 hour and 1 day after EOD, depending on the project. The initial unit side resistance ($f_{so}$) from the restrike will be considered depending on the initial normalized time, $t_o$ (i.e., 1 hour or 1 day). Equations (42) - (44) [recommended equation (42)] can be used to estimate the unit side resistance set-up if the restrike is performed at 1 hour; while equations (34), (36) or (38) [recommended equation (34)] can be used to estimate the unit side resistance set-up if the restrike is performed at 1 day. However, if the restrike is performed between 1 hour and 1 day, then the unit side resistance ($f_{so}$) at 1 hour or 1 day will be calculated first using equations (42) - (44) or equations (34), (36), (38), respectively, depending on which

normalized time $t_o$ is closer to restrike time. If the restrike is performed at or earlier than 12 hours after EOD, then equations (42) - (44) will be used to back-calculate the initial unit side resistance ($f_{so}$) at the normalized $t_o$ = 1 hour. However, if the restrike is performed later than 12 hours after EOD, then equations (34), (36), (38) will be implemented to calculate the initial unit side resistance ($f_{so}$) at the normalized $t_o$ = 1 day.

For example, using first approach, if the first restrike is performed at 5 hours after EOD, then equations (42) will be used to calculate the initial unit side resistance ($f_{so}$) at $t_o$ = 1 hour.

$$\frac{f_{s(5\text{-hr})}}{f_{so(1\text{-hr})}} = 1 + \left[\frac{1.02*\left(\frac{PI}{100}\right)+0.26}{\left(\frac{S_u}{1\ tsf}\right)^{0.68}+0.50}\right] \log \frac{t_{(5\text{-hr})}}{t_{o(1\text{-hr})}}$$

After calculating the $f_{so}$ at 1 hour, then equation (42) will be used to predict the unit side resistance set-up at any specific time, t (e.g., 30 days) as follows:

$$\frac{f_{s(30\text{-day})}}{f_{so(1\text{-hr})}} = 1 + \left[\frac{1.02*\left(\frac{PI}{100}\right)+0.26}{\left(\frac{S_u}{1\ tsf}\right)^{0.68}+0.50}\right] \log \frac{t_{(30\text{-day})}}{t_{o(1\text{-hr})}}$$

In the case of several restrikes are performed in the field, the set-up parameter "A" can be verified, adjusted and used to estimate the unit side resistance set-up at any specific time, t.

**First Approach: Implementation procedure for individual soil layers**

Equations (34), (36), (38), (42), (43), (44) that incorporate different soil properties can be implemented to estimate the increase in unit side resistance ($f_s$) of individual clayey soil layer due to set-up at any time after the initial normalized time $t_o$ (i.e., 1 hour to 1 day). The unit side resistance ($f_s$) value will be first multiplied with the contact area of the soil layer ($A_{si}$) to calculate the side resistance ($R_{si}$) of that layer. In the absence of sandy soil layers, the side resistance of all clayey soil layers ($R_{si}$) along the pile length can be added to evaluate the total side resistance ($R_s$) of the pile. In the presence of mixed (i.e., clayey and sandy) soil layers, the total resistance ($R_t$) due to set-up can be calculated using the following procedure:

(1) Identify and classify the soil layers along the length of the pile from laboratory and/or in-situ tests (i.e., PCPT) and evaluate the required subsurface soil properties for the selected set-up model level (i.e., $S_u$, PI, OCR, $c_v$, $S_t$) for all soil layers.

(2) Evaluate the initial unit side resistance ($f_{so}$) of each soil layer from the initial restrike (i.e., 1 hour, 1 day, or any other time restrike).

(3) If the restrike is performed between 1 hour and 1 day, then use equations (34), (36), (38) to estimate the unit side resistance ($f_{so}$) at 1 day, or use equations (42) - (44) to estimate the unit side resistance ($f_{so}$) at 1 hour, depending on which normalized time $t_o$ is closer to the restrike time.

(4) Depending on the soil type and recommendations provided in Table 27, select a maximum set-up time frame, t, for each soil layer (i.e., 3 days for medium dense and loose sands, 30 days for stiff clay, 75 days for medium clay and 120 days for soft clay).

(5) Use equations (42) - (44) (initial normalized time $t_o$ = 1 hour) or equations (34), (36), (38) (initial normalized time $t_o$ = 1 day) to calculate the unit side resistance ($f_{si}$) of clayey soil layers due to set-up, and multiply the $f_{si}$ value with the contact area ($A_{si}$) of the corresponding layer to estimate the side resistance of that soil layer ($R_{si\ (set\text{-}up)} = f_{si\ (set\text{-}up)} \times A_{si}$).

(6) Use a constant value of A = 0.28 (if $t_o$ = 1 hour) or A = 0.15 (if $t_o$ = 1 day) as set-up parameter (the average value of "A" parameter of all sandy soil layers in this study) to estimate the unit side resistance ($f_{si}$) due to set-up for the sandy soil layers, and calculate the side resistance ($R_{si}$) of the sandy soil layers.

(7) Sum the set-up side resistances for all soil layers ($R_{s1}$, $R_{s2}$…$R_{sn}$) to estimate the total side resistance ($R_s$) of the pile.

$R_{s\ (set\text{-}up)} = R_{s1\ (set\text{-}up)} + R_{s2\ (set\text{-}up)} + \ldots\ldots\ldots + R_{sn\ (set\text{-}up)}$

(8) Since no set-up was observed in the tip ($R_{tip}$) resistance in this study as well as reported in the literature, no set-up is considered in the tip resistance ($R_{tip}$).

(9) The total resistance ($R_t$) of the pile due to set-up can be calculated by adding the set-up side resistance ($R_s$) and the tip resistance measured at 1st restrike (i.e., 1 hour or 1 day).

$R_{t\ (set\text{-}up)} = R_{s\ (set\text{-}up)} + R_{tip\ (1st\ restrike)}$

**Second Approach: Implementation Procedure for Weighted Average Methods**

The developed model can also be implemented through calculating the weighted average set-up parameter ($A_{av}$) as described earlier in the design phase, or by using the weighted average values of soil properties for clayey soil layers to calculate the set-up parameter "A." The following steps can be followed to calculate the total resistance ($R_t$) due to "set-up" using he weighted average values of soil properties:

(1) Evaluate the subsurface soil properties (i.e., $S_u$, PI, OCR, $c_v$, $S_t$) for each soil layer.

(2) Determine the weighted average values of each soil properties for the total height of the clayey soil layers. For example:

$$S_{u\ (WAV)} = \frac{(Su1 \times H1)+(Su2 \times H2)\ldots.+(Sun \times Hn)}{H\ (Clayey\ soil\ layer)}$$

$$PI_{\ (WAV)} = \frac{(PI_1 \times H_1)+(PI_2 \times H_2)\ldots.+(PI_n \times H_n)}{H\ (Clayey\ soil\ layer)}$$

(3) The set-up rate value for the clayey soil layers ($A_{-clay}$) can be calculated using equations (39)-(41) (if $t_o$ = 1 hour) or equations (33), (35) or (37) (if $t_o$ = 1 day) using the weighted average values of soil properties from step-2.

(4) As stated earlier, for sandy soil layers set-up parameter $A_{sand}$ = 0.28 (if $t_o$ = 1 hour) or $A_{sand}$ = 0.15 (if $t_o$ = 1 day).

(5) The set-up rate value for the total length of the pile ($A_{-Total\ pile}$) can be calculated as:

$$A_{(Total\ pile)} = \frac{(A\ clay \times H\ clay) + (A\ sand \times H sand)}{H\ (Total\ length\ of\ pile)}$$

The value of $A_{-Total\ pile}$ can be verified and adjusted if two or more restrikes are performed in the field.

(6) The "A" value from step-5 can be implemented into the following equation to determine the total side resistance ($R_s$) of the pile due to set-up.

$$\frac{R_s}{R_{so}} = 1 + A_{(Total\ pile)} \log \frac{t}{t_o}$$

(7) The total resistance ($R_t$) due to set-up can be calculated as the sum of total set-up side resistance ($R_s$) obtained from step-6 with and the tip resistance measured at 1st restrike (i.e., 1 hour or 1 day).

$R_{t\ (set\text{-}up)} = R_{s\ (set\text{-}up)} + R_{tip\ (1st\ restrike)}$

**Time Frame to Implement the Set-up Models**

Pile resistance increase due to set-up is expected to continue as long as the consolidation process (dissipation of excess PWP) of the surrounding soil is not completed. After the completion of consolidation process, pile resistance may continue to increase during the "aging" set-up phase at much slower rate, which is usually considered insignificant to be considered in the design of piles. The duration of the consolidation process for each soil layer due to pile installation can be estimated using the coefficient of horizontal consolidation ($c_h$), which can be determined either from laboratory oedometer consolidation test (for $c_v$ value) and using the ratio of horizontal to vertical coefficient of permeability ($k_h/k_v$) to evaluate $c_h$ [i.e., $c_h = (k_h/k_v)\, c_v$], or directly measured from in-situ piezocone dissipation tests (first option), and applying the consolidation theory on pile face to estimate $t_{90}$ (time for 90% consolidation). Teh and Houlsby *[73]* interpretation equation can be used to estimate $t_{90}$ on the pile face ($t_{90} = T_{90}\, D^2/c_h$, where D = equivalent pile diameter). In this study, the duration of consolidation phase was measured by the piezometers installed on the pile face. In the absence of $c_h$ parameters, the recommended time frame values presented in Table 27 can be used (second option) to implement the set-up models effectively. The time frames to estimate pile set-up are proposed here based on the results of this study, which are grouped according to soil type and soil properties. No significant set-up is expected for dense sand, and in contrary, sometimes it might be subjected to relaxation.

However, set-up continues for a short time period in medium dense and loose sands (up to 3 days). Depending on the PI and $S_u$, three different time frames are proposed for clayey soil layers to implement the set-up equations (33)-(44) effectively. It is recommended to use a time frame of 30 days for stiff clayey soil layers with PI < 20% and $S_u$ > 1.0 tsf. For medium clayey soil layers with PI = 20% to 50% and $S_u$ = 0.5 tsf to 1.0 tsf, it is recommended to use a time frame of 75 days. A time frame of 120 days can be used for soft clayey soil layers with PI > 50% and $S_u$ < 0.5 tsf. However, set-up resistance increase can be extended beyond 120 days for very soft clayey soils ($S_u$ < 0.25 tsf) provided the duration of consolidation phase is verified using estimated $c_h$ and consolidation theory.

**Table 27**

**Proposed time frame to predict pile set-up resistance**

| Soil Type | | | | Time Frame |
|---|---|---|---|---|
| Sand | Dense Sand | - | | No set-up |
| | Medium Dense and Loose Sand | | | 3 days |
| | | PI | $S_u$ (tsf) | |
| Clay | Stiff Clay | 4% to 20% | (1.0 - 1.5) tsf | 30 days |
| | Medium Clay | 20% to 50% | (0.5 – 1.0) tsf | 75 days |
| | Soft Clay | 50% to 80% | (0.1 -0.5) tsf | >120 days |

**Implementation Example**

**First Approach: Individual Soil Layers**

The following example illustrates the implementation procedure for the proposed set-up model (equation 34) using the first approach (i.e., calculate resistance for individual soil layers) to estimate set-up for test pile-1of Bayou Lacassine site. The subsurface soil layering and properties are presented in Figure 11. The first restrike was performed at 1 day after EOD ($t_o$ = 1 day). Equation (34) is implemented to calculate the unit side resistance ($f_s$) due to set-up at t = 53 days for each clayey soil layer separately as follows:

$$\frac{f_s}{f_{so}} = 1 + \left[\frac{0.79\left(\frac{PI}{100}\right) + 0.49}{\left(\frac{S_u}{1\ tsf}\right)^{2.03} + 2.27}\right] \log\frac{t}{t_o};$$

$$\frac{f_{s2}}{0.31} = 1 + \left[\frac{0.79\left(\frac{25}{100}\right) + 0.49}{\left(\frac{0.72}{1\ tsf}\right)^{2.03} + 2.27}\right] \log\frac{53}{1};\ f_{s2} = 0.44\ tsf$$

$R_{S2}$ = 0.44 tsf x 110 $ft^2$ (area of the layer) = 48.4 ton

$$\frac{f_{s3}}{0.38} = 1 + \left[\frac{0.79\left(\frac{18}{100}\right) + 0.49}{\left(\frac{1.12}{1\ tsf}\right)^{2.03} + 2.27}\right] \log\frac{53}{1};\ f_{s3} = 0.50\ tsf$$

$R_{S3}$ = 0.50 tsf x 50 $ft^2$ (area of the layer) = 25 ton

$\frac{f_{s5}}{0.50} = 1 + [\frac{0.79\left(\frac{25}{100}\right) + 0.49}{\left(\frac{1.23}{1\ tsf}\right)^{2.03} + 2.27}] \log\frac{53}{1}$; $f_{s5}$ = 0.66 tsf

$R_{S5}$ = 0.66 tsf x 100 $ft^2$ (area of the layer) = 66 ton

$\frac{f_{s6}}{0.40} = 1 + [\frac{0.79\left(\frac{12}{100}\right) + 0.49}{\left(\frac{1.22}{1\ tsf}\right)^{2.03} + 2.27}] \log\frac{53}{1}$; $f_{s6}$ = 0.51 tsf

$R_{S6}$ = 0.51 tsf x 50 $ft^2$ (area of the layer) = 25.5 ton

$\frac{f_{s7}}{0.34} = 1 + [\frac{0.79\left(\frac{4}{100}\right) + 0.49}{\left(\frac{1.05}{1\ tsf}\right)^{2.03} + 2.27}] \log\frac{53}{1}$; $f_{s7}$ = 0.43 tsf

$R_{S7}$ = 0.43 tsf x 50 $ft^2$ (area of the layer) = 21.5 ton

$\frac{f_{s8}}{0.26} = 1 + [\frac{0.79\left(\frac{17}{100}\right) + 0.49}{\left(\frac{1.17}{1\ tsf}\right)^{2.03} + 2.27}] \log\frac{53}{1}$; $f_{s8}$ = 0.34 tsf

$R_{S8}$ = 0.34 tsf x 50 $ft^2$ (area of the layer) = 17 ton

For the sandy soil (layer-4), a value of A = 0.15 is used as calculated in this study.

$\frac{f_{s4}}{f_{so}} = 1 + A \log\frac{t}{t_o}$; $\frac{f_{s4}}{0.45} = 1 + 0.15 \log\frac{3}{1}$; $f_{s4}$ = 0.48 tsf; $R_{s4}$ = 0.48 tsf x 50 $ft^2$ = 24 ton

[t =3 days is used as no set-up is considered after 3 days for sand]

The total side resistance ($R_s$) due to set-up of the pile can be calculated as follows:
$R_s = \sum_{i=1}^{n=8} R_{Si}$ = 227.4 ton (455 kips) (The top 21 ft. is not considered due to casing)

The total side resistance ($R_s$) due to set-up estimated using the proposed model at t = 53 days (the 2nd SLT) after EOD is very close to the measured $R_s$ value (i.e., 427 kips) at 53 days. The total resistance ($R_t$) due to set-up can be calculated as: $R_t = R_{s\ (set\text{-}up)} + R_{tip\ (1\text{-}Day)}$ = 455 kips + 79 kips = 534 kips, which is very close to the measured total resistance ($R_t$) (i.e., 500 kips) at 53 days.

**Second Approach: Weighted Average Methods**

The following example illustrates the implementation procedure for the proposed set-up model at Level-1 using the 2nd approach (i.e., weighted average method) to estimate set-up for test pile-1 of Bayou Lacassine site. The test pile had 7 soil layers along the length of the pile (Figure 11). The weighted average value of PI for the six clayey soil layer is:

$$PI_{(WAV)} = \frac{(PI_1 \times L_1)+(PI_2 \times L_2)....+(PI_n \times L_n)}{L\ (Clayey\ soil\ layer)}$$

$$= \frac{(25x11)+(18x5)+(25x10)+(12x5)+(4x5)+(17x5)}{11+5+10+5+5+5}$$

$$= 19$$

The weighted average value of $S_u$ for the six clayey soil layer is:

$$S_{u\ (WAV)} = \frac{(Su1 \times L1)+(Su2 \times L2)....+(Sun \times Ln)}{L\ (Clayey\ soil\ layer)}$$

$$= \frac{(0.72x11)+(1.12x5)+(1.23x10)+(1.22x5)+(1.05x5)+(1.17x5)}{11+5+10+5+5+5}$$

$$= 1.05$$

Now set-up parameter "A" for clayey soil layers can be calculated using the developed model at Level-1[equation (33)] as:

$$A = \frac{0.79\left(\frac{PI}{100}\right) + 0.49}{\left(\frac{S_u}{1\ tsf}\right)^{2.03} + 2.27}$$

$$= \frac{0.79\left(\frac{19}{100}\right) + 0.49}{\left(\frac{1.05}{1\ tsf}\right)^{2.03} + 2.27}$$

$$= 0.19$$

Set-up parameter "A" for the total length of the test pile is

$$A_{\ (Total\ pile)} = \frac{(0.19 \times 41) + (0.15 \times 5)}{46} = 0.18$$ (The top 21 ft. is not considered due to casing)

The side resistance ($R_s$) due to set-up can be calculated as:

$$\frac{R_S}{R_{so}} = 1 + A \log\frac{t}{t_o}$$

$$\frac{R_S}{348} = 1 + 0.18 \log\frac{53}{1}$$

$R_s$ = 456 kips

The total resistance ($R_t$) due to set-up can be calculated as: $R_t = R_{s\ (set\text{-}up)} + R_{tip\ (1\text{-}Day)}$ = 456 kips + 79 kips = 535 kips, which is very close to the measured total resistance ($R_t$) (i.e., 500 kips) at 53 days. However, it is recommended to use the 1st approach (i.e., calculated resistance by individual soil layers) over 2nd approach (i.e., weighted average method).

# SUMMARY AND CONCLUSIONS

The accurate prediction/estimation of the increase in pile resistance with time (or set-up) can be incorporated into a rational design through reducing the number of piles, shortening pile lengths, reducing pile cross-sectional area (using smaller-diameter piles). Incorporating any or a combination of these benefits will result in a cost reduction and savings to pile foundation design in Louisiana. For this purpose, this research study was carried out to investigate the pile set-up phenomenon for clayey soils, to develop empirical models to predict the increase in pile resistance (pile set-up or freeze) at certain time after end of driving (EOD), and to incorporate set-up into the LRFD design of pile foundations in Louisiana. A total number of twelve prestressed concrete (PSC) test piles were driven in different soil conditions of Louisiana. The test piles were instrumented with vibrating wire strain gages to measure the distribution of load transfer along the length of the piles during the static load tests, and vibrating wire piezometers and pressure cells to measure the dissipation of excess PWP and the corresponding increase in effective stress with time. Static and dynamic load tests were performed at different times after EOD to verify the axial resistances of piles and to quantify the amount of increase in pile resistance (i.e., set-up) compared to the EOD. The focus of this research study was to develop empirical models to estimate the increase in resistance of individual soil layers with time along the piles. Logarithmic set-up parameter "A" of individual soil layers were calculated using the unit side resistance with respect to initial normalized time, $t_o$ (i.e., 1 hour and 1 day). The set-up parameter "A" was correlated with different soil properties such as $S_u$, PI, $c_v$, $S_t$ and OCR. Three different levels of empirical models were developed to estimate the magnitude of pile set-up with time for each initial normalized time, $t_o$ (i.e., 1 hour and 1 day). Reliability-based analyses were performed to calibrate the set-up resistance factors ($\phi_{set\text{-}up}$) of different empirical models for incorporating it into the LRFD pile design methodology. Based on the findings of this research study, the following conclusions can be drawn:

- The testing program and the results of the SLTs and DLTs demonstrated set-up behavior that follows a linear logarithmic rate with time after EOD, similar to Skov and Denver model for all the test piles *[7]*. The tip resistances ($R_{tip}$) were almost constant, with the majority of set-up was mainly attributed to increase in side resistance ($R_s$).

- The piezometers that were installed on the piles' faces demonstrated that the dissipation of excess PWP generated during pile driving correlates very well with the pile set-up process. Both the total resistances $R_t$ of the piles and the side resistances of the individual soil layers exhibited high rate of set-up during the initial restrikes. The rate of set-up became slower once the excess PWP was dissipated. The horizontal effective stress increased significantly

for the test piles during the dissipation of the excess PWP. However, after the excess PWP was completely dissipated, the rate of increase in horizontal effective stress became much slower.

- Logarithmic rate of set-up parameter "A" was back-calculated for individual soil layers using Skov and Denvers' model for two initial normalized time (i.e., $t_o$ =1 hour and i.e., $t_o$=1 day) *[7]*. The unit side resistance ($f_s$) was used in this study instead of the total resistance ($R_t$) or side resistance to evaluate set-up behavior. A total of 94 pile segments were considered in this study and clayey soil behavior was dominant on 70 soil layers. The corresponding average values of the rate of the set-up parameter "A" for clayey and sandy soil layers were 0.58 and 0.28, respectively for initial normalized time, $t_o$ = 1 hour; and for $t_o$ = 1 day the average values of the rate of the set-up parameter "A" for clayey and sandy soil layers were 0.31 and 0.15, respectively.

- The magnitude and rate of set-up were found to correlate with the different soil properties. The $S_u$, PI, $c_v$, $S_t$ and OCR have significant influence on the set-up parameter "A." The set-up parameter "A" was found to decrease with increasing $S_u$, $c_v$, and OCR, and to increase with increasing PI and $S_t$.

- Multivariable non-linear regression empirical models were developed to estimate the increase of unit side resistance ($f_s$) with time (or set-up) for individual clayey soil layers. Three different empirical models with different levels of incorporated soil properties were developed with respect to two different initial normalized time (i.e., $t_o$ = 1 hour and $t_o$ = 1 day)**.** The proposed empirical models are:

  The developed models with respect to the normalized time $t_o$ = 1 hour

$$\frac{f_s}{f_{so(1\text{-}hr)}} = 1 + \left[\frac{1.02*\left(\frac{PI}{100}\right)+0.26}{\left(\frac{S_u}{1\ tsf}\right)^{0.68}+0.50}\right] \log \frac{t}{t_{o(1\text{-}hr)}}$$

$$\frac{f_s}{f_{so(1\text{-}hr)}} = 1 + \left[\frac{1.18*\left(\frac{PI}{100}\right)+0.32}{\left[\left(\frac{S_u}{1\ tsf}\right)^{0.40}\right]*\left[\log\left(\frac{c_v}{0.01\frac{in^2}{hour}}\right)\right]^{0.37}+0.53}\right] \log \frac{t}{t_{o(1\text{-}hr)}}$$

$$\frac{f_s}{f_{so(1\text{-}hr)}} = 1 + \left[\frac{0.11*\left(\frac{PI}{100}\right)(S_t)+0.23}{\left[\left(\frac{S_u}{1tsf}\right)^{0.07}\right]*\left[\log\left(\frac{c_v}{0.01\frac{in^2}{hour}}\right)\right]^{0.17}-0.06}\right] \log \frac{t}{t_{o(1\text{-}hr)}}$$

The developed models with respect to the normalized time $t_o$ = 1 day

$$\frac{f_s}{f_{so(1\text{-day})}} = 1 + \left[\frac{0.79*\left(\frac{PI}{100}\right)+0.49}{\left(\frac{S_u}{1\ tsf}\right)^{2.03}+2.27}\right] \log \frac{t}{t_{o(1\text{-day})}}$$

$$\frac{f_s}{f_{so(1\text{-day})}} = 1 + \left[\frac{1.12*\left(\frac{PI}{100}\right)+0.69}{\left[\left(\frac{S_u}{1\ tsf}\right)^{1.44}\right]*\left[\log\left(\frac{C_v}{0.01\frac{in^2}{hour}}\right)\right]^{0.54}+3.19}\right] \log \frac{t}{t_{o(1\text{-day})}}$$

$$\frac{f_s}{f_{so(1\text{-day})}} = 1 + \left[\frac{0.44*\left(\frac{PI}{100}\right)(S_t)+2.20}{\left[\left(\frac{S_u}{1tsf}\right)^{1.94}\right]*\left[\log\left(\frac{C_v}{0.01\frac{in^2}{hour}}\right)\right]^{1.06}+10.65}\right] \log \frac{t}{t_{o(1\text{-day})}}$$

- Reliability-based analyses using FOSM, FORM, and the Monte Carlo simulation were performed to calibrate the set-up resistance factors ($\phi_{set\text{-}up}$) of the three empirical models with respect to $t_o$ = 1 hour and $t_o$ = 1 day for incorporating the effect of set-up into the LRFD pile design methodology. Four different time intervals were selected for this reliability analysis, i.e., at 30 days, 45 days, 60 days and 90 days after EOD. The results showed that the set-up resistance factors ($\phi_{set\text{-}up}$) obtained using the FORM and Monte Carlo simulation methods are higher than those obtained from the FOSM method. The resistance factors ($\phi_{set\text{-}up}$) for the additional set-up resistance (measured from 14 days) at 30 days, 45 days, 60 days and 90 days after EOD are in the range of 0.26 to 0.29, 0.29 to 0.34, 0.30 to 0.37 and 0.32 to 0.37, respectively, for the three empirical models at a target reliability index ($\beta$) of 2.33. The set-up resistance factor ($\phi_{set\text{-}up}$) corresponds to a dead load to live load ratio ($Q_{DL}/Q_{LL}$) of 3 at a target reliability index ($\beta_T$) of 2.33 is recommended to be $\phi_{set\text{-}up}$ = 0.35 for all time intervals.

# RECOMMENDATIONS

1. The authors strongly recommend that DOTD design engineers begin implementing the proposed set-up models, especially model 1 (using both $t_o$ = 1 hour and $t_o$ = 1 day), and the corresponding set-up resistance factor ($\phi_{set\text{-}up}$) in the design and analysis of piles driven in cohesive soil for all future state projects.

2. It is recommended to select several project sites to compare between the design of pile foundations with and without considering the pile set-up to conduct a cost benefit study and to demonstrate the cost savings.

3. It is recommended to initiate a new research project to study and investigate the set-up behavior of open-ended pipe piles, develop an empirical set-up prediction model for local soil conditions, and calibrate the corresponding resistance factors for LRFD design of open-ended pipe piles.

4. It is recommended to hold a workshop should to train DOTD engineers and local geotechnical design engineers on how to incorporate the pile set-up in the analysis and LRFD design of deep pile foundations.

5. It is highly recommended to continue collecting pile set-up data from instrumented test piles for new project sites (as a follow-up study) for evaluation, verification/validation and possible future re-calibration of the proposed models in different soil conditions and re-calibrate the corresponding resistance factors. A database of a minimum 30 pile is considered statistically reliable to perform LRFD calibration.

6. It is recommended to initiate a new research project focusing on evaluating the pile set-up phenomenon using piezocone penetration and dissipation test data.

7. It is recommended to implement the pile set-up resistance in the analysis and design of piles using the “Louisiana Pile Design by Cone Penetration Test (LPD-CPT)” software.

# ACRONYMS, ABBREVIATIONS, AND SYMBOLS

| | |
|---|---|
| AASHTO | American Association of Highway and Transportation Officials |
| $c_v$ | Vertical Coefficient of Consolidation |
| $c_h$ | Horizontal Coefficient of Consolidation |
| CAPWAP | Case Pile Wave Analysis Program |
| CDF | Cumulative Density Function |
| COV | Coefficient of Variation |
| DOTD | Department of Transportation and Development |
| DLT | Dynamic Load Test |
| EOD | End of Driving |
| FOSM | First Order Second Moment |
| FORM | First Order Reliability Method |
| FHWA | Federal Highway Administration |
| $f_s$ | Unit Side Resistance |
| $f_{so}$ | Initial Unit Side Resistance |
| ft. | Feet |
| in. | Inch |
| $k_h$ | Horizontal Permeability |
| LA | Louisiana |
| LRFD | Load and Resistance Factor Design |
| LTRC | Louisiana Transportation Research Center |
| M | Constrained Modulus |
| NCHRP | National Cooperative Highway Research Program |
| OCR | Overconsolidation Ratio |
| OCLT | Osterberg Load Cell Test |
| PCPT | Piezocone Penetration Test |
| PDF | Probability Density Function |
| PI | Plasticity Index |
| PSC | Prestressed Concrete Pile |
| PWP | Pore Water Pressure |
| $q_c$ | Tip resistance |
| $q_t$ | Corrected Cone Tip Resistance |
| $Q_{DL}$ | Dead Load |
| $Q_{LL}$ | Live Load |
| $R^2$ | Coefficient of Correlation |
| $R_{14}$ | Resistance at 14 Days |

| | |
|---|---|
| $R_{s14}$ | Side Resistance at 14 Days |
| $R_{si}$ | Side Resistance of Individual Soil Layers |
| $R_{soi}$ | Initial Side Resistance of Individual Soil Layers |
| $R_{st}$ | Total Side Resistance |
| $R_t$ | Total Resistance |
| $R_{tip}$ | Tip Resistance |
| SLS | Serviceability Limit State |
| SLT | Static Load Test |
| $S_u$ | Undrained Shear Strength |
| $S_t$ | Sensitivity |
| SPT | Standard Penetration Test |
| SSE | Sum of Square Error |
| $t_o$ | Initial Normalized Time |
| TP | Test Pile |
| ULS | Ultimate Limit State |
| WSD | Working Stress Design |
| $\beta_T$ | Target Reliability Index |
| $\phi$ | Resistance Factor |
| $\phi_{14}$ | Resistance Factor at 14 Days |
| $\phi_{set\text{-}up}$ | Set-up Resistance Factor after 14 Days |

# REFERENCES


1. Bullock, P. J., Schmertmann, J. H., McVay, M. C., and Townsend, F. C. "Side shear setup I: Test piles driven in Florida." *Journal of Geotechnical and Geoenvironmental Engineering*, Vol. 131(3), 2005, pp. 292-300.
2. Fellenius, B. H. "Effective stress analysis and set-up for shaft capacity of piles in clay." *From Research to Practice in Geotechnical Engineering*, ASCE, Alberta, Canada, 2008, pp. 384-406.
3. Lee, W., Kim, D., Salgado, R., and Zaheer, M. "Setup of driven piles in layered soil." *Soils and Foundations*, Vol. 50(5), 2010, pp. 585-598.
4. Paikowsky, S. G. and Hajduk, E. L. "Design and construction of three instrumented test piles to examine time dependent pile capacity gain." *Geotechnical Testing Journal*, Vol. 27 (6), 2004, pp. 515-531.
5. Schmertmann, J. H. "The mechanical aging of soils." *Journal of Geotechnical Engineering,* Vol. 117(9), 1991, pp. 1288-1330.
6. Komurka, V. E., Wagner, A. B., and Edil, T. B. "Estimating soil/pile set-up." *Wisconsin Highway Research Program #0092-00-14*, Wisconsin Department of Transportation, 2003.
7. Skov, R. and Denver. H. "Time dependence of bearing capacity of piles." *Proceedings of the 3rd International Conference on the Application of Stress-Wave Theory to Piles*, B. H. Fellenius (Ed.), Ottawa, Ontario, Canada, May 25-27, 1988, pp. 879-888.
8. Svinkin, M. R., Morgano, C. M., and Morvant, M. "Pile capacity as a function of time in clayey and sandy soils." *Proceedings of the DFI 5th International Conference on 'Piling and deep foundations*', Stresa, Italy, April, 1994, pp. 451-456.
9. Svinkin, M. R. and Skov, R. "Set-up effect of cohesive soils in pile capacity." *Proceedings of the 6th International Conference on Application of Stress Waves to Piles*, S. Niyama and J. Beim, (Ed.), Sao Paulo, Brazil, Sep 11-13, 2000, pp. 107-111.
10. Karlsrud, K., Clausen, C. J. F., and Aas, P. M. "Bearing capacity of driven piles in clay, the NGI approach." *Proceedings of the 1st International Symposium on Frontiers in Offshore Geotechnics*, Taylor & Francis, University of Western Australia, Perth, Sep 19-21, 2005, pp. 775-782.
11. Ng, K. W., Suleiman, T. M., and Sritharan, S. "Pile setup in cohesive soil. II: Analytical quantifications and design recommendations." *Journal of Geotechnical and Geoenviromental Engineering*, Vol. 139(2), 2013, pp. 210-222.
12. Guang-Yu, Z. "Wave equation application for piles in soft ground." *Proceedings of the 3rd International Conference on the Application of Stress-Wave Theory to Piles*, B. H. Fellenius, (Ed.), Ottawa, Ontario, Canada, May 25-27, 1988, pp. 831-836.

13. Huang, S. “Application of dynamic measurement on long H-pile driven into soft Ground in Shanghai.” *Proceedings of the 3rd International Conference on the Application of Stress-Wave Theory to Piles*, B. H. Fellenius (Ed.), Ottawa, Ontario, Canada, May 25-27, 1988, pp. 635-643.
14. Lim, J. K. and Lehane, B. M. “Characterisation of the effects of time on the shaft friction of displacement piles in sand.” *Geotechnique,* Vol. 64(6), 2014, pp. 476-485.
15. Bullock, P. J., Schmertmann, J. H., McVay, M. C., and Townsend, F. C. “Side shear setup II: Test piles driven in Florida.” *Journal of Geotechnical and Geoenvironmental Engineering*, Vol. 131(3), 2005, pp. 301-310.
16. Yang, L. and Liang, R. “Incorporating setup into reliability-based design of driven piles in clay.” *Canadian Geotechnical Journal,* Vol. 43(9), 2006, pp. 946-955.
17. Ng, K. W. and Sritharan, S. “A procedure for incorporating setup into load and resistance factor design of driven piles.” *Acta Geotecnica,* 2015, DOI: 10. 1007/s11440-014-0354.
18. Chow, F. C., Jardine, R. J., Brucy, F., and Nauroy, J. F. “Effects of time on capacity of pipe piles in dense Marine sand.” *Journal of Geotechnical and Geoenvironmental Engineering*, Vol. 124(3), 1998, pp. 254-264.
19. Wang, J. X., Verma, N. and Steward, E. J. “Estimating Pile Set-up using 24-h restrike resistance and computed static capacity for PPC piles driven in soft Louisiana Coastal deposits.” *Geotech Geol. Eng*., Vol. 1, 2015, pp. 1-17.
20. McVay, M. C., Schmertmann, J., Townsend, F., and Bullock, P. “Pile friction freeze: A field investigation study.” *Research Report No. WPI 0510632,* Vol. 1*,* Report submitted to Florida Department of Transportation, 1999.
21. Axelsson, G. “Long term setup of driven piles in non-cohesive soils evaluated from dynamic tests on penetration rods.” *Proceedings of the 1st International Conference on Geotechnical Site Characterization*, P. K. Robertson and P. W. Mayne, (Ed.), Atlanta, Georgia, April 19-22, Vol. 2, 1998, pp. 895-900.
22. Basu, P., Prezzi, M., Salgado, R., and Chakraborty, T. “Shaft resistance and setup factors for piles jacked in clay.” *Journal of Geotechnical and Geoenvironmental Engineering*, Vol. 140(3), 2013.
23. Chen, Q., Haque, Md. N., Abu-Farsakh, M., and Fernandez, B. A. “Field investigation of pile setup in mixed soil.” *Geotechnical Testing Journal,* Vol. 37(2), 2014, pp. 268-281, DOI: 10.1520/GTJ20120222.
24. Doherty, P. and Gavin, K. “Shaft capacity of open-ended piles in clay.” *Journal of Geotechnical and Geoenvironmental Engineering,* Vol. 137(11), 2011, pp. 1090-1102.
25. Randolph, M. F., Carter, J. P., and Wroth, C. P. “Driven piles in clay – The effects of installation and subsequent consolidation.” *Geotechnique*, Vol. 29(4), 1979, pp. 361-393.

26. Haque, Md. N., Abu-Farsakh, M., Chen, Q., and Zhang, Z. "Case study on instrumenting and testing full scale test piles for evaluating setup phenomenon." *Journal of the Transportation Research Board No 2462*, National Research Council, Washington, D.C., 2014, pp. 37-47, DOI: 10.3141/2462-05.
27. Doherty, P. and Gavin, K. "Pile aging in cohesive soils." *Journal of Geotechnical and Geoenvironmental Engineering,* Vol. 139(9), 2013, pp. 1620-1624.
28. Haque, Md. N., Abu-Farsakh, M., Tsai, C., and Zhang, Z. "Developing a model to estimate pile set-up for individual soil layers on the basis of PCPT data." *Journal of the Transportation Research Board No 2579*, National Research Council, Washington, D.C., 2016, DOI. 10.3141/2579-03.
29. Azzouz, Amr S., Baligh, Mohsen M., and Whittle, Andrew J. "Shaft Resistance of Piles in Clay," *Journal of Geotechnical Engineering,* Volume 116(2), 1990, pp. 205-221.
30. Long, J. H., Kerrigan, J. A., and Wysockey, M. H. "Measured time effects for axial capacity of driven piling." *Journal of Transportation Research Record 1663,* National Research Council, Washington, D.C., 1999, pp. 57-63.
31. Samson, L. and Authier, J. "Change in pile capacity with time: case histories." *Canadian Geotechnical Journal*, Vol. 23(1), 1986, pp. 174-180.
32. Sawant, V. A., Shukla, S. K., Sivakugan, N., and Das, B. M. "Insight into pile set-up and load carrying capacity of driven piles." *International Journal of Geotechnical Engineering,* Vol. 7(1), 2013, pp. 71-83.
33. Astedt, B., Weiner, L., and Holm, G. "Increase in Bearing Capacity with Time of Friction Piles in Sand," *Proc., Nordic Geotech. Meeting*, 1992, pp. 411-416.
34. Hannigan, P. J., Goble, G. G., Thendean, G., Likins, G. E., and Rausche, F. "Design and construction of driven foundations-Vol. I." *Research Report No. FHWA-HI-97-013,* 1998.
35. Holloway, D. M. and Beddard, D. L. "Dynamic testing results, indicator pile test program – I-880, Oakland, California." *Proceedings of the Deep Foundation Institute 20th Annual Members Conference and Meeting*, Charleston, SC, Oct 13-18, 1995, pp. 105-126.
36. Walton, P. A. and Borg, S. L. "Dynamic pile testing to evaluate quality and verify capacity of driven piles." Transportation research Board, 1998.
37. Yang, N. C. "Relaxation of piles in sand and inorganic silt." *Journal of Soil Mechanics Foundation Division*, Vol. 96, (1970), pp. 395-409.
38. Axelsson, G. "A conceptual model of pile set-up for driven piles in non-cohesive soils." *Proceedings of the Conference of Deep Foundation: An International Perspective on Theory, Design, Construction and Performance (International Deep Foundations Congress 2002)*, Geotechnical Special Publication No. 116, M. W. O'Neill and F. C. Townsend, (Ed.), Orlando, FL, Vol. 1, Feb 14-16, 2002, pp. 64-79.

39. Titi, H. H. and Wathugala, G. W. “Numerical procedure for predicting pile capacity setup/ freeze.” *Journal of the Transportation Research Board No. 1663*, National Research Council, Washington, D.C., 1999, pp. 25-32.
40. Abu-Farsakh, M. Y., Rosti, F. and Souri, A. “Evaluating pile installation and subsequent thixotropic and consolidation effects on setup by numerical simulation for full scale pile load tests.” *Canadian Geotechnical Journal,* 52(11), 2015, pp. 1734-1746.
41. York, D. L., Brusey, W. G., Clemente, F. M., and Law, S. K. “Setup and relaxation in glacial sand.” *Journal of Geotechnical Engineering*, Vol. 120(9), 1994, pp. 1498-1513.
42. Koutsoftas, Demetrious C. “High capacity piles in dense sands.” Deep Foundation Congress, GSP no. 116, Vol. 1, ASCE, 2002, pp. 632-646.
43. Dudler, E. V., Durante, V. A. and Smirnov, C. D. “Experience gained in using the penetrometer probe for soil investigation in conjunction with energy-related constructions in the soviet union,” INFORM-ENERGO, Moscow, Soviet Union, 63, 1968.
44. Camp III, W. M. and Parmar, H. S. “Characterization of pile capacity with time in the Cooper Marl: a study of the applicability of a past approach to predict long time pile capacity.” *Journal of Transportation Research Record 2004*, 1999, pp. 12-19.
45. Yang, N. C. “Redriving characteristics of piles.” *Journal of Soil Mechanics Foundation Division*, Vol. 82, 1956, 1026.
46. Preim, M. J., March, R., and Hussein, M. “Bearing capacity of piles in soils with time dependent characteristics.” *Proceedings of the 3rd International Conference on ‘Piling and Deep foundation’,* J. B. Burland and J. M. Mitchell, (Ed.), London, England, May 15-18, 1989, pp. 363-370.
47. Chow, F. C., Jardine, R. J., Nauroy, J. F., and F, Brucy. “Time related increase in shaft capacities of driven piles in sand.” *Geotechnique*, Vol. 47(2), 1997, pp. 353-361.
48. Haque, Md. N., Chen, Q., Abu-Farsakh, M., and Tsai, C. “Effects of pile size on set-up behavior of cohesive soils.” *Proceedings of Geo-Congress 2014, GeoCharacterization and Modeling for Sustainability,* GSP No 234*,* Georgia, Feb 23-26, 2014, pp. 1743-1749.
49. Bullock, P. J. “Pile friction freeze: A field and laboratory study.” *PhD Dissertation*, University of Florida, Gainesville, USA, 1999.
50. Lukas, R. G. and Bushell, T. D. “Contribution of soil freeze to pile capacity” *Proceedings of Foundation Engineering: Current Principles and Practices*, Evanston, Illinois, June 25-29, Vol. 2, 1989, pp. 991-1001.
51. Mesri, G., Feng, T. W., and Benak, J. M. “Postdensification penetration resistance of clean sands.” *Journal of Geotechnical Engineering*, Vol. 116(7), 1990, pp. 1095-1115.
52. Flaate, K. “Effects of pile driving in clays.” *Canadian Geotechnical Journal*, Vol. 9(1), 1972, pp. 81-88.

53. Withiam, J. L., Voytko, E. P., Barker, R. M., Duncan, J. M., Kelly, B. C., Musser, S. C. and Elias, V. "Load and Resistance factor Design (LRFD) for Highway Bridge Substructure." *FHWA HI-98-032*, Federal Highway Administration, Washington, D. C.
54. Nowak, A.S. *Calibration of LRFD Bridge Design Code*, Publication NCHRP-368, Transportation Research Board, Washington, D.C., 1999. pp.218.
55. Becker, D. E. "Eighteenth Canadian Geotechnical Colloquium: Limit state design for foundation. Part I and II. An Overview of the Foundation Design Process." *Canadian Geotechnical Journal*, Vol. 33, 1996, pp. 956-1007.
56. AASHTO. *LRFD Bridge Design Specifications*, 4th Edition, American Association of State Highway and Transportation Officials, Washington, D.C., USA, 2007. pp.582.
57. Abu-Farsakh, Y. M., Yoon, S., and Tsai, C. *Calibration of Resistance Factors Needed in the LRFD Design of Driven Piles*. Report No. 449, Louisiana Transportation Research Center, May, 2009.
58. Hansell, W. C. and Viest, I. M. "Load factor design for steel highway bridges." AISC Engineering Journal, Vol. 8(4), 1971, pp. 113-123.
59. McVay, M. C., L. B. Birgisson, L. Zhang, A. Perez, and S. Putcha. "Load and resistance factor design (LRFD) for driven piles using dynamic methods-A Florida Perspective." *Geotechnical Testing Journal,* Vol. 23 (1), 2000, pp 55-66.
60. Paikowsky, S. G. "NCHRP Report 507: Load and Resistance Factor Design (LRFD) for Deep Foundation." *Transportation Research Board of the National Academics*, Washington, D. C., 2004.
61. Ng, K. W., Suleiman, M. T., Sritharan, S., Roling, M., and AbdelSalam, S. S. "Development of LRFD design procedures for bridge pile foundations in IOWA-Field testing of steel piles in clay, sand and mixed soils and data analysis." *Final Report. Vol. 2*, Institute for Transportation, Iowa State University, Ames, IA, 2011.
62. Hasofer, A. M. and Lind, N. C. "An exact and invariant First-Order Reliability Format." *Journal of Engineering Mechanics*, Vol. 100, No. EM1, 1974, pp. 111-121.
63. Nowak, S. A. and Collins, K. R. "Reliability of structures" McGraw Hill, International Edition, 2000.
64. Rackwitz, R. and Fiessler, B. "Structural reliability under combined random loads." *Computers and Structures*, Vol. 9, 1978.
65. Allen, T.M., Nowak, A., and Bathurst, R. *Calibration to Determine Load and Resistance Factors for Geotechnical and Structural Design*. Publication TRB Circular E-C079, Transportation Research Board, Washington, D.C., 2005. pp.93.
66. Harr, M. E. "Reliability based design in civil engineering." Dover, Mineola, NY, 1996.

67. Abu-Farsakh, M. Y., Chen, Q., and Haque, Md. N. "Calibration of Resistance factors for Drilled Shafts for the New FHWA Design Method*" Report no FHWA/LA. 12/495,* Louisiana Transportation Research Center, 2013.
68. Chen, Q., Abu-Farsakh, M. Y., and Haque, Md. N. "Comparison of resistance factors between 1999 and 2010 FHWA design methods for LRFD design of drilled shafts.*" In Proceedings of Transportation Research Board 94th Annual Meeting,* 2015, Washington D.C.
69. Barker, R. M., Duncan, J. M., Rojiani, K. B., Ooi, P. S. K., Tan, C. K., and Kim, S. G. *Manuals for the Design of Bridge Foundations*. NCHRP-343, Transportation Research Board, National Research Council, Washington, D.C., 1991, pp. 306.
70. Zhang, Z. and Tumay, M. T. "Statistical to fuzzy approach toward CPT soil classification." *Journal of Geotechnical and Geoenvironmental Engineering*, Vol. 125(3), 1999, pp. 179-186.
71. Abu-Farsakh, M. Y. "Evaluation of consolidation characteristics of cohesive soils from Piezocone Penetration Tests." Report: 386, Louisiana Transportation Research Center, Baton Rouge, LA, 2004.
72. Robertson, P. K. "Estimating in-situ soil permeability from CPT and CPTu." *In Proceedings to the 2nd International Symposium on Cone Penetration Testing (CPT' 10)*, May 9-11, 2010, Huntington Beach, California, USA.
73. Teh, C. I. and Houlsby, G. T. "An analytical study of the Cone Penetration Test in clay." *Geotechnique*, Vol. 41, No. 1, 1991, pp. 17-34.
74. ASTM D4945-12. "Standard test method for high-strain dynamic testing of deep foundations." ASTM International West Conshohocken, PA, 2013.
75. ASTM D1143/D1143M-07. "Standard test methods for deep foundations under static axial compression load." ASTM International West Conshohocken, PA, 2012.
76. Haque, Md. N. "Field instrumentation and testing to study set-up phenomenon of driven piles and its implementation in LRFD design methodology." *Ph.D. Dissertation*, Louisiana State University, Baton Rouge, USA, 2016.
77. Haque, Md. N., Abu-Farsakh, M. Y. and Chen, Q. "Pile set-up for individual soil layers along instrumented test piles in clayey soil." *In Proceedings of the 15th Pan-American Conference on Soil Mechanics and Geotechnical Engineering (From Fundamentals to Applications in Geotechnics)*, D. Manzanal and A.O. Sfriso (Eds.) November 15–18, Buenos Aires, Argentina, 2015, pp. 390-397.
78. Haque, Md. N., Abu-Farsakh, M. Y. and Tsai, C. "Field investigation to evaluate the effects of pile installation sequence on pile setup behavior for instrumented test piles." *Geotechnical Testing Journal,* Vol. 39(5), 2016, pp. 1-17, DOI. 10.1520/GTJ20140259.

79. Davisson, M. T. “High capacity piles.” *Proceedings of the Soil Mechanics Lecture Series on Innovations in Foundation Construction,* ASCE, Reston, VA, 1972, pp. 81-112.
80. Briuad, J. L. and Tucker, L. M. “Measured and predicted axial response of 98 piles.*”* *Journal of Geotechnical and Geoenvironmental Engineering*, Vol. 114(8), 1988, pp. 984-1001.

# APPENDIX A

1. Bayou Liberty (State project No. 852-21-0024)

(a) Test Pile Information

| | |
|---|---|
| Pile Type | PSC |
| Width | 24 in. |
| Length | 68 ft. |
| Station No | 111+62 |

(b) Set-up information of the test pile

| Time | Resistance (kips) | | |
|---|---|---|---|
| | Side, $R_s$ | Tip, $R_{tip}$ | Total, $R_t$ |
| EOD | 49.3 | 30.9 | 80.2 |
| 72 hrs | 193.6 | 46.3 | 239.9 |
| 432 hrs | 350.8 | 58.2 | 409 |

2. US 90 LA-668 (Interchange) (State project No. 424-04-0026)

(a) Test Pile Information

| | |
|---|---|
| Pile Type | PSC |
| Width | 14 in. |
| Station No | 123+80 |

(b) Set-up information of the test pile

| Time | Resistance (kips) | | |
|---|---|---|---|
| | Side, $R_s$ | Tip, $R_{tip}$ | Total, $R_t$ |
| EOD | 16.5 | 33.7 | 50.2 |
| 24 hrs | 78 | 119.7 | 197.7 |
| 384 hrs | 86.5 | 119.7 | 206.2 |

3. New Starc (TP-2) (State project No. 064-01-0040)

(a) Test Pile Information

| | |
|---|---|
| Pile Type | PSC |
| Width | 24 in. |
| Length | 55 ft. |
| Station No | 108+85 |

(b) Set-up information of the test pile

| Time | Resistance (kips) | | |
|---|---|---|---|
| | Side, $R_s$ | Tip, $R_{tip}$ | Total, $R_t$ |
| EOD | 348.7 | 185.9 | 534.6 |
| 24 hrs | 481.8 | 185.5 | 667.3 |
| 960 hrs | 734.5 | 185.5 | 920 |

4. JCT LA-1 LA-983 US-190

(a) Test Pile Information

| | |
|---|---|
| Pile Type | PSC |
| Width | 16 in. |
| Length | 75 ft. |
| Station No | 22+965 |

(b) Set-up information of the test pile

| Time | Resistance (kips) | | |
|---|---|---|---|
| | Side, $R_s$ | Tip, $R_{tip}$ | Total, $R_t$ |
| EOD | 64.7 | 101.7 | 166.4 |
| 24 hrs | 195.1 | 97.6 | 292.7 |
| 336 hrs | 216.4 | 112.9 | 329.3 |

5. Calcasieu River (TP-1) (State project No. 700-58-0141)

(a) Test Pile Information

| | |
|---|---|
| Pile Type | PSC |
| Width | 24 in. |
| Length | 73.8 ft. |
| Station No | 11+100 |

(b) Set-up information of the test pile

| Time | Resistance (kips) | | |
|---|---|---|---|
| | Side, $R_s$ | Tip, $R_{tip}$ | Total, $R_t$ |
| EOD | 484 | 210 | 694 |
| 24 hrs | 630 | 286 | 916 |
| 456 hrs | 1001 | 238 | 1239 |

6. Calcasieu River (TP-2) (State project No. 700-58-0141)

(a) Test Pile Information

| | |
|---|---|
| Pile Type | PSC |
| Width | 24 in. |
| Length | 70.8 ft. |
| Station No | 11+315 |

(b) Set-up information of the test pile

| Time | Resistance (kips) | | |
|---|---|---|---|
| | Side, $R_s$ | Tip, $R_{tip}$ | Total, $R_t$ |
| EOD | 370 | 599 | 969 |
| 96 hrs | 837 | 533 | 1370 |
| 504 hrs | 1009 | 662 | 1671 |

7. St. Louis Canal Bridge

(a) Test Pile Information

| | |
|---|---|
| Pile Type | PSC |
| Width | 16 in. |
| Length | 92 ft. |

(b) Set-up information of the test pile

| Time | Resistance (kips) | | |
|---|---|---|---|
| | Side, $R_s$ | Tip, $R_{tip}$ | Total, $R_t$ |
| EOD | 20 | 20 | 40 |
| 24 hrs | 84.5 | 44.8 | 129.3 |
| 360 hrs | 106.6 | 32.9 | 139.5 |

8. Joyce Lasalle (IND 1)

(a) Test Pile Information

| | |
|---|---|
| Pile Type | PSC |
| Width | 16 in. |

(b) Set-up information of the test pile

| Time | Resistance (kips) | | |
|---|---|---|---|
| | Side, $R_s$ | Tip, $R_{tip}$ | Total, $R_t$ |
| EOD | 96.4 | 203.6 | 300 |
| 24 hrs | 180.5 | 299.6 | 480.1 |
| 360 hrs | 182.5 | 367.5 | 550 |

9. Joyce Lasalle (IND 2)

(a) Test Pile Information

| | |
|---|---|
| Pile Type | PSC |
| Width | 16 in. |

(b) Set-up information of the test pile

| Time | Resistance (kips) | | |
|---|---|---|---|
| | Side, $R_s$ | Tip, $R_{tip}$ | Total, $R_t$ |
| EOD | 76.3 | 113.8 | 190.1 |
| 24 hrs | 152 | 142.2 | 294.2 |
| 360 hrs | 207 | 138 | 345 |

10. Morman Slough (TP-1) (State project No. 012-02-0029)

(a) Test Pile Information

| | |
|---|---|
| Pile Type | PSC |
| Width | 24 in. |
| Length | 68 ft. |

(b) Set-up information of the test pile

| Time | Resistance (kips) | | |
|---|---|---|---|
| | Side, $R_s$ | Tip, $R_{tip}$ | Total, $R_t$ |
| EOD | 196.5 | 118.1 | 314.6 |
| 24 hrs | 357.1 | 107 | 464.1 |
| 672 hrs | 490.5 | 100.5 | 591 |

11. Bayou Bouef (west) (State project No. 424-05-0081)

(a) Test Pile Information

| | |
|---|---|
| Pile Type | PSC |
| Width | 14 in. |
| Length | 75 ft. |
| Station No | 591+00 |

(b) Set-up information of the test pile

| Time | Resistance (kips) | | |
|---|---|---|---|
| | Side, $R_s$ | Tip, $R_{tip}$ | Total, $R_t$ |
| EOD | 40.9 | 92 | 132.9 |
| 24 hrs | 171.7 | 127.7 | 299.4 |
| 336 hrs | 207.9 | 109.9 | 317.8 |

12. Fort Buhlow (State project No. 840-43-0001)

(a) Test Pile Information

| | |
|---|---|
| Pile Type | PSC |
| Width | 14 in. |
| Length | 60 ft. |
| Station No | 108+85 |

(b) Set-up information of the test pile

| Time | Resistance (kips) | | |
|---|---|---|---|
| | Side, $R_s$ | Tip, $R_{tip}$ | Total, $R_t$ |
| EOD | 53.8 | 38.4 | 92.2 |
| 24 hrs | 122.6 | 56.5 | 179.1 |
| 384 hrs | 193.5 | 56.5 | 250 |

13. Caminada Bay (TP-3) (State project No. 064-01-0040)

(a) Test Pile Information

| | |
|---|---|
| Pile Type | PSC |
| Width | 36 in. |
| Length | 153 ft. |

(b) Set-up information of the test pile

| Time | Resistance (kips) | | |
|---|---|---|---|
| | Side, $R_s$ | Tip, $R_{tip}$ | Total, $R_t$ |
| EOD | 30 | 95 | 125 |
| 48 hrs | 333.7 | 256.3 | 590 |
| 1320 hrs | 1110.3 | 289.7 | 1400 |

14. Caminada Bay (TP-5) (State project No. 064-01-0040)

(a) Test Pile Information

| | |
|---|---|
| Pile Type | PSC |
| Width | 36 in. |
| Length | 148 ft. |

(b) Set-up information of the test pile

| Time | Resistance (kips) | | |
|---|---|---|---|
| | Side, $R_s$ | Tip, $R_{tip}$ | Total, $R_t$ |
| EOD | 68.3 | 91.7 | 160 |
| 1 hr | 175.6 | 89.2 | 264.8 |
| 48 hrs | 449.1 | 110.9 | 560 |
| 768 hrs | 680.8 | 269.5 | 950.3 |

15. Caminada Bay (TP-6) (State project No. 064-01-0040)

(a) Test Pile Information

| | |
|---|---|
| Pile Type | PSC |
| Width | 36 in. |
| Length | 133 ft. |

(b) Set-up information of the test pile

| Time | Resistance (kips) | | |
|---|---|---|---|
| | Side, $R_s$ | Tip, $R_{tip}$ | Total, $R_t$ |
| EOD | 29.9 | 97.1 | 127 |
| 1 hr | 199 | 201 | 400 |
| 24 hrs | 370.2 | 279.8 | 650 |
| 984 hrs | 770.2 | 229.5 | 999.7 |

16. Caminada Bay (TP-7) (State project No. 064-01-0040)

(a) Test Pile Information

| | |
|---|---|
| Pile Type | PSC |
| Width | 36 in. |
| Length | 73 ft. |

(b) Set-up information of the test pile

| Time | Resistance (kips) | | |
|---|---|---|---|
| | Side, $R_s$ | Tip, $R_{tip}$ | Total, $R_t$ |
| EOD | 40 | 10 | 50 |
| 48 hrs | 230 | 135 | 365 |
| 672 hrs | 397.5 | 142.6 | 540.1 |

17. LA-1 (TP-6) (State project No. 829-32-0007 and 064-30-0035)

(a) Test Pile Information

| | |
|---|---|
| Pile Type | PSC |
| Width | 24 in. |
| Length | 150 ft. |

(b) Set-up information of the test pile

| Time | Resistance (kips) | | |
|---|---|---|---|
| | Side, $R_s$ | Tip, $R_{tip}$ | Total, $R_t$ |
| EOD | 162 | 39 | 201 |
| 2 hrs | 351 | 89 | 440 |
| 4 hrs | 471 | 62 | 533 |
| 6 hrs | 480 | 87 | 567 |
| 24 hrs | 649 | 77 | 726 |
| 48 hrs | 653 | 102 | 755 |
| 72 hrs | 674 | 118 | 792 |
| 150.5 hrs | 747 | 106 | 853 |
| 147.3 hrs (Static) | - | - | 888 |

18. LA-1 (TP-10) (State project No. 829-32-0007 and 064-30-0035)

(a) Test Pile Information

| | |
|---|---|
| Pile Type | PSC |
| Width | 24 in. |
| Length | 78 ft. |

(b) Set-up information of the test pile

| Time | Resistance (kips) | | |
|---|---|---|---|
| | Side, $R_s$ | Tip, $R_{tip}$ | Total, $R_t$ |
| 2 hrs | 372 | 212 | 584 |
| 4 hrs | 564 | 260 | 824 |
| 7 hrs | 769 | 249 | 1018 |
| 24 hrs | 899 | 233 | 1132 |
| 72 hrs | 1149 | 215 | 1364 |
| 1200 hrs | 1393 | 215 | 1608 |
| 167 hrs (Static) | - | - | 801 |

This public document is published at a total cost of $250
42 copies of this public document were published in this first printing at a cost of $250. The total cost of all printings of this document including reprints is $250. This document was published by Louisiana Transportation Research Center to report and publish research findings as required in R.S. 48:105. This material was duplicated in accordance with standards for printing by state agencies established pursuant to R.S. 43:31. Printing of this material was purchased in accordance with the provisions of Title 43 of the Louisiana Revised Statutes.